Investigation into the relevance of BCR-ABL for the survival of cancer stem cells in chronic myeloid leukaemia

by

Ashley Hamilton

A thesis submitted for the degree of Doctor of Philosophy

June 2010

Section of Experimental Haematology

Division of Cancer Sciences and Molecular Pathology

Faculty of Medicine

ABSTRACT

Chronic myeloid leukaemia (CML) is a clonal myeloproliferative disorder of the haemopoietic stem cell, defined by the Philadelphia chromosome (Ph) - the outcome of a balanced, reciprocal translocation between the long arms of chromosomes 9 and 22. The novel fusion oncogene generated on chromosome 22 as a result of this translocation is called *BCR-ABL*. In the majority of patients, this oncogene transcribes a 210-kDa constitutively active protein tyrosine kinase, often referred to as $p210^{BCR-ABL}$, which is necessary for the transformation of the disease. The introduction of the orally available, tyrosine kinase inhibitor (TKI) - imatinib mesylate (IM) - marked a major advance in CML treatment in terms of efficacy and tolerability and has now become the first line of therapy. IM acts by competing with ATP to block ABL-kinase activity, resulting in the selective apoptosis induction of $BCR-ABL^{+}$ cells. However, despite the success of IM as standard therapy for CML, only a small proportion of patients obtain a complete molecular response, where they become negative for *BCR-ABL* transcripts by RT-PCR. It is hypothesised that this minimal residual disease is the result of a primitive quiescent subpopulation of leukaemic cells, which may be the cause for relapse at a later date. Another major clinical concern is the observation of molecular resistance in IM-treated patients. Proposed mechanisms of resistance include BCR-ABL amplification, decreased intracellular IM concentrations caused by drug efflux proteins such as multi drug resistance-1 and the development of point mutations within the ABL-kinase domain. In an attempt to overcome IM-resistance, a second generation of BCR-ABL inhibitors has been developed. Dasatinib (BMS-354825, Sprycel) is a TKI developed for the treatment of IM-resistant or -intolerant patients with Ph^{+} leukaemias, which has a 325-fold greater potency than IM against cells expressing wild-type BCR-ABL, and is effective

against all IM-resistant BCR-ABL mutants tested *in vitro*, except T315I. Previously, we showed that dasatinib induced durable inhibition of BCR-ABL and impressive clearance of Ph^+ cells, however, the primitive quiescent cell population did not appear to undergo apoptosis even after several days TKI exposure. Therefore, it was still not clear whether early CML progenitor cells depend on BCR-ABL for their growth and survival. In this study we have attempted to determine whether CML stem cells are dependent on BCR-ABL TK activity for their survival and/or proliferation using dasatinib treatment and aimed to characterise the cells which survived drug exposure. We found that 10% of the CML cells were able to survive the dasatinib treatment. We also showed that maximal BCR-ABL TK inhibition was achieved in the surviving CML cells, both in the bulk population of cells and the more problematic primitive stem cell population. Those cells which survived the dasatinib treatment were found to be primitive, residing mainly in the undivided cell fraction and the very early cell divisions. Since these BCR-ABL TK-inhibited, resistant cells were also able to grow when re-cultured in cytokines and form long-term culture-initiating cell (LTC-IC) colonies; these data suggested that ~10% of primitive $CD34^+$ CML cells are not addicted to BCR-ABL TK activity for their survival. This also suggested that these primitive, resistant CML cells appeared to survive and proliferate by BCR-ABL-independent mechanisms. Therefore, the next experiments were then designed to investigate the cellular process of autophagy as a potential means of primitive CML cell survival. Analysis of the properties of $CD34^+$ CML cells which remained viable following dasatinib treatment, revealed the existence of cytoplasmic autophagic structures determined by electron microscopy and significantly increased autophagosome-asociated LC3-II, particularly in the cells cultured without growth factors (GF)s. This suggested that autophagy is induced following GF deprivation of CML cells and is significantly increased within these cells, upon BCR-ABL inhibition following dasatinib

treatment. Furthermore, we also found that the inhibition of autophagy greatly potentiated the effect of TKI treatment on the reduction of primitive CML progenitor cells, in terms of the effective eradication of functionally defined colony forming cells and LTC-ICs.

Overall, this thesis has shown for the first time that the most TKI-resistant primitive CML cells are likely to be independent of BCR-ABL TK activity for their proliferation and/or survival. Furthermore, we have shown that these resistant CML stem cells rely on the BCR-ABL independent autophagy process for survival in response to stressful conditions, such as, GF deprivation and TKI treatment.

TABLE OF CONTENTS

LIST OF TABLES

LIST OF FIGURES

RELATED PUBLICATIONS

Hamilton A, Gallipoli P, Nicholson E, TL Holyoake. Targeted therapy in haematological malignancies. [Review] *The Journal of Pathology* (2009);220(4):404-18.

Schemionek M, Elling C, Steidl U, Bäumer N, **Hamilton A**, Spieker T, Göthert JR, Stehling M, Wagers A, Huettner CS, Tenen DG, Tickenbrock L, Berdel WE, Serve H, Holyoake TL, Müller-Tidow C, Koschmieder S. BCR-ABL enhances differentiation of long-term repopulating hematopoietic stem cells. *Blood* (2010);115(16):3185-95.

Bellodi C, Lidonnici MR, **Hamilton A**, Helgason GV, Soliera AR, Ronchetti M, Galavotti S, Young KW, Selmi T, Yacobi R, Van Etten RA, Donato N, Hunter A, Dinsdale D, Tirrò E, Vigneri P, Nicotera P, Dyer MJ, Holyoake T, Salomoni P, Calabretta B. Targeting autophagy potentiates tyrosine kinase inhibitor-induced cell death in Philadelphia chromosome-positive cells, including primary CML stem cells. *Journal of Clinical Investigation* (2009); 119(5):1109-23. doi: 10.1172/JCI35660. (first three authors joint first)

Allan EK, **Hamilton A**, Hatziieremia S, Zhou P, Jørgensen HG, Vigneri P, Holyoake TL. Nuclear entrapment of BCR-ABL by combining imatinib mesylate with leptomycin B does not eliminate CD34+ chronic myeloid leukaemia cells. *Leukemia* (2009); 23(5):1006-8.

Hamilton A, Alhashimi F, Myssina S, Jorgensen HG, Holyoake TL. Optimization of methods for the detection of BCR-ABL activity in Philadelphia-positive cells. *Experimental Hematology* (2009); 37(3):395-401.

Myssina S, Helgason GV, Serrels A, Jørgensen HG, Bhatia R, Modi H, Baird JW, Mountford JC, **Hamilton A**, Schemionek M, Koschmieder S, Brunton VG, Holyoake TL. Combined BCR-ABL inhibition with lentiviral-delivered shRNA and dasatinib augments induction of apoptosis in Philadelphia-positive cells. *Experimental Hematology* (2009); 37(2):206-14.

Copland M, Pellicano F, Richmond L, Allan EK, **Hamilton A**, Lee FY, Weinmann R, Holyoake TL. BMS-214662 potently induces apoptosis of chronic myeloid leukemia stem and progenitor cells and synergizes with tyrosine kinase inhibitors. *Blood*. 2008 Mar 1; 111(5):2843-53. Erratum in: *Blood* (2008); 111(9):4830.

Copland M, **Hamilton A**, Holyoake TL. Response: Conventional Western blotting techniques will not reliably quantify p210 BCR-ABL**.** *Blood* (2007); 109: 1336.

PUBLICATIONS IN PREPARATION

Hamilton A, Helgason G.V., Schemionek M, Myssina S, Allan E, Nicolini F.E., Bhatia R, Brunton V.G., Müller-Tidow C, Koschmieder S, Holyoake T. L. Chronic Myeloid Leukaemia Stem Cells are not Oncogene Addicted and Survive via Bcr-Abl independent Mechanisms. *In preparation*

ACKNOWLEDGEMENTS

I would like to thank a number of people who, without their help, would have made the undertaking of this PhD far more difficult. Firstly, I am indebted to my main supervisor Tessa Holyoake, who has given me invaluable guidance and support both during and prior to the PhD. This thesis would not have happened without Tessa's encouragement. I would also like to thank my second supervisor Vignir Helgason for all of his help and useful advice towards the end of my PhD. Special thanks to my colleagues at the Paul O'Gorman Leukaemia Research Centre who have helped me along the way and have most of all, made this experience fun.

Also I would like to thank the people who helped me undertake some of the research presented in this thesis, namely, Alan Hair, Elaine Allan, Sandrine Hayette and David Dinsdale.

I would especially like to thank my family and friends for their constant support and encouragement.

I am indebted to the Leukaemia Research Fund and Medical Research Council for funding this research. I am also grateful to the Medical Research Council/TSCRC for funding the clinical trial associated with this thesis.

AUTHOR'S DECLARATION

Unless otherwise stated, I declare that all the work presented in this thesis is my own.

DEFINITIONS AND ABBREVIATIONS

4EBP1	eukaryotic translation initiation factor 4E
7-AAD	7 aminoactinomycin D
Ab	antibody
ABC	adenosine triphosphate-binding cassette
ALBA	human albumin solution
ALDH	aldehyde dehydrogenase
ALL	acute lymphoblastic leukaemia
alloSCT	allogeneic stem cell transplantation
A-loop	activation loop
AML	acute myeloid leukaemia
AMP	adenosine monophosphate
AMPK	AMP-kinase
AP	accelerated phase
Ara-C	cytosine arabinoside
ATP	adenosine triphosphate
Bad	Bcl-2-associated death promoter
BAF	bafilomycin A_1
Bap	BRCA1-associated protein
BC	blast crisis
Bcl	B-cell lymphoma
BCA	bicinchoninic acid
BCR-ABL	breakpoint cluster region-abelson
BIT	bovine serum albumin/insulin /transferrin
BM	bone marrow
BRCA1	breast cancer 1
BSA	bovine serum albumin
C-C	coiled-coil
CCR	complete cytogenetic response
CFC	colony-forming cell
CFSE	carboxyfluorescein diacetate succinimidyl ester
CHR	complete haematological response
CIS	cytokine-induced SH2-containing
CLP	common lymphoid progenitors
CML	chronic myeloid leukaemia
CMP	common myeloid progenitors
CMR	complete molecular response
COOH	carboxy
CP	chronic phase
CQ	chloroquine
CrkL	Crk-like
DMEM	Dulbecco’s Modified Eagle Medium
DMSO	dimethyl sulfoxide
Dok	docking protein
DT	diphtheria toxin
EDTA	ethylenediaminetetraacetic acid
eIF4E	eukaryoytic initiation factor 4E
ELISA	enzyme-linked immunosorbent assay
EM	electron microscopy
ERK	extracellular signal-regulated kinase
FACS	fluorescence-activated cell sorting

Fak	focal adhesion kinase
FAM	6-carboxyfluorescein reporter
FCS	foetal calf serum
FDA	Food and Drug Administration
FISH	fluorescence in situ hybridisation
FOXO	forkhead box, subgroup O
FRET	Fluorescence Resonance Energy Transfer
FSC	forward-angle light scatter
FTI	farnesyl transferase inhibitors
GAP	GTPase activating protein
GAPDH	Glyceraldehyde-3-phosphate-dehydrogenase
G-CSF	granulocyte-colony stimulating factor
GEF	guanine-nucleotide-exchange factor
GF	growth factor
GFP	green fluorescent protein
GM-CSF	granulocyte macrophage-colony stimulating factor
G-protein	guanine-nucleotide-binding protein
Grb-2	growth-receptor-binding-2
GSK3β	Glycogen synthase kinase 3 beta
HBSS-CMF	Hank's buffered salt solution - calcium and magnesium free
HCl	hydrochloric acid
HCQ	hydroxychloroquine
HRP	horseradish peroxidase
HSC	haemopoietic stem cell
Hst	Hoechst 33342
IC_{50}	50% inhibitory concentration
IF	immunofluorescence
IFNα	interferon alpha
IL	Interleukin
IM	imatinib mesylate
IMDM	Isocove's Modified Dulbecco's Medium
IRIS	International Randomized Study of Interferon and STI571
JAK	Janus family of activated kinases
KCl	potassium chloride
LC3	microtubule-associated protein 1 light chain 3
LSC	leukaemic stem cell
LTBMC	long-term bone marrow culture
LTC-IC	long-term culture-initiating cell
LT-HSC	long-term HSC
MAPK	mitogen-activated protein kinase
mcl	myeloid cell leukaemia
MCR	major cytogenetic response
mdm2	murine double minute 2
MDR-1	multi-drug resistance-1
MEK	MAPK kinase
$MgCl_2$	magnesium chloride
MFI	mean fluorescence intensity
MNC	mononuclear cells
MPP	multipotent progenitor
MRD	minimal residual disease
mTOR	mammalian target of rapamycin
NH2	amino
NLS	nuclear localisation signal

NOD/ SCID	non-obese diabetic/severe combined immunodeficient
PBS	phosphate buffered saline
PCR	polymerase chain reaction
p-CrkL	phospho-CrkL
PDGF-R	platelet-derived growth factor receptor
PE	phosphatidylethanolamine
Ph	Philadelphia chromosome
PI3K	phosphatidylinositol 3-kinase
PIP_2	PI-(4,5)-bisphosphate
PIP_3	PI-(3,4,5)-triphosphate
PLCγ	phospholipase Cγ
P-loop	ATP binding site
Plt	peripheral blood platelet count
PTEN	phosphatase and tensin homologue deleted on chromosome 10
PTK	protein TK
p-Tyr	phospho-tyrosine
PVDF	polyvinylidene fluoride
PY	Pyronin Y
qRT-PCR	quantitative reverse transcriptase-polymerase chain reaction
raptor	regulatory-associated protein of mTOR
Rho	Rhodamine-123
rictor	rapamycin-insensitive companion of mTOR
S6K	p70 ribosomal protein S6 kinase
SAHA	suberoylanilide hydroxamic acid
SCF	stem cell factor
SDF-1α	stromal cell-derived factor-1 alpha
SDS-PAGE	sodium dodecyl suphate-polyacrylamide gel electrophoresis
Ser	serine
SFK	SRC family kinase
SH	SRC homology
sh	short hairpin
SHIP	SH2-containing inositol-5-phosphatase
si	small interfering
SL-IC	SCID leukaemia-initiating cells
SOCS	suppressors of cytokine signalling
SOS	son of sevenless
SP	side population
SSC	side-angle light scatter
STAT	signal transducer and activator of transcription
ST-HSC	short-term HSC
TAMRA	tetramethylrhodamine
TBS	Tris-buffered saline
TBST	TBS-Tween
TEL	translocated ets leukaemia
tet-O	tetracycline-responsive element
Thr	threonine
TK	tyrosine kinase
TKI	tyrosine kinase inhibitor
TSC	tuberous sclerosis
UD	undivided
WC	white cell count
WHO	World Health Organisation
Y177	tyrosine 177

1. INTRODUCTION

1.1 Haemopoietic stem cells and normal haemopoiesis

Haemopoiesis is the process of blood cell formation within an organism and results in the development and differentiation of haemopoietic stem cells (HSCs) (1, 2). In adult mammals, HSCs are predominantly found in the bone marrow (BM), with the majority being relatively short-lived within the circulation (3). In order to maintain the haemopoietic system, it is necessary for the BM to produce up to 10^{13} cells per day (4). Terminally differentiated cells are incapable of further growth themselves and therefore, to prevent the depletion of the BM stem cell pool, they must be replaced through the development and proliferation of HSCs.

A key criterion which defines an HSC is the ability to replicate symmetrically, through the mitotic process of self-renewal. This results in the generation of progeny that are identical copies of the HSC and allows the BM cellularity to remain in a constant steady state. Multipotency is a further criterion which defines an HSC, with a single cell being able to give rise to a number of differentiated cell types. In order to achieve this, the stem cell also replicates asymmetrically, producing one copy of itself and a second which is able to differentiate (5, 6). It is estimated that one stem cell is capable of producing approximately 10^6 mature blood cells after around twenty cell divisions.

The haemopoietic system is often assessed using a transplantation assay, whereby the transplantation of a single HSC from the BM into a lethally irradiated animal can rescue the entire haemopoietic system (7-9). On the basis of these experiments using murine haemopoietic cells, transplanted HSCs can be further

classified into three distinct populations: long-term HSCs (LT-HSC) which are capable of producing all blood cell types indefinitely and generate progeny that demonstrate similar potentiality on secondary transplant; short-term HSCs (ST-HSC) which reconstitute the myeloid and/or lymphoid compartments for a limited period of time; and multipotent progenitor (MPP) cells which have little or no detectable ability to self-renew (10, 11). These MPP cells then commit either to the lymphoid or myeloid lineage by differentiating to common lymphoid progenitors (CLP) (12) or common myeloid progenitors (CMP) (13), which are able to give rise to cells which are functionally mature (Figure 1-1).

At steady state, only a small proportion of HSCs reconstitute the haemopoietic system, as it is believed that HSCs cycle infrequently, with the majority of cells existing in a quiescent state, or G_0 stage of cell cycle (14, 15). This infrequent proliferation is important for the maintenance of tissue homeostasis and allows time to repair any DNA damage which may arise from life-long HSC self-renewal (16).

The fate of the HSC to self-renew, differentiate or remain quiescent is thought to be controlled by signals from their microenvironment, commonly known as the stem cell niche (17). The BM haemopoietic niche utilises signals from osteoblasts and mesenchymal stromal cells (18), to secrete factors like stromal cell-derived factor-1 (SDF-1) (CXCL12), which activate the CXCR4 receptor expressed on HSCs. This instructs circulating HSCs to home to and engraft in the BM (19) and thereby maintains HSC quiescence and potential for self-renewal (20-22). Loss of this mechanism would typically result in the stem cell leaving the niche to either divide, differentiate or apoptose (23).

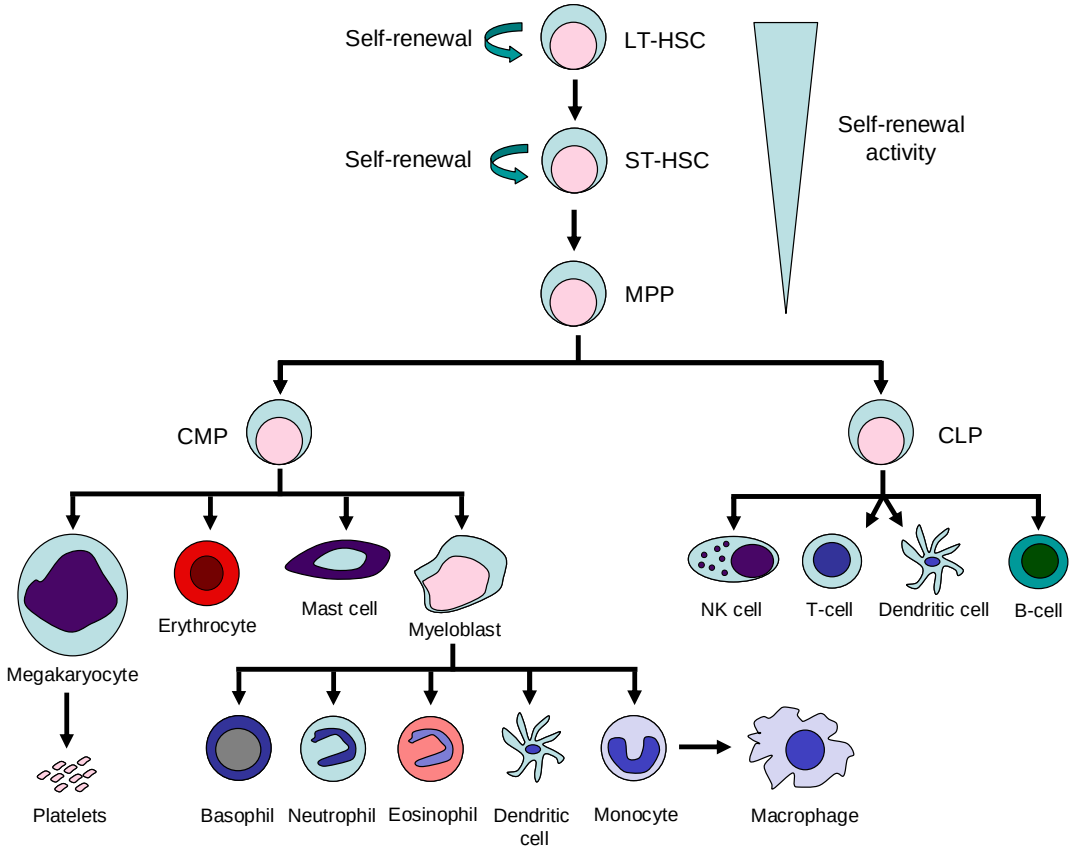

Figure 1-1 The haemopoietic hierarchy model

Only LT-HSC and ST-HSC have the capacity for self-renewal, which is lost once the cell has become an MPP. These give rise to the CLP and CMP, which undergo several proliferation and differentiation steps to give rise to mature, terminally differentiated progeny. [LT- long term, ST - short term, HSC- haemopoietic stem cell, CMP- common myeloid progenitor, CLP- common lymphoid progenitor, MPP- multi-potent progenitor]

The CD34 molecule is a 115-kDa type I transmembrane glycoprotein, which is strongly expressed on human HSCs and shows a progressive decline in expression as these cells undergo differentiation (24). Studies suggest that CD34 may play a role in cell adhesion and signal transduction in HSC and progenitor cells, although despite its importance, its exact function and regulation are still not completely understood (25). Since its discovery, CD34 has become the most widely used marker to obtain enriched populations of human HSCs and progenitors for research or clinical use. However, the total $CD34^+$ population is heterogeneous and it is thought that the frequency of the true HSC population is low (<0.5% in total BM and 1-10% of all $CD34^+$ cells (26)). HSCs do not express a variety of surface markers which are associated with terminal differentiation. The lack of expression of these markers can, therefore, be used to distinguish the most primitive cells from differentiated cells within a total haemopoietic cell population. For example, the type II transmembrane glycoprotein, CD38, which was originally described as a lymphoid cell surface differentiation marker (27), is expressed at intermediate to high levels on >90% of $CD34^+$ cells. These $CD34^+38^+$ cells are able to give rise to a transient repopulation of irradiated mice (28). By contrast, $CD34^+38^-$ haemopoietic cells are capable of continuous, multi-lineage reconstitution following transplant into irradiated mice (29), indicating that true HSC exist only within this rare cell population. Therefore, a population of cells enriched for HSC can be identified by cell surface phenotype - $CD34^+lin^-CD38^-$ (30). Alternative strategies for HSC enrichment include positive selection of cells that express surface markers, such as CD133 (31, 32), in combination with CD34 expression (Table 1-1).

Cell type	Phenotype
HSC	$CD34^+$ Lin^- $CD38^-$ $CD33^-$ $HLA\text{-}DR^{low}$ $c\text{-}Kit^+$ $CD133^+$ $CD90^+$
MPP and lineage-committed progenitors	$CD34^+$ $Lin^{+/-}$ $CD38^+$ $CD33^+$ $HLA\text{-}DR^{high}$
Mature cell	$CD34^-$ Lin^+

Table 1-1 Lineage phenotypes of the human haemopoietic system

Other than cell surface phenotype, primitive haemopoietic cells can be identified and purified based on their ability to efflux certain fluorescent dyes, such as Rhodamine-123 (Rho) and Hoechst 33342 (Hst). The majority of the HSCs in adult human and murine tissues are Rho-/lo (33) and this phenotype is attributed to the activity of the adenosine triphosphate-binding cassette (ABC) transporter, multi-drug resistance-1 (MDR-1), expressed at the HSC surface (34).

In 1996, Goodell et al. identified a new population of HSCs, by staining with Hst and visualising the dual wavelength by flow cytometry. These cells were able to efflux Hst and were designated as side population (SP) cells, because they form a cluster of events to the lower left side of a dual wavelength flow cytometric plot. The ability of SP cells to efflux Hst has been attributed to the high expression of the ABC transporter, breast cancer resistance protein (ABCG2) (35). The SP population was also thought to be enriched for stem or progenitor cells, as they

were subsequently shown to have a primitive phenotype and were capable of reconstituting lethally irradiated recipients (36).

In order to isolate the most quiescent HSCs and distinguish between cells in G_0 and G_1 phases of cell cycle, it is necessary to combine DNA- and RNA-labelling. Pyronin Y (PY) is an RNA-selective dye, which was first used in combination with Hst, by Shapiro in 1981, for two-parameter cell cycle assessment of intact cells (37). Using this technique, quiescent cells in G_0 phase and out of cycle, can be detected as they have diploid DNA content and low RNA content, reflecting a low number of ribosomes. As the cells enter G_1, they accumulate RNA and are able to uptake PY. As the cells progress through cell cycle to the S/G_2 and M phase, they accumulate tetraploid DNA and appear double positive for both Hst and PY.

Primitive haemopoietic cells are also relatively resistant to alkylating agents, such as the active derivatives of cyclophosphamide (38). This resistance is due to the expression of the enzyme aldehyde dehydrogenase (ALDH) on HSCs (39). The highest expression of ALDH has been found on the $CD34^{+}38^{-}$ subset of human BM cells and therefore, fluorescent ALDH-substrates have also been used to identify and isolate HSCs by FACS (40).

1.1.1 The leukaemic stem cell hypothesis

The characterisation of HSCs has allowed parallels to be drawn between their identity and that of cancer cells, with human leukaemias frequently called stem cell diseases (41). Early experiments by the group led by Philip Fialkow, where they used patterns of inactivation in X-linked genes, demonstrated that leukaemias such as chronic myeloid leukaemia (CML) (42) and acute myeloid leukaemia (AML) (43) are clonal disorders with origins in a multipotent stem cell (44). The

concept of a tumourigenic or leukaemic stem cell (LSC) was further explored in studies where only a small fraction of leukaemic cells was capable of extensive proliferation *in vitro* and *in vivo*. Park and colleagues demonstrated that only 1 in 10000 to 1 in 100 murine myeloma cells were capable of forming colonies *in vitro* in clonal colony-forming assays (45). Furthermore, only 1-4% of the total number of leukaemic cells was able to form colonies within the spleen when transplanted *in vivo* (46).

In 1997, adaptation of the existing quantitative assays for normal HSC repopulation *in vivo*, allowed the first direct evidence for the LSC hypothesis to be demonstrated in AML (47, 48). Bonnet and Dick demonstrated that only a small proportion of leukaemic blasts, which were referred to as 'SCID leukaemia-initiating cells' (SL-IC) and possessed the immature phenotype, $CD34^{+}38^{-}$, were capable of causing human AML in non-obese diabetic/severe combined immunodeficient (NOD/SCID) mice. Additionally, these primitive cells were found to possess a high self-renewal capacity in serial transplantation experiments. Based on these findings, the authors proposed that AML forms a stem cell hierarchy that is similar to normal haemopoiesis. This concept suggests that many tumours may be maintained by a small population of LSCs which are capable of life-long self-renewal, differentiation and proliferation.

Due to the phenotypic and functional similarities between the HSC and LSC, the authors also propose that the initial transforming events occur within a stem cell rather than a committed progenitor cell. HSCs already have the self-renewal pathways activated, therefore may require fewer mutations to maintain self-renewal properties than more differentiated cells. Indeed, other studies support this model, whereby the transduction of the potent oncogene *BCR-ABL*, did not

confer similar self-renewal properties to committed progenitor cell populations (49). However, the idea that an LSC must arise from a normal stem cell is not universally accepted, with the alternative view suggesting that the LSC could be a more restricted or differentiated mature cell, which has transformed and reacquired the stem cell capability of self-renewal. Evidence for this was first demonstrated in murine models of leukaemia (50). Populations of murine progenitor cells, which lacked the capacity for self-renewal, were retrovirally transduced with either the *MLL-ENL* or *MOZ-TIF2* human leukaemia oncogenes. This led to the reacquisition of self-renewal properties in these progenitor populations, as they were able to form colonies in serial methylcellulose-plating experiments *in vitro*. Similarly the transduced cells were also able to induce AML when transplanted into irradiated mice, which could then be transferred to secondary recipients. Furthermore, expression of the MLL-AF9 oncoprotein has also since been shown to initiate AML in isolated granulocyte-macrophage progenitor cells (51). More recently, Bonnet has herself demonstrated transplantation capacity for $CD34^{+}38^{+}$ AML cells in at least a proportion of AML samples (52), thus expanding the LSC compartment and beginning to separate LSC from HSC phenotypes (Figure 1-2).

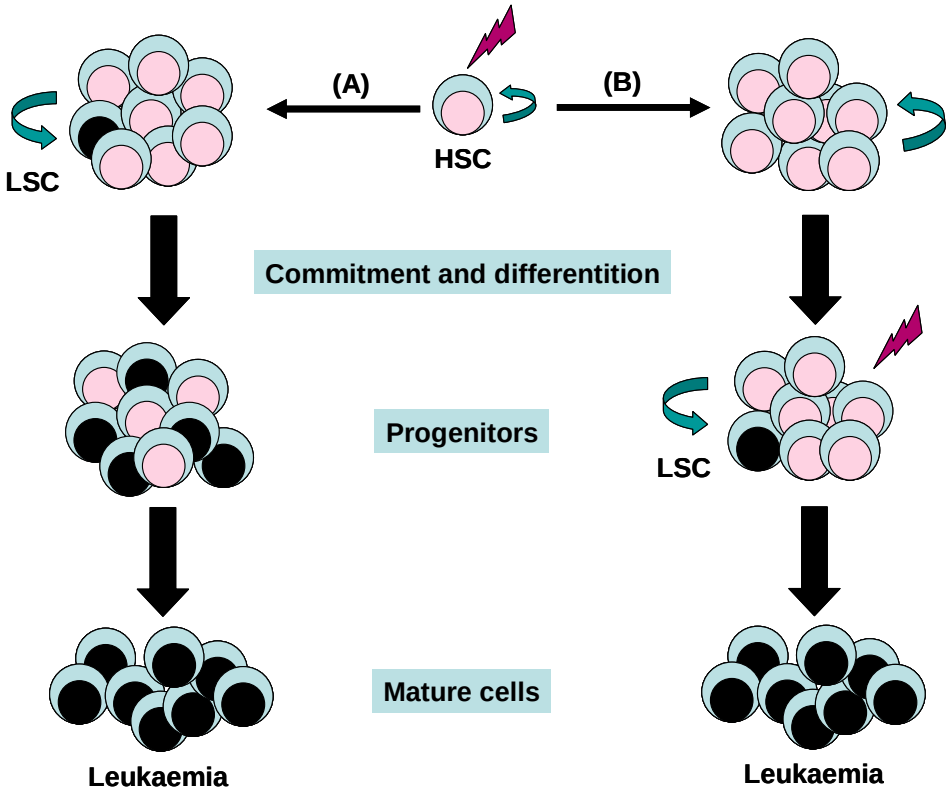

Figure 1-2 Schematic models of leukaemic initiation and progression

(A) The initial transforming mutation disrupts the normal development of an HSC and gives rise to a self-renewing LSC, which is present in the stem cell compartment. (B) Conversely, the transforming mutation may occur in the downstream progeny. These cells have then reacquired the stem cell capability of self-renewal, to generate the LSCs.

1.2 CML

Compelling evidence suggests that CML is one such malignancy which is driven by LSCs. CML is a clonal myeloproliferative disorder of primitive haemopoietic progenitor cells, which accounts for 15% of all adult leukaemias and has an incidence of 1-2 cases per 100,000 population (53). It is defined by the Philadelphia chromosome (Ph), which results from the reciprocal translocation between the 3' end of the c-ABL (Abelson) gene from chromosome 9 and the 3' end of the BCR (Breakpoint Cluster Region) gene on chromosome 22 (t(9;22)(q34;q11)) (54). The novel fusion oncogene generated on chromosome 22 as a result of this translocation is called BCR-ABL (breakpoint cluster region-abelson) (55, 56) (Figure 1-3). In the majority of CML patients, this oncogene transcribes a 210-kDa constitutively active non-receptor tyrosine kinase (TK), often referred to as $p210^{BCR\text{-}ABL}$, which is necessary for the transformation of the disease (57).

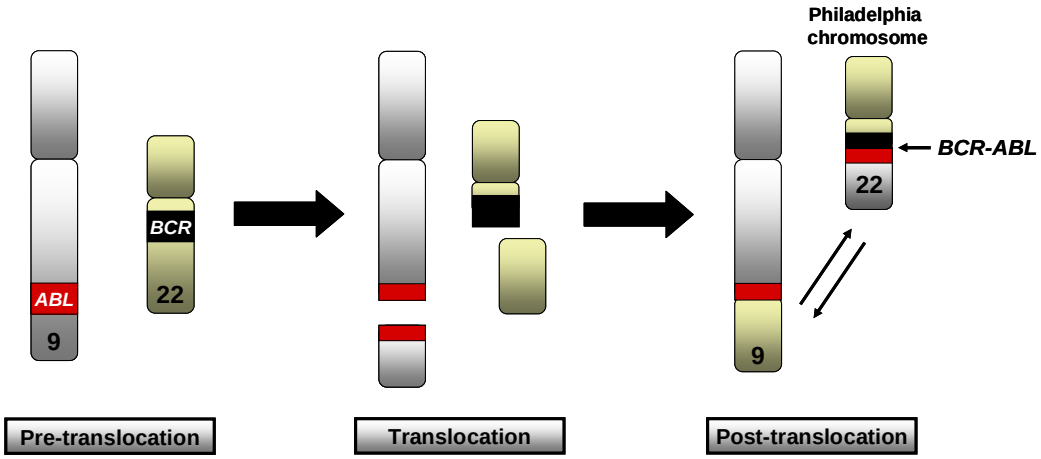

Figure 1-3 The Ph chromosome

The reciprocal translocation between chromosomes 9 and 22 results in the formation of the Ph chromosome. This is the shortened chromosome 22 and results in the production of the fusion gene product BCR-ABL.

CML is a clinically triphasic disorder, where the majority of patients present in chronic phase (CP), a stage which is characterised by an abnormal blood count, increased megakaryocytes in BM and splenomegaly (58). Diagnosis is confirmed by the detection of the Ph chromosome by BM cytogenetics and by measurement of *BCR-ABL* transcripts, in peripheral blood or BM, by highly sensitive quantitative reverse transcriptase-polymerase chain reaction (qRT-PCR) (59). If left untreated, the initial CP lasts for approximately 3-6 years, before progressing to accelerated phase (AP). As the disease develops, additional cytogenetic abnormalities arise and eventually terminate in blast crisis (BC). This is a period of overproduction of immature leukaemic blast cells within the BM compartment, where prognosis is generally poor (58). The most widely used criteria for AP and BC CML diagnosis are defined by the World Health Organisation (WHO) and are outlined below (60):

AP CML Diagnosis if one or more of the following is present:

- Blasts 10 to 19% of peripheral blood white cells or BM cells
- Peripheral blood basophils at least 20%
- Persistent thrombocytopenia (100 x 10^9/L) unrelated to therapy, or persistent thrombocytosis (1000 x 10^9/L) unresponsive to therapy
- Increasing spleen size and increasing WC count unresponsive to therapy
- Cytogenetic evidence of clonal evolution

BC CML Diagnosis if one or more of the following is present:

- Blasts 20% or more of peripheral blood white cells or BM cells
- Extramedullary blast proliferation
- Large foci or clusters of blasts in BM biopsy

Table 1-2 Criteria for diagnosis of AP and BC CML

1.2.1 BCR-ABL structure and function

The mammalian c-ABL gene is ubiquitously expressed and encodes a non-receptor TK, with two 145-kDa isoforms arising from alternative splicing of the first exon (61). The amino-terminus of human c-ABL protein contains three SRC homology domains (SH1-SH3) that mediate TK (SH1), phospho-tyrosine protein-binding (SH2) and kinase inhibitory (SH3) functions. The centre of the protein contains proline-rich sequences which can in turn interact with the SH3 domains of other adaptor-proteins, such as Crk. The carboxyl-terminus of c-ABL encodes a lysine-rich motif required for nuclear localisation, a DNA-binding domain and actin-binding domains. In c-ABL, the structural motifs which are thought to be necessary for cellular transformation are the SH1, SH2 and actin-binding domains (62-64). The c-ABL proto-oncoprotein is commonly distributed in both the nucleus where it is bound to chromatin and in the cytoplasm where it is bound to F-actin (65). Normal c-ABL protein is predominantly nuclear and appears to be involved in the regulation of cell cycle, suppression of cell growth, regulation of gene transcription and integrin signalling. In contrast, transforming c-ABL proteins are often localised in the cytoplasm, implying that the cytoplasmic fraction of c-ABL may normally be involved in the signalling cascades that induce mitogenesis (65).

Like c-ABL, the 160-kDa BCR protein is ubiquitously expressed and localised within the cytoplasm, although its exact function is not clearly defined. The amino-terminus of BCR contains a serine/threonine kinase domain, including at least three SH2 binding sites which can bind with substrates such as, BRCA1 (breast cancer 1)-associated protein (Bap)-1, a member of the 14-3-3 family of proteins (66). A coiled-coil (C-C) domain (amino acids 1-63) at the amino-terminus of BCR-ABL allows dimer formation *in vivo*. The C-C structural motif, along with the tyrosine 177 (Y177) phosphorylation site, which is necessary for the binding of

growth-receptor-binding-2 (Grb-2) and subsequent activation of the Ras pathway, are thought to be necessary for the transforming function of BCR-ABL (67-69).

The most important structural domains of BCR and c-ABL proteins are demonstrated in Figure 1-4.

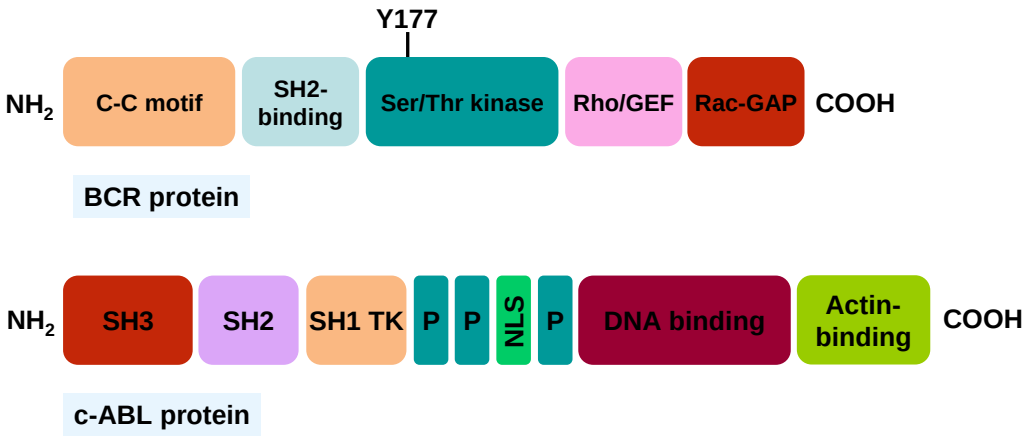

Figure 1-4 The important structural motifs of BCR and c-ABL proteins

In BCR, the coiled-coil (C-C) (also known as the oligomerisation domain) resides at the amino (NH2) terminus. This is followed by a domain which is thought to facilitate binding to SRC-homology 2 (SH2)-domain-containing proteins. BCR also contains a serine/threonine (Ser/Thr) kinase domain, a tyrosine at position 177 (Y177), a Rho guanine-nucleotide-exchange factor (Rho-GEF) domain and a Rac GTPase activating protein (Rac-GAP) homology domain. In ABL, there are SH3, SH2 and SH1 tyrosine kinase (TK) domains at the amino terminus, several proline-rich domains (P) and a nuclear localisation signal (NLS). At the carboxy terminus (COOH) there are DNA- and actin-binding domains.

Three predominant products are formed depending on which breakpoint located within the BCR gene is fused with exon a2 of ABL. These different forms of BCR-ABL are associated with three distinct forms of leukaemia. In the majority of CML cases, the breakpoint occurs within the major BCR (M-BCR), which spans exons b1-4. This results in the formation of fusion transcripts with b2a2 or b3a2 junctions, which encode the $p210^{BCR-ABL}$ oncoprotein. A second breakpoint is located upstream of M-BCR - minor BCR (m-BCR) - and encodes a 190-kDa protein, referred to as $p190^{BCR-ABL}$. This commonly occurs in Ph^{+} acute B lymphoblastic leukaemia (ALL) (70), occasionally in AML (71) and in rare cases of CML (72). Lastly, a third downstream BCR (μ-BCR) encodes a 230-kDa protein ($p230^{BCR-ABL}$), which is found in chronic neutrophilic leukaemia and some cases of CML (73).

The first evidence that BCR-ABL was responsible for the malignant transformation of HSCs in CML was provided by Daley et al., who demonstrated that mice transplanted with BM transduced with $p210^{BCR-ABL}$, developed many features of CML (74). The importance of BCR-ABL was further demonstrated in transgenic mice in which the tetracycline-responsive element (tet-O) was used to induce BCR-ABL1 expression in HSCs. The BCR-ABL1-tet-O mice then developed a CML-like disease upon the withdrawal of tetracycline treatment (75).

It is suggested that BCR-ABL gives rise to this malignant transformation through a number of mechanisms, namely, alteration of the BM microenvironment, anti-apoptotic defences, constitutive activation of proliferation and survival pathways and growth factor (GF) independence.

1.2.2 BCR-ABL and alteration of the BM microenvironment

In normal haemopoiesis, progenitor cell proliferation is negatively regulated by the microenvironment through adhesion of integrin receptors, such as the β1-integrin receptors, to BM stromal cells (76). The increased proliferation and abnormal circulation of primitive CML cells may, in part, be explained by perturbed adhesion between the BM microenvironment and the CML progenitors (77, 78). CML progenitors express a variant of the β1-integrin receptor that is not present on normal cells and evade this regulation through impaired adhesion. Following receptor-binding, integrins are capable of initiating normal signal transduction; therefore, it is possible that in CML cells, the signalling that usually inhibits proliferation is impaired. BCR-ABL may have a further impact on this altered signalling, as proteins that are also involved in signal transduction through β1-integrins, such as paxillin, and phosphatidylinositol 3-kinase (PI3K) (79), are constitutively activated by BCR-ABL in cell lines transduced with the oncogene. Bhatia et al., have demonstrated that treatment with interferon alpha (IFNα), a therapeutic agent in CML, can restore β1-integrin mediated adhesion of CML progenitors to BM stroma and restore this anti-proliferative mechanism (80).

SDF-1α-CXCR4 signalling positively regulates the homing of HSC to the BM (81). In primary blast CML cells, BCR-ABL has been shown to down-regulate CXCR4 expression resulting in attenuated adhesion and migratory responses to SDF-1α, increasing the ability of these immature cells to escape from the marrow (82). Inhibition of BCR-ABL kinase activity, has been demonstrated to restore CXCR4 expression in CML cells co-cultured with mesenchymal stem cells. This resulted in the migration of CML cells to the BM niche and an acquisition of stroma-mediated resistance of CML progenitor cells (21). These results suggest that the SDF-1α-

CXCR4 interaction contributes to the resistance of CML cells against agents which inhibit BCR-ABL activity in the BM microenvironment.

1.2.3 BCR-ABL and anti-apoptosis

CML stem cells demonstrate elevated and continuous growth and expansion as compared to their normal counterparts, but do not exhibit greater proliferation potential (83). This indicates that the increased TK activity of BCR-ABL within CML progenitors may act to suppress the normal programmed cell death process, apoptosis. The “protection from apoptosis” hypothesis has been confirmed in transformed haemopoietic cell lines, whereby transfection with BCR-ABL upregulated the anti-apoptotic survival proteins, B-cell lymphoma (Bcl)-2 (84), myeloid cell leukaemia (mcl)-1 (85) and Bcl-XL (86).

1.2.4 BCR-ABL and constitutive activation of proliferation and survival pathways

A consequence of BCR-ABL is an increase in cellular proliferation. At first the “discordant maturation hypothesis” was proposed, where it was assumed that the most mature proliferating cells in CP CML caused the expansion of Ph^+ cells. However, this was refuted by other investigations demonstrating that the myeloid expansion is a result of increased numbers of primitive CML progenitor cells (87).

BCR-ABL is localised exclusively to the cytoplasm and is able to constitutively tyrosine phosphorylate a host of substrates. Importantly, due to autophosphorylation, there is increased phospho-tyrosine (p-Tyr) on the BCR-ABL oncoprotein itself. This then, generates many binding sites for the SH2 domains of other proteins. A number of target substrates of BCR-ABL have been reported as shown in Table 1-3. Substrates of BCR-ABL can be grouped into three broad

categories, depending on function: (1) adaptor molecules such as CrkL and p62^{Dok}; (2) cell membrane and cytoskeleton related proteins such as talin and paxillin and (3) proteins with catalytic function such as Ras-GAP and phospholipase Cγ (PLCγ) (88). Tyrosine phosphorylation of these BCR-ABL substrates results in the constitutive activation of multiple cytoplasmic and nuclear signalling cascades, which are shared with cytokines known to regulate the proliferation, differentiation and survival of haemopoietic cells (Figure 1-5).

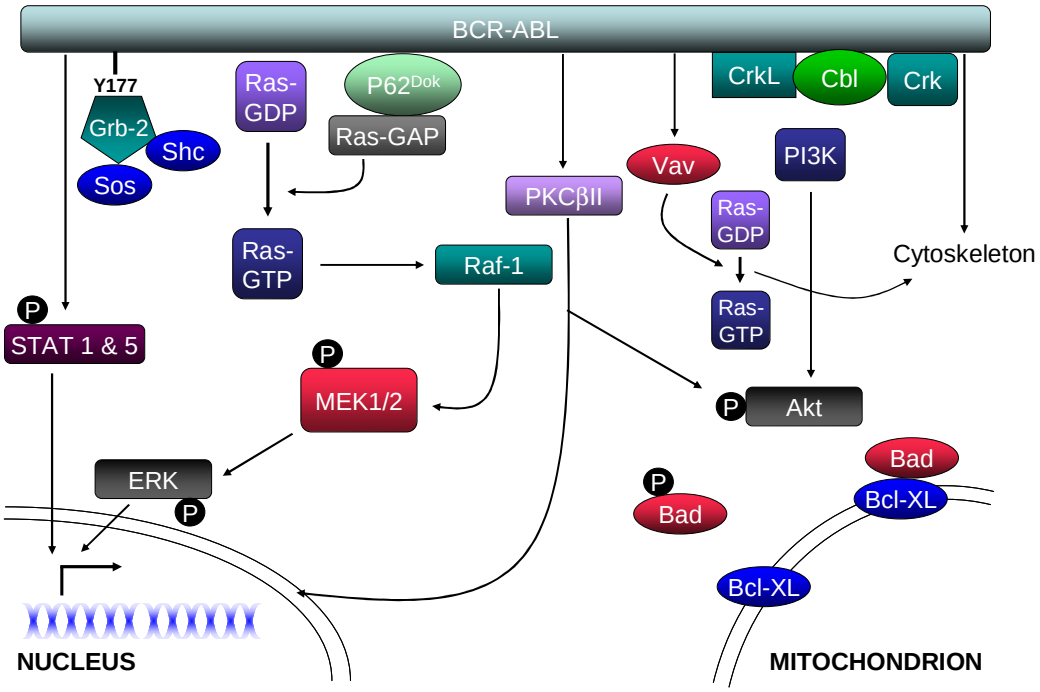

Figure 1-5 BCR-ABL associated signalling cascades that contribute to cellular proliferation, differentiation and survival

Substrate	Function	References
Grb-2	Adapter molecule	(69)
P62^{Dok}	Adapter molecule	(89)
CrkL	Adapter molecule	(90)
Crk	Adapter molecule	(91)
Ras-GAP	Ras-GTPase activation	(92)
Ras	Signalling switch; cellular oncogene	(93)
Raf-1	Serine/threonine kinase	(94)
Cbl	E3 ligase for ubiquitination	(95)
PI3 kinase (p85 subunit)	Serine kinase	(96)
STAT1 and 5	Transcriptional activators	(97, 98)
Paxillin	Cytoskeleton	(99)
Fak	Cytoskeleton	(100)
Talin	Cytoskeleton	(101)
PLCγ	Phospholipase	(102)
Bap-1	14-3-3 adaptor protein	(66)
Vav	Guanine-nucleotide-exchange factor	(103)

Table 1-3 Examples of BCR-ABL PTK substrates

[Grb- growth-receptor-binding protein; Dok- docking protein; CrkL- Crk-like; GAP- GTPase-activating protein; PI3K- phosphatidylositol 3-kinase; STAT- signal transducer and activator of transcription; Fak- focal adhesion kinase; PLC- phospholipase C; Bap- BRCA1 (breast cancer 1)-associated protein.] Table adapted from Smith et al. 2003 (88).

1.2.4.1 BCR-ABL and the Ras-Raf-MEK-ERK pathway

Ras is a small guanine-nucleotide-binding protein (G-protein) that is active when bound to GTP, or inactive when GDP-bound. Ras is activated when GEFs catalyse the exchange of Ras-bound GDP for GTP. In contrast, GAPs inactivate Ras by catalysing its intrinsic GTPase activity.

In normal cells, activation of Ras by haemopoietic GFs, such as IL-3, leads to the recruitment of the serine/threonine Raf-1 kinase to the cell membrane. Activated Raf-1 can then phosphorylate mitogen-activated protein kinase (MAPK) kinase (MEK) on both serine and threonine residues. MEK is then able to phosphorylate and activate extracellular signal-regulated kinase; ERK, which can, in turn, phosphorylate transcription factors, such as c-Jun and c-Fos and thereby direct gene regulation (93).

It has also been demonstrated that elevated Ras activation occurs in CML cells (104). Autophosphorylation of Y177 on BCR-ABL provides a docking site for the adapter molecule Grb-2 (69). Activated Grb-2 can then bind the positive regulator, Son of sevenless (SOS; a GEF) and then stabilise Ras in the active form. Grb-2 mutants that lack SH3 domains block the activation of Ras and suppress the transforming capability of BCR-ABL (105). Two other BCR-ABL adaptor molecules, Shc and CrkL, can also activate Ras (90, 106). The importance of Ras in CML cell growth was demonstrated in cell line models in which the introduction of a dominant-negative Ras into BCR-ABL-transfected cells inhibited malignant transformation (107). Further investigations have shown that, in BCR-ABL-transformed haemopoietic cells, the constitutive activation of Ras is likely to lead to the activation of an anti-apoptotic pathway (108, 109). These data highlight an

important role for the Ras-Raf-MEK-ERK pathway in the pathogenesis of BCR-ABL$^+$ leukaemias.

1.2.4.2 BCR-ABL and the JAK-STAT pathway

The JAK-STAT pathway is activated by cytokines, such as IL-3, IFNα and granulocyte macrophage-colony stimulating factor (GM-CSF). Janus family of activated kinases (JAK1, JAK2, JAK3, Tyk2) are cytoplasmic protein TKs (PTKs) that mediate signalling downstream of cytokine receptors. Activated JAKs phosphorylate a family of downstream transcription factors called the STAT family members. STAT proteins then translocate to the nucleus and activate the transcription of specific genes necessary for the growth, survival and differentiation of haemopoietic cells. The JAK-STAT pathway is tightly regulated by the suppressors of cytokine signalling (SOCS) and cytokine-induced SH2-containing (CIS) family of proteins (110).

The constitutive activation of STATs is observed in BCR-ABL expressing cell lines and primary CML cells (111, 112) and the activation of STAT5 appears to contribute to malignant transformation (113). The effect of STAT5 activation in BCR-ABL$^+$ cells appears to be predominantly anti-apoptotic, as the activation of STAT5 in CML cells contributes to upregulated expression of the anti-apoptotic family members, mcl-1 and Bcl-XL (114, 115). Although BCR-ABL is known to activate JAKs, there may also be a distinct BCR-ABL-mediated pathway for the phosphorylation of STAT5, as the introduction of dominant-negative JAK mutants in BCR-ABL transformed cells did not abrogate STAT5 phosphorylation (112).

1.2.4.3 BCR-ABL and the PI3K pathway

PI3K is a heterodimer consisting of an 85-kDa (p85) regulatory subunit containing one SH3 domain and two SH2 domains and a 110-kDa (p110) catalytic subunit (116). PI3K is found in cellular complexes with ligand-activated GF and oncogene PTKs (117). These interactions are mediated by the SH2 and SH3 domains of p85 (118). The PI3K signalling pathway plays an important role in many biological processes, such as survival, proliferation, differentiation, mobility and metabolism in a number of cell types (119, 120).

PI3K can bind to activated haemopoietic GF receptors via its SH2 and SH3 domains and is recruited to the cell membrane following haemopoietic GF stimulation. Activated PI3K can produce PI-(4,5)-bisphosphate (PIP_2) which may be converted to PI-(3,4,5)-triphosphate (PIP_3), an important second messenger (121). PIP_3 and other PI3K lipid products on the inner cell membrane generate binding sites for other proteins that contain pleckstrin homology domains. PI3K signalling is negatively regulated by phosphatases, such as, phosphatase and tensin homologue deleted on chromosome 10 (PTEN) which removes the 3-phosphate from PIP_3 (122). SH2-containing inositol-5-phosphatase (SHIP) - removes the 5-phosphate from PIP_3 to generate PIP_2, a second messenger which may have different signalling functions (Figure 1-6).

$$\text{PI-(4,5)-P}_2 \underset{\text{PTEN}}{\overset{\text{PI3K (class I)}}{\rightleftharpoons}} \text{PI-(3,4,5)-P}_3 \xrightarrow{\text{SHIP}} \text{PI-(3,4)-P}_2$$

Figure 1-6 Diagram of PI3K inositol lipid second messenger synthesis and degradation

PI3K signalling is deregulated in a large number of cancers and has also thought to contribute to cellular transformation by BCR-ABL. Skorski et al. demonstrated

that PI3K activity was regulated by BCR-ABL and required for the growth of CML cells, using antisense oligonucleotides against PI3K expression (84). Furthermore, a specific inhibitor of the p110 subunit of PI3K, wortmannin, was shown to inhibit the proliferation of BCR-ABL$^+$ cells, but not normal haemopoietic cells (96). These findings are corroborated by the fact that BCR-ABL-transformed cells have increased PI3K class 1A activity and an accumulation of PIP_3 (79).

A YXXM motif is contained within the ABL sequence of BCR-ABL, which when phosphorylated corresponds to the optimal binding sequence for the SH2 domains of the p85 regulatory subunit of PI3K (123). However, the BCR-ABL-PI3K interaction does not appear to be direct as mutation of the YXXM motif does not attenuate PI3K activity. This finding indicates that PI3K activation occurs through associations with other tyrosine-phosphorylated proteins that are recruited to BCR-ABL (123).

1.2.4.3.1 The adapter protein Gab2

The majority of evidence indicates that the main pathway for PI3K activation in BCR-ABL$^+$ cells occurs via the Y177 autophosphorylation site on the BCR portion of the fusion protein. The Y177 site is important for Grb2 binding via its SH2 and generates a docking site for Gab2 through its SH3 domain (124). BCR-ABL can then phosphorylate Gab2 on tyrosines within its YXXM motif which, in turn, act as binding sites for the SH2 domains of PI3K regulatory subunits. Mutations within the Y177 site resulted in decreased transformation by BCR-ABL. Similarly, loss of Gab2 inhibited myeloid transformation both *in vitro* and *in vivo* (124).

1.2.4.3.2 The adapter protein CrkL

A further possible Gab2-independent mechanism of PI3K activation involves the 39-kDa protein CrkL. CrkL was originally identified by ten Hoeve et al. (125) and is one of the most prominent tyrosine-phosphorylated proteins detected in BCR-ABL-transformed cells (90). CrkL belongs to the Crk family of adapter proteins which includes v-Crk and c-Crk. It is ubiquitously expressed and contains one SH2 domain, an SH2' domain (has no known function) and two SH3 domains (126). It is thought to be involved in the regulation of cellular motility and integrin-mediated cell adhesion by association with other focal adhesion proteins such as paxillin (99). In CML, CrkL interacts and is phosphorylated on tyrosine 207 (127) directly by the BCR-ABL oncoprotein (90, 125, 128). Tyrosine phosphorylated CrkL then binds to c-CBL with its SH2 domain and forms a multimeric complex with PI3K, c-ABL and BCR-ABL through its SH3 domain (95, 129). The exact function of CrkL tyrosine phosphorylation in leukaemic cell signalling remains to be determined, however, it seems likely that CrkL binding to other tyrosine phosphorylated proteins, such as PI3K, leads to the activation of pathways that could contribute to leukaemic transformation. Due to the specificity of BCR-ABL signalling to CrkL activation and also the inherent instability of the BCR-ABL oncoprotein, detection of the activated form of CrkL (p-CrkL) has become a standard indirect method to assess BCR-ABL status, as illustrated by our own laboratory (130, 131) and others (132, 133).

1.2.4.3.3 Akt - a major downstream signalling effector of PI3K

Akt is a serine/threonine kinase (also known as protein kinase B) which is activated by PI3K and is the effector most closely associated with cellular transformation. Activated Akt has a number of different substrates which regulate

proliferation, metabolism and survival, as illustrated in Figure 1-7 and described below.

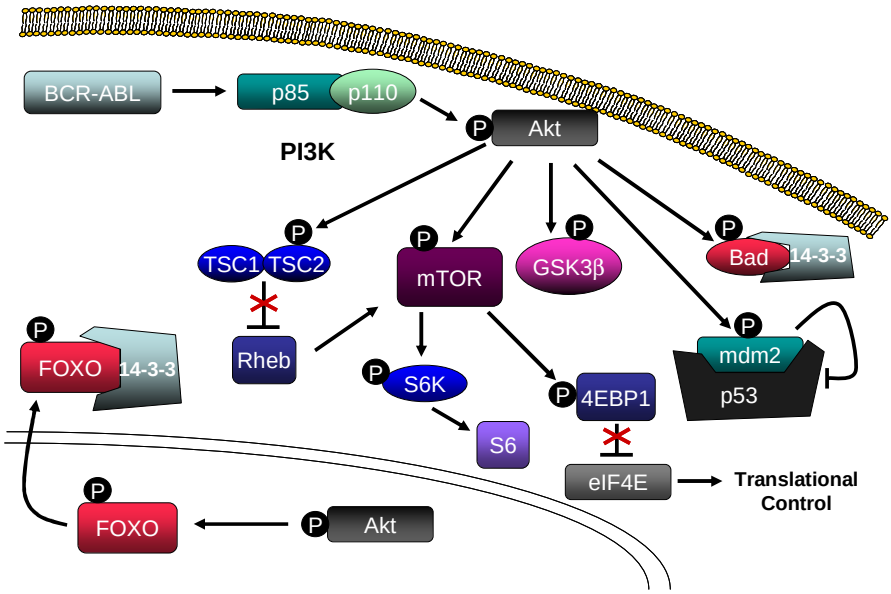

Figure 1-7 Downstream substrates of PI3K/Akt phosphorylation

Signalling via GF stimulation of cognate receptors or by BCR-ABL, results in the activation of PI3K and the subsequent recruitment of Akt. Activated Akt then phosphorylates many substrates to promote cell growth, proliferation and survival. See text for details. [TSC- tuberous sclerosis, mTOR- mammalian target of rapamycin, GSK3β- Glycogen synthase kinase 3β, FOXO- forkhead box, subgroup O, Bad- Bcl-2-associated death promoter, mdm2- murine double minute 2, 4EBP1-eukaryotic translation initiation factor 4E, eIF4E-eukaryotic initiation factor 4E]

1.2.4.3.3.1 Forkhead Box, Subgroup O

The forkhead box, subgroup O (FoxO) family of transcription factors are a sub-class of the Fox forkhead transcription factors that have a variety of roles in the regulation of proliferation, cellular metabolism and survival (134). The mammalian members of the FoxO transcription factors include FoxO1, FoxO3a, FoxO4 and FoxO6 and contain three evolutionarily conserved Akt phosphorylation sites within each of the FoxO proteins. Following GF stimulation, Akt phosphorylates FoxO transcription factors within the nucleus. This allows for the binding of the 14-3-3 chaperone protein (135, 136), resulting in the efficient export and re-localisation of FoxO transcription factors to the cytoplasm. Cytoplasmic sequestration prevents the FoxO-dependent transcription of genes that may antagonise cell survival, such as Bim and Trail (137, 138) and also promote cell cycle arrest, such as the downregulation of cyclins D1 and D2 (139). Recent investigations have demonstrated the importance of FoxO function in haematological malignancies. BCR-ABL transformation was shown to inhibit FoxO3a, via the constitutive activation of PI3K/Akt signalling and the subsequent cytoplasmic sequestration of Foxo3a (140). The expression of a constitutively active FoxO3a triple mutant in BCR-ABL^{+} cells resulted in the induction of apoptosis (140, 141). Furthermore, FoxO3a inhibition by BCR-ABL was also shown to affect the expression of the cell cycle regulatory gene, cyclin D2 (142). These data indicate that the inhibition of FoxO3a by BCR-ABL may represent a potentially important mechanism in CML tumourogenesis.

1.2.4.3.3.2 Bcl-2-associated death promoter

The Bcl-2-associated death promoter (Bad) protein is a pro-apoptotic member of the Bcl-2 gene family which is involved in initiating apoptosis. Non-phosphorylated

Bad exerts pro-apoptotic effects through binding to, and preventing the function of anti-apoptotic proteins such as Bcl-2 and Bcl-XL (143). Conversely, Bad phosphorylation by Akt (triggered by PIP_3) causes the formation of the Bad-(14-3-3) protein homodimer. This results in the sequestration of Bad in the cytoplasm and leaves Bcl-2 free to inhibit Bax-triggered apoptosis (144). *In vitro* studies have demonstrated that BCR-ABL can promote the phosphorylation and inactivation of Bad. However, within the same study, it was also noted that BCR-ABL-mediated phosphorylation of Bad was not essential for BCR-ABL-induced cell survival, as the cells continued to survive in the absence of Bad phosphorylation (145). This thereby suggests that the transforming ability of BCR-ABL is not due to one pathway, it is rather the activation of complex network of signalling cascades.

1.2.4.3.3.3 Murine double minute 2

Murine double minute 2 (Mdm2) is an E3 ubiquitin ligase which, when phosphorylated by Akt, acts as an important negative regulator of the tumour suppressor, p53 (146). Studies suggest that BCR-ABL may promote cell survival by p53 downregulation via increased expression of Mdm2 (147).

1.2.4.3.3.4 Glycogen synthase kinase 3β

Glycogen synthase kinase 3β (GSK3β) is a serine/threonine kinase that is a downstream target of Akt and becomes inactivated following phosphorylation (148). Two downstream targets of GSK3β, include cyclin D1 and β-catenin. Activated GSK3β phosphorylates these proteins and targets them from proteasome-mediated degradation (149). Recent studies have demonstrated that HSCs which were deficient in β-catenin, demonstrated a reduction in long-term

self-renewal as measured by serial transplantation assays. Furthermore, BCR-ABL-transduced cells deficient in β-catenin, failed to develop CML (150). These data highlight an important role for β-catenin in the maintenance of both normal and CML stem cells. However, a direct functional role for the inactivation of GSK3β downstream of PI3K/Akt in BCR-ABL transformed cells has yet to be determined.

1.2.4.3.3.5 Tuberous Sclerosis-2 and the Mammalian Target of Rapamycin pathway

The serine/threonine kinase, mammalian target of rapamycin (mTOR) functions as both a nutrient sensor and an important downstream substrate of PI3K/Akt signalling, following GF or oncoprotein stimulation (151). The activation of mTOR results in the regulation of processes, such as cell growth, cell-cycle progression, protein synthesis and autophagy (152, 153).

mTOR can form at least two multi-protein complexes, mTORC1 and mTORC2 (152). mTORC1 is a heterotrimeric protein kinase that consists of the mTOR catalytic subunit and two associated proteins - regulatory-associated protein of mTOR (raptor) and mLST8. mTORC1 has been demonstrated to be involved in cellular proliferation, autophagy and translation in response to nutrients. mTORC2 also contains mTOR and mLST8 but, instead of raptor, it contains two other proteins - rapamycin-insensitive companion of mTOR (rictor) and mSin1. mTORC2 is less well understood than the first mTOR-containing complex, however studies suggest that it is involved in the PI3K/Akt pathway as it directly phosphorylates Akt (154).

The mTOR pathway has proven to be an attractive target for the drug treatment of several malignancies which display excessive PI3K/Akt signalling, including breast and ovarian cancers (155). Furthermore, rapamycin was observed to enhance the anti-leukaemic effects of IM on both IM-sensitive and -resistant CML cells both *in vitro* and *in vivo* (156, 157).

The exact mechanism by which BCR-ABL activates mTOR in CML cells has yet to be defined but appears to be PI3K/Akt-dependent (156). PI3K/Akt-signalling regulates mTOR indirectly through activation of tuberous sclerosis complex 2 (TSC2). TSC2 forms a heterodimer with TSC1 which acts as a brake on mTOR-dependent signalling in the absence of GF/oncogene signals. When TSC2 is phosphorylated by activated Akt, the TSC1/TSC2 complex becomes inactive and its ability to inhibit the small G-protein Rheb is blocked. Rheb is then able to activate mTOR once released from this inhibition (158) (see Figure 1-7).

The mTOR pathway controls cell growth through regulators of translation, such as, eukaryotic translation initiation factor 4E (4EBP1) and the p70 ribosomal protein S6 kinases 1 and 2 (S6K1 and S6K2) (159). Phosphorylation of 4EBP1 by mTOR blocks its ability to inhibit eukaryotic initiation factor 4E (eIF4E). The eIF4E protein is then released and is free to bind the 5'-cap structure of mRNAs to allow an increase in cap-dependent translation (159). The S6K activation of the S6 protein of 40S ribosomes promotes cell growth and proliferation by an unknown mechanism (160).

1.2.4.3.3.5.1 mTOR and autophagy

As described previously, mTOR mediates the control of cellular growth. mTOR is active under favorable growth conditions, and promotes the initiation of translation and nutrient import. However, during conditions of nutrient starvation, rapamycin treatment or mTOR depletion there is a dramatic downregulation of general protein synthesis and an activation of a process known as autophagy.

The term autophagy is derived from the Greek, “auto” - oneself and “phagy” - to eat; and refers to a cellular catabolic degradation process. During autophagy, a cell’s own long-lived proteins and organelles are degraded through a lysosome-dependent pathway and recycled to sustain metabolism (161). Autophagy occurs at low basal levels in virtually all cells and has an important homeostatic function, to maintain organelle and protein turnover. It has a critical role during early mammalian development as mice lacking essential autophagy genes die within hours after birth. This is possibly due to their inability to adapt to the neonatal starvation period (162). Autophagy is also thought to have a critical role in response to conditions of cellular stress, such as nutrient deprivation, hypoxia and pathogen infection (163).

Macroautophagy (herein referred to as autophagy) involves the delivery of cellular material sequestered inside double membrane vesicles to the lysosome in eukaryotic cells. In conditions of starvation or GF deprivation, a drop in intracellular nutients allows “protective” autophagy to occur. Initially, an isolation membrane (also called a phagophore) is formed (vesicle nucleation) and expanded (vesicle elongation). This structure sequesters the cytoplasmic material to be degraded, which may include mitochondria, endoplasmic reticulum, and ribosomes (Figure 1-8). The edges of the phagophore then fuse to form a double-

membrane structure, known as the autophagosome. This is followed by a fusion of the outer membrane of the autophagosome with the lysosome, where the sequestered material, together with the inner membrane is degraded. Degradation of the sequestered material generates nucleotides, amino acids, and free fatty acids that may be recycled by the cell for protein synthesis and adenosine triphosphate (ATP) generation, thereby promoting cell survival (161).

One of the main regulators of autophagy is mTOR, which is the key inhibitory signal that turns off autophagy in the presence of GFs or an abundance of nutrients. The binding of GFs to cell surface receptors activates class I PI3K/Akt signalling, leading to activation of mTOR. This results in the negative regulation of autophagosome formation and prevents the autophagy process from occuring (164). Autophagy may also be pharmacologically inhibited by targeting the fusion of autophagosomes with lysosomes, using inhibitors of the lysosomal H^+ATPase proton pump, such as, bafilomycin A_1 (BAF) or lysosomotropic alkalines, such as chloroquine (CQ) or 3-hydroxychloroquine (HCQ). Conversely, autophagy can be pharmacologically induced by targeting mTOR with rapamycin (163).

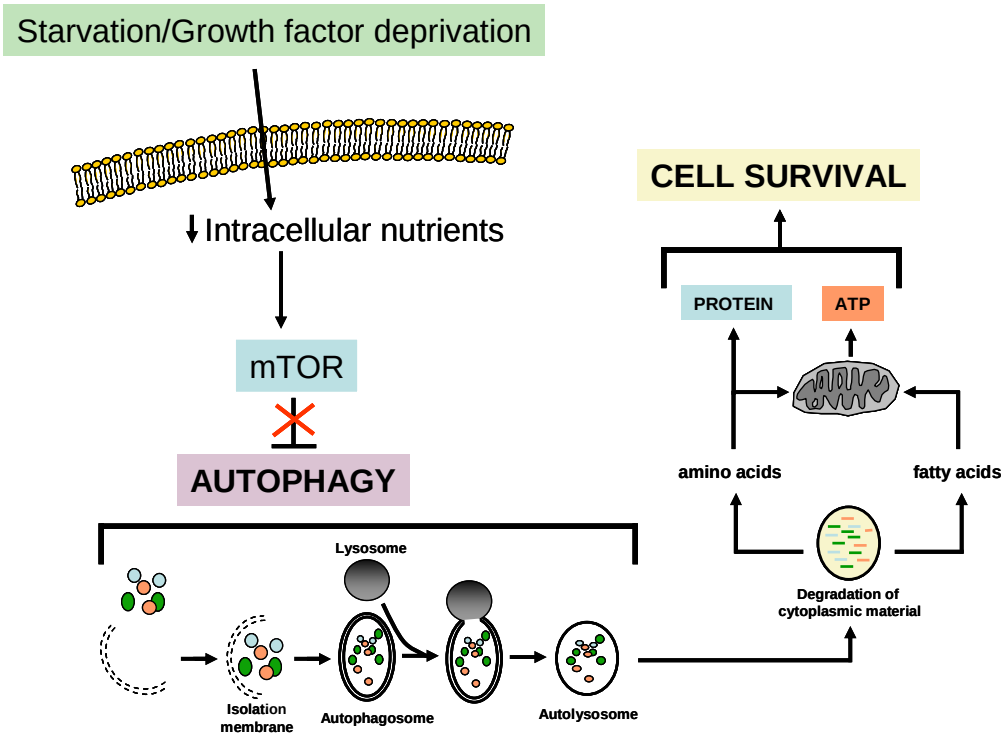

Figure 1-8 The autophagy pathway and its role in cellular adaptation in response to nutrient deprivation

Autophagy is activated by a decrease in intracellular nutrients and involves the sequestration of cytoplasmic material by an isolation membrane to form the autophagosome. The autophagosome then fuses with a lysosome, to form an autolysosome, where the sequestered material is degraded. Degradation of this material by the autolysosome generates free fatty acids and amino acids that can be used by the cell to maintain mitochondrial ATP energy production and protein synthesis, thus promoting cell survival.

In yeast, approximately 30 genes (known as the Atg genes), which are essential for autophagy or autophagy-related processes, are located downstream of TOR kinase. Most of these genes have homologues in higher eukaryotes and encode proteins that act in different stages of autophagosome formation. The Atg proteins can be divided into 5 functional groups depending on function. They include a protein serine/threonine kinase complex that responds to upstream signals such as mTOR (Atg1, Atg13, Atg17); a lipid kinase signalling complex that mediates the formation of the isolation membrane (Atg6 (or beclin 1), Atg14, Vps34, and Vps15), ubiquitin-like conjugation pathways that allow vesicle expansion (the Atg8-Atg-7 and Atg12-Atg7 systems), a recycling pathway that mediates the disassembly of Atg proteins from matured autophagosomes (Atg2, Atg9, Atg18) and vacuolar permeases that alow the efflux of amino acids from the degradative compartment (Atg22) (165).

The identification of the genes and signals which regulate the autophagy process has also allowed the cellular manipulation and detection of autophagy. Classically, electron microscopy (EM) was used as the gold-standard to demonstrate autophagosomes in cells. However, more recently the autophagosome-associated protein microtubule-associated protein 1 light chain 3 (LC3) (mammalian homologue of yeast Atg8) has been used as a marker of autophagy. When autophagy is not activated, LC3 is localised in the cytoplasm; however, upon the execution of autophagy, LC3 links up with the isolation membrane and remains associated with the autophagosome membrane. For this reason, transfection with the green fluorescent protein-linked LC3 (GFP-LC3) chimeric plasmid is useful for the detection of autophagosomes by fluorescence microscopy (166). LC3 has two forms: type I is cytosolic and type II is membrane-bound. During autophagy, LC3-II increases by conversion from LC3-I. Therefore,

the increase of LC3-II can be detected by immunoblot analysis because LC3-I and LC3-II have different molecular weights (166).

Increasing evidence suggests that autophagy is important in tumour development. In all eukaryotic organisms, autophagy promotes the survival of normal cells during nutrient starvation. Similarly, autophagy might promote the survival of rapidly growing cancer cells that have outgrown their vascular niche and face conditions of hypoxia or metabolic stress (167).

It has also been shown that autophagy may also enhance the survival of cancer cells by targeting damaged mitochondria and other organelles for lysosomal degradation (168), thus, evading the oxidative stress response that can be triggered by activated cancer-causing genes or by anti-cancer treatments. Recent data suggests that CML cells undergo autophagy in response to TK inhibitor (TKI) treament (169, 170). Moreover, combination therapy with autophagy inhibitors, augmented the anti-leukaemic effects of both suberoylanilide hydroxamic acid (SAHA) (171) and dasatinib (to be discussed further later in this thesis) (172) on human primary CML cells *in vitro*.

In the majority of circumstances, autophagy serves as an adaptation pathway to cellular stress that promotes cell survival. However, an apparent paradox is the fact that autophagy is also considered as a form of non-apoptotic cell death or “type II” cell death. Indeed, allelic loss of the essential autophagy gene beclin 1 is found with high frequency in human breast, prostate and ovarian cancers (173, 174). Furthermore, inactivation of beclin1 leads to increased tumourigenesis in mice (175, 176). Therefore, whether autophagy protects against or causes disease is controversial and whether to turn autophagy on or off in a cancer cell

also remains a subject of much debate. This further highlights the need to clarify the mechanisms of autophagy and its inhibition in more detail.

1.2.5 GF independence of BCR-ABL$^+$ cells

1.2.5.1 Interleukin-3

Interleukin-3 (IL-3) is a 17-kDa cytokine which functions as a multipotent haemopoietic GF. Through activation of the IL-3 receptor, IL-3 induces activation of JAK-STAT, PI3K/Akt and Ras signalling pathways, to promote the proliferation, maturation, survival and probably self-renewal of pluripotent HSCs and cells of myeloid, erythroid and megakaryocytic lineages (177).

1.2.5.2 Granulocyte-Colony Stimulating Factor

Granulocyte-colony stimulating factor (G-CSF) is a 25-kDa secreted glycoprotein which also functions as a cytokine and was named for its specific induction of growth of haemopoietic progenitor cells in semi-solid cultures (178). The main biological effect of G-CSF is to cause an increase in proliferation and differentiation of cells in the neutrophil lineage, from HSCs to mature neutrophils, through the activation of JAK-STAT, PI3K/AKt and Ras signalling (179).

Neutropenia is a significant side effect of many cytotoxic chemotherapy regimes used to treat cancer. Therefore, the actions of G-CSF meant that it was initially tested in clinic for its ability to prevent or reduce severe neutropenia (180). Other functional roles for G-CSF include the mobilisation of HSCs from the BM into the peripheral blood (181) and the possible regulation of immune responses (182).

1.2.5.3 The autocrine production of IL-3 and G-CSF in CML cells

Several studies suggest that the aberrant production of haemopoietic cytokines, such as IL-3 and G-CSF, could play a role in CML pathogenesis. Investigations

have shown that similar biochemical changes, which occur in normal cells following exposure to high concentrations of IL-3, can be demonstrated in both BCR-ABL-transformed cell lines and primary CML cells (183). Murine models have demonstrated that the transplantation of BM cells, retrovirally transduced or transgenically-engineered to produce IL-3, may induce the development of a myeloproliferative disorder (184-186). Further *in vitro* investigations have shown that retroviral introduction of $p210^{BCR-ABL}$ into cytokine-dependent cell lines induced GF-independent proliferation, in association with autocrine production of IL-3 and G-CSF (187-189). However, one group did note that IL-3 and GM-CSF were not required for the induction of a BCR-ABL-mediated CML-like disorder in mice, but may be required for disease maintenance (189). Jiang et al. furthered this work by showing that primitive $CD34^+$ cells, isolated from patients with CP CML, express aberrant RNA transcripts for IL-3 and G-CSF. This was associated with an autocrine production of IL-3 and G-CSF which resulted in increased STAT5 phosphorylation and autonomous proliferation in cytokine-free cultures (190). Other groups have shown that normal progenitor cells die when cultured under the same conditions (83, 191). This evidence suggests that the autocrine GF loop is a further mechanism for selective CML cell proliferation and survival.

1.2.6 Historical Treatment of CML

The management of CML has changed significantly since the first treatment attempts with arsenic (Fowler' solution) in 1856. Other early treatment strategies included benzene, radiotherapy and splenectomy which were used as palliative therapies and did not affect the overall survival of patients (192).

In the 1950's, the oral alkylating agent bulsulfan was introduced for the treatment of patients with CP CML. Bulsulfan was convenient to administer and was

relatively specific for the haemopoietic tissue. However, bulsulfan therapy was associated with severe side effects such as prolonged myelosuppression, idiosyncratic pulmonary reactions ("bulsulfan lung") and BM fibrosis (193).

In the 1970's, bulsulfan therapy was largely replaced by hydroxyurea, a cell cycle-specific inhibitor of DNA synthesis. It produces rapid but transient haematological control and is well tolerated with fewer adverse effects. Both bulsulfan and hydroxyurea produced complete haematologic responses in 50 to 80% of treated patients with CML and these responses could be maintained for several years. However, cytogenetic responses were rare and most patients progressed to the BC stage (194). Although these agents did provide some clinical benefit for patients with CML they did not significantly alter the natural history of the disease.

Allogeneic stem cell transplantation (alloSCT) was introduced in the 1980's, which for the first time, offered a curative potential for younger CML patients (<50-55 years of age) with HLA-matched donors (195). Indeed, the complete elimination of the malignant clone in CML, defined by inability to detect *BCR-ABL* transcripts by qRT-PCR, is only possible with alloSCT (196). However, this procedure has a significant morbidity and mortality rate of between 20-40%, due to the associated graft-versus-host disease and frequent infections (58). Further, the majority of patients are not eligible for this therapy, due to age, the lack of a suitable donor and the associated high risk of mortality (197).

The early 1980's also saw the introduction of IFNα and began a new era for the treatment of CML. IFNα is given by subcutaneous injection and provides a significant survival advantage when compared to bulsulfan or hydroxyurea treatment (198). It is effective in reducing the leukocyte count and reversing the

clinical and laboratory features of CML. Additionally, it was observed that 5-15% of IFNα-treated patients achieved a significant reduction in Ph^+ metaphases (199). Combination with cytosine arabinoside (AraC) further improved response rates, with the induction of a complete haematological response (CHR) of 66% and major cytogenetic response (MCR) of 41% with a survival rate of 85.7% within three years (200). Cytogenetic response is an important prognostic factor for improved survival. Definitions of response are given in Table 1-4. These early studies with IFNα demonstrated that cytogenetic responses could be achieved using drug treatment. Therefore, this became the overall therapeutic target for patients with CML

Haematological response	Cytogenetic response¥	Molecular response†
Complete*	**Complete Ph^+ 0%**	**Complete**
Plt <450x10^9/L	**Partial Ph^+ 1-35%**	**Undetectable**
WC <10x10^9/L	**Minor Ph^+ 36-65%**	**Major <0.10%**
normal differential	**Minimal Ph^+ 66-95%**	
spleen not palpable	**None Ph^+ >95%**	

Table 1-4 CML disease response definitions

[*Plt- Peripheral blood platelet count, WC- white cell count with normal differential implying a lack of immature granulocytes and <5% basophils. ¥Ph+ as % of total metaphases (at least 20) examined in the BM. †BCR-ABL to control gene ratio. Undetectable levels depend on the sensitivity of assay. A major response may also be defined as a 3 log reduction from baseline.

1.2.6.1 The development of an ABL TKI

Studies investigating the structure of BCR-ABL and its importance in the malignant transformation of HSCs in CML provided the rationale for targeting BCR-ABL function therapeutically. This led to one of the most important advances in CML therapy to date - the development of imatinib mesylate (IM).

In the early 1990's, Anafi et al. first reported that the tyrphostins, AG568 and AG112 inhibited the TK activity of BCR-ABL in a BC-derived CML cell line, K562 (201). Tyrphostins have competitive activity towards ATP and/or substrate. However, despite showing effective activity *in vitro*, these compounds were not developed for clinical use. A further early compound which demonstrated activity towards BCR-ABL was the benzoquinonoid ansamycin antibiotic, herbimycin A. Herbimycin A was shown to inhibit the growth of a number of $p210^{BCR-ABL}$ transformed cells, without affecting the growth of Ph^- haemopoietic cell lines (202) and also prolonged the survival in a SCID mouse model of a disease akin to human Ph^+ ALL (203). It was originally thought that herbimycin A inhibited the BCR-ABL kinase, however, it was later shown to promote the degradation of BCR-ABL protein (204). Taken together, the data from investigations using these early compounds suggested that the development of a specific inhibitor towards BCR-ABL would be an effective therapeutic agent in CML and other Ph^+ leukaemias.

1.2.7 The development of IM

Scientists at Ciba Geigy (now Novartis) led the early development of IM by initiating a screen of a large number of ATP-competitive 2-phenylaminopyrimidine compounds for protein TK inhibitory activity. STI 571 (formerly CGP 57148B, now IM; GlivecTM or GleevecTM, Novartis Pharmaceuticals, Basel, Switzerland) emerged from the screen as the lead TKI for preclinical development (Figure 1-9).

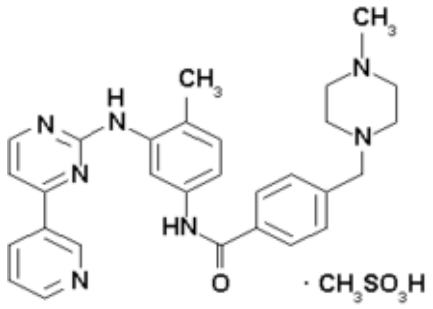

Figure 1-9 Structure of IM

IM was found to have potent inhibitory activity towards ABL, c-Kit and platelet-derived GF receptor (PDGF-R). It exerts effect on BCR-ABL by competitive inhibition of ATP. It selectively binds to the NH2-terminal anchor region of the ATP-binding pocket or “activation loop” thereby preventing BCR-ABL autophosphorylation, TK activity and subsequent phosphorylation of downstream target substrates (205) (Figure 1-10). The activation loop controls the catalytic activity of the kinase by switching between the active and inactive states. Crystallographic studies show that IM binds to the ATP site only when the activation loop is closed, thereby stabilizing the inactive state and thus, preventing the conformational change to the active form of the oncoprotein (206).

IM was found to inhibit ABL-kinase activity with 50% inhibitory concentration (IC_{50}) values ranging between 0.1 and 0.35μM using *in vitro* kinase assays, in a range of cell lines expressing constitutively active ABL, such as viral ABL (v-ABL) (207), $p210^{BCR-ABL}$ (205), $p185^{BCR-ABL}$ (208, 209) and translocated ets leukaemia (TEL)-ABL (208). Activity against the PDGFR and Kit were found to be in a similar range. Conversely, the IC_{50} values were at least 100-fold higher for a large number of other tyrosine and serine/threonine kinases, indicating that IM functions with a high level of selectivity (210).

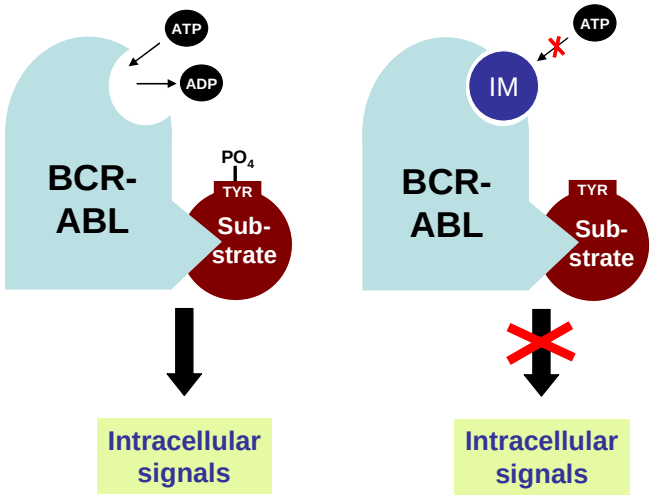

Figure 1-10 Mechanism of action of IM

BCR-ABL requires ATP binding for phosphorylation of substrates and subsequent activation of downstream pathways that promote cell survival, proliferation and regulation. IM can compete with ATP, binding to the inactive state of BCR-ABL, preventing the phosphorylation of substrates that would activate intracellular signals.

In initial cellular studies, IM was shown to specifically inhibit the proliferation of myeloid cell lines expressing BCR-ABL or CML BC cell lines *in vitro* (205, 211, 212). The inhibition of proliferation with cell death through apoptotic mechanisms was demonstrated to occur between 0.5 and 1μM of IM, whereas concentrations of up to 10μM IM did not affect the growth of BCR-ABL$^-$ cell lines (205, 211). Additional experiments showed that IM was equally potent in p185- and p210-expressing cells (208, 209). Colony-formation assays were also performed, using mononuclear cells (MNC)s from CML patients and normal individuals, to assess the effects of IM on committed haemopoietic progenitors. In these studies, IM induced a 92-98% decrease in the number of BCR-ABL$^+$ colonies formed with no or minimal inhibition of normal colony formation at concentrations up to 1μM (205,

211). These findings were then confirmed in stroma-dependent long-term cultures (213, 214).

Animal studies demonstrated a dose-dependent inhibition of tumour growth in animals inoculated with BCR-ABL-transformed 32D cells and treated daily with IM, with inactivity against v-SRC-expressing tumours. However, using a once-per-day injection schedule of up to 50mg/kg, tumour growth was inhibited, but not eradicated (205). This modest *in vivo* activity could be explained by the murine pharmacokinetic profile of IM. It revealed a short drug half-life in mice, where a single dose of IM inhibited BCR-ABL kinase activity for only 2 to 5 hours. This was not seen in any other species - ie. rat, dog or human. In nude mice, a 3-times daily administration of IM resulted in continuous inhibition of BCR-ABL kinase activity. This led to an eradication of tumours in 87% of IM-treated mice (215). From this data, it was suggested that IM was able to target some, but not all leukaemic clones and therefore, it was likely that continuous exposure to IM would be required for optimal therapeutic effects.

1.2.7.1 IM and Phase I Clinical Trials

Phase I studies with IM began in June 1998 and were designed to establish the maximum tolerated dose. The study consisted of patients with CP CML who were refractory or resistant to therapy with IFNα (216). IM was given as a once daily oral therapy and was well tolerated. Side effects were generally mild and included occasional nausea, periorbital oedema, and muscle cramps. 98% of CP CML patients, who had failed IFNα therapy and were treated with IM at 300mg and above, achieved a CHR. Furthermore, only one of these patients had relapsed at one-year of follow-up. Pharmacokinetic studies showed that with a dose of 300mg, plasma levels of IM were equivalent to the effective *in vitro* concentration of 1μM.

Using the current standard dose for CP CML of 400mg IM, a peak plasma level of approximately 4.6μM and trough level of approximately 2.13μM could be achieved, with a half-life of 19.3 hours. These data indicated that the once-daily dosing schedule would be sufficient to cause continuous kinase inhibition.

Following these promising results, the initial study was expanded to include patients with myeloid or lymphoid BC CML and relapsed or refractory Ph^+ ALL patients (217). With doses at or exceeding 300mg per day, 21 of 38 (55%) myeloid BC patients responded, with 11% achieveing a CHR. In patients with lymphoid BC or ALL, 70% responded, including 20% who had complete responses. However, all but one patient with lymphoid BC or ALL had relapsed within weeks to months.

1.2.7.2 IM and Phase II Clinical Trials

The successful data from the Phase I trial led to the commencement of Phase II studies, which began in late 1999 using IM as a single agent for all stages of CML. In CP patients who had failed IFNα therapy, 95% achieved a CHR and 60% a MCR, which was defined as a reduction to less than 35% Ph^+ metaphases. Only 13% of these patients had relapsed at the median follow-up of 29 months (218). However, although the response rates in AP and BC CML patients were also quite high, the relapses were much more common, with the majority of BC patients relapsing during the first year of therapy (219, 220). Overall, these clinical trials confirmed the promising results of the phase I studies. This led to Food and Drug Administration (FDA) approval of IM for the treatment of CML in advanced phase and after failure of IFNα therapy.

1.2.7.3 IM and Phase III Clinical Trials - A Randomised Comparison of IM with IFNα Plus Ara-C

The next clinical trial was a phase III study of newly diagnosed CP CML patients which compared IM treatment with the standard therapy of IFNα plus Ara-C. This was named the International Randomized Study of Interferon and STI571 (IRIS) study and was initiated in June 2000. The trial managed to reach its goal of recruiting more than 1000 patients in a 7-month period (221). At the median follow-up of 18 months, patients who had been randomised to IM therapy responded significantly better than the patients treated with IFNα plus Ara-C in all measured parameters, as shown in Table 1-5.

	IM (% responding at 400mg/day) (n=553)	IFNα plus Ara-C (n=553)
CHR	**97**	**69**
MCR	**87**	**35**
CCR	**76**	**14**
Intolerence	**3**	**31**
Progressive disease	**3**	**8.5**

Table 1-5 Phase III results of IM versus IFNα plus Ara-C for newly diagnosed CP patients with CML - taken from (221).

Results are with a median follow-up of 18 months. [CHR- complete hematologic response; MCR- major cytogenetic response; CCR- complete cytogenetic response; intolerance leading to discontinuation of first-line therapy; progressive disease, progressing to AP or BC. All of these differences are highly significant, with p < 0.001.]

The apparent superiority of IM treatment, led to the results being disclosed early and most of the patients were crossed over into the IM arm.

Five year follow-up studies have shown more impressive results for IM. In the most recent update of the IRIS study, the estimated overall survival for newly diagnosed CP CML patients, who received IM as an initial therapy was 89%. The best observed rate of CHR (normal white count and loss of symptoms) was 97% and the CCR (no Ph^+ metaphases) rate was 87%. Furthermore, an estimated 93% of IM-treated patients remained free from disease progression to AP or BC phase CML (222).

1.2.8 Molecular persistence

The monitoring of residual disease in CML patients is generally performed by qRT-PCR for *BCR-ABL*. It was observed that in the Phase III trial, for complete cytogenetic responders, the risk of disease progression was inversely correlated with the reduction of *BCR-ABL* transcripts as compared with pre-treatment levels (223). However, despite the fact that the majority of patients randomised to the IM arm achieved a CCR, most of these patients still had detectable leukaemia. Only a small proportion (4%) of patients obtained a complete molecular response (CMR), where they became negative for *BCR-ABL* transcripts by qRT-PCR. Therefore, for the majority of IM-treated patients, there is persistence of the leukaemic clone and most have relapsed if treatment was discontinued. It is hypothesised that this minimal residual disease (MRD) is a result of a primitive “quiescent” subpopulation of leukaemic cells (224), which may be the cause for relapse at a later date. Holyoake et al. were the first to isolate such primitive, quiescent cells - which were found to account for around 0.5% of the $CD34^+$ compartment - from CML cells using two different approaches (224, 225). The authors first obtained viable G_0

and G_1/S/G_2/M fractions by fluorescence-activated cell sorting (FACS), using Hst and PY staining, with quiescence being confirmed by the subsequent analysis of Ki67 and cyclin D expression. In GF-supplemented serum-free cultures, this non-proliferating population could also be isolated by first labelling $CD34^+$ CML progenitor cells with carboxyfluorescein diacetate succinimidyl ester (CFSE), in order to track cell division at high resolution by FACS. The group found that these quiescent cells were Ph^+ and expressed high levels of CD34, but lacked expression of lineage markers, CD38, CD45RA or CD71. They also had *in vitro* progenitor activity as demonstrated by colony-forming cell (CFC) and long-term culture-initiating cell (LTC-IC) assays and were capable of engrafting NOD/SCID mice (224). Significantly, these studies also demonstrated that quiescence is a temporary phenomenon, whereby the G_0 cells can re-enter the cell cycle, via a mechanism associated with the upregulation of IL-3 expression (225). Therefore, the existence of a transiently quiescent leukaemic clone may account for the fact that IM is unable to completely eradicate CML and also provides a feasible explanation for patients often relapsing at a later date.

In vitro studies have also demonstrated that these BCR-ABL^+ quiescent cells appear to be inherently resistant to IM therapy, at concentrations up to 10 times higher than those achievable *in vivo*, whereas the more mature, proliferating cells remain sensitive (226, 227). Bhatia and colleagues also found that $CD34^+$ cells taken from IM-treated patients, who had achieved CCR, were able to form colonies in both CFC and LTC-IC assays (228). Jorgensen et al. identified a second subset of primitive cells within a total CML cell population. These cells were found to undergo cell cycle arrest and accumulate in the G_0/G_1 phase in the presence of anti-proliferative agents, including IM (229). It was also demonstrated that these cells could be encouraged into cell cycle with sequential pulsed therapy.

Overall, these data suggest that IM is able to control the disease, through inhibition of stem cell proliferation, but is unable to eliminate the quiescent malignant clone. This has also since been postulated by a mathematical model which has demonstrated that during IM treatment, the clearance of *BCR-ABL* transcripts follows a biphasic decline. The initial phase is characterised by a rapid clearance of transcripts, whereas the second phase shows a slower rate of clearance. This model predicts that this biphasic decline is likely due to the differential susceptibility of a total CML population to IM treatment. The more mature differentiated cells are readily cleared by the drug, whereas the G_0 CML cells escape IM-induced apoptosis, simply by virtue of their quiescent state (230).

1.2.9 Molecular resistance

Another major clinical concern is the observation of molecular resistance in IM-treated patients. This is generally observed in CML patients at the advanced stage of disease, with an estimated 4-year resistance rate of 20% in later CP and 70% to 90% in AP/BC phases (220, 222), although, it has also been seen in CP CML patients. IM resistance can be described either as primary ("refractoriness"), defined as a failure to achieve CHR at 3 months, a cytogenetic response at 6 months or a MCR at 12 months; or secondary ("acquired"), defined as loss of established IM response or progression to AP or BC (231). It has also been speculated that there are 2 broad categories of IM resistance: BCR-ABL-independent and BCR-ABL-dependent.

1.2.9.1 BCR-ABL-independent mechanisms of resistance

BCR-ABL-independence suggests that the leukaemia cells are no longer reliant on BCR-ABL to drive proliferation; but have acquired additional oncogenic mutations and mechanisms, which are responsible for their growth and survival. Donato et

al. demonstrated that compensatory SRC activation within a CML cell may play a role in CML progression to BP and BCR-ABL independent IM resistance (232, 233). It was found that patients who have progressed whilst being treated with IM had an elevated SRC kinase activity, while the *BCR-ABL* transcripts and protein were reduced. Furthermore, it has also been shown that the SRC family kinase (SFK), LYN, is persistently activated in patients who have failed IM therapy and who harbour no *BCR-ABL* mutations (234). These data have led to the development of new agents that target the SRC kinase and inhibit other non-ATP binding sites (to be discussed further later). The induction of autocrine GF secretion is another potential mechanism for IM resistance. Adaptive autocrine secretion of GM-CSF was shown to mediate BCR-ABL-independent TKI resistance via activation of the anti-apoptotic JAK2-STAT5 pathway. This GM-CSF-induced resistance could then be overcome by the inhibition of JAK2 (235). A further possibility is that IM resistant cells are inherently refractory to TKI treatment and resistance reflects intrinsic properties of CML stem cells, to sustain survival in the presence of drug treatment. Thus, BCR-ABL is no longer a relevant target for IM in these cells and any specific BCR-ABL inhibitor would be ineffective in this situation.

1.2.9.2 BCR-ABL-dependent mechanisms of resistance

Conversely, resistance in Ph^+ leukaemias may be dependent on BCR-ABL. Proposed mechanisms of resistance include BCR-ABL amplification- where multiple copies of BCR-ABL gene can be detected in the interphase nuclei in patients who relapse after initially responding to IM, resulting in overexpression of the BCR-ABL oncoprotein (236-238). However, BCR-ABL dependent IM resistance is most often attributed to the development of point mutations within the ABL-kinase domain, which are found in more than 50% patients with acquired

resistance (132, 238-240). In 2001, Gorre and colleagues described the development of BCR-ABL mutations in 11 patients with BC phase CML or Ph^+ ALL who relapsed on IM therapy (238). BCR-ABL gene amplification was only detected in three patients. Following sequencing of the ATP-binding pocket and the activation loop of the kinase domain, an identical cytosine to thymidine mutation at ABL nucleotide 944 in 6 of 9 assessable patients was identified. This mutation resulted in a single amino-acid change at position 315, is designated T315I. Threonine 315 (also known as the “gatekeeper” residue) is located at the binding site of ABL and forms a crucial hydrogen bond interaction with IM (241). The T315I mutation disrupts this bond interaction which, along with the bulkier isoleucine side chain, sterically inhibits IM binding. This results in complete insensitivity to IM therapy at clinically achievable doses (238). The T315I mutant remains the most clinically significant as it linked to poor prognosis in CML patients (242). To date, more than 100 kinase domain mutations have been described *in vivo* and from *in vitro* screens (240, 241, 243, 244), each conferring a different transforming potential and level of resistance relative to wild-type BCR-ABL. These include mutations within the ATP binding site (P-loop), activation loop (A-loop) or the caboxy terminus. Some mutations only confer a moderate degree of resistance; however, the mutations within the P-loop are often associated with a poorer outcome (239). This is probably due to the restriction of IM-binding due to mutations altering and destabilising the conformation of the ATP-binding site (240). However, it is also worth noting that the presence of BCR-ABL mutations does not always explain resistance in IM-treated patients (245).

It has been noted that the concentration of drug within a target cell is a further important treatment consideration; therefore, the active efflux of chemotherapeutic drugs from target cells could be a mechanism of drug resistance. The ABC

transporter (ABCB1 (or MDR-1)) is a cell-surface transmembrane protein that mediates multi-drug resistance in a variety of malignancies through the regulation of chemotherapeutic agent efflux. Cells from BC CML patients have demonstrated a higher expression of ABCB1 compared with those from CP patients and has been linked to the development of IM resistance (237). Several groups have also shown that IM is a substrate for ABCB1 (246, 247). However, the role of ABCB1 in CML remains unclear as *in vitro* studies have shown that overexpression of ABCB1 in K562 cells does not confer resistance to IM (248). Furthermore, inhibition of ABCB1 did not enhance the therapeutic effect of IM against BCR-ABL activity in primitive CML cells (249). Another related ABC transporter, ABCG2, is also present on HSCs and has been suggested as another candidate for regulating intracellular IM availability. However, Jordanides and colleagues demonstrated that IM is an inhibitor of, but not a substrate for ABCG2 and therefore does not modulate the intracellular IM concentrations within CML stem cells (250).

1.2.10 Second generation TKIs

In an attempt to overcome IM-resistance, a second generation of BCR-ABL inhibitors have been developed. These include the ATP-competitive compounds, nilotinib, bosutinib and dasatinib.

1.2.10.1 Nilotinib (AMN107, Tasigna™)

Nilotinib (Tasigna™; AMN107, Novartis, Basel, Switzerland) is an orally administered second-generation TKI which inhibits ABL-kinase, PDGFR, Kit and ephrin receptor kinase and is currently approved by the FDA for the treatment of CP CML or AP CML (Figure 1-11). Nilotinib is an analogue of IM, which disrupts the ATP-phosphate-binding pocket, binding exclusively to the inactive

conformation of the ABL-kinase domain. Nilotinib has additional alterations in its structure that allow higher binding affinity and in IM-sensitive cell lines, demonstrates 43- to 60-fold greater potency than IM. In IM-resistant cell lines, nilotinib demonstrates at least 20-fold more potency than IM. Indeed, nilotinib inhibited 32 of 33 IM-resistant mutant cell lines *in vitro*, except for cells containing the T315I mutation (251, 252), and also prolonged survival in mice injected with cells expressing both wild-type and IM-resistant BCR-ABL mutants (253).

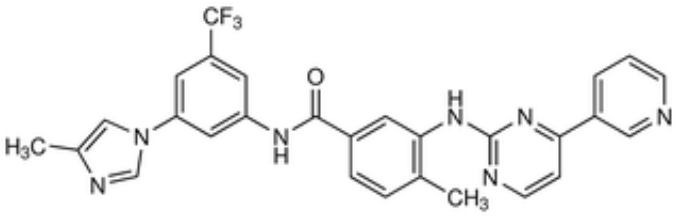

Figure 1-11 Structure of nilotinib

Phase I studies determined the appropriate dosing of nilotinib and established its clinical safety and efficacy in patients with CML or Ph^+ B-ALL who were resistant or intolerant to IM. Promising response rates were observed in patients with CP disease, with a CHR achieved in 92% (11 of 12). Responses in advanced stage disease were lower, with 72 (33 of 46) and 48% (22 of 46) of patients with AP disease achieving haematological and cytogenetic responses, respectively. Among patients with BP disease, 39% (13 of 33) achieved a haematological response and 27% (9 of 33) achieved a cytogenetic response (254).

Subsequent clinical evaluation has since confirmed the safety and efficacy of nilotinib treatment. In Phase II studies, IM-resistant or -intolerant CP CML patients, who were treated with 400 mg nilotinib twice daily, demonstrated MCR and CCR rates of 48 and 31% at 6 months, respectively. The estimated overall survival rate at 12 months was 95% (255). Within the group of patients whose baseline BCR-ABL mutation status was available, IM-resistant patients with no BCR-ABL

mutations showed similar MCR rates as patients with mutated BCR-ABL - 51 versus 42%, respectively. Furthermore, consistent with the *in vitro* data, 4 out of 4 patients with the T315I mutation showed no response to IM treatment (255).

Further *in vitro* studies have shown that nilotinib has anti-proliferative effects on $CD34^+$ CML cells, but does not eradicate the most primitive cells within the stem cell compartment (256). Therefore, whether nilotinib like IM, contributes to the disease persistence phenomenon still remains to be seen.

SFKs comprise of nine structurally homologous cytoplasmic non-receptor TKs (SRC, FYN, YES, BLK, YRK, FGR, HCK, LCK and LYN) which regulate signalling pathways involved in cell growth, differentiation and survival (257). As stated previously, studies have shown that the overexpression of SFK, such as LYN, plays a role in the proliferation and survival of CML cells, and in some cases, IM resistance (233). Further, experiments with SRC-dominant-negative mutants suggest that SFKs are involved in the proliferation of BCR-ABL^+ cell lines (258),(259). Therefore, the simultaneous inhibition of BCR-ABL and SRC kinase makes a further attractive option for CML therapy.

1.2.10.2 Bosutinib (SKI-606)

Bosutinib (SKI-606, Wyeth, Madison, NJ) is an orally available 4-anilino-3-quinolinecarbonitrile derivative (Figure 1-12) that is a potent dual inhibitor of the SF and ABL TK activity with an IC50 of 1.2 and 1nM, respectively.

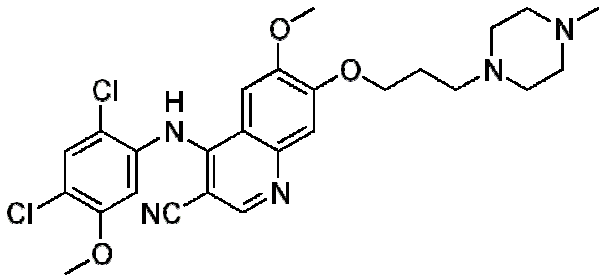

Figure 1-12 Structure of bosutinib

Bosutinib showed *in vitro* activity against all IM-resistant mutants, except T315I, and caused regression of large K562 xenografts in nude mice (260). Unlike both IM and nilotinib, bosutinib does not significantly inhibit PDGFR and Kit activity, which may result in a safer toxicity profile *in vivo*. Indeed, bosutinib demonstrated favourable toleribility in Phase I and II trials with patients who are resistant or intolerant to IM. Responses up to CCR were achieved in patients who harboured various BCR-ABL mutants, however, no patient with the T315I mutation responded (261). Recent *in vitro* studies suggest that bosutinib does not demonstrate increased ability to eliminate primitive CML progenitors by apoptosis, as compared to IM (262), however due to its toleribility; bosutinib may be a good option for patients who have failed therapy with IM or any other second generation TKI.

1.2.10.3 Dasatinib (BMS-354825; Sprycel®)

Dasatinib (BMS-354825; Sprycel, Bristol-Myers Squibb, Princeton, NJ) is a second-generation TKI for the treatment of IM-resistant or -intolerant patients with Ph^+ leukaemias, that was approved by the FDA in 2006 (263) (Figure 1-13).

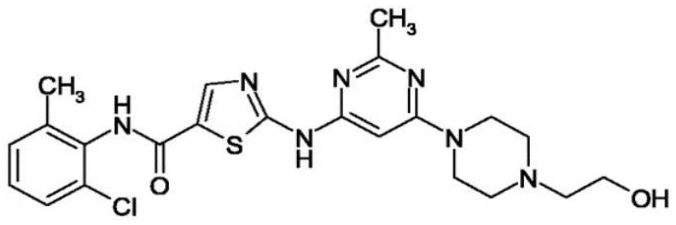

Figure 1-13 Structure of dasatinib

Like bosutinib, dasatinib is also a potent oral inhibitor of SFKs and BCR-ABL, and has added activity against Kit, PDGFR and Ephrin receptor TKs (264). Dasatinib has a 325-fold greater potency than IM against cells expressing wild-type BCR-ABL, with an IC_{50} of less than 1nM, and is effective against all IM-resistant BCR-ABL mutants tested *in vitro*, except T315I (252). Dasatinib binds to the ATP-binding site in a similar position to IM, but is also able to bind both the active and inactive conformation of ABL-kinase (265). This less stringent conformation requirement for ABL-kinase inhibition may be a further way of overcoming IM resistance.

The clinical efficacy of dasatinib was demonstrated in a series of Phase II studies called the SRC/ABL Tyrosine Kinase Inhibition Activity Research Trials (START). The START-C trial was a Phase II multicentre study for the assessment of dasatinib treatment of patients with CP CML who were resistant or intolerant to IM (266). At the median follow-up of 24 months, data was available from 387 patients (288 IM-resistant and 99 IM-intolerant). In 91% of the patients, a CHR was

achieved, with 62% obtaining a MCR. Responses were observed across all BCR-ABL mutations, irrespective of the location (with the exception of T315I), thus demonstrating that dasatinib has activity across the subgroups, including those patients with P-loop mutations (266). At the 24-month follow-up, progression-free and survival rates were determined as 80 and 94%, respectively. Impressive responses have even been noted in myeloid and lymphoid BC CML with a CCR rate of more than 20% (267, 268). However, despite these promising *in vivo* results, recent *in vitro* data showed that although dasatinib demonstrated increased efficacy over IM against earlier progenitor populations, it did not target the quiescent stem cell population (131). Therefore, dasatinib treatment alone may not have the ability to completely eradicate the disease.

1.2.11 Oncogene Addiction

The term 'oncogene addiction' was first coined by IB Weinstein (269-271) to describe the phenomenon by which some cancers acquire dependency on one or a few genes for the maintenance of the malignant phenotype and cell survival. Evidence for this concept has now been obtained from a number of systems such as, transgenic mice, where switching off the overexpressed "dependent" oncogene leads to growth inhibition, apoptosis and/or tumour regression. The dependence on a single oncogene for survival has been observed in murine models for a number of different cancers including, lung tumours induced by the K-ras oncogene (272), melanoma induced by the H-ras oncogene (273), T-cell and AML induced by c-myc (274) and acute B-cell leukaemia induced by BCR-ABL (275). Similarly, mechanistic studies using human cancer cell lines have also illustrated the oncogene addiction phenomenon. The inhibition of HER2 (276), cyclin D1 (277), K-ras (278) and β-catenin (279) expression using antisense DNA or RNA interference systems attenuated the growth various human cancer cell lines. The

most convincing evidence for the apparent dependency on oncogenes for tumour cell survival comes from examples of patients treated with molecularly-targeted drugs. The targeting of BCR-ABL by TKI has shown remarkable therapeutic efficacy. TKI treatment has been demonstrated to efficiently kill a subset of cells expressing the oncogene, particularly in early CP CML (223). However, despite the impressive clearance of the majority of Ph^+ cells by IM and dasatinib, the primitive $CD34^+38^-$ cell population does not appear to undergo apoptosis even after several days TKI exposure (131). Therefore, it is still not clear whether early CML progenitor cells depend on BCR-ABL for their survival.

2. MATERIALS AND METHODS

2.1 Materials

2.1.1 Small molecule inhibitors

IM was provided as a white powder under a Materials Transfer Agreement from Novartis Pharma (Basel, Switzerland). It was dissolved in sterile H_2O and stored as a 100mM stock solution at 4℃. Dasatinib was provided as a white powder under a Materials Transfer Agreement from Bristol-Myers Squibb (Princeton, NJ, USA). It was dissolved in dimethyl sulfoxide (DMSO) to give a stock concentration of 20mM and stored in multiple aliquots at -20℃ prior to use. All small molecule inhibitors were made up fresh and diluted to the appropriate concentration with PBS prior to use.

2.1.2 Tissue culture supplies (including $CD34^+$ selection)

Abbot Diagnostics Maidenhead, UK	**LS1 BCR-ABL Dual Colour FISH probe**
Baxter Healthcare Nottingham, UK	**Sterile water**
Becton Dickinson Plymouth, UK	**Luer lock syringes**
Bio-Rad Hercules, CA, USA	**Triton-X-100**
Chugai Pharma London, UK	**Recombinant human G-CSF**
Greiner bio one Gloucestershire, UK	**25 and 75cm^3 tissue culture flasks 96-well plates FACS tubes Pipette tips**
Hendley Essex, UK	**Multispot microscope slides**
Invitrogen Paisley, UK	**2-Mercaptoethanol Colcemid Foetal calf serum (FCS) L-glutamine 200mM (100x) Phosphate buffered saline (PBS)**

	Penicillin-streptomycin solution (5000U/mL) **RPMI 1640 medium**
Miltenyi Biotec **Bisley, UK**	**CliniMACS CD34 reagent** **CliniMACS PBS/EDTA buffer** **CliniMACS tubing set**
Nalge Nunc International **Roskilde, Denmark**	**35mm non-adherent tissue culture dishes** **75cm^3 non-adherent tissue culture flasks** **Cryotubes** **Cryofreezer container** **Vacubottles**
Sartorius **Hannover, Germany**	**Minisart 0.2μM sterile filters** **Minisart 0.45μM sterile filters**
Scottish National Blood Transfusion Service **Glasgow, UK**	**20% human albumin solution (ALBA)** **4.5% ALBA**
Sigma-Aldrich **Dorset, UK**	**Bovine serum albumin (BSA)** **Carbonate-bicarbonate buffer** **DMSO** **Dulbecco's Modified Eagle Medium (DMEM)** **E-64d protease inhibitor (1mg/mL)** **Ficoll/histopaque solution (1.077g/mL)** **G418 disulphite salt solution** **Hank's buffered salt solution – calcium and magnesium free (HBSS-CMF)** **Hydrochloric acid (HCl)** **Hygromycin B** **Isocove's Modified Dulbecco's Medium (IMDM)** **Magnesium chloride ($MgCl_2$)** **Pepstatin A protease inhibitor (1mg/mL)** **Poly-L-lysine** **Potassium chloride (KCl)** **Sodium azide** **Trisodium citrate** **Trypan blue** **Trypsin-EDTA**
Stem Cell Technologies **British Columbia, Canada**	**Bovine pancreatic deoxyribonuclease (DNAse I) 1mg/mL** **Bovine serum albumin/insulin /transferrin (BIT) serum substitute** **Flt-3 ligand** **Hydrocortisone 21-hemisuccinate** **IL-3** **IL-6** **Methocult^{TM}** **Myelocult^{TM}** **Stem cell factor (SCF)**

Sterlin Ltd Hounslow, UK	**Iwaki Type I Collagen-coated 6-well plates Pastettes 5mL, 10mL and 25mL disposable pipettes 15 and 50mL sterile plastic falcon tubes 90mm Petri dishes**
Thermo Fisher Scientific Loughborough, UK	**Immulon II HB 96-well flat bottomed plates Acetic acid Methanol**
Weber Scientific International, West Sussex, UK	**Hawksley Neubauer counting chamber**

2.1.3 Flow cytometry reagents

BD Biosciences, Oxford, UK	**Anti-human IgG FITC isotype control Anti-human IgG PE isotype control Anti-human IgG APC isotype control FACS flow FACS clean Mouse anti-human-active caspase-3-PE antibody Mouse anti-human-Ki67-FITC antibody Mouse anti-human-annexin-V-FITC antibody Mouse anti-human-CD34-APC Mouse anti-human-CD38-FITC Viaprobe- 7 aminoactinomycin D (7-AAD)**
Caltag Laboratories Silverstone, UK	**Fix and Perm® A and B**
Cell Signaling (New England Biolabs), Hitchin, UK	**Rabbit anti-human-p-CrkL antibody Rabbit anti-human-p-STAT5 antibody**
Molecular probes Eugene, OR, USA	**CFSE**
Sigma-Aldrich Dorset, UK	**Anti-rabbit IgG-FITC conjugate Anti-rabbit IgG-PE conjugate Formaldehyde solution**

2.1.4 Molecular biology supplies

Abcam, Cambridge, UK	**Anti-rabbit IgG**
Amersham Pharmacia Biotech Ltd Buckinghamshire, UK	**Rainbow marker (RPN756)**
Applied Biosystems, Foster City, CA, USA	**High capacity cDNA archive kit Taqman gene expression assays- cyclin D1 and glyceraldehydes-3-phosphate dehydrogenase (GAPDH) qPCR mastermix plus**
Bio-Rad Hercules, CA, USA	**4-15% Tris-HCl gradient gels Laemmli sample buffer Immun-star ECL reagents Nitrocellulose membrane Tris/Glycine/SDS running buffer Tris/Glycine transfer buffer Tween-20 Triton-X-100**
Cell Signaling (New England Biolabs), Hitchin, UK	**Anti-rabbit IgG horseradish peroxidase (HRP)-linked secondary antibody Rabbit anti-human-p-CrkL antibody Rabbit anti-human-LC3b antibody Rabbit anti-human-GAPDH antibody Rabbit anti-human-p-S6K antibody Rabbit anti-human-FoxO3a antibody**
Chemicon International Temecula, CA, USA	**Re-blot™ Plus Strong Antibody Stripping Solution**
Eurogentec Ltd Southampton, UK	**BCR-ABL p210 detection: ENF501 (FORWARD PRIMER): TCCGCTGACCATCAAYAAGGA ENF561 (REVERSE PRIMER): CACTCAGACCCTGAGGCTCAA ENP541 (PROBE): FAM- CCCTTCAGCGGCCAGTAGCATCTGA- TAMRA**
Fisher Scientific Loughborough, UK	**Methanol**
Invitrogen (Molecular Probes) Paisley, UK	**Anti-rabbit-Alexa Fluor 488**
Perbio Northumberland, UK	**BCA kit**
Qiagen, Crawley, UK	**RNeasy mini kit**
Roche, Burgess Hill, UK	**PCR grade water**
Sigma-Aldrich Dorset, UK	**Ethylenediaminetetraacetic acid (EDTA) Ficoll/histopaque solution 36.5% Formaldehyde solution NP-40**

	Protease inhibitor cocktail **Sodium chloride** **Tris (hydroxymethyl)aminomethane hydrochloride (Tris-HCl)** **Tris base** **Osmium tetroxide** **Uranyl acetate** **25% gluteraldehyde solution** **Sodium cacodylate**
SPI Supplies Loughborough, UK	**300-mesh formvar-coated grids**
Taab Laboratories Equipment Ltd, Aldermaston, UK	**Taab epoxy resin**
Upstate (Millipore) Watford, UK	**Anti-phosphotyrosine (4G10) antibody**
Vector Laboratories Inc Burlingame, CA, USA	**VECTASHIELD® mounting medium with DAPI**

2.2 Preparation of media and solutions

2.2.1 Tissue culture media

2.2.1.1 RPMI^{++}

RPMI 1640	**500mL**
FCS	**50mL**
L-glutamine	**5mL**
Penicillin/Streptomycin solution	**5mL**

2.2.1.2 Serum free medium (SFM)

BIT	**25mL**
2-Mercaptoethanol	**250µL**
L-glutamine	**1.25mL**
Penicillin/Streptomycin solution	**1.25mL**
IMDM	**97.25mL**

- ***Made up in a Vacubottle and filter sterilised***

2.2.1.3 SFM supplemented with GF cocktail (SFM+5GF)

SFM	**50mL**
IL-3 (50μg/mL)	**20μL**
IL-6 (50μg/mL)	**20μL**
G-CSF (50μg/mL)	**20μL**
Flt-3 ligand (50μg/mL)	**100μL**
SCF (50μg/mL)	**100μL**

- ***Filter sterilised through 0.22μM filter***

2.2.1.4 RPMI for maintenance of stromal cell line M2-10B4 for LTC-IC

RPMI 1640	**500mL**
FCS	**50mL**
L-glutamine	**10mL**
Penicillin/streptomycin solution	**10mL**

2.2.1.5 DMEM for maintenance of stromal cell line Sl/Sl for LTC-IC

DMEM	**500mL**
FCS	**75mL**
L-glutamine	**10mL**
Penicillin/streptomycin solution	**10mL**

2.2.1.6 Myelocult

Myelocult™	**100mL**
Hydrocortisone hemisuccinate ($1x10^{-4}$M)	**1mL**

2.2.2 Tissue culture solutions

2.2.2.1 PBS/2% FCS

PBS	**490mL**
FCS	**10mL**

2.2.2.2 PBS/20% FCS

PBS	**80mL**
FCS	**20mL**

2.2.2.3 'DAMP' solution for thawing cryopreserved $CD34^+$ or unmanipulated cell (MNC) aliquots from -150℃

DNAse II solution (1mg/mL)	**1 vial**
Magnesium chloride (400x; 1M)	**625μL**
Trisodium citrate (0.155M)	**26.5mL**
20% ALBA	**12.5mL**
PBS (magnesium/calcium free)	**To 250mL**

2.2.2.4 20% DMSO/4.5% ALBA

DMSO	**20mL**
4.5% ALBA	**80mL**

2.2.2.5 IMDM/2% FCS

IMDM	**98mL**
FCS	**2mL**

2.2.3 Flow cytometry solutions

2.2.3.1 PBS/0.4% formaldehyde

PBS	**48mL**
10% formaldehyde solution	**2mL**

2.2.3.2 PBS/0.2% Triton-X-100

PBS	**50mL**
Triton-X-100	**100μL**

2.2.3.3 Annexin/viaprobe buffer

Annexin/viaprobe buffer (10X)	**1mL**
Distilled water	**9mL**

2.2.3.4 Fix perm wash – PBS/1% BSA

BSA	**10g**
PBS	**To 1L**

2.2.4 Molecular biology solutions

2.2.4.1 Lysis buffer for protein lysates (RIPA)

dH_2O	**7.75mL**
1.5M NaCl	**1mL**
1M Tris-HCl	**0.5mL**
150mM EDTA	**333µL**
NP-40	**50µL**
10% (w/v) Sodium deoxycholate	**250µL**

- ***Immediately prior to use, 100mL of protease inhibitor cocktail was added***

2.2.4.2 Running buffer

10x TGS buffer	**100mL**
PBS	**900mL**

2.2.4.3 Transfer buffer

10x TG buffer	**100mL**
PBS	**700mL**
Methanol	**200mL**

2.2.4.4 Tris-buffered saline (TBS) (1x)

Sodium chloride	**8g**
Potassium chloride	**0.2g**
Tris base	**3g**
dH_2O	**To 1L**

- ***Adjusted to pH 7.4 with 1M HCl***

2.2.4.5 Wash buffer (TBS-Tween; TBS-T)

TBS	**1000mL**
Tween	**100µL**

2.2.4.6 Blocking buffer

TBS	**100mL**
BSA	**5g**

2.2.4.7 3.65% Formaldehyde (Immunofluorescence)

PBS	**10mL**
36.5% Formaldehyde solution	**1mL**

2.2.4.8 0.5% Triton-X-100 (Immunofluorescence)

PBS	**50mL**
Triton-X-100	**250µL**

2.2.4.9 0.1M Sodium cacodylate (pH 7.4)

dH_20	**100mL**
Sodium cacodylate	**2.14mg**

- ***Buffer to pH 7.4 with 0.2M HCl***

2.2.4.10 Fixing solution for EM

25% gluteraldehyde solution	**1mL**
0.1M Sodium cacodylate (pH 7.4)	**9mL**

2.2.4.11 Post-fixation solution for EM

Osmium tetroxide	**0.1g**
0.1M Sodium cacodylate (pH 7.4)	**10mL**

2.2.4.12 5% uranyl acetate

dH_20	**10mL**
Uranyl acetate	**0.5g**

2.2.4.13 2% uranyl acetate

dH_20	**10mL**
Uranyl acetate	**0.2g**

2.3 Methods

2.3.1 Cell culture

2.3.1.1 Culture of cell lines

The BC CML cell lines K562, LAMA84 and BV173 (BCR-ABL^{+}) and the AML cell line HL60 (BCR-ABL^{-}), which were all available "in-house", were grown in suspension culture in RPMI^{++} medium in tissue culture flasks. Ba/F3 cells (murine IL-3 dependent pro-B cells) which stably expressed either wild-type p210 or *BCR-ABL* with kinase domain mutations (M351T and T315I) were donated as a kind gift from Professor Junia Melo and also maintained in RPMI^{++}. M2-10B4 and Sl/Sl murine fibroblast cell lines were cultured in RPMI (see Section 2.2.1.4) and DMEM (see Section 2.2.1.5), respectively.

All cell lines were maintained at 10ml in 25cm^3 tissue culture flasks, counted and passaged every two days with warm fresh media, to maintain a density of between 1x10^5-1x10^6.

2.3.1.2 Cell counting and cell viability assessment

Cell counts and assessment of viability were performed using a counting chamber. Cells were counted with trypan blue exclusion. Trypan blue dye was first diluted 1:10 with PBS and 90μL was added to 10μL of cell suspension to give a 1:10 dilution of cells. Approximately 10μL of the mixture was transferred to a haemocytometer and a minimum of 100 viable cells were counted. Cells that have damaged membranes are porous and absorb the trypan blue dye, appearing dark-blue under the microscope, whereas the cells with an intact membrane do not absorb the dye. Hence, the unstained cells were counted and the remaining stained dead cells were deemed non-viable.

2.3.1.3 Cryopreservation of cells

Between $4x10^6$-$2x10^7$ $CD34^+$ selected CP CML cells, $1x10^8$ unselected (MNC) CP CML cells and $5x10^6$-$1x10^7$ cell line cells were cryopreserved at -150℃ until use. To each cell suspension, an equal volume of 20% DMSO in 4.5% ALBA was added to give a final concentration of 10% DMSO. The cryotubes were transferred to a cryofreezer container and first cooled at -80°C to provide a controlled temperature reduction and then transferred to a -150℃ freezer for long-term storage.

2.3.1.4 Collection of human primary cell samples

All samples were collected with the approval from the Local Research and Ethics Committee and with written informed patient consent from patients at diagnosis of CP CML. Cells were collected by leukapheresis prior to any drug treatment. Each sample was determined to be Ph^+ by D-FISH and BCR-ABL^+ by PCR. Further samples were also obtained from patients, with normal BM undergoing autologous stem cell collection for either non-Hodgkin's lymphoma or multiple myeloma, who had been mobilised with G-CSF following chemotherapy and had excess $CD34^+$ cells remaining after those required for clinical use had been processed.

2.3.1.5 Purification of the MNC fraction from whole blood cell samples

Either 6mL of ficoll/histopaque solution was added to a 15mL falcon tube, or 20mL of ficoll/histopaque solution was added to a 50mL falcon tube (depending on the volume of blood sample) and brought to room temperature. The whole blood sample was first diluted (1:2) with PBS, carefully layered drop-wise onto the ficoll/histopaque solution, until it reached the top of the centrifuge tube and centrifuged at 1500rpm for 20 minutes at room temperature. Following centrifugation, the opaque interface containing the MNCs was carefully aspirated

with a pastette. The interface was then transferred into a sterile centrifuge tube with a pastette and washed twice with sterile PBS (centrifuge at 1000rpm for 5 minutes). The resultant MNCs were either used fresh or cryopreserved according to Section 2.3.1.3 until required.

2.3.1.6 Selection of $CD34^+$ cells from MNC samples

Enrichment for $CD34^+$ cells was achieved using the sterile CliniMACS system (Miltenyi Biotec, Bisley, UK), which positively selects for $CD34^+$ cells according to the manufacturers' instructions. Briefly, total MNCs were incubated with a specific anti-CD34 monoclonal antibody (Miltenyi Biotec) to which super-paramagnetic MACS beads (~50nM in diameter) had been conjugated. The cell sample was then passed through a high-gradient magnetic separation column, where the target $CD34^+$ cells were retained in the column and the unlabelled $CD34^-$ cells flushed through and discarded. The bound $CD34^+$ cells were then eluted after removal from the magnetic field, collected and an aliquot was removed for flow cytometry assessment of CD34 purity, which confirmed that all samples were >95% $CD34^+$ post-selection (Figure 2-1). All samples were for stored at the indicated concentrations (see Section 2.3.1.3) in cryotubes at -150℃, until required for use.

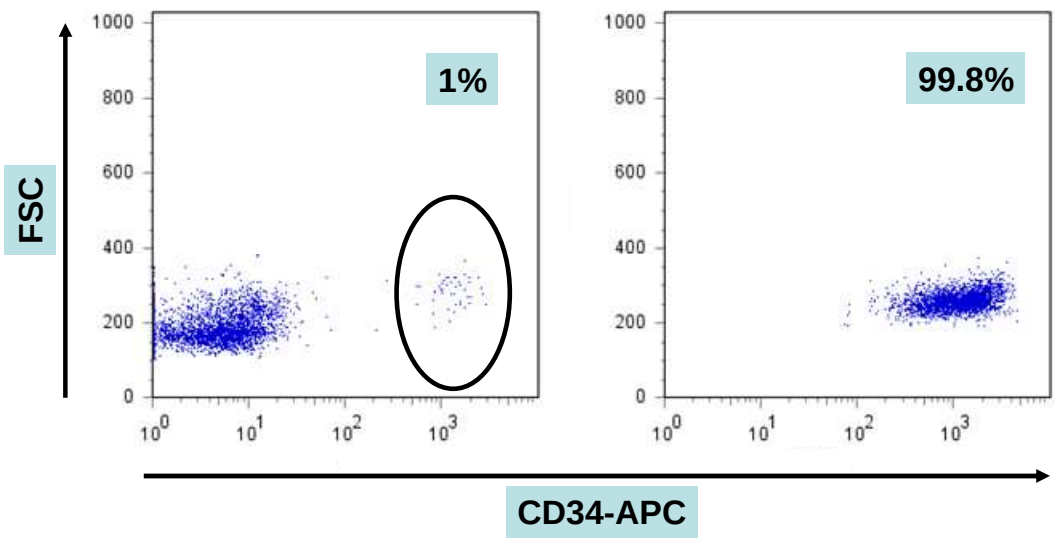

Figure 2-1 Example of cellular CD34 purity following CliniMACS selection

The left panel shows the percentage of $CD34^+$ cells, within a total MNC population, prior to the selection. The right panel shows the purified cells following CD34 selection.

2.3.1.7 Recovering frozen cells

CML cells were removed from -150℃ and immediately thawed at 37℃ in a water bath until the ice crystals had melted. Using a pastette, the cells were added to a 15ml sterile tube and recovered by slowly adding 10ml of thawing solution (DAMP) drop-wise over a 20 minute period. This step was performed at room temperature to enhance the activity of the DNAse II, with constant agitation to prevent clumping of the cells. The cells were centrifuged at 1000rpm for 10 minutes, the supernatant was poured away and the pellet loosened by flicking the tube. The pellet was then washed twice in DAMP and centrifuged, then resuspended in SFM for counting and cell viability. The CML cells were then plated in $25cm^3$ tissue culture flasks at ~$2x10^6$/mL.

Cell lines were thawed in a 37℃ water bath and rec overed slowly as above but in $RPMI^{++}$. The cells were then washed twice more with $RPMI^{++}$ and resuspended in 10ml of $RPMI^{++}$, then plated in $25cm^3$ tissue culture flasks.

NB. The exception to this was with M2-10B4 and Sl/Sl murine fibroblast cell lines, which were thawed and cultured in RPMI (see Section 2.2.1.4) and DMEM (see Section 2.2.1.5), respectively.

2.3.1.8 Selection of $CD34^+38^-$ cells from total $CD34^+$ samples

Total $CD34^+$ cells ($2x10^7$) were centrifuged (1000rpm, 5 minutes) and resuspended in 100µl PBS/2% FCS. Aliquots of cells ($2x10^4$ cells per tube) were removed for appropriate isotype controls which were used to correctly set the detectors, so that the negative isotype population was placed in the first log decade for each flow cytometry channel. CD34 APC and CD38 FITC positive controls (5µL of antibody per tube) were also set up. The remaining test cells were stained with 15µL of both CD34 APC and CD38 FITC antibodies and all samples were incubated for 20 minutes at room temperature in the dark. Following incubation, samples were washed twice with PBS/2% FCS (1000rpm, 5min). The controls were resuspended in 100µL PBS/2% FCS and the test cells were resuspended in 2mL PBS/2% FCS. All samples were sterile filtered through a 0.22µM filter before sorting. The controls were then run first and the compensation adjusted. The $CD34^+38^-$ cells were then sorted using a Becton Dickinson FACSAria.

2.4 Cellular techniques

2.4.1 CFSE staining

In 1994, Lyons and Parish introduced a technique for tracking the cell division of lymphocytes by flow cytometry, using the serial dilution of a fluorescein-based dye - CFSE (280). CFSE is a lipophilic molecule which passively enters cells, where it is converted to a reactive dye by non-specific intracellular esterases. Once inside a cell, it binds irreversibly to the free amines of cytoplasmic proteins, resulting in stable long-term retention. The dye is then equally partitioned between two daughter cells during mitosis, so fluorescence intensity is halved with every cell division. This property allows both the identification of cell progeny and the division-tracking of individual cells that have undergone up to ten sequential division cycles. Li et al. have demonstrated, using a mixture of CFSE-stained human and unstained rat cells in an *in vitro* co-culture, that no dye leaks from the stained cells and that the fluorescence intensity of the undivided cells remains constant (281). This therefore, confirms the reliability of this technique for the identification of undivided cells. Figure 2-2A shows the intensity of CFSE halving with each cell division and Figure 2-2B demonstrates the subsequent FACS histogram identifying the ‘peaks’, which each represent a cell division.

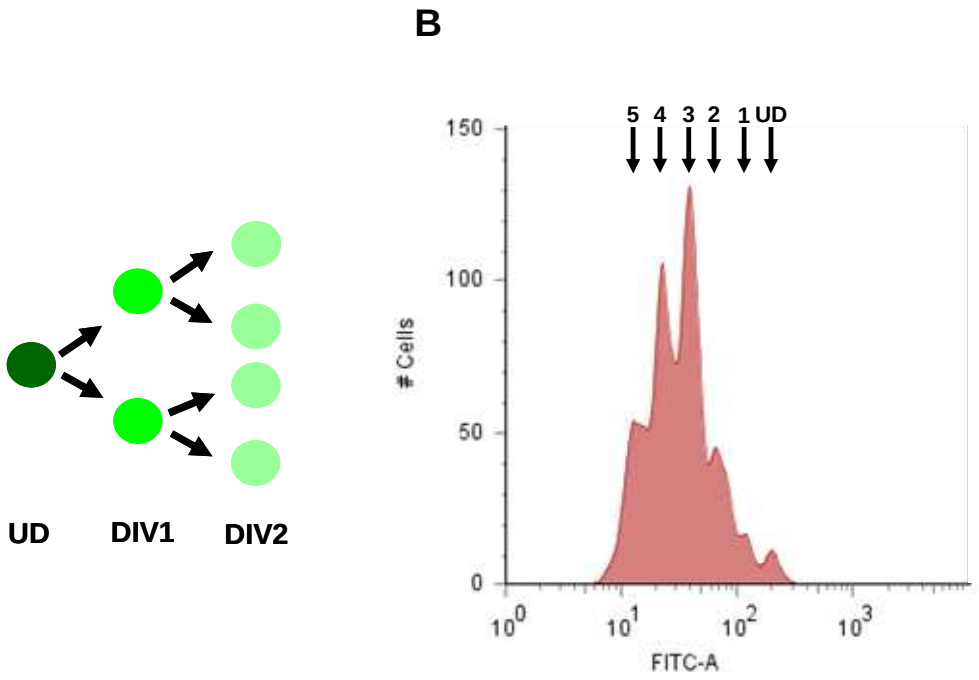

Figure 2-2 Tracking a cell with CFSE stain

(A) A schematic diagram of the brightness of the CFSE stain in a cell halving in the daughter cells with each division. (B) A histogram of a FACS plot showing the classic 'peaks' pattern with the undivided cells showing the highest fluorescence and the intensity halving with each division. A single peak can be gated to determine the percentage of cells in the total population that have undergone the equivalent number of divisions. [UD: undivided]

Following successful recovery of cells and resuspension in PBS/2% FCS, an aliquot (~10%) of the $CD34^+$ cells was removed and set up in culture in SFM+5GF as an unstained control. A stock solution of 5mM CFSE (in DMSO) was diluted at 1 in 10 dilution with PBS/2% FCS and 10µL added to 5mL of the remaining cells to give a final concentration of 1µM. The cells were then incubated in a water bath at 37℃ for exactly 10 minutes, after which the cells were removed and the CFSE was quenched by adding 10x volume of ice-cold PBS/20% FCS. The cells were

then centrifuged for 10 minutes at 1000rpm, the supernatant was discarded and the cells washed in fresh PBS/2% FCS. The cells were cultured overnight in 10mL SFM+5GF in non-adherent ($75cm^3$) tissue culture flasks ($1\text{-}2x10^7$ $CD34^+$ cells/flasks) at 37℃, 5% CO_2.

After CFSE staining and overnight incubation, the CFSE-stained cells were removed from the tissue culture flask and placed in a sterile tube. The flask was then washed out with PBS/2% FCS and this was also added to the tube. The cells were then centrifuged at 1000rpm for 10 minutes and washed again in PBS/2% FCS. Following this, the $CFSE^+$ cells were resuspended in PBS/2% FCS and the cell count and viability was determined. An aliquot of cells (~$2x10^4$) was removed for flow cytometry to assess the position of the undivided (CFSEmax; $CD34^+$) cell population prior to culture in different treatment conditions. For every experiment, a colcemid control was set up using $CFSE^+$ cells to determine the position of the CFSEmax peak after culture. One μL of the colcemid stock (100μg/mL) was added per mL of the tissue culture medium to give a final concentration of 100ng/mL. The cells unstained for CFSE were used to alter the voltage settings and optimally compensate for spectral overlap.

2.4.2 Culture of $CD34^+$ cells

Following either recovery from -150℃ or CFSE staining, cells were cultured in SFM or SFM+5GF (as indicated in the text) in 35mm suspension dishes at an initial cell concentration of ~$5x10^5$/mL for 1 to 12 days at 37℃, 5% CO_2. Drugs were added to each experiment as appropriate to the described conditions. The cells were harvested at indicated time-points, washed in PBS/2% FCS and aliquots were removed for performing a cell count and FACS analysis. In Chapter 4, the cells were harvested every 4 days and at the end of the final cycle of each

experiment (day 12), as well as performing a cell count and FACS analysis, an aliquot of cells was prepared for FISH to determine if the cells remaining after culture were BCR-ABL^{+}. Furthermore aliquots of cells were also taken for protein lysate and RNA preparation (methods described in Sections 2.6.1 and 2.8.1 respectively).

2.4.3 LTC-IC

Primitive haemopoietic cells, with proliferative potential, can be maintained in culture for extended periods of time, typically several months. These culture conditions have been called long-term bone marrow culture (LTBMC) (282). Briefly, LTBMC requires the formation of a supportive stromal layer which supplies the necessary microenvironment to allow the primitive haemopoietic cells to proliferate over time. An application of LTBMC is an assay that measures the number of LTC-IC (283, 284). In this assay, the cells of interest are overlayed on pre-established, irradiated stromal layers. After 5 weeks culture the contents of each plate are set up in a committed progenitor assay for a further two weeks. At the end of this, the number of colonies formed is counted and this allows the frequency of LTC-IC to be determined. Figure 2-3 shows a schematic diagram for the method used in the LTC-IC assay.

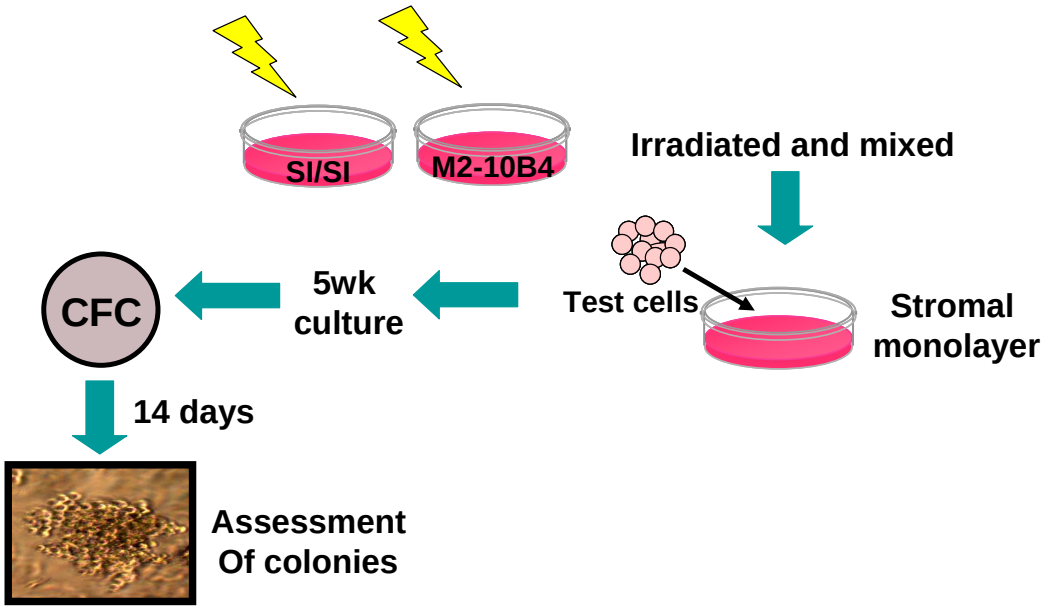

Figure 2-3 Schematic diagram for the assessment of LTC-IC

Test cells are overlayed on a supportive stromal cell monolayer and cultured for 5 weeks before being added to a commited progenitor assay (CFC). The number of colonies counted at the end of the assay correlates with the number of LTC-IC within the test cell sample.

Two genetically-modified murine fibroblast cell lines, M2-10B4 and Sl/Sl fibroblasts (both kindly provided by the Terry Fox Laboratories, Vancouver, BC, Canada) were used to provide the stromal support necessary for the LTC-IC. The M2-10B4 cells have been genetically modified to express G-CSF and IL-3, and Sl/Sl fibroblasts have been genetically modified to express SCF and IL-3. After thawing, these cell lines were maintained in culture at 37℃, 5% CO_2. The cells were trypsinised and passaged when the monolayer was semi-confluent to allow propagation of sufficient cells for LTC-IC. To minimise the proliferation of untransduced wild-type cells, the cultures were fed on alternate weeks with hygromycin B (final concentration 62.5μg/mL for M2-10B4 and 125μg/mL for Sl/Sl

fibroblasts) and G418 (final concentration 400μg/mL for M2-10B4 and 800μg/mL for Sl/Sl fibroblasts).

Before the stromal layers were seeded with the test cells, it was necessary to irradiate the stromal cells to render them incapable of proliferation. Prior to irradiation, the stromal cells were trypsinised and counted. A total of $1.5x10^5$ M2-10B4 and $1.5x10^5$ SI/SI fibroblasts were required for each test well. The stromal cell layers were then irradiated at 80Gy. Following this, the M2-10B4 and SI/SI fibroblasts were mixed and resuspended in Myelocult™ supplemented with hydrocortisone, to give a final cell concentration of $3x10^5$/mL. Two millilitres of this stromal cell suspension was then aliquoted into the required number of wells of a Type I Collagen coated 6-well plate (to facilitate stromal adherence). The plates were then incubated at 37℃, 5% CO_2. After the stromal cells had been incubated for 24 hours, the test cells ($CD34^+$ cells treated under different drug conditions as described in Section 2.4.2) were inoculated onto the stromal monolayers. Following drug treatment, the remaining CML cells were washed in PBS/2% FCS and then resuspended in 300μL of SFM. Duplicate LTC-IC wells were set up with 150μL of treated $CD34^+$ cell suspension. The cells were then incubated for a total of 5 weeks at 37℃, 5% CO_2. Every week, 1mL of Myelocult™ medium was removed from each well and 1mL of fresh Myelocult™ was added and this constituted a half medium change.

At the end of 5 weeks culture, the LTC-IC were harvested and set up in committed progenitor CFC assays. For each LTC-IC culture well, the culture supernatant (containing non-adherent cells) was pipetted into a sterile 15mL centrifuge tube (harvest tube). Two millilitres of HBSS-CMF was added to remove any serum-containing Myelocult™ medium and the plate swirled gently before the HBSS-CMF

was transferred to the harvest tube. One millilitre of trypsin-EDTA was then added to each well and swirled gently at intervals until all the adherent cells had detached (up to 5 minutes). Detachment was facilitated by repeatedly pipetting the trypsin-EDTA over the surface of each well, helping to generate a single cell suspension. The supernatant was transferred to the harvest tube. Immediately, 2mL of IMDM/2% FCS was added to the LTC-IC well, swirled gently and transferred to the harvest tube. A further 2mL of HBSS-CMF was added to the well and swirled gently before being transferred to the harvest tube. The harvest tubes were then centrifuged at 1000rpm for 10 minutes. Following this, the supernatant was gently poured off and the cells resuspended in the remaining supernatant. The volume of the remaining cell suspension was noted and a cell count performed.

2.4.3.1 CFC assay

Duplicate committed progenitor cell assays were set up for each cell volume of each treatment condition at two different cell concentrations - $2.5x10^4$/mL and $5x10^4$/mL. The appropriate volume of cell suspension for duplicate wells was added to 2mL of Methocult™ methylcellulose medium for committed progenitor cell assays. The cell suspension and Methocult™ medium were thoroughly mixed and 1mL of this mixture was added to a 35mm tissue culture dish. The dish was then gently swirled, so that the bottom of the dish was completely coated, and then incubated for 14 days at 37℃, 5% CO_2. At the end of this time, the number of viable colonies was counted in each dish and this allowed a comparison of the LTC-IC present in the different treatment conditions.

In experiments where CFC assays were performed alone (without LTC-IC), exactly the same methodology (described directly above) was carried out.

2.4.4 Dual-colour fluorescence in situ hybridisation

CML cells, pre- and post-culture, and colonies from LTC-IC experiments were assessed for the presence of BCR-ABL by dual-colour fluorescence in situ hybridisation (D-FISH). Aliquots of at least 5000 cells were transferred to a 1.5mL eppendorf, washed in PBS/2% FCS and re-suspended in 500μL pre-warmed (37℃) hypotonic solution (0.075M potassium chloride). Samples were then incubated at room temperature for 20 minutes. One hundred microlitres of freshly made fixative (methanol:acetic acid [3:1]) was added to the cells and the samples were incubated for a further 5 minutes at room temperature. The cells were then centrifuged at 5000rpm for 5 minutes; the supernatant removed and a further 500μL fixative added, the cells incubated for a further 5 minutes and then centrifuged for 5 minutes. This step was repeated a further twice. The cell pellet was finally resuspended in 50μL of fixative and then stored at -20℃ prior to further preparation for D-FISH.

Aliquots of 20μL of cell solution were spotted onto multi-spot microscope slides previously coated with poly-L-lysine and air-dried overnight. The prepared slides were wrapped in parafilm and stored at -20℃ until D-FISH was performed with the LS1 *BCR-ABL* Dual Colour, Dual Fusion translocation probe according to the manufacturer's instructions. Interphase nuclei were evaluated using a Leica fluorescence microscope with a triple band pass filter for DAPI, Spectrum Orange and Spectrum Green. All D-FISH slides were prepared and scored by Mrs Elaine Allan.

2.5 Flow Cytometry

Flow Cytometry also known as FACS is a quantitative technique that permits the visualisation and sorting of cells by multiple parameters according to their fluorescence. A flow cytometer can also measure the size of a cell using forward-angle light scatter (FSC) and the granularity of a cell using side-angle light scatter (SSC). Therefore, in comparison to spectrophotometry, flow cytometry allows the measurement of fluorescence per cell, hence allowing accurate analysis of single cells. All the flow cytometric analyses were carried out on a Becton Dickinson FACSCanto.

2.5.1 Intracellular antibody staining

First, $5x10^4$ -$1x10^5$ cells were resuspended in 100µL of fixing reagent (reagent A) from the Fix & Perm® Cell Permeabilisation kit and incubated for 15 minutes. The cells were then washed with PBS, the supernatant completely removed using a graduated pipette and the cell pellet resuspended in 50µL permeabilising reagent (reagent B) from the Fix & Perm® Cell Permeabilisation kit. To this the appropriate volume of intracellular antibody was added (anti-active-caspase-PE; 1:10 dilution) and the cells incubated for 45 minutes at room temperature in the dark. Finally the cells were washed twice in PBS (1200rpm for 5 minutes) prior to FACS analysis.

2.5.2 Assessment of phospho-proteins by flow cytometry

There is no specific antibody that is able to detect the activity of BCR-ABL.

However, it is known that one of the prominent downstream substrates constitutively phosphorylated by the BCR-ABL oncoprotein is the 39-kDa adaptor protein CrkL. It has previously been shown that CrkL phosphorylation is inhibited in a concentration dependent manner when CML cells are treated with IM, correlating with BCR-ABL phosphorylation (130).

The rabbit anti-human phospho-CrkL (p-CrkL) antibody used for this assay detected endogenous levels of CrkL only when it was phosphorylated at tyrosine 207 - the BCR-ABL phosphorylation site. Measuring the difference in the geometric mean fluorescence intensity (MFI) of p-CrkL peaks between drug-treated samples and untreated controls, determined the effect of the treatments on the inhibition of BCR-ABL. Samples for analysis of p-CrkL levels were prepared by permeabilisation and staining using the Fix & Perm® Cell permeabilisation kit as above (Section 2.5.1), but with minor modifications. Following fixation with 100µl fixing reagent, the cells were resuspended in 25µl of permeabilising reagent with 2.5µl of the p-CrkL antibody for 40 minutes. The cells were washed twice and resuspended in 100µl fix perm wash with 2µl of the secondary anti-rabbit IgG FITC conjugate (1: 50 dilution), or 10µl of the secondary anti-rabbit IgG PE conjugate (1: 10 dilution) and incubated at room temperature in the dark for 30 minutes. Different secondary antibodies were added depending on the requirements for multi-parametric FACS. For example, in non CFSE-stained cells, anti-rabbit IgG FITC conjugated secondary antibody was used, whereas in $CFSE^{+}$ cells, anti-rabbit IgG PE conjugated secondary antibody was used. Following incubation, the cells were then washed twice and then analysed immediately by flow cytometry.

The amount of p-CrkL in an untreated CML sample was assessed as the geometric MFI of the cell sample minus the geometric MFI of the isotype control. The p-CrkL status of the drug-treated samples was expressed as a percentage of the untreated control (100%).

Assessment of phospho-STAT5 (p-STAT5) was carried out in exactly the same way, except the p-CrkL primary antibody was replaced by the p-STAT5 antibody at the same concentration

2.5.3 High resolution cell cycle analysis

Differing culture and treatment conditions may alter progression of cells through the cell cycle. Therefore, it was important to determine the effects of the different treatment conditions on progression of CML cells through the cell cycle.

Ki67 is an antigen present in the nuclei of cells which are in the active phases of cell cycle - G_1, S/G_2 and M - and is not expressed in G_0 cells. The precise function of Ki67 still remains unclear, however, since it is only present in proliferating cells (normal and malignant) (285); it has become a widely accepted marker for cellular proliferation. 7AAD is a fluorescent compound with a strong affinity for DNA, which has been used in chromosome analysis, cell cycle studies and, most commonly, to quantify apoptosis. Using the Ki67 stain in conjunction with an intercalating DNA stain such as 7AAD, allows for a high resolution of cell cycle analysis, as it distinguishes between the different phases of cycling cells (286). G_0 cells can be identified as they have low DNA content and are negative for Ki67. Cells in G_1 phase have the same DNA content; however, begin to express low amounts of Ki67. Both DNA content and Ki67 expression increase within cells from S and G_2 phases and staining is maximal in mitosis. Since LSCs exist within G_0 phase of cell cycle, this staining technique has also proven invaluable for the discovery and isolation of primitive, quiescent malignant cells in CML (224).

Approximately $3x10^5$ cells were washed in PBS (1200rpm for 5 minutes), the supernatant discarded and then resuspended in 500µL of PBS/0.4% formaldehyde for fixing and incubated for 30 minutes on ice. Following this, 500µL of PBS/0.2% Triton-X-100 was added to permeablise the cells, which were then incubated overnight at 4℃. The following morning, the cells were washed once in PBS and then resuspended in 1mL PBS. The cell suspension was then divided equally between two FACS tubes (500µL each) and either 20µL of Ki67-FITC labelled

antibody or 20µL of FITC isotype control was added to the tubes. The cells were then vortexed and incubated for 40 minutes at room temperature in the dark. After one further wash, the cells were resuspended in 1mL PBS and 5µL of 7AAD (1µg/mL) was added and then incubated for at least 6 hours, but preferably overnight, at 4℃ prior to FACS analysis. Before FA CS analysis, the cells were washed once in PBS. To separate the cells from debris, the cell population was gated on using FSC versus FL3. The gated population was then analysed in FL1 versus FL3 and this allowed the relative percentages of cells at each stage of the cell cycle.

2.5.4 FACS for CFSE experiments

CFSE stained cells were surface stained as described in Section 2.4.1. Flow cytometry analysis of CFSE-stained cells was performed at baseline to determine the position of the undivided peak and confirm uniform staining of the cell population (which allowed resolution of the peaks at subsequent analyses), and again at the time-points stated for each set of experiments. Isotype controls were used to correctly set the detectors, so that the negative isotype population was placed in the first log decade for each flow cytometry channel. A CFSE positive control was then run and the compensation adjusted. Because CFSE is a very bright fluorescent stain which has substantial spectral overlap into other FACS channels, considerable levels of compensation were required.

2.5.4.1 Calculation of the undivided (CFSEmax) cell population

To determine the anti-proliferative effect of different treatment conditions and assess the size of the non-proliferating primitive progenitor population, the percentage recovery of viable CML cells in the undivided population remaining after culture was assessed. At each analysis time-point, the number of viable cells

harvested from each culture condition was recorded, as was the percentage of CML cells found in the undivided fraction (CFSEmax). Percentage recovery of input cells in the undivided peak could then be calculated by dividing the absolute number of CFSEmax CML cells by the total number of input CML cells and multiplying by 100%. This allowed direct comparison of different treatment conditions on the non-proliferating primitive progenitor population.

2.5.5 Assessment of apoptosis and necrosis

For analysis of cell death, cells were incubated with 5μL annexin-V-FITC and 10μL viaprobe in 100μL annexin buffer for 15 minutes in the dark. The cells were then topped with 300μL annexin buffer and read by flow cytometry within the hour to identify necrotic (viaprobe detected in FL-3) and apoptotic (annexin-V detected in FL1) cells.

2.6 Western blotting

The Western blot, alternatively known as the protein immunoblot, is an analytical technique used to detect specific proteins in a given cell sample. A specific protein can be identified after fractionation on either one or two dimensional gels, by exposing all proteins present to a specific antibody coupled to an easily detectable enzyme such as HRP, a radioactive isotope or fluorescent dye. This is done after the proteins separated on the gel have been transferred or ‘blotted’ onto a membrane - typically nitrocellulose paper or polyvinylidene fluoride (PVDF) as this is more robust than the gel.

2.6.1 Preparation of protein lysate

The RIPA lysis buffer was prepared immediately prior to use. Equal cell numbers from different treatment conditions were washed twice with ice cold PBS (1200rpm

for 5 minutes). The cells were then transferred to a 1.5mL eppendorf and washed again in ice cold PBS (3000rpm for 5 minutes in a bench-top micro-centrifuge). The lysis buffer was added to the cells (50µL per 1-3x10^5 cells), mixed by pipetting up and down and incubated for 15 minutes on ice. Following this incubation, the cells were gently vortexed and then spun at 14,000rpm for 10 minutes at 4℃ to clarify the supernatant which was then saved as a protein lysate and stored at -20℃ until use.

2.6.2 Protein quantification

Protein quantification was performed using the bicinchoninic acid (BCA) method for colorimetric detection and quantification of total protein according to the manufacturers' instructions. This method utilises the reduction of Cu^{2+} to Cu^{1+} by protein in an alkaline medium (the biuret reaction with the colorimetric detection of the cuprous cation (Cu^{1+}) using a reagent containing BCA (287). The purple reaction product of this assay is formed by chelation of one cuprous ion with two molecules of BCA. The water-soluble complex exhibits a strong absorbance at 562nm that is nearly linear over a broad range of protein concentrations (20-2000µg/mL)

First the BSA standards were prepared. BSA was dissolved in 0.9% saline to give a concentration of 2mg/mL. Serial dilutions of this stock were then made to produce a concentration gradient for the controls. The following concentrations of BSA control were prepared: 1500; 1000; 750; 500; 250; 125; 50; 25; 5µg/mL and a blank (dH_2O). The controls were then stored at -20℃ for use on multiple occasions. To prepare the assay, 25µL of each control was pipetted onto the well of a 96-well plate in duplicate. Protein lysate (5µl) was added to 20µL of PBS in duplicate test wells. BCA solutions A and B were mixed in a 50:1 ratio (A:B) and

200μL of the BCA mixture was added to each well. The 96-well plate was then incubated at 37℃ for 30 minutes and the plate was read using an enzyme-linked immunosorbent assay (ELISA) plate reader according to the manufacturers' instructions. This allowed accurate protein quantification so that equal amounts of protein could be compared in Western blotting.

2.6.3 Sodium dodecyl sulphate-polyacrylamide-gel electrophoresis

Sodium dodecyl suphate-polyacrylamide gel electrophoresis (SDS-PAGE) is a denaturing separation method commonly used to analyse protein samples, which uses a highly cross-linked gel as the inert matrix through which the proteins migrate. The proteins are in solution that includes SDS, a negatively charged detergent, which binds to hydrophobic regions of the protein molecules, causing them to unfold into long polypeptide chains and become freely soluble in the solution. A reducing agent such as β-mercaptoethanol is also added to break any disulphide bonds present in the proteins, so that all the constituent polypeptides can be analysed separately. Each protein molecule binds many of the negatively charged detergent molecules, which masks the protein's inherent positive charge. An electric current is then applied, resulting in migration of the protein towards the positive electrode. The direction, distance, and speed of migration are dependent on the size and shape of the polypeptides and the pore-size of the gel matrix; with smaller polypeptides travelling more rapidly through the gel. Common gel materials are agarose (a polysaccharide) and acrylamide (a 3-carbon amide which is polymerized to form long chains with cross-links between the chains). The pore size of the gel is influenced by the percentage of gel material used and, in the case of acrylamide, the amount of cross-linking.

To perform SDS-PAGE, equal volumes of protein lysate and Laemmli 2x sample buffer were mixed together in a 1.5mL eppendorf and then heated to 95℃ for 5 minutes. The samples were then loaded onto a 4-15% gradient gel. Ten microlitres of rainbow ladder marker was loaded onto a lane of the gel to allow determination of protein size. The gel was electrophoresed in a 1xTGS running buffer for 90 minutes at 120V using the Bio-rad Mini-PROTEAN^{TM} electrophoresis system.

2.6.4 Transfer to nitrocellulose membrane

The protein bands were then transferred from the gel to the nitrocellulose membrane. Sponges, blotting paper and nitrocellulose membrane were first soaked in transfer buffer and the transfer sandwich was prepared as shown in Figure 2-4.

Figure 2-4 Preparation of transfer sandwich for wet transfer of protein from gel to nitrocellulose membrane

The sandwich then underwent electrophoresis for 1 hour at room temperature at 80V.

2.6.5 Immunolabelling

After transfer, the nitrocellulose membrane was briefly washed in TBS-T and blocked in blocking buffer, with shaking at room temperature for 1-2 hours. Following this, the blocking buffer was discarded and the membrane incubated with the primary antibody solution (p-CrkL, LC3B, GAPDH; p-S6K; 1:1000 dilution in blocking buffer) overnight at 4℃ with gentle ag itation. The following morning, the nitrocellulose membrane was washed twice (15 minutes per wash) in TBS-T and then incubated with anti-rabbit HRP-conjugated secondary antibody (1:3000 dilution) in blocking solution for 1 hour at room temperature with gentle agitation. The membrane was then washed twice (15 minutes per wash) in TBS-T and then developed with the Immun-star ECL reagents A and B (first diluted 1:2) and developed directly using a Biorad Molecular Imager ChemiDoc XRS$^+$ System.

2.6.6 Stripping and reblotting

The Re-Blot Plus Strong stripping solution was diluted 1:10 with distilled water. The nitrocellulose membrane was then incubated in the stripping solution for 10-15 minutes and then washed twice (5 minutes per wash) in TBS-T. The membrane was then re-blocked for 1 hour, prior to being incubated with another antibody. This allowed the re-blotting of the membrane 3-4 times.

2.7 ELISA for the measurement of p-Tyr

Whole cell protein lysates were prepared from 10^5-10^6 cells according to Section 2.6.1. Lysates were diluted in carbonate-bicarbonate coating buffer, added to each well of an Immulon II HB 96-well flat bottom ELISA plate in triplicate (5µg protein in 100µl carbonate-bicarbonate buffer/well) and plates were then incubated at 4℃, with shaking, overnight. Following incubation, plates were washed with TBS-T four times, surfaces were blocked with 100µl of blocking buffer (except those wells

reserved for chromagen blanks) and plates incubated for 1 hour at room temperature with shaking. Plates were then washed as previously and incubated with 100µl per well of 1:1000 4G10 anti-p-Tyr antibody or 1:500 anti-GAPDH in blocking buffer for 2 hours at room temperature on a shaker. Plates were washed with TBS-T four times and incubated with 100µl per well of 1:1000 anti-mouse IgG-HRP secondary antibody (anti-P-Tyr samples) or 1:1000 anti-rabbit IgG-HRP secondary antibody (anti-GAPDH samples) for 1 hour at room temperature on a shaker. Plates were then washed four times with TBS-T, 100µl of chromagen substrate (tetramethylbenzidine) was added to each well and plates incubated for 20 minutes in the dark. The reaction was stopped by adding 50µl of 2N HCl and plates were then read at 460nm absorbance on an ELISA plate reader.

Negative control wells were included in the assay (lysate only and antibody only) and these values were subtracted as background, where indicated, from each relevant test well.

2.8 mRNA transcript measurement and mutation analysis

2.8.1 RNA synthesis

Total RNA was isolated from pellets using the RNeasy Mini Kit according to the manufacturer's instructions. The resulting RNA was quantitated using a nanodrop spectrophotometer Nd-1000 (Labtech International, East Sussex, UK). An absorbance at 260nm quantified nucleic acid and the ratio of 260/280 determined purity (pure RNA ratio is 2.0).

2.8.2 cDNA synthesis

RNA was synthesised to cDNA by the High Capacity cDNA Archive kit according to the manufacturer's instructions.

2.8.3 qRT-PCR using Taqman

The TaqMan probe principle relies on the 5´-3´ nuclease activity of Taq polymerase to cleave a dual-labelled probe during hybridization to the complementary target sequence. As in other qRT-PCR methods, the resulting fluorescence signal permits quantitative measurements of the accumulation of the product during the exponential stages of the PCR; however, the TaqMan probe significantly increases the specificity of the detection. TaqMan probes consist of a reporter fluorophore covalently attached to the 5'-end of the oligonucleotide probe and a quencher at the 3'-end (Figure 2-5). The quencher molecule quenches the fluorescence emitted by the reporter fluorophore via Fluorescence Resonance Energy Transfer (FRET), when excited by the thermal cycler's light source. As long as the reporter and the quencher are in proximity, quenching inhibits any fluorescence signals. The probes anneal within a DNA region amplified by a specific set of primers. As the Taq polymerase extends the primer and synthesises the nascent strand, the 5' to 3' exonuclease activity of the polymerase degrades the probe that has annealed to the template. Degradation of the probe releases the fluorophore from it and breaks the close proximity to the quencher, thus relieving the quenching effect and allowing fluorescence of the reporter fluorophore. Hence, fluorescence detected in the RT-PCR thermal cycler is directly proportional to the fluorophore released and the amount of DNA template present in the PCR.

The mRNA levels of cyclin D1 and the endogenous reference gene GAPDH were measured using the ABI PRISM 7900HT sequence detector (Applied Biosystems (ABI), Warrington, U.K.). The cyclin D1 PCR products were detected using a probe containing a 6-carboxyfluorescein (FAM) reporter and tetramethylrhodamine (TAMRA) quencher. For the GAPDH reaction VIC replaced FAM. The cyclin D1

and GAPDH mRNA levels were measured using the pre-developed Taqman Gene Expression Assays (primer and probe mix). For each reaction, 2.5µl of cDNA was used as template and added to 6.25µl q-PCR Mastermix Plus, 0.62µl of relevant Taqman Gene Expression Assay and made to a total volume of 12.5µl with PCR-grade water. Each reaction was carried out in triplicate. Samples were run on the ABI PRISM 7900 with the following reaction conditions: 50℃ for 2 minutes, 95 °C for 10 minutes followed by 40 cycles of 95℃ for 15 seconds and 60℃ for 1 minute. The levels of cyclin D1 were calculated using the validated $2^{-\Delta\Delta CT}$ method to calculate the relative expression.

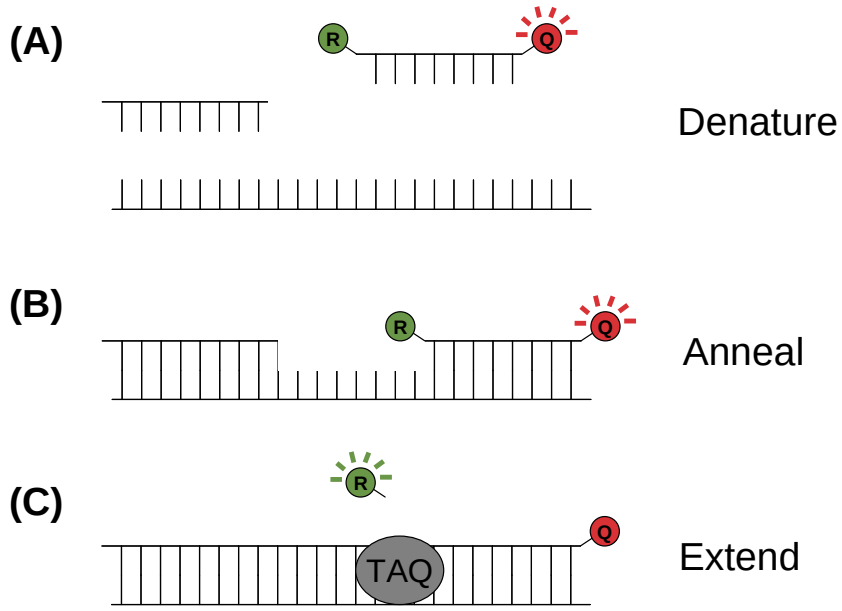

Figure 2-5 Schematic diagram on the mechanism of Taqman qRT-PCR

(A) While the probe is attached or unattached to the template DNA and before the polymerase acts, the quencher (Q-fluorophore) reduces the fluorescence from the reporter (R-fluorophore). (B) Following denaturation, both the TaqMan® probe and the primers anneal to the specific target DNA, allowing *Taq* polymerase to create a complementary strand. (C) *Taq* polymerase then adds nucleotides and removes the Taqman® probe from the template DNA. This separates the quencher from the reporter, and allows the reporter to emit its energy which is then quantified using a computer.

2.8.4 RT-PCR and BCR-ABL kinase domain mutation analyses

Quantitative RT-PCR to amplify *BCR-ABL* fusion transcript was performed according to Standardised EAC (European Against Cancer) protocols previously described (288). The final results are expressed as *BCR-ABL*/*ABL* ratios in percent according to the international scale (244). The mutation was detected by direct sequencing (on both strands) according to the methods described by Branford et al. (239) with some modification (289). *BCR-ABL* transcript measurement and mutation analysis was performed by Dr Sandrine Hayette, Hôpital Lyon, Lyon, France.

2.9 Immunofluorescence

2.9.1 Fixing cell samples onto multi-spot slides

Cells were washed in PBS/2% FCS and pellet resuspended in PBS. Twenty thousand cells were added to each relevant well of a poly-L-lysine-coated multi-spot slide and cell samples were added in duplicate. Samples were allowed to adhere to the slides for 90 minutes at room temperature. Following this, the excess PBS was gently removed and 30μL of the 3.65% formaldehyde solution was added per well, in order to fix the cells. The slides were then incubated for 20 minutes at room temperature and then washed twice, 5 minutes each in PBS. The slides were then either antibody-stained straight away or stored at 4℃ in a humidified chamber (with enough PBS to cover the cells on the slides) until required for immunofluorescence (IF) analysis.

2.9.2 Intracellular antibody-staining for IF

All slides were first air-dryed until no moisture remained and 30μL of the 0.5% Triton-X-100 solution was added per well, in order to permeablise the cells. The slides were then incubated for 10 minutes at room temperature and then washed twice, 5 minutes each in PBS. Following this the slides were dried and each spot was blocked with 30μL blocking buffer for 1 hour at room temperature. The blocking buffer was then gently soaked away with a tissue and antibody (LC3B or FoxO3a) at a concentration of 0.5μg/mL in blocking buffer was added to each relevant well. Thirty microlitres of anti-rabbit IgG (Abcam) (0.5μg/mL in blocking buffer) was added to the two wells reserved for isotype control. The slides were then incubated for 90 minutes at room temperature. Following incubation, the slides were washed 4 times with PBS (5 minutes per wash). The slides were then incubated with anti-rabbit-Alexa Fluor 488 secondary antibody (1μg/mL in blocking buffer; 30 μL per spot) for 1 hour at room temperature. Following incubation, the slides were washed 4 times with PBS (5 minutes per wash) and then air-dryed until no moisture remained. Two drops of VECTASHIELD® mounting medium with DAPI were added to the centre of each slide and a coverslip was placed on the top. The coverslip was carefully pushed down, so that the mounting medium spread over each well of the slide and was then sealed with nail varnish. The slides were stored at 4℃ until analysis.

All slides were analysed using a Zeiss Imager M1 microscope at 100x magnification using oil immersion and Axiovision software.

2.10 EM

CML cells ($2x10^5$-$1x10^6$) were pelleted in a 1.5mL eppendorf (1000rpm; 5 mins) immediately prior to fixation. One millilitre of fixing solution for EM (Section 2.2.4.10) was added, without resuspending pellet and the samples were left to incubate for 1 hour. The fixing solution was then carefully removed, without disturbing the pellet, and replaced with 1mL 0.1M sodium cacodylate solution, as a rinse. The cells were then post-fixed with 1mL post-fixation solution for EM (Section 2.2.4.11) for 1 hour. After 3 changes in distilled water (10 minutes each), specimens were stained with 1mL 5% uranyl acetate, and embedded in Taab epoxy resin. Sections (100nm) were stained with aqueous 2% uranyl acetate for 10 minutes and viewed on 300-mesh formvar-coated grids by zero-loss imaging on a LEO 912 AB energy filtering transmission electron microscope (Olympus).

All EM procedures were performed by Dr David Dinsdale from the microscopy facility at the University of Leicester, Leicester, UK.

2.11 Statistics

The results are shown as the mean ± standard error values unless otherwise stated. All statistical analyses were performed using the Student's T-test on the Graph Pad prism software package. A level of $p<0.05$ was deemed significant.

3. RESULTS (I) Optimisation of methods to assess BCR-ABL activity in Ph^+ cell lines and primary CML cells

There is now an expanding set of scenarios in which the ability to accurately assess degrees of BCR-ABL inhibition by TKIs, either in the laboratory or in patient samples, would be extremely valuable. With the development of second generation TKIs, including dasatinib (264), nilotinib (251) and bosutinib (260), clinicians would like to be able to predict response for individual patients at diagnosis, or at the time of a proposed change in therapy, in order to select the agent with the best chance of success. Great progress has been made in this application by the group of Tim Hughes (290). Here, the group have demonstrated that the IC_{50} of IM, determined by Western blotting for the level of inhibition of phosphorylation of CrkL, on peripheral blood from individual patients, was highly predictive of molecular response to IM therapy.

Since its introduction, a minority of patients have developed resistance to IM. For the individual patient with IM-resistant disease, methods to select the TKI likely to produce maximal BCR-ABL inhibition would be beneficial. Schultheis et al. (291) have developed a FACS-based assay that demonstrated differences in total p-Tyr inhibition by IM between $CD34^+$ cells from cytogenetic responders and non-responders to IM treatment. Our own group have since developed another rapid method for the detection of p-CrkL in CML cell lines, cell lines with known BCR-ABL mutations and human primary CML cells, at the single cell level by flow cytometry (130). This method also appeared to be predictive of response to IM therapy. Figure 3-1 shows the p-CrkL profiles of two patients' CML $CD34^+$ cells cultured in the presence and absence of 5μM IM for 16 hours. Panel A

demonstrates the p-CrkL profile of a CML patient who did not respond optimally to IM treatment (i.e. did not achieve any degree of cytogenetic response by 6 months). It was observed that the IM-treated $CD34^+$ CML cells showed no reduction in p-CrkL, consistent with the presence of IM-resistant cells. Panel B shows a representative p-CrkL profile of a CML patient who responded well to IM treatment (i.e. CHR by 4 weeks and CCR by 6 months). Following IM treatment, there was only 7% phosphorylation of CrkL in IM-treated $CD34^+$ CML cells, relative to no drug control (100%), indicating that most of the cells were sensitive to IM.

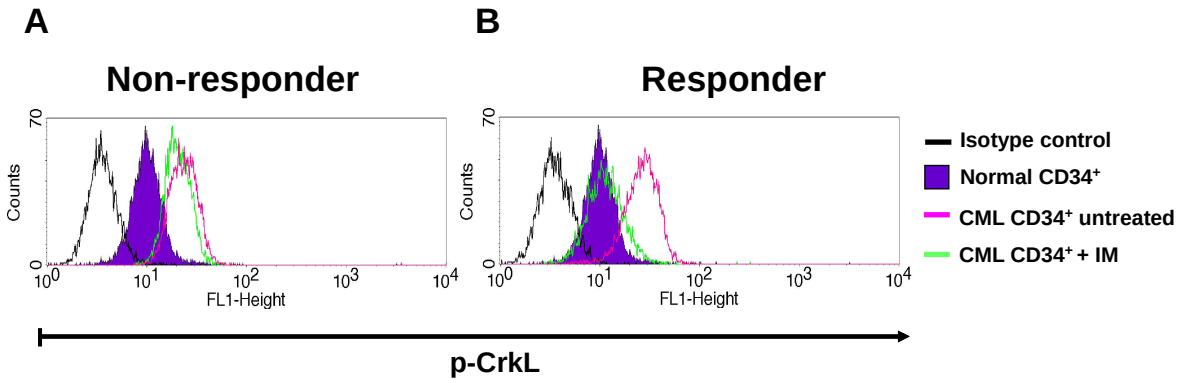

Figure 3-1 The effect of IM treatment on BCR-ABL activity within $CD34^+$ CML cells as measured by flow cytometry

$CD34^+$ CML cells were cultured ± 5μM IM for 16 hours, before p-CrkL levels were determined by FACS and compared to the levels obtained from normal $CD34^+$ cells at baseline. Panels A and B demonstrate the p-CrkL profile from a 'non-responder' and 'responder' to IM, respectively.

To fully understand the mechanism(s) of resistance in CML stem cells it is essential to be able to measure inhibition of BCR-ABL activity at the stem cell level and using very small cell samples. The phosphorylation of proteins in signal transduction is traditionally studied by means of techniques such as ELISA, which

reliably provide information regarding homogeneous or purified cell populations. Hence, to further investigate the potential methods for the measurement of BCR-ABL activity, the following studies were designed for the:

1. Development of a novel ELISA method for the detection of BCR-ABL activity in CML cells
2. Comparison of the ELISA method with established techniques for the measurement of BCR-ABL activity in CML cells

3.1 Development of a novel ELISA method for the measurement of BCR-ABL activity in CML cells

3.1.1 Comparison of plastics for use in a novel ELISA assay for the determination of BCR-ABL activity in CML cells

To further explore alternative methods for assessment of BCR-ABL, a novel ELISA method was developed. Initially, 96-well plates from two different companies (Greiner bio-one and Thermo Fisher Scientific) were tested for their suitability for the ELISA method. For Western blot, 10μg of protein is generally added per lane and the blot probed with a 1:1000 dilution of relevant antibody. Therefore, for this preliminary ELISA, each well of an ELISA plate was first coated with 10μg of K562 protein lysate and a 1:1000 dilution of p-Tyr antibody in 5% BSA/TBST was added to each relevant test well. Absorbance was then read at 460nm using an ELISA plate reader. Figure 3-2 shows that the ELISA plate from Greiner bio-one gave the best discrimination in absorbance between the test wells (lysate + Ab) and background (no lysate + Ab and lysate - Ab), with a significant difference between the two different plates ($p= 0.032$). Therefore, the 96-well ELISA plates from Greiner bio-one were used for all subsequent experiments.

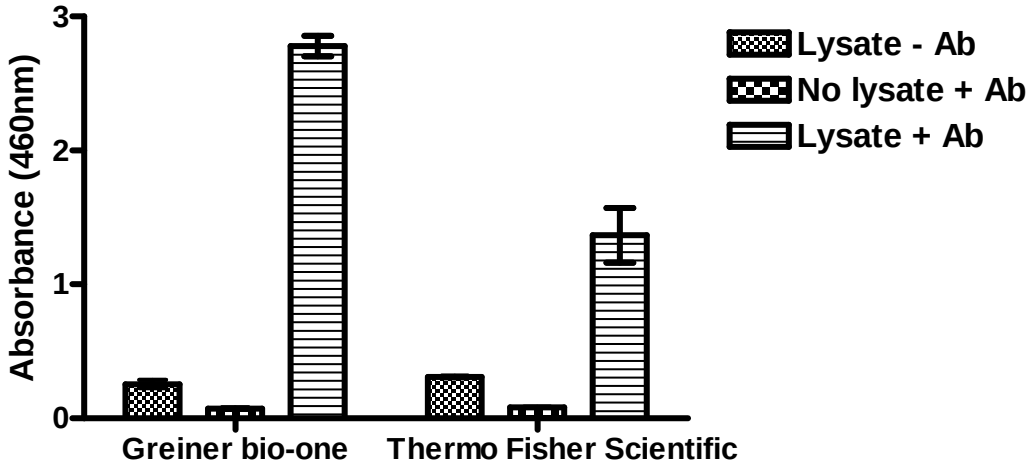

Figure 3-2 Comparison of plastics for use in a novel ELISA assay for the determination of BCR-ABL activity in CML cells

ELISA plates from indicated companies were coated with 10µg of protein lysate from K562 cells and p-Tyr antibody was added to each relevant test well in triplicate (p=0.032). Negative controls were included- lysate without antibody and no lysate with antibody. Absorbance was read at 460nm. [Ab: antibody]

3.1.2 Optimisation of blocking solution for use in a novel ELISA method

Next, different buffers were tested to determine the optimal blocking solution for the p-Tyr antibody for use in the novel ELISA method. Each well of the ELISA plates were first coated with 10μg of protein lysate from K562 cells and blocked in either 5% BSA/TBST or 5% MILK/TBST, with a 1:1000 dilution of p-Tyr antibody in either 5% BSA/TBST or 5% MILK/TBST added to each relevant test well in triplicate. Figure 3-3 demonstrates that the 5% BSA/TBST blocking buffer gave the greatest discrimination in absorbance between the test wells and background, with a significant difference observed between the two buffers (p=0.037). Therefore, the 5% BSA/TBST blocking buffer was used in the ELISA for all subsequent experiments.

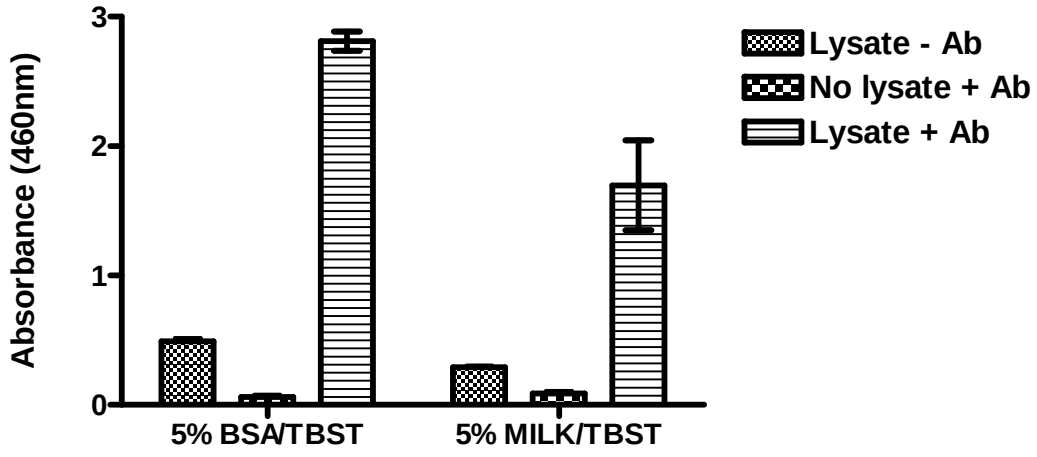

Figure 3-3 Optimisation of blocking solution for use in a novel ELISA method

ELISA plates were coated with 10μg of protein lysate from K562 cells and blocked in either 5% BSA/TBST or 5% MILK/TBST, with a 1:1000 dilution of p-Tyr antibody in either 5% BSA/TBST or 5% MILK/TBST added to each relevant test well in triplicate (p=0.037). Negative controls were included- lysate without antibody and no lysate with antibody.

3.1.3 Antibody and protein concentration titration for optimal use in a novel ELISA method

Since cellular material is limited when working with primitive populations of primary CML cells, it is important to be as efficient with the protein lysate as possible. Furthermore, since antibodies are relatively expensive it is also essential that they are not wasted unnecessarily. Therefore an ELISA was performed using different concentrations of protein lysate and probed with different concentrations of the p-Tyr antibody. ELISA plates were first coated with either 1μg (A), 5μg (B) or 10μg (C) of K562 protein lysate, before the indicated concentrations of p-Tyr were added to the plate in triplicate (Figure 3-4). Both 5 and 10μg of K562 protein lysate were found to give significantly increased absorbance levels as compared to 1μg of lysate ($p= 0.0007$ and 0.0011 for 1:2000 dilution; $p= 0.0005$ and 0.0029 for 1:1000 dilution; $p= 0.0023$ and 0.0053 for 1:500 dilution and $p= 0.0009$ and 0.0005 for 1:250 dilution for 1μg versus 5μg and 10μg of K562 protein lysate, respectively). Each of the antibody concentrations consistently gave absorbance levels of over 2.0 units using both 5 (B) and 10μg (C) of protein lysate. Therefore, it was decided that 5μg of protein lysate per well, using the lowest antibody concentrations would be sufficient to give effective p-Tyr absorbance readings. However, since K562 cells express multiple copies of BCR-ABL and hence, have much higher TK activity than human primary CML cells, it was thought best to err on the side of caution in terms of the amount of p-Tyr antibody used.

Therefore, in order to give the best results, whilst also being as economical as possible with both the amount of protein and antibody used, it was decided that the optimal conditions for the ELISA were a 1:1000 dilution of p-Tyr antibody, using 5μg of protein lysate.

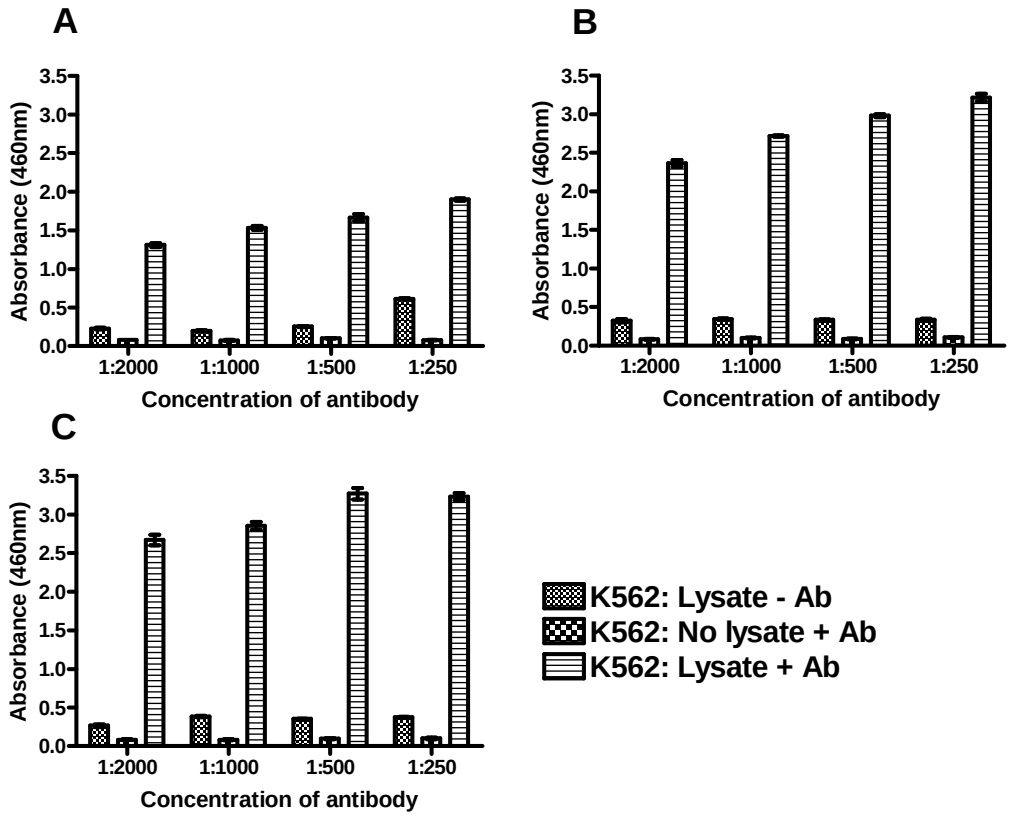

Figure 3-4 Antibody and protein concentration titration for optimal use in a novel ELISA method

ELISA plates were first coated with either 1µg (A), 5µg (B) or 10µg (C) of K562 protein lysate, before the indicated concentrations of p-Tyr were added to the plate in triplicate. Negative controls were included- lysate without antibody and no lysate with antibody. Absorbance was read at 460nm.

3.1.4 Comparison of antibodies for optimal use in a novel ELISA method

As the measurement of total tyrosine phosphorylation is not entirely specific to BCR-ABL, other antibodies were also tested in the ELISA method. Anti-p-ABL and anti-p-CrkL were compared to the anti-p-Tyr antibody, for the measurement of BCR-ABL activity within the Ph^+ cell line, K562, in 3 replicate experiments. As shown in Figure 3-5, the anti-p-Tyr antibody gave the best discrimination in absorbance between Ph^+ cells against background (p= 0.015 and 0.016 for p-Tyr versus p-CrkL and p-Abl, respectively). Therefore, this antibody was used in the ELISA for all subsequent experiments.

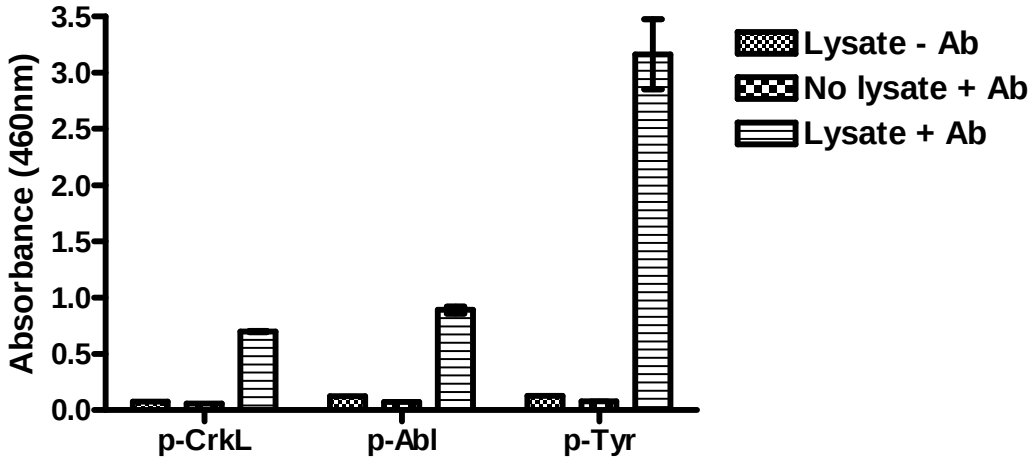

Figure 3-5 Comparison of antibodies for optimal use in a novel ELISA method

Activity was measured in K562 cells by ELISA using the indicated antibodies, in triplicate (p= 0.015 and 0.016 for p-Tyr versus p-CrkL and p-Abl, respectively).

3.1.5 Confirmation of effective protein-coating in a novel ELISA method

In order to confirm good reproducibility of protein coating, several ELISAs were initially performed using anti-GAPDH antibody. Figure 3-6 demonstrates that the results were very consistent, with an average reading of 1.59 absorbance units (460nm) (n=6) (range: 1.5253 - 1.6439; coefficient of variation: 5.24%) per 5μg of protein per well from K562 cells and an average reading of 1.57 absorbance units (460nm) (n=6) (range: 1.455 - 1.674; coefficient of variation: 5.54%) per 5μg of protein per well from HL60 cells. No significant difference was observed between the two cell lines (p=0.595). This, therefore, confirmed good protein-coating efficacy and to save on cell samples, the following ELISAs were conducted using the anti-p-Tyr antibody only.

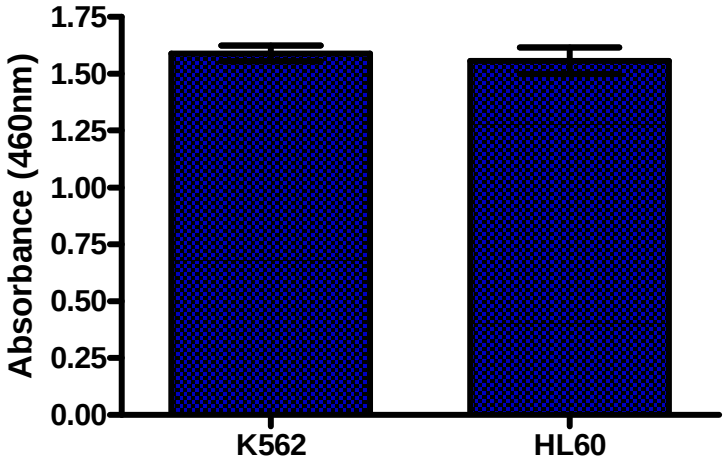

Figure 3-6 Confirmation of effective protein-coating in a novel ELISA method

GAPDH levels were measured in K562 and HL60 cells by ELISA in 6 replicates.

3.1.6 Assessment of p-Tyr in BCR-ABL positive and negative cell lines using a novel ELISA method

The ELISA was further tested using other Ph^+ BC CML cell lines, LAMA84 and BV173, in comparison with K562 cells and also the Ph^- cell line, HL60 (Figure 3-7). The results were very consistent between the Ph^+ cell lines. The anti-p-Tyr antibody produced absorbance readings of >3 absorbance units (460nm) for all Ph^+ cell lines, whereas the reading was around 0.5 absorbance units (460nm) for the Ph^- cell line, HL60. Further negative controls which consisted of lysate without antibody and antibody without lysate, consistently gave readings of <0.5 absorbance units (460nm).

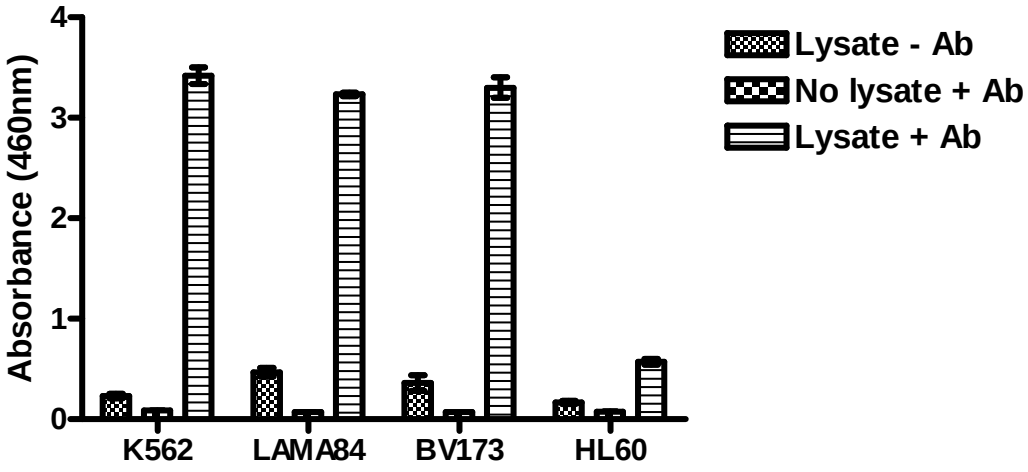

Figure 3-7 Assessment of p-Tyr in BCR-ABL positive and negative cell lines using a novel ELISA method

Total p-Tyr status was measured by ELISA for each of the cell lines, in triplicate.

3.1.7 The effect on total p-Tyr levels upon drug treatment of K562 and HL60 cell lines measured by ELISA

The ELISA's ability to detect changes in p-Tyr levels in CML cells following TKI treatment was next investigated. K562 and HL60 cells were first treated for 16 hours with either IM or dasatinib and p-Tyr was measured by ELISA. Figure 3-8 shows that in response to increasing concentrations of TKI, the absorbance readings decreased in K562 cells, reaching the background level of HL60 cells with 5μM IM and 150nM dasatinib treatment ($p=0.000794$ for no drug versus 1μM IM; $p=0.000646$ for no drug versus 2.5μM IM; $p=0.000218$ for no drug versus 5μM IM; $p=0.000381$ for no drug versus 10nM dasatinib and $p=0.000274$ for no drug versus 150nM dasatinib). As expected, neither IM nor dasatinib reduced the absorbance for HL60 cells ($p=0.612664$ for no drug versus 1μM IM; $p=0.097389$ for no drug versus 2.5μM IM; $p=0.658101$ for no drug versus 5μM IM; $p=0.255663$ for no drug versus 10nM dasatinib; and $p=0.290042$ for no drug versus 150nM dasatinib).

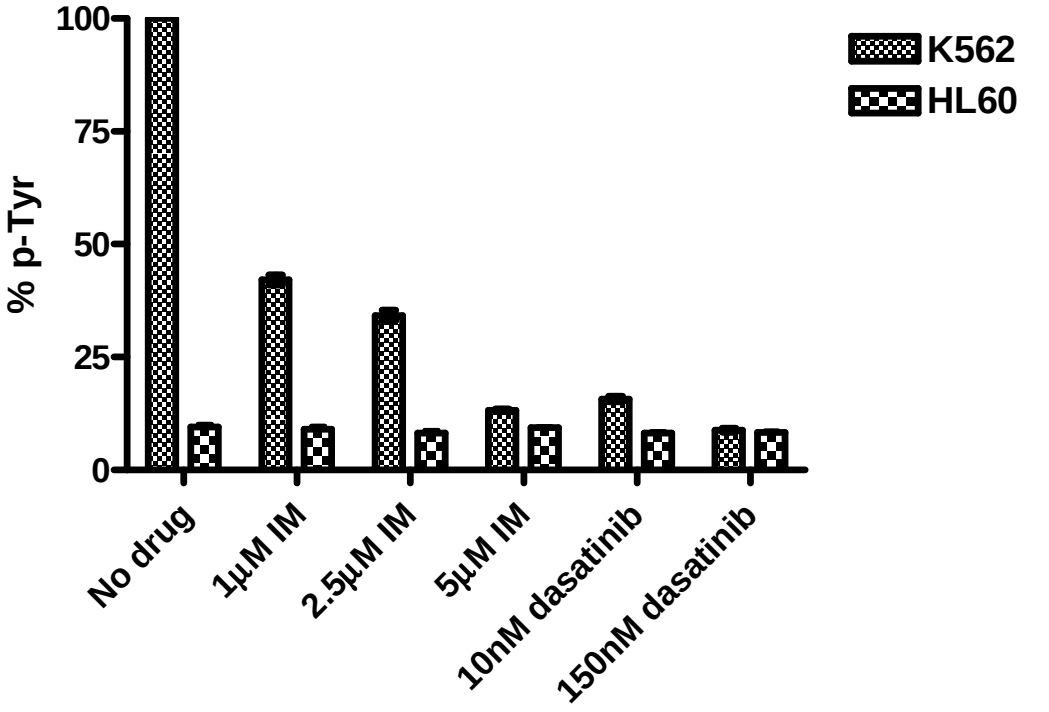

Figure 3-8 The effect on total p-Tyr levels upon drug treatment of K562 and HL60 cell lines measured by ELISA

K562 and HL60 cells were treated ± increasing concentrations of IM (1, 2.5 and 5μM) and dasatinib (10 and 150nM) for 16 hours (n=3). No significant differences were observed between no drug and each condition in HL60 cells, whereas significant differences were observed between no drug and each condition in K562 cells, (p=0.612664 and 0.000794 for 1μM IM; p=0.097389 and 0.000646 for 2.5μM IM; p=0.658101 and 0.000218 for 5μM IM; p=0.255663 and 0.000381 for 10nM dasatinib; p=0.290042 and p=0.000274 for 150nM dasatinib) for HL60 and K562 cells, respectively.

3.1.8 Effect of increasing concentrations of IM and dasatinib on Ba/F3 cell lines containing *BCR-ABL* mutations

The ELISA was further tested by assessing the response of cells with known *BCR-ABL* mutations to TKI treatment (Figure 3-9). Ba/F3 cells transduced with either *BCR-ABL*-p210 wild-type, M351T or T315I were exposed to IM (A) or dasatinib (B) for 16 hours. Following this, p-Tyr levels were assessed by ELISA. As expected, dasatinib was found to be more potent than IM, inducing 100% inhibition of p-Tyr in cells transduced with wild-type p210 at 150nm, as compared to 80% maximal inhibition with IM at 5μM. Consistent with the literature (292), dasatinib also inhibited the M351T mutation as effectively as the wild-type p210 at each concentration of drug. The specific type of mutation is a key factor in the level of resistance conferred to IM (293). The M351T mutation confers only moderate resistance to IM, which implies that dose escalation may be able to recapture a cellular response. This is indeed reflected in Figure 3-9A, where the level of p-Tyr inhibition reaches that of wild-type p210 at the highest concentration of IM. The T315I mutation was fully resistant to both agents as expected.

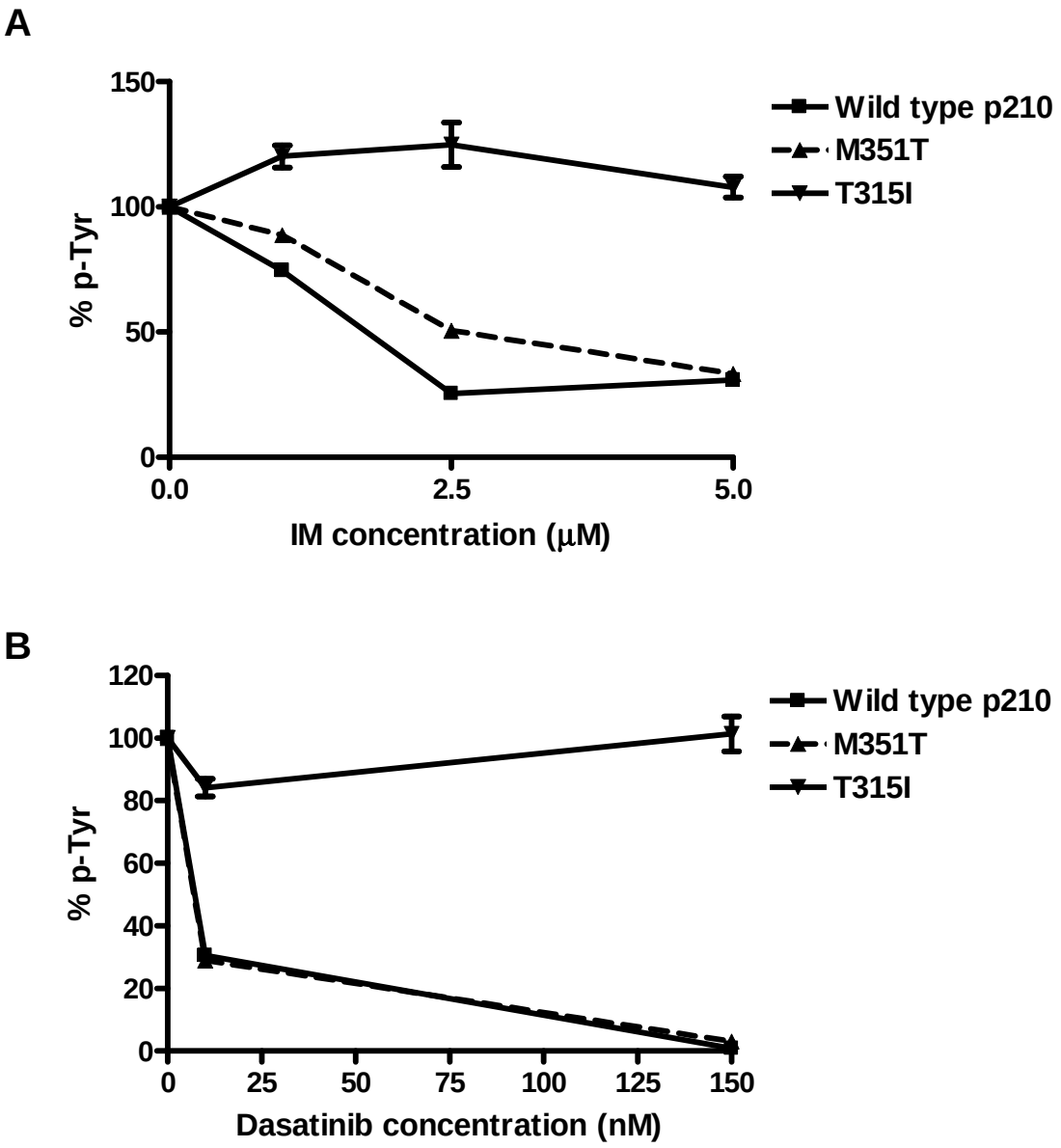

Figure 3-9 Effect of increasing concentrations of IM and dasatinib on Ba/F3 cell lines containing *BCR-ABL* mutations

Ba/F3-*BCR-ABL* p210, M351T, and T315I were cultured ± increasing concentrations of IM and dasatinib for 16 hours (n=3). Total p-Tyr levels were then determined by ELISA, in triplicate. The above figures demonstrate that the level of p-Tyr detected correlated with each Ba/F3-*BCR-ABL* mutant's degree of IM (A) or dasatinib (B) resistance.

3.1.9 Assessment of p-Tyr in primary CML CD34$^+$ and mature cells by ELISA

Finally, the ELISA's suitability for measuring BCR-ABL activity in both mature and primitive primary human CML samples was investigated. Primary CML CD34$^+$ (n=3) and MNC samples (n=6) were found to have increased levels of p-Tyr at baseline, as compared to Ph$^-$ samples from both CD34$^+$ (n=3) (p=0.012) and MNC (n=3) (p=0.0007) cell fractions (Figure 3-10).

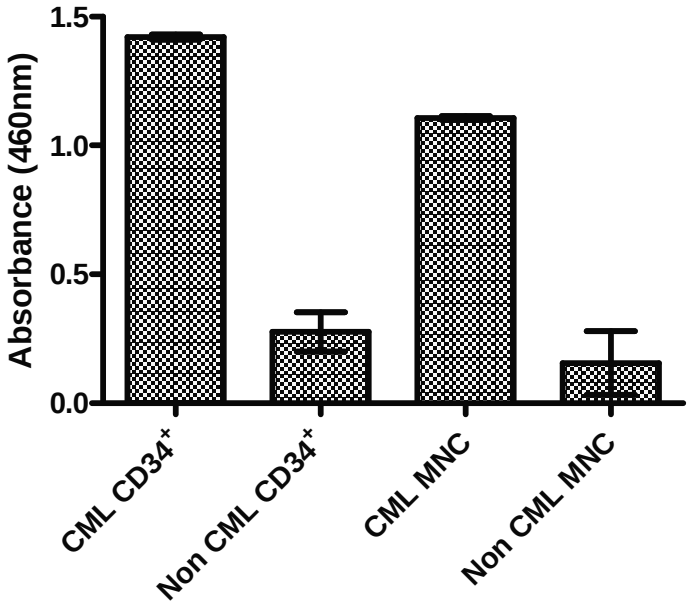

Figure 3-10 Assessment of p-Tyr in primary CML CD34$^+$ and mature cells by ELISA

Total p-Tyr status was measured by ELISA in CD34$^+$ (n=3) and MNC (n=6) CML cells and compared to non CML cell samples from both fractions (n=3). Levels of p-Tyr were found to be significantly increased in the CML cell samples as compared to the Ph$^-$ cell samples (p=0.012 for CML versus non CML CD34$^+$ cells and p=0.0007 for CML versus non CML MNC cells).

Overall, these data confirm the novel ELISA's ability to assess total p-Tyr levels in Ph$^+$ cell lines, cells with known *BCR-ABL* mutations and both mature and primitive primary human CML cells.

3.2 Comparison of the novel ELISA method with established techniques for the measurement of BCR-ABL activity in CML cells

Western blot is a well established and reliable method which has previously been shown to reproducibly measure p-CrkL. However, it is time-consuming and laborious which makes the testing of large sample numbers difficult. Furthermore, it requires a relatively large number of cells, which is often unrealistic when working with a small pool of primitive CML cells. More recently, flow cytometric methods have been developed to detect p-Tyr (291) and p-CrkL (130) levels in small numbers of primary CML cells. Although this technique requires few cells and is rapid, even within our own group we have found it to be less reproducible between individuals than Western blot. In order to determine how the novel ELISA method compared with the more established techniques, further investigations were carried out.

3.2.1 Equivalence between Western blot, flow cytometry and ELISA methods as a means of detecting BCR-ABL activity in K562 cells

K562 cells were first treated with IM (0, 1, 5μM) for 48 hours, before p-CrkL was measured by Western blot and FACS and p-Tyr was detected by ELISA. When phosphorylation levels from 3 independent experiments were compared, the methods appeared equivalent, with no significant differences observed between the 3 techniques ($p=0.87$ and 0.15 for Western versus flow cytometry; $p=0.19$ and 0.24 for Western versus ELISA and $p=0.2$ and 0.13 for ELISA versus flow cytometry) for 1 and 5μM IM treatment, respectively (Figure 3-11).

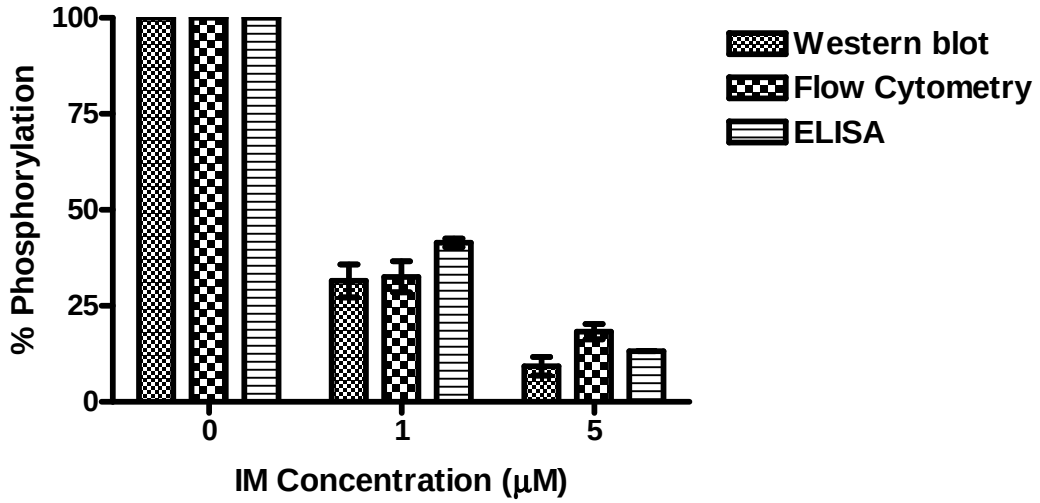

Figure 3-11 Equivalence between Western blot, flow cytometry and ELISA methods as a means of detecting BCR-ABL activity in K562 cells

K562 cells were treated with IM (0, 1, 5μM) for 48 hours. Reduction of p-CrkL was then detected by Western blot and flow cytometry and total p-Tyr was measured by ELISA. No significant differences were observed between the 3 methods (p=0.87 and 0.15 for Western versus flow cytometry; p=0.19 and 0.24 for Western versus ELISA and p=0.2 and 0.13 for ELISA versus flow cytometry) for 1 and 5μM IM treatment, respectively.

3.2.2 Comparison of flow cytometry and ELISA methods used to measure the effect of IM treatment on Ba/F3 cell lines containing *BCR-ABL* mutations

The ELISA was further investigated by assessing the response of Ba/F3 cells transduced with either *BCR-ABL*-p210 wild-type, M351T or T315I, to 16 hours treatment with 5μM IM, and the results were compared with data obtained from the p-CrkL flow cytometry method (Figure 3-12). Inhibition of p-Tyr was maximal in *BCR-ABL*-p210 wild-type (80% reduction as compared to no drug control (100%)) and each mutant was inhibited according to their degree of low and high IM-resistance. Furthermore, the techniques appeared equivalent with no significant differences observed between the 2 methods (p=0.55 for *BCR-ABL*-p210 wild-type; p=0.08 for M351T and p=0.06 for T315I).

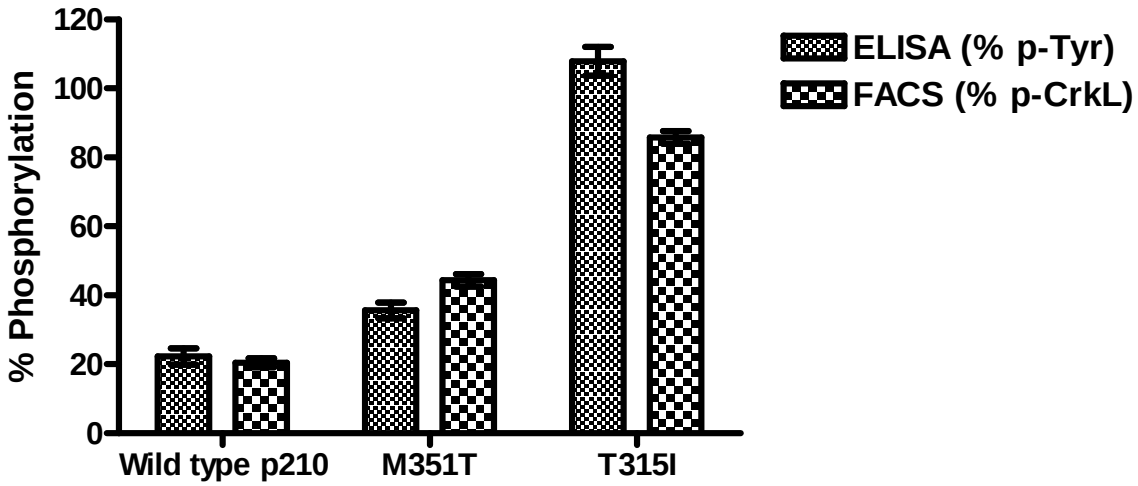

Figure 3-12 Comparison of flow cytometry and ELISA methods used to measure the effect of IM treatment on Ba/F3 cell lines containing *BCR-ABL* mutations

Ba/F3-*BCR-ABL* p210, M351T and T315I were cultured ± 5μM IM for 16 hours. Total p-Tyr levels were then determined by ELISA, and compared to p-CrkL levels measured by flow cytometry. Percentage phosphorylation was calculated based on the relevant no drug control (100%). The level of p-Tyr detected correlated with each Ba/F3-*BCR-ABL* mutant's degree of IM resistance, with no significant differences detected between the methods (p=0.55 for wild-type p210; p=0.08 for M351T and p=0.06 for T315I).

3.2.3 Equivalence between ELISA and flow cytometry methods as a means of detecting BCR-ABL activity in CML CD34$^+$ cells

It was noted that the comparison made between p-Tyr and p-CrkL levels is not strictly accurate and that the assessment of total tyrosine phosphorylation assayed by ELISA and flow cytometry, would allow a better evaluation of the ELISA method. Therefore, primary CML CD34$^+$ cells (n=4, >90% Ph$^+$), were treated ± 5μM IM before p-Tyr levels were measured by both ELISA and flow cytometry. Incomplete inhibition of p-Tyr was achieved following IM treatment (around 70% inhibition as compared to no drug control (100%)), with no significant difference observed between the ELISA and flow cytometric methods (p=0.54) (Figure 3-13). This level of BCR-ABL inhibition in response to IM is consistent with data previously published (131).

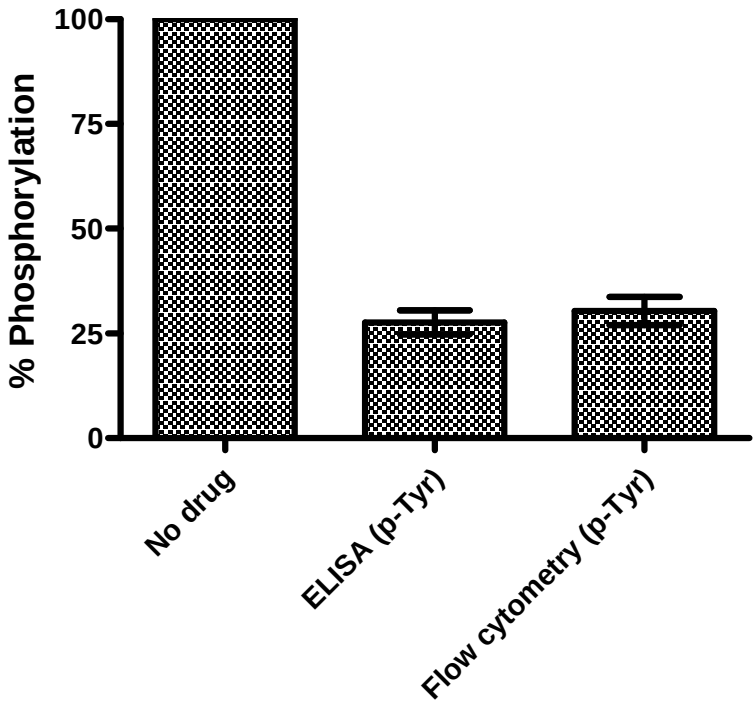

Figure 3-13 Equivalence between ELISA and flow cytometry methods as a means of detecting BCR-ABL activity in CML CD34$^+$ cells

CML CD34$^+$ cells (n=4) were treated ± 5μM IM for 16 hours and samples were taken for p-Tyr measurement by ELISA and flow cytometry. The IM-treated CD34$^+$ cells showed a 70% reduction in BCR-ABL activity as compared to no drug control (100%). No significant differences were observed between the methods (p=0.54).

3.3 Summary

The advantages and disadvantages of the techniques to assess the activity of BCR-ABL that have been described in this chapter and in the literature (130, 131, 290, 291, 294-297) are described in brief in Table 3-1. Although Western blot has been shown to be a reliable and reproducible technique for the assessment of p-CrkL, it requires >100 times the number of cells needed for flow cytometry. This is often not feasible when attempting to characterise a rare population of CML stem cells. The main advantages of the p-Tyr ELISA are that it is reproducible between individuals and also allows the assay of many samples at once, so could be adapted for high throughput applications. However, large cell numbers are also required, as one sample performed in triplicate would require a total of 15μg of protein lysate. The experiments performed in this chapter were performed without verification of sample protein-coating. However, to be more exact, a loading control, such as GAPDH should be included for each sample, taking the total amount of protein required up to 30μg. This is more than is necessary for a Western blot and an unrealistic amount when it comes to working with very primitive CML cells. When analysing small numbers of immature CML cells the only reasonable option is flow cytometry. It also provides an accurate assessment of a viable cell population, as any dead cells or debris can be gated out prior to analysis, which would be impossible with either Western blot or ELISA. Furthermore, multi-parameter flow cytometry offers the valuable advantage of characterising certain cell surface and intracellular markers, to identify cellular subpopulations in response to a stimulus or drug treatment. This is a key factor when attempting to identify CML stem cells, track their survival and proliferation, and also assess BCR-ABL activity in response to TKI treatment.

In summary, for the single measurement of BCR-ABL activity, it would be advisable to use anti-p-CrkL antibody in Western blot in all situations where sufficient cells are available and the number of samples to be tested is low. When a large quantity of samples requires to be tested, then ELISA for p-Tyr can be used. Where cell numbers are limited and a number of parameters require to be tested simultaneously, flow cytometry should be used. However, wherever possible key results should be confirmed using a limited number of Western blots to reassure the investigator that their interpretation of results obtained by flow cytometry and ELISA are consistent with the gold standard.

	Western blot (BCR-ABL) (295-297)	Western blot (p-CrkL) (130, 131, 290, 294)	Flow cytometry (p-Tyr) (291)	Flow cytometry (p-CrkL) (130, 131)	ELISA (p-Tyr)
Required number of cells	$10^5 – 10^6$ (≥10µg/ well)	$10^5 – 10^6$ (≥10µg/ well)	$10^3 – 10^5$	$10^3 – 10^5$	$10^5 – 10^6$ (5µg/well)
Ease of throughput	+	+	++	++	+++
Time required	≥ 2 days	≥ 2 days	2-4 hours	2-4 hours	1 day
Reproducib -ility	+++	+++	++	++	+++
Suitability for cell lines	+++	+++	+++	+++	+++
Suitability for mature primary cells	X	+++	+++	+++	+++
Suitability for $CD34^+$ primary cells	+++	+++	+++	+++	+++
Suitability for multi-parametric analysis	X	X	+++	+++	X

Table 3-1 Summary of methods to assess BCR-ABL activity in Ph^+ cell lines and primary CML cells

4. RESULTS (II) Is BCR-ABL relevant for the survival of cancer stem cells in CML?

The importance of BCR-ABL for the malignant transformation of CML has led to the development of TKIs, such as IM. Despite IM's initial therapeutic success, only a small proportion of patients obtain a CMR, where they become negative for *BCR-ABL* transcripts by RT-PCR. It is hypothesised that this MRD is the result of a primitive subpopulation of LSCs, which may cause relapse at a later date. Another major clinical concern is the observation of molecular resistance in IM-treated patients. There are 2 broad categories of IM resistance: BCR-ABL-independent and BCR-ABL-dependent. In most cases of acquired resistance to IM, BCR-ABL-dependence is found. Postulated mechanisms include BCR-ABL amplification with over-expression and decreased intracellular IM concentrations caused by reduced drug-uptake and increased drug-efflux through drug transporters (298). However, BCR-ABL dependent IM resistance is most often attributed to the development of point mutations within the ABL-kinase domain (240)·(299). A further possibility is that IM resistant stem cells are simply refractory to TKI treatment due to poorly understood properties that allow them to survive drug exposure. For example, we and others (131, 298, 300) have demonstrated that CML stem cells over-express BCR-ABL, which may be sufficient to render them IM resistant.

BCR-ABL-independence suggests that resistance is a result of stem cell-related or intrinsic mechanisms whereby the leukaemia cells either do not require BCR-ABL for survival and the maintenance of a quiescent state; or are no longer reliant on BCR-ABL to drive proliferation. These cells may employ additional mechanisms

which are responsible for their growth and survival. Although examples of this type of resistance have been demonstrated in more advanced phase CML (301, 302), this has not yet been proven for the CP CML stem cell population.

In an attempt to understand the mechanisms of IM resistance in CML, the primary aim of this chapter is to determine whether CML stem cells are dependent on BCR-ABL kinase activity for their survival. Hence, the following experiments were designed for the:

1. Optimisation of culture conditions to maximise targeting of BCR-ABL kinase activity within CP CML cells.
2. Characterisation of primitive CML cells following kinase inhibition of BCR-ABL
3. Analysis of functionality of the CML cells remaining following prolonged BCR-ABL kinase inhibition

If the CML stem cells are proven to be dependent on BCR-ABL kinase activity for survival then efforts to enhance intracellular concentration and binding of potent TKIs selective for BCR-ABL should lead to improved responses/cures for patients. If CML stem cell survival is proven to be independent of BCR-ABL kinase activity then alternative approaches to develop CML stem cell therapies would be required.

4.1 Optimisation of culture conditions to maximise targeting of BCR-ABL kinase activity within CP CML cells

4.1.1 Comparison of GF culture conditions in TKI-treated CML cells

In order to determine the optimal culture conditions for maximal BCR-ABL inhibition, preliminary experiments were carried out. CML stem cells produce autocrine cytokines at low levels and are able to survive in culture in the absence of added GFs (190), however, these cells may also respond to supplemental cytokines. There has therefore been concern that the addition of cytokines at high concentration to these cultures may support the survival of CML stem cells during exposure to TKIs (303),(235). Thus, an experiment was performed to compare the effects of TKI treatment on CML $CD34^+$ cells, cultured in SFM with and without added GF support. Figure 4-1 shows total cell numbers, determined by trypan blue dye exclusion, following treatment ± either 2μM IM or 150nM dasatinib and cultured ± 5GF for 3 days (n=3). As predicted, untreated CML $CD34^+$ cells were able to survive and proliferate in the absence of GFs. However, this condition resulted in significantly reduced cell numbers as compared to untreated cells cultured with GFs ($p=0.05$). Treatment with either IM or dasatinib in the presence of GFs resulted in a significantly decreased cell number as compared to the corresponding untreated control ($p=0.05$ for no drug +GF versus IM +GF and $p=0.04$ for no drug +GF versus dasatinib +GF). Interestingly, TKI treatment in the presence of GFs also gave the same effect as removing the GF support from untreated control cells, with no significant difference observed between the conditions ($p=0.70$ for no drug versus IM and $p=0.94$ for no drug versus dasatinib). This demonstrates the protective effect that cytokines may have over TKI treatment of CML cells. Due to the compelling evidence that autocrine stimulation

via cytokines such as, G-CSF, IL-3 and GM-CSF could be of importance for the regulation of the growth and survival of CML cells (187, 190); it is perhaps not surprising that the exogenous GF support mediated such resistance against the TKI treatment of these CML cells. The greatest effect was observed with TKI treatment minus GFs, with a significantly decreased cell number as compared to TKI treatment plus GFs (p=0.03 for IM -GF versus IM +GF; p=0.04 for IM -GF versus dasatinib +GF; p=0.02 for dasatinib -GF versus IM +GF and p=0.03 for dasatinib -GF versus dasatinib +GF). There was no significant difference in cell number observed between IM- and dasatinib-treated cells cultured without GFs (p=0.774).

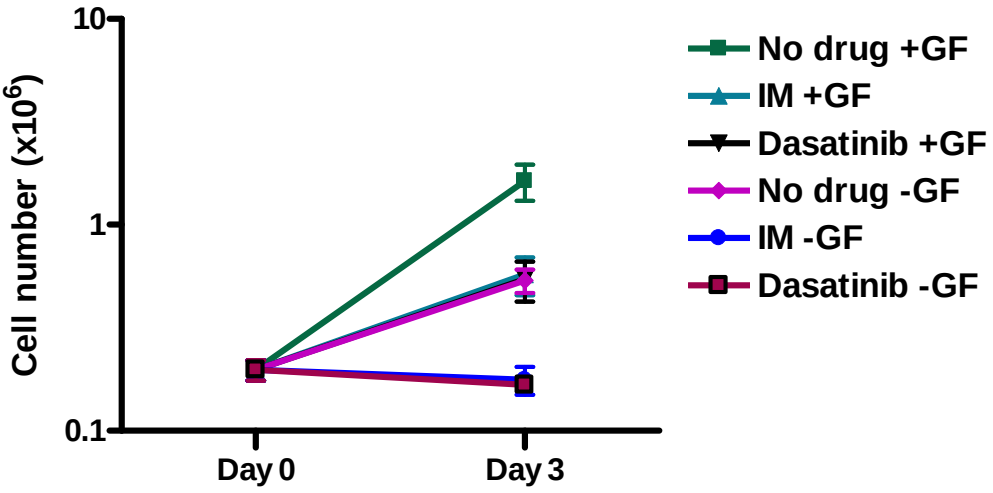

Figure 4-1 Comparison of GF culture conditions in TKI-treated CML cells

CML CD34$^+$ cells (n=3) were treated ± either 2μM IM or 150nM dasatinib and cultured in SFM ± a 5GF cocktail for 3 days. Viable cell counts were determined by trypan blue dye exclusion.

4.1.2 Comparison of TKI treatments and exposure times in primary CML cells

In order to compare the effects of different TKI treatments, studies were performed whereby $CD34^+$ CML cells were cultured in SFM without exogenous GF support and treated for 1, 2, 3, 4, 24 and 72 hours with increasing concentrations of either IM, nilotinib or dasatinib. At each treatment time-point, the cells were washed twice with PBS to remove any trace of drug and put back into culture with fresh medium. A viable cell count was then performed by trypan blue dye exclusion at the 72 hour time-point. Figure 4-2 demonstrates the percentage of viable CML cells remaining following the treatment timecourse with IM (A), nilotinib (B) or dasatinib (C). The percentage of viable cells was significantly increased, following exposure for the shortest treatment time (1 hour), as compared to the longest treatment time (72 hours), using the lowest concentration of IM (1μM) ($p=0.009$). However, no significant difference in cell number was observed as the concentration was increased ($p=0.11$ for 5μM IM; $p=0.18$ for 10μM IM and $p=0.5$ for 20μM IM). Furthermore, no significant difference in viable cell number was observed between the 1 and 20μM concentrations of IM at both the shortest and longest treatment time-point ($p=0.07$ and 0.14) for 1 and 72 hours, respectively (Figure 4-2A).

No significant differences in viable cell number were observed between the shortest (1 hour) and longest (72 hours) treatment times using both the lowest and highest concentration of nilotinib ($p=0.47$ and $p=0.436$) (Figure 4-2B) and dasatinib ($p=0.06$ and 0.1475) (Figure 4-2C) for the lowest and highest concentrations of drug, respectively. Similarly, no significant difference in viable cell number was detected between 10 and 1000nM dasatinib treatment ($p=0.1255$

and 0.081) and 1 and 20μM nilotinib treatment (p=0.27 and p=0.23) at both the shortest and longest treatment time-point, respectively.

Figure 4-2D demonstrates a comparison of each TKI treatment at clinically achievable concentrations. Although no significant differences in cell number were observed between each condition by the 72 hour time-point (p=0.31 for IM versus nilotinib; p=0.074 for IM versus dasatinib and p=0.19 for nilotinib versus dasatinib), there was a trend towards a greater reduction in viable cells following 150nM dasatinib treatment.

In general, these data show that transient exposure with relatively low concentrations of TKI is as effective as continuous treatment with increased concentrations of TKI, which are clinically unachievable.

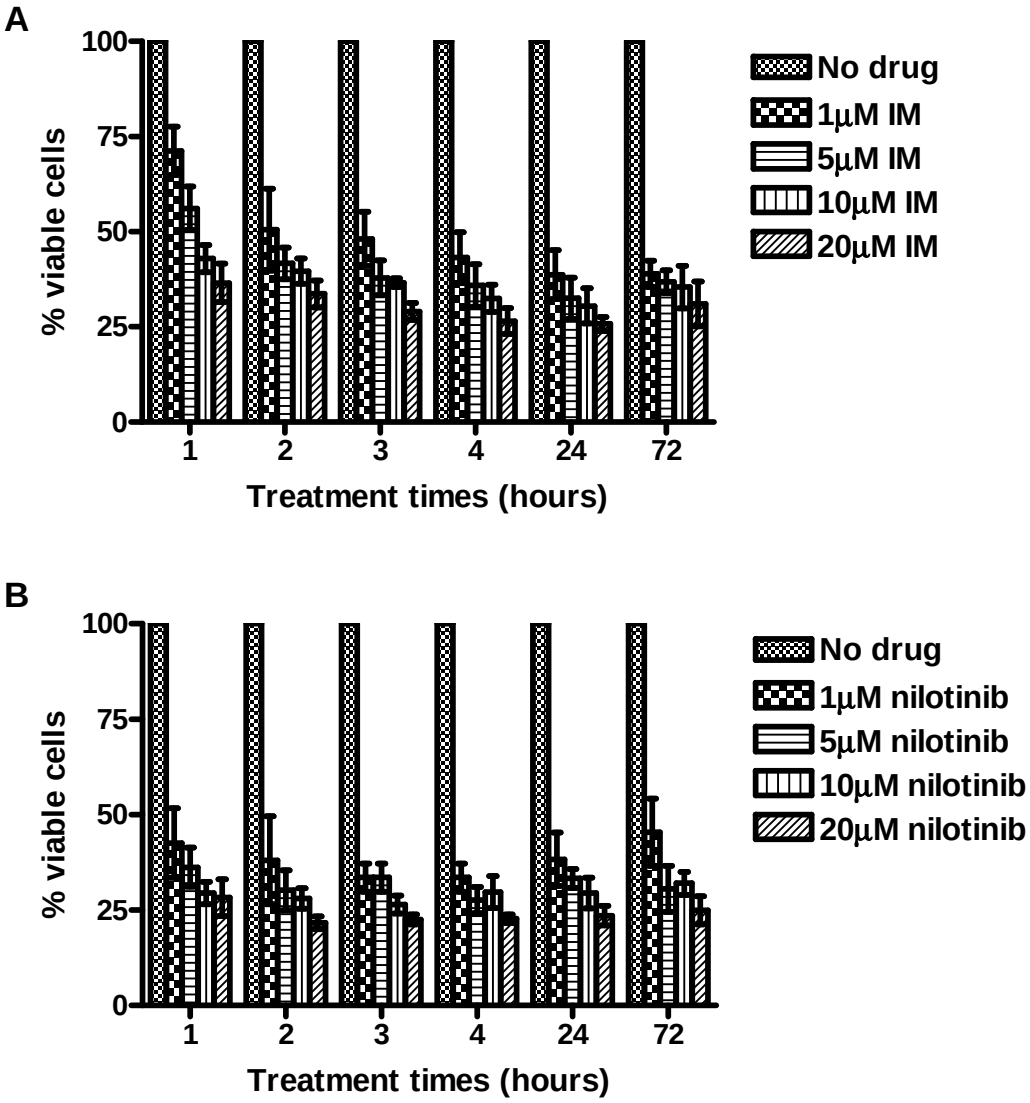
A
100
75
50
25
0
% viable cells
1
2
3
4
24
72
Treatment times (hours)
No drug
1μM IM
5μM IM
10μM IM
20μM IM
B
100
75
50
25
0
% viable cells
1
2
3
4
24
72
Treatment times (hours)
No drug
1μM nilotinib
5μM nilotinib
10μM nilotinib
20μM nilotinib

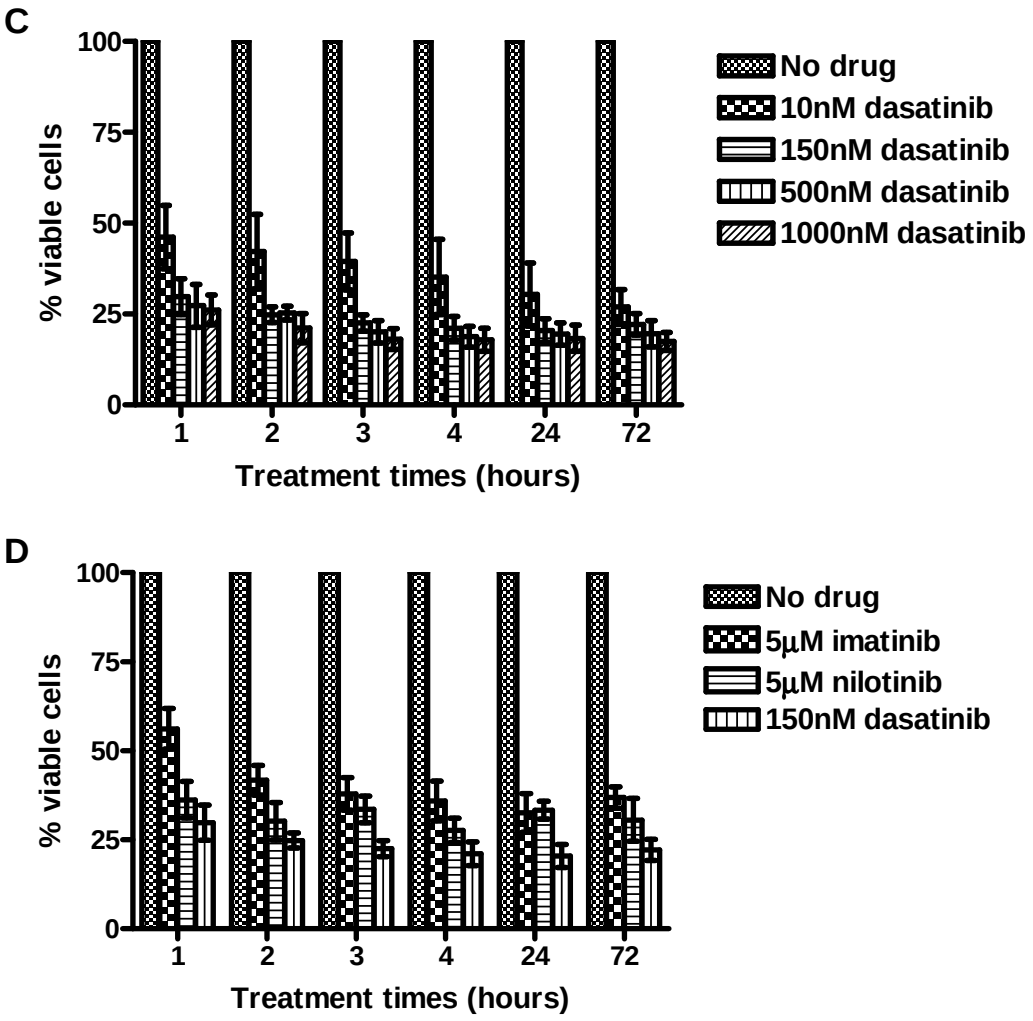

Figure 4-2 Comparison of TKI treatments and exposure times in primary CML cells

$CD34^+$ CML cells (n=3) were treated with increasing concentrations of IM (A), nilotinib (B) and dasatinib (C) for the indicated treatment times. Following each time-point, the cells were washed with PBS and put back into culture with fresh media. Viable cell counts were performed by trypan blue dye exclusion at the 72 hour time-point and compared to no drug control cells (100%). A comparison of each TKI treatment at a clinically achievable dose is shown in Panel D.

4.1.3 Effect of TKI treatment on apoptosis induction within CD34$^+$ CML cells

In order to determine which TKI had the greatest effect on CML cells, further characterisation was carried out. First, CML CD34$^+$ cells were cultured without GFs and treated ± either 5μM IM or 150nM dasatinib for 48 hours. Apoptosis was then determined by annexin-V and viaprobe staining as measured by flow cytometry (n=3). Figure 4-3 demonstrates the relative fold change in the percentage of early and late apoptotic cells (i.e. the cells which stained positive for both annexin-V and viaprobe) for each condition, as compared to no drug control. IM treatment significantly increased the number of apoptotic cells as compared to no drug control (p=0.05). Dasatinib treatment significantly increased the number of apoptotic cells as compared to both no drug control and IM treatment (p=0.02 and p=0.05, respectively).

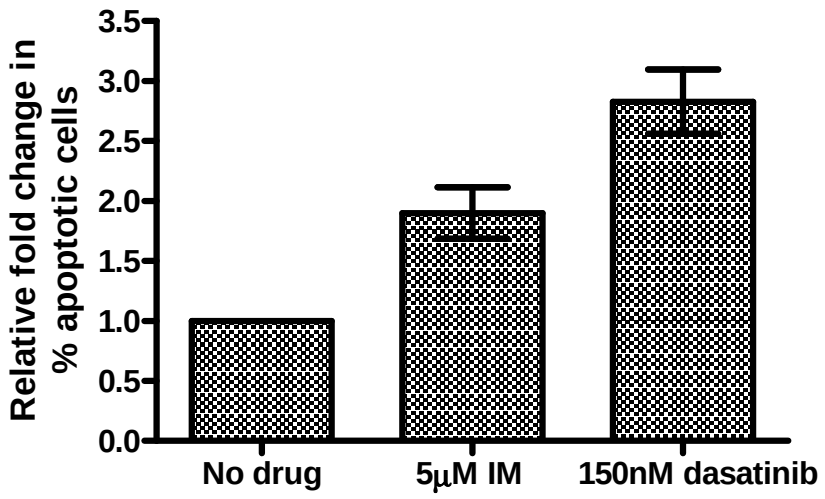

Figure 4-3 Effect of TKI treatment on apoptosis induction within CD34$^+$ CML cells

CML CD34$^+$ cells were cultured for 48 hours in SFM without GFs and treated ± either 5μM IM or 150nM dasatinib (n=3). Apoptosis was determined at this time-point by annexin-V and viaprobe staining measured by flow cytometry. Each condition was then compared relative to a no drug control.

4.1.4 Effect of TKI treatment on p-CrkL levels within CML cells

To compare the effects of TKI treatment on BCR-ABL activity within CML cells, p-CrkL was measured. $CD34^+$ CML cells were cultured in SFM and treated ± an IC_{90} concentration of TKI (5μM IM and 150nM dasatinib) for a total of 72 hours. The levels of p-CrkL were then measured by Western blot of whole cell protein lysates, prepared at 16 hours in order to measure the immediate effects of TKI inhibition of BCR-ABL and then at 72 hours to measure the effects of TKI on cells which survive the initial drug treatment. Pan-actin was included as a protein loading control. Figure 4-4 demonstrates that IM treatment resulted in a reduction of p-CrkL, as compared to no drug control after 16 hours of treatment, suggesting that the majority of cells were IM-sensitive. However, despite re-exposure to IM 12 hours before the 72 hour time-point, those cells that survived treatment showed no reduction in p-CrkL, consistent with enrichment, following cell death, of an IM-resistant population. Dasatinib treatment inhibited p-CrkL both at the early time-point and also, unlike IM, at the later time-point.

Overall, these data show that the greatest effect of TKI on CML cells is seen in culture conditions without added GF support. Further, that dasatinib is superior to IM, in terms of inducing apoptosis (which should lead to a reduction in CML cell numbers) and provides the greatest inhibition of BCR-ABL. Therefore, dasatinib treatment without added GFs was the culture condition used for all subsequent experiments.

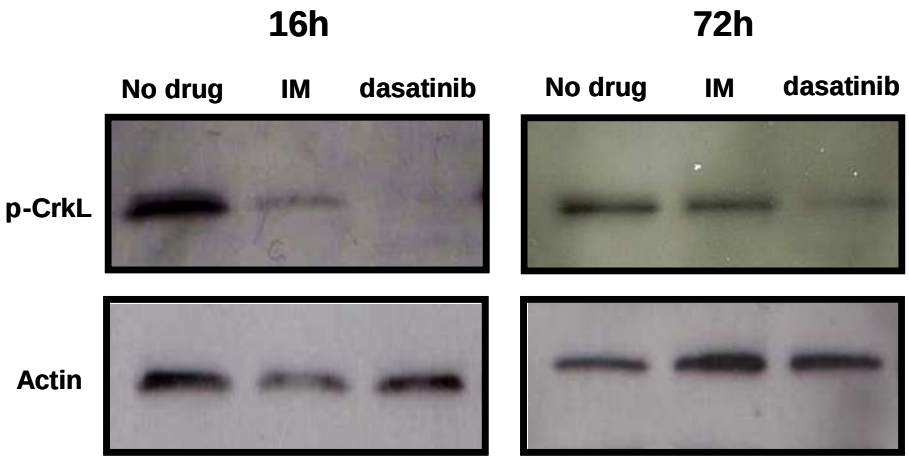

Figure 4-4 Effect of TKI treatment on p-CrkL levels within CML cells

Whole cell protein lysates were prepared from $CD34^+$ CML cells treated ± either 5μM IM or 150nM dasatinib for a total of 72 hours. The levels of p-CrkL were assessed in each sample at the 16 and 72 hour time-point by Western blot. Pan-actin levels were also measured as a protein loading control.

4.2 Characterisation of primitive CML cells following kinase inhibition of BCR-ABL

4.2.1 Assessment of CML cell viability following treatment with dasatinib

The studies described in Figure 4-1 demonstrate that up to 6 days dasatinib treatment does not completely eradicate CML $CD34^+$ cells, cultured without GFs. Timecourse studies also demonstrated that any CML cells which were sensitive to TKI, were likely to be targeted within the first few hours of treatment. In an attempt to completely isolate and then characterise the CML cells which are not initially targeted by TKI treatment, the exposure time to dasatinib was increased. Figure 4-5A demonstrates the cell counts as determined by trypan blue dye exclusion, following treatment ± 150nM dasatinib for 12 days. Every 3 days, cells were washed twice with PBS, cultured with fresh medium and re-drugged with dasatinib, to ensure no degradation of drug over the timecourse. As with previous data, untreated cells were able to expand despite being cultured without GFs, whereas, dasatinib-treated cells were significantly reduced in viable cell number to $3.4x10^5$ total cells by day 12 (<2% cells remaining relative to no drug control, p=0.01). Figure 4-5B shows the percentage viability, as compared to input cell number, for dasatinib-treated cells. At the end of the timecourse, residual viable cells represented <10% of the starting cell number.

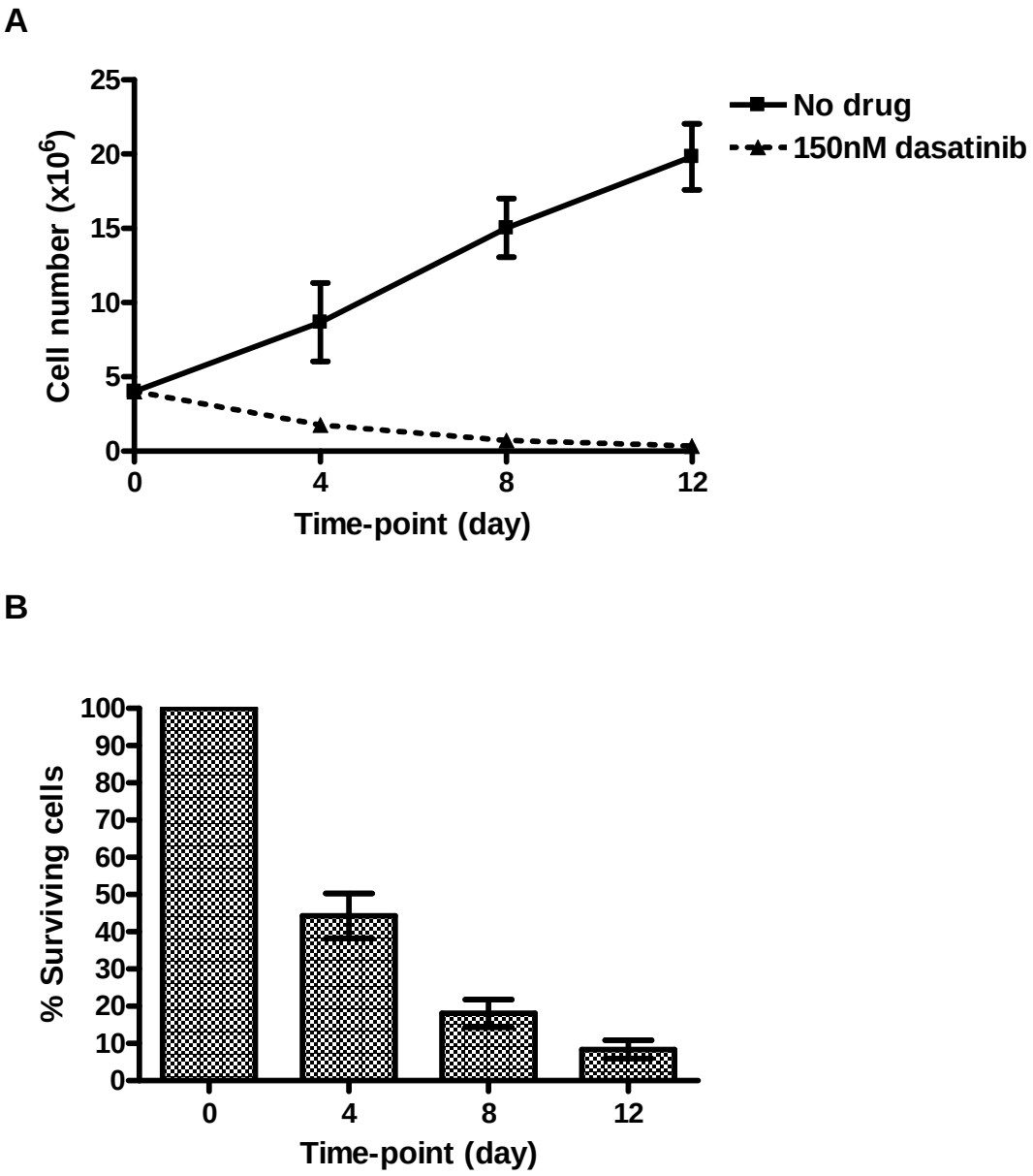

Figure 4-5 Assessment of CML cell viability following treatment with dasatinib

Panel A demonstrates the viable cell counts from $CD34^+$ CML cells treated ± 150nM dasatinib and cultured without exogenous GF support, as measured by trypan blue dye exclusion at each time-point. Panel B shows the percentage of surviving cells at each time-point, calculated based on starting cell number (100%).

4.2.2 D-FISH profiles of CML cells treated with dasatinib

Previous studies have reported BCR-ABL amplification in primary cells from patients with advanced phase CML and that this may be a mechanism of acquired drug resistance (238). In order to determine whether the cells which survived dasatinib exposure showed evidence of oncogene amplification, D-FISH was performed. Only a single copy of the BCR-ABL gene was detected in each of the samples. Figure 4-6 demonstrates the D-FISH profile of one representative patient's CML cells following 12 days treatment ± 150nM dasatinib. In each of the three patients samples kindly tested by Mrs Elaine Allan, >95% of the cells were shown to be BCR-ABL positive by D-FISH, both before and after dasatinib treatment. Although normal cells would not survive 12 days culture in SFM without GF support; these data definitively rule out both the presence of normal cells and oncogene amplification as explanations for resistance.

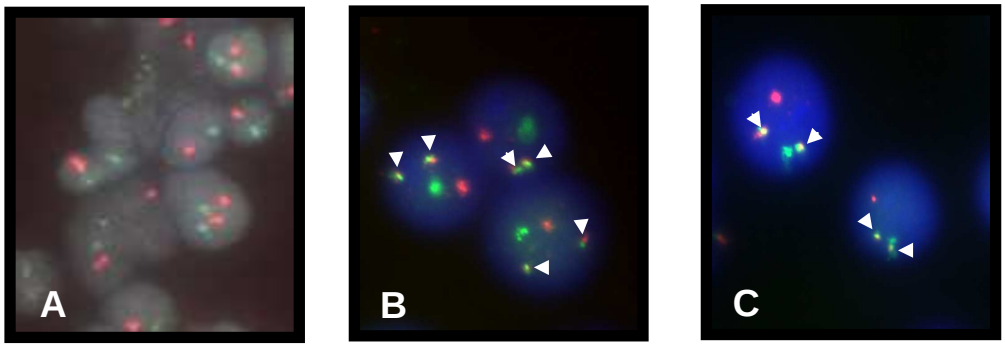

Figure 4-6 D-FISH profiles of CML cells treated with dasatinib

Representative FISH profile from non CML CD34$^+$ cells at baseline (A), untreated CD34$^+$ CML cells following the 12 day timecourse (B) and 150nM dasatinib-treated CD34$^+$ CML cells following the 12 day timecourse (C). Green signals represent BCR; red signals represent ABL and yellow signals represent the BCR-ABL fusion gene (denoted by the white arrows).

4.2.3 Analysis of ABL-kinase domain mutations in CML cells treated with dasatinib

IM resistance is most often attributed to the development of point mutations within the ABL-kinase domain. To investigate whether this was a potential mechanism for the cells to remain resistant to dasatinib, a mutation screen of the ABL-kinase domain of BCR-ABL was kindly performed by Dr Sandrine Hayette (Hôpital Lyon, Lyon, France) on RNA purified from CML cells, both before and after ± 12 days dasatinib exposure. No mutation was detected in any of the patients' samples (n=3). Direct sequencing of the ABL-kinase domain has a sensitivity of about 10-20% (244), therefore if a mutation was present, it would be in less than 20% of the surviving cells following dasatinib treatment. This then rules out mutation as a means of dasatinib resistance, in the majority of the cells which remained following prolonged dasatinib treatment.

4.2.4 Expression of BCR-ABL in CML cells following dasatinib treatment

Previously, it has been demonstrated that patients treated with allogeneic transplantation had Ph^+ cells detected by D-FISH, but remained BCR-ABL negative by RT-PCR. To determine whether the primitive CML cells from this study were transcriptionally silent, the expression of BCR-ABL was measured in the untreated and 150nM dasatinib-treated cells at day 12 of the timecourse by qRT-PCR and these levels were compared to the same patients' cells at baseline. Figure 4-7 demonstrates that CML cells at baseline expressed 82.7% BCR-ABL as compared to total ABL. For 12 day untreated and 150nM dasatinib-treated cells BCR-ABL as compared to total ABL was 71 and 59%, respectively, with no significant differences observed between the conditions ($p=0.427$ for baseline versus no drug; $p=0.109$ for baseline versus 150nM dasatinib and $p=0.215$ for no drug versus 150nM dasatinib). These data suggest that although BCR-ABL kinase activity has been inhibited within these surviving CML cells, BCR-ABL is still expressed at the transcript level.

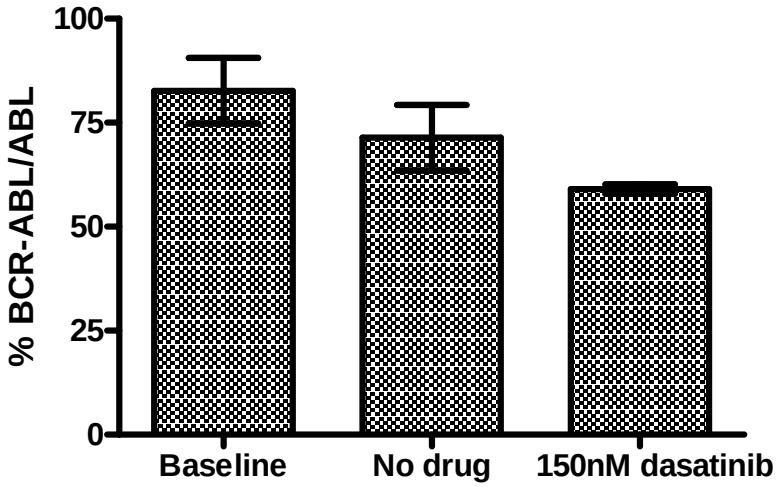

Figure 4-7 Expression of BCR-ABL in CML cells following dasatinib treatment

BCR-ABL **mRNA transcripts were measured by qRT-PCR in CD34^{+} CML cell samples (n=3) either at baseline or following treatment ± 150nM dasatinib for 12 days.**

4.2.5 Analysis of p-CrkL within normal cells and compared to CML cells

Since the previous experiments ruled out the most common means of resistance in TKI-treated CML cells, the level of inhibition of BCR-ABL kinase activity was next investigated. As stated in the introduction, p-CrkL has been found to be an excellent marker for the measurement of BCR-ABL kinase activity in CML cells. However, in addition to its role in CML, CrkL is also implicated in signal transduction by integrins, B- and T-cell receptors, and cytokines such as erythropoietin, IL-3, SCF, and thrombopoietin (304-309). This, therefore, implies that some level of CrkL phosphorylation is evident in normal cells. In order to test this, non CML $CD34^+$ cells (n=3) and CML $CD34^+$ cells (n=3) were treated ± 150nM dasatinib for 24 hours and p-CrkL levels were compared. The 24 hour time-point was chosen in order to reflect the early effects of TKI treatment. The percentage of p-CrkL present in each sample was then calculated based on the levels of p-CrkL detected in untreated CML $CD34^+$ cells (n=3) (100%). Figure 4-8 demonstrates that a level of 34 and 32.3% p-CrkL was observed in the non CML cells untreated and treated with dasatinib, respectively, as compared to 37% p-CrkL in dasatinib-treated CML cells. No significant differences in p-CrkL levels were observed between the conditions ($p=0.35$ for dasatinib-treated CML cells versus untreated non CML cells; $p=0.14$ for dasatinib-treated CML cells versus dasatinib-treated non CML cells and $p=0.28$ for untreated non CML cells versus dasatinib-treated non CML cells).

In all subsequent experiments, the level of p-CrkL present in normal cells was subtracted from the level present in CML cells treated ± dasatinib, in order to give a true measure of BCR-ABL inhibition.

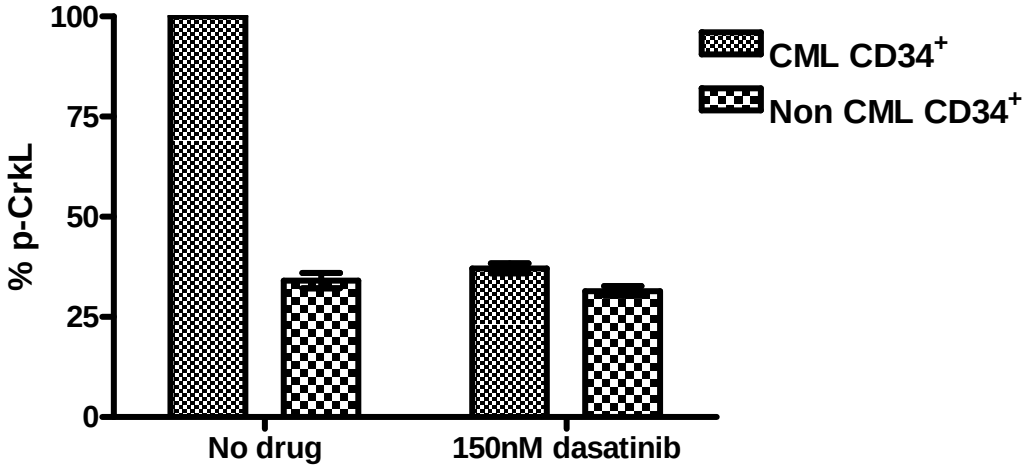

Figure 4-8 Analysis of p-CrkL within normal cells and compared to CML cells

Levels of p-CrkL were measured by flow cytometry in non CML (n=3) versus CML CD34$^+$ cells (n=3) treated ± 150nM dasatinib for 24 hours.

4.2.6 Flow cytometric analysis of p-CrkL expression within a total population of CML cells treated with dasatinib

In order to determine whether prolonged dasatinib exposure could completely inhibit BCR-ABL activity within the total CML cell population, flow cytometry was used to measure p-CrkL levels within the 12 day dasatinib-treated CML samples. Figure 4-9 demonstrates that within the bulk population of CML cells, dasatinib induced a maximal inhibition of p-CrkL by day 12 of treatment, with no significant difference observed between the time-points ($p=0.54$ for day 4 versus day 8; $p=0.84$ for day 4 versus day 12 and $p=0.3$ for day 8 versus day 12).

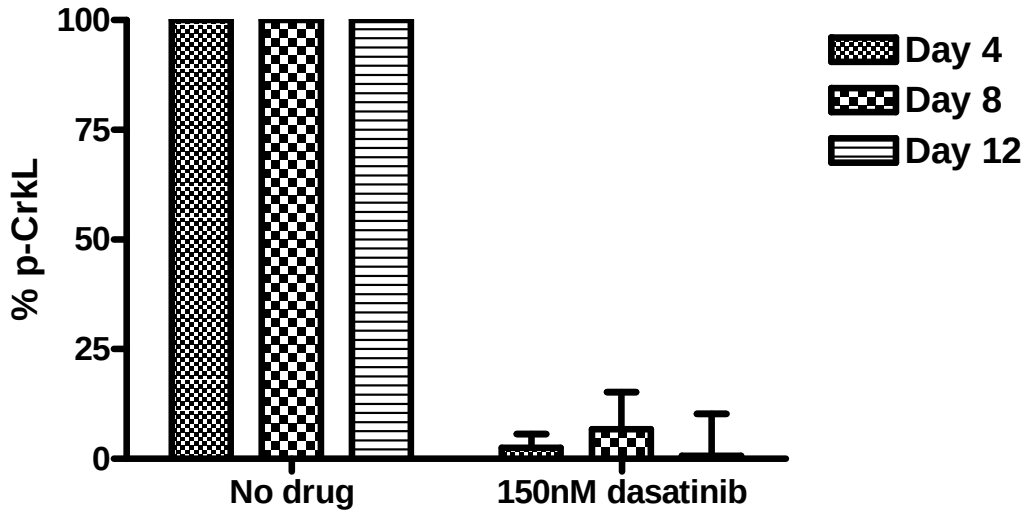

Figure 4-9 Flow cytometric analysis of p-CrkL expression within a total population of CML cells treated with dasatinib

$CD34^+$ CML cells (n=3) were cultured in SFM minus GFs and treated ± 150nM dasatinib for 12 days. The levels of p-CrkL were then measured by flow cytometry at each indicated time-point.

4.2.7 Western blot analysis of p-CrkL expression within a total population of CML cells treated with dasatinib

In order to confirm the results from the flow cytometric anaysis of p-CrkL within the bulk population of dasatinib-treated cells (as described in Figure 4-9), a Western blot for p-CrkL was performed on the cells remaining after 12 days treatment. Figure 4-10A shows that near complete inhibition of p-CrkL was achieved in 2 of the patients' dasatinib-treated CML cells (CML 232 and 219) and that complete inhibition was reached in 1 patient's CML cells (CML 235). To determine the percentage of p-CrkL in each sample, densitometry was performed on the blots shown in Figure 4-10A, with correction on each arm for its corresponding pan-actin loading control. Figure 4-10B demonstrates that 94.5% inhibition of p-CrkL was achieved in the total population of dasatinib-treated CML cells, as determined by Western blot ($p=0.00014$ for dasatinib-treated cells versus no drug control (100%)).

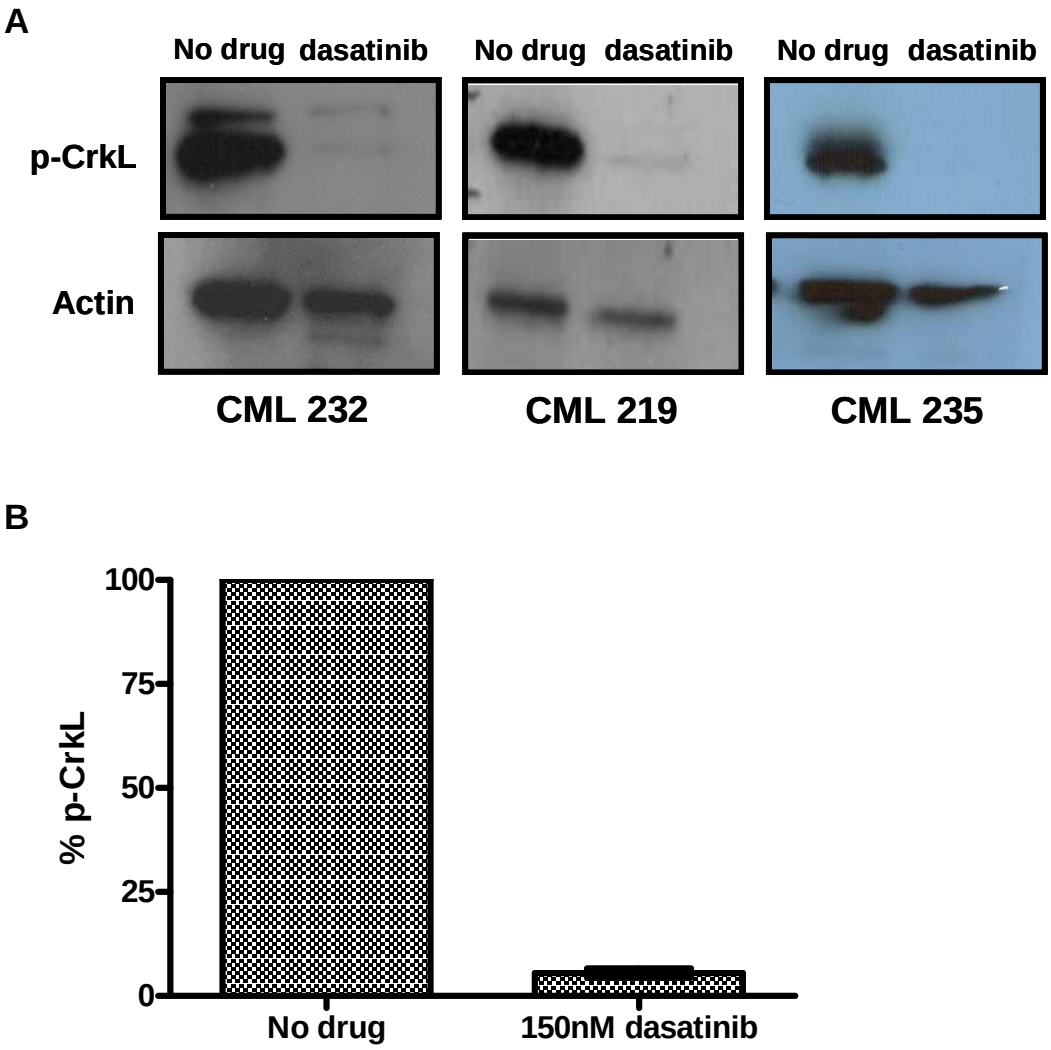

Figure 4-10 Western blot analysis of p-CrkL expression within a total population of CML cells treated with dasatinib

Panel A shows p-CrkL profiles from 3 patients' $CD34^+$ CML cells treated ± 150nM dasatinib for 12 days. Pan-actin was included in each experiment as a protein loading control. Panel B shows the mean percentage of p-CrkL expressed in the samples shown in panel A, as measured by densitometry. Each sample was corrected for its corresponding pan-actin control (p=0.00014 for dasatinib treatment versus no drug control (100%)).

4.2.8 Levels of p-CrkL within each cell division of CML cells treated with dasatinib

It has previously been demonstrated by our own group (131) and others (300),(298), that BCR-ABL is over-expressed within very primitive populations of CML cells. Therefore, it is unclear whether the level of inhibition of p-CrkL following dasatinib treatment, as seen in the total population of CML cells (Figure 4-10), is representative of all cells, or potentially 100% inhibition in the majority of cells and 0% inhibition in a smaller subpopulation. To determine whether prolonged dasatinib exposure could completely inhibit BCR-ABL activity, specifically within the undivided primitive CML cell population and also in each subsequent cell division, multi-colour flow cytometry was used. In the CML $CD34^+$ cells described in Figure 4-10, intracellular p-CrkL measurement was combined with CFSE analysis by flow cytometry. Cells that retain maximal CFSE fluorescence (CFSEmax), as compared to a colcemid control, represent the primitive $CD34^+$ cells that remain undivided. Figure 4-11A shows the levels of p-CrkL within each cell division following 150nM dasatinib treatment, as calculated based on the levels of p-CrkL in each corresponding untreated control (100%). Statistical analysis revealed no difference in p-CrkL levels between the total CML cell population and each cell division at every time-point (Table 4-1).

	Day 4	Day 8	Day 12
Undivided population	0.152	0.578	0.377
Division 1	0.312	0.457	0.645
Division 2	0.748	0.391	0.805
Division 3	0.061	0.743	0.776

Table 4-1 p values for the total CML cell population versus each division of CML cells treated with 150nM dasatinib for 12 days

In order to determine whether this was the maximal amount of BCR-ABL inhibition achievable by dasatinib, CML $CD34^+$ cells (n=3) were also treated with a much increased dose of dasatinib (1000nM; not achievable in patients). Figure 4-11B demonstrates that, using a higher concentration of dasatinib, no significant difference was observed between the total population and each cell division at every time-point (Table 4-2). Furthermore, no significant difference was observed between 150nM and 1000nM dasatinib treatment (Table 4-3).

	Day 4	Day 8	Day 12
Undivided population	0.787	0.382	0.455
Division 1	0.529	0.441	0.940
Division 2	0.319	0.984	0.273
Division 3	0.616	0.185	0.191

Table 4-2 p values for the total CML cell population versus each division of CML cells treated with 1000nM dasatinib for 12 days

	Day 4	Day 8	Day 12
Total population	0.827	0.718	0.768
Undivided population	0.748	0.947	0.494
Division 1	0.954	0.567	0.715
Division 2	0.694	0.143	0.877
Division 3	0.945	0.422	0.425

Table 4-3 p values for the 12 day 150nM dasatinib-treated CML cells versus the 12 day 1000nM dasatinib-treated CML cells

Although there looks to be a trend towards increased p-CrkL inhibition in later cell divisions as compared to earlier ones (specifically, division 3 versus undivided cells) in both 150 and 1000nM dasatinib-treated cells, the difference was not significant (Table 4-4).

	Day 4	Day 8	Day 12
150nM dasatinib	0.174	0.409	0.357
1000nM dasatinib	0.803	0.332	0.329

Table 4-4 p values for the undivided population of cells versus cell division 3 of both 12 day 150nM dasatinib-treated CML cells and 1000nM dasatinib-treated CML cells

These data indicate that maximal pharmacological inhibition of BCR-ABL is achieved with 150nM dasatinib and that every subpopulation of CML cells is inhibited equally.

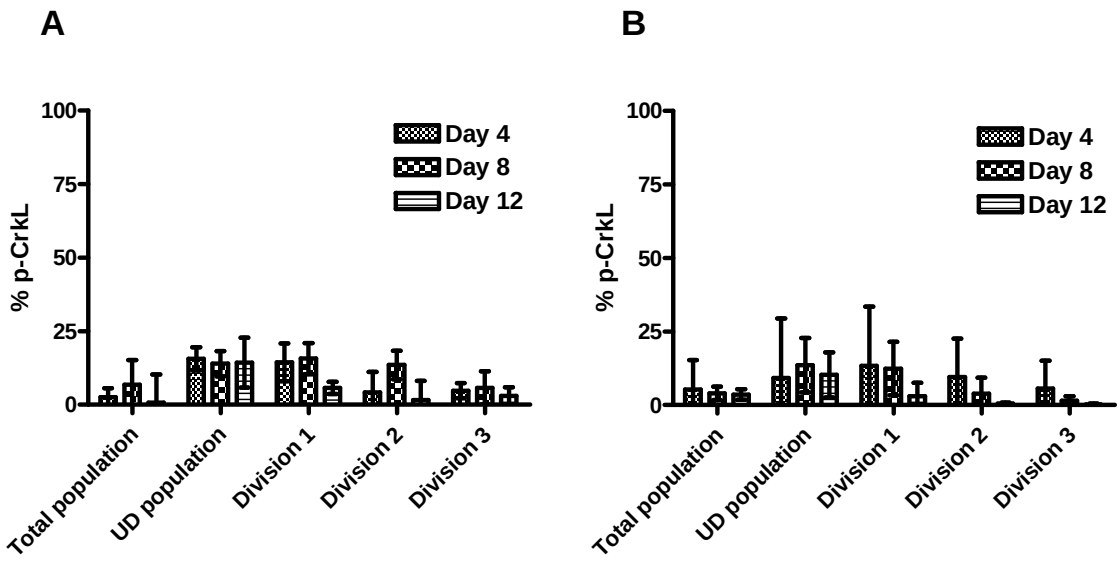

Figure 4-11 Levels of p-CrkL within each cell division of CML cells treated with dasatinib

CFSE-stained CML CD34$^+$ cells (n=3) were treated with either 150nM dasatinib (A) or 1000nM dasatinib (B) for 12 days. Measurement of p-CrkL was performed by flow cytometry at the indicated time-points, within each cell division. The level of p-CrkL was calculated based on the relevant untreated control (100%).

4.2.9 Comparison of the phosphorylation levels of CrkL and STAT5 within dasatinib-treated CML cells

Shah and colleagues have recently suggested that, since CrkL is physically associated to- and highly phosphorylated by- BCR-ABL, the detection of p-CrkL may not be sensitive enough to detect modest changes in BCR-ABL activity. The authors suggest that other endpoints should also be measured in order to make an accurate assessment of BCR-ABL inhibition (310). Therefore, in order to verify whether the measurement of p-CrkL gave an exact representation of the amount of BCR-ABL inhibition achieved, the phosphorylation of another downstream substrate, STAT5, was also measured. Figure 4-12 demonstrates the levels of p-STAT5 within each cell division of CFSE-stained CML $CD34^+$ cells, treated for 12 days with 150nM dasatinib, as measured by flow cytometry. These data were then compared to the p-CrkL results at day 12 which were demonstrated in Figure 4-11A. No significant differences were observed between the two methods for determining the inhibition of BCR-ABL kinase activity ($p=0.4$ for the total population; $p=0.95$ for the undivided population; $p=0.83$ for division 1; $p=0.8$ for division 2 and $p=0.52$ for division 3).

It should be noted that, since non CML samples are relatively rare, it was not feasible to use one sample solely for the purpose of measuring the baseline levels of p-STAT5. Therefore, the levels of p-STAT5 and p-CrkL were compared within $CD34^+$ CML cells only, without any non CML background correction.

These data further confirmed the reliability of the p-CrkL flow cytometric method for the measurement of BCR-ABL activity.

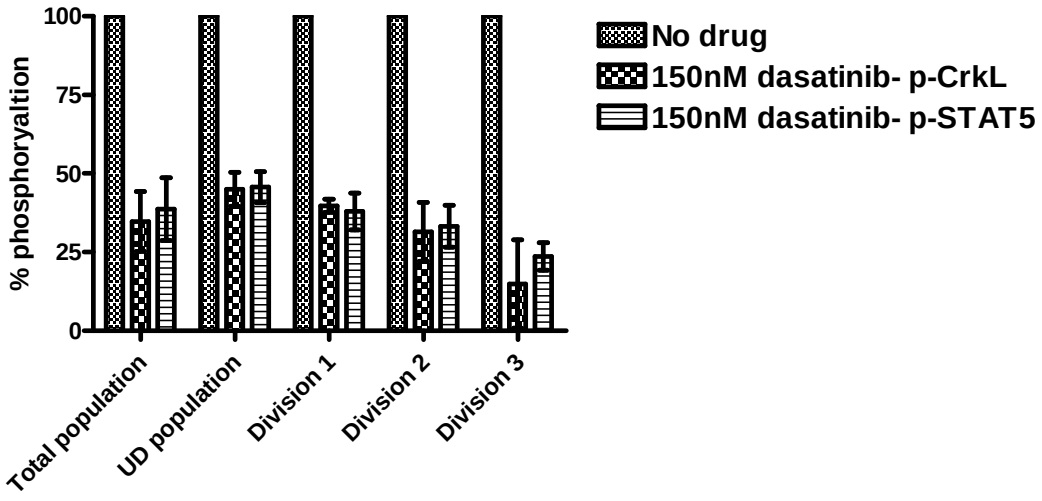

Figure 4-12 Comparison of the phosphorylation levels of CrkL and STAT5 levels in dasatinib-treated CML cells

CFSE-stained CML $CD34^+$ cells (n=3) were treated ± 150nM dasatinib for 12 days. Measurement of p-STAT5 was performed by flow cytometry at day 12, within each cell division. The level of p-STAT5 was calculated based on the relevant untreated control (100%) and compared to the p-CrkL data described in Figure 4-11A.

4.2.10 Undivided CML cell recoveries as measured by CFSE-staining

Previous studies by our lab have demonstrated the anti-proliferative effect of both IM (226) and dasatinib (131). Since the quiescent CML stem cell population resides within the CFSEmax population, it is important to measure the percentage of cells within this gate, in order to determine whether these cells have been targeted following TKI treatment. Therefore, CFSE staining was used to assess the most primitive CML cell recovery during the 12 day treatment timecourse of CML $CD34^+$ cells (n=3) with 150nM dasatinib. Figure 4-13 demonstrates the percentage of CML cells which remain undivided at day 12 of treatment, as compared to the input cell number from the start of the timecourse. The percentage of dasatinib-treated CML cells which remained undivided was significantly increased as compared to untreated control (0.21% versus 0.07%; p=0.03). This corroborates previous data which showed an enrichment for the CFSEmax undivided population following TKI treatment (131, 226).

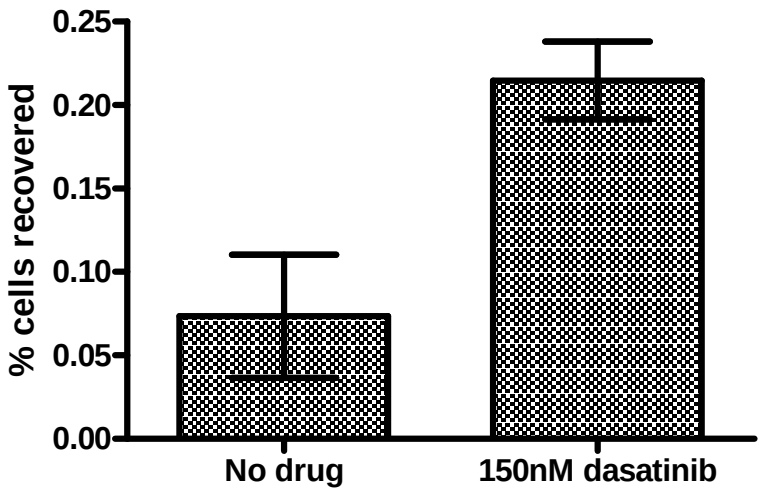

Figure 4-13 Undivided CML cell recoveries as measured by CFSE-staining

CFSE-stained CML CD34^{+} cells (n=3) were treated ± 150nM dasatinib for 12 days and measurement of CFSE was performed by flow cytometry. The percentage of undivided cells recovered at day 12 was calculated based on the input cell number at day 0.

4.2.11 CML cell recoveries within each division as measured by CFSE-staining

Next, a further analysis of the cell division status of the cells which remained following the 12 day timecourse was performed. Figure 4-14 demonstrates the percentage of cells within each cell division, recovered following 12 days treatment ± 150nM dasatinib. Consistent with previous data, an anti-proliferative effect was observed with dasatinib treatment as compared to no drug control. The data described in Figure 4-13 showed enrichment for the undivided population of CML cells following TKI treatment. However, Figure 4-14 shows that it is not only the quiescent population of CML cells which is able to survive the prolonged dasatinib exposure. It would appear that a further resistant CML cell population, which is able to reach the earlier cell divisions, exists. CFSE analysis of the CML cells which survived the 12 days treatment with 150nM dasatinib revealed that the majority of recovered cells resided within cell division 2 (Table 4-5).

	No drug (%)	150nM dasatinib (%)
undivided population	0.55	3.01
Division 1	0.483	40.05
Division 2	14.81	48.71
Division 3	43.52	7.99
Division 4	26.53	0.23
Division 5	9.26	0
Division 6	4.84	0

Table 4-5 Percentages of CML cells residing within each division, following 12 days treatment ± 150nM dasatinib

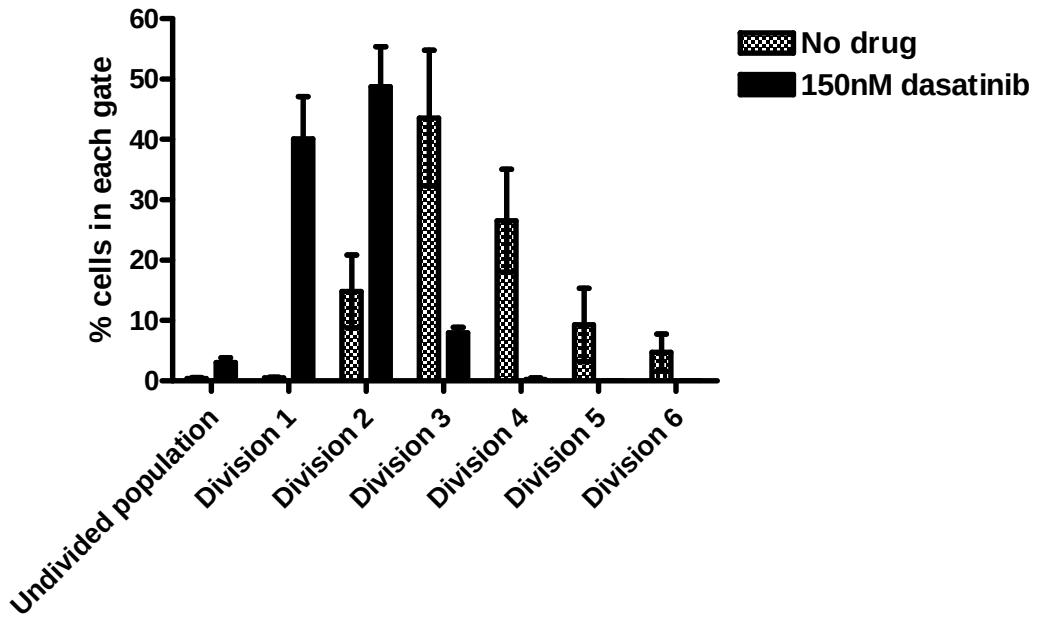

Figure 4-14 CML cell recoveries within each cell division as measured by CFSE-staining

$CD34^+$ CML cells were first stained with CFSE, cultured in SFM minus GFs and treated ± 150nM dasatinib for 12 days. The percentages of cells residing within each cell division were then determined by CFSE-staining, as measured by flow cytometry.

4.2.12 CML cell cycle status as measured by Ki67 and 7AAD staining

Although CFSE staining has proven to be a reliable technique for the identification of undivided cells, it should be noted that cell quiescence cannot be directly confirmed by this method, as it does not give any information on cell cycle status i.e. cells within the undivided gate may either be quiescent or in G_1 arrest. In order to determine the cell cycle status of the CML cells which have been treated ± 150nM dasatinib, Ki67/7AAD staining was carried out. Figure 4-15 shows representative patient's CML cells left untreated (A) and treated with 150nM dasatinib (B); cultured with (right hand panel) and without (left hand panel) GFs at day 12 of treatment. Panel A shows that the majority of untreated CML cells, which have been cultured with exogenous GF support, are in division (G_0: 26.5%; G_1: 48.56%; S/G_2/M: 24.47%). As expected, fewer cells had gone into division in the CML cells which were untreated and cultured without GFs (G_0: 55.34%; G_1: 36.48%; S/G_2/M: 7.24%). Panel B demonstrates the anti-proliferative effect of dasatinib, with the majority of cells residing within the G_0 stage of cell cycle. Again, far fewer cells had gone into division in the CML cells which had been cultured without GFs versus the cells which had been cultured with GFs by day 12 of dasatinib treatment (G_0: 86.49% and 51.23%; G_1: 6.99% and 40.31%; S/G_2/M: 2.17% and 7.57%, respectively). This finding is consistent with previous data, whereby a detailed analysis of CML cells revealed very little/no detectable levels of Ki67 expression within the quiescent stem cell population (224). This would suggest that the dasatinib-treatment without GFs in the culture media has selected for a quiescent population of CML cells. However, since the CFSE data (described in Figure 4-14) shows that the majority of the cells have been able to divide to division 2, it may mean that the cells divided early in the timecourse and had stopped almost all cell division by the day 12 time-point.

It is also interesting to note that the percentage of cells in G_0 was approximately equal in the untreated cells cultured without GFs and the dasatinib-treated cells cultured with GFs (G_0: 55.34% versus 51.23%, respectively). This finding corroborates the data presented in Figure 4-1, where TKI treatment in the presence of GFs gave the same effect as removing the GF support from untreated control cells.

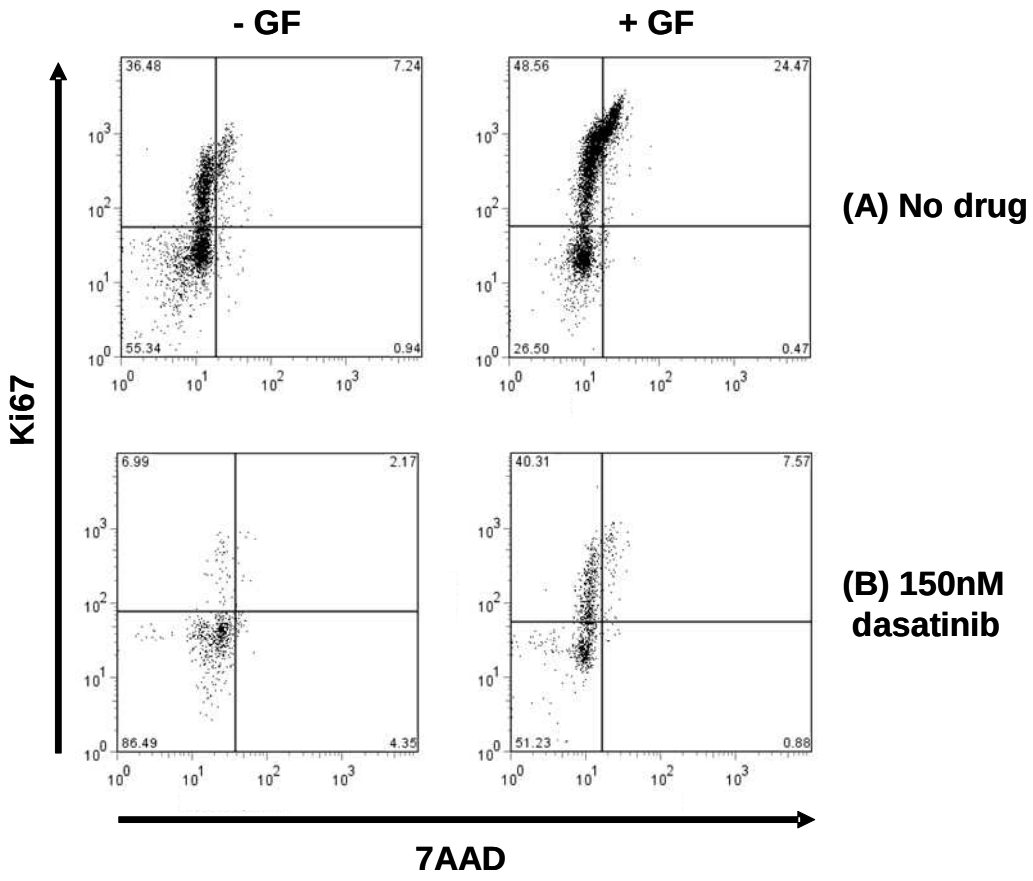

Figure 4-15 CML cell cycle status as measured by Ki67 and 7AAD staining

Representative Ki67/7AAD FACS profile from one patient's $CD34^+$ CML cells left either untreated (A) or treated with 150nM dasatinib (B) and cultured ± GFs for 12 days.

4.2.13 The effect of dasatinib treatment on the localisation of FoxO3a within CML cells

The previous data demonstrated that dasatinib treatment exerted a potent anti-proliferative effect on CML cells, consistent with other studies (131, 226). However, the mechanism by which dasatinib causes these anti-proliferative effects is still not fully understood. Since the nuclear localisation of FoxO3a and its subsequent transcriptional activity, has been shown to be important for the induction of cell cycle arrest (311); this was next investigated. CML $CD34^+$ cells were first cultured in SFM ± GF and treated with 150nM dasatinib for 12 days, before being fixed onto slides and stained with anti-FoxO3a antibody. Nuclei were counterstained with then DAPI and levels of FoxO3a were then visualised within these cells by IF. Figures 4-16A and B demonstrate a representative FoxO3a IF profile and corresponding surface plot profile (using ImageJ software) from one patient's cells, respectively. In the untreated CML cells cultured with (top left panel) and without (top right panel) GFs, FoxO3a was found to be predominantly localised to the cytoplasm where it is transcriptionally inactive. The greatest amount of cytoplasmic FoxO3a-positive puncta was observed in the untreated cells cultured with GFs. Treatment of the CML cells with dasatinib in the presence of GFs (bottom left panel), resulted in a localisation of FoxO3a to both the nucleus and cytoplasm. However, treatment of the CML cells with dasatinib without exogenous GF support (botton right panel), resulted in FoxO3a to be predominantly localised to the nucleus and therefore, in a transcriptionally active state. Since FoxOs transcription factors are direct targets of activated Akt, it could be said that the activation of the PI3K/Akt pathway within CML cells, by BCR-ABL and/or GF stimulation, induces the cytoplasmic localisation and hence inhibition of FoxO3a, which is consistent with previous studies (312-314). Treatment of CML cells with dasatinib induces the nuclear localisation and hence activation of

FoxO3a transcriptional activity. However, this can be partially overcome by the addition of exogenous GF support.

A

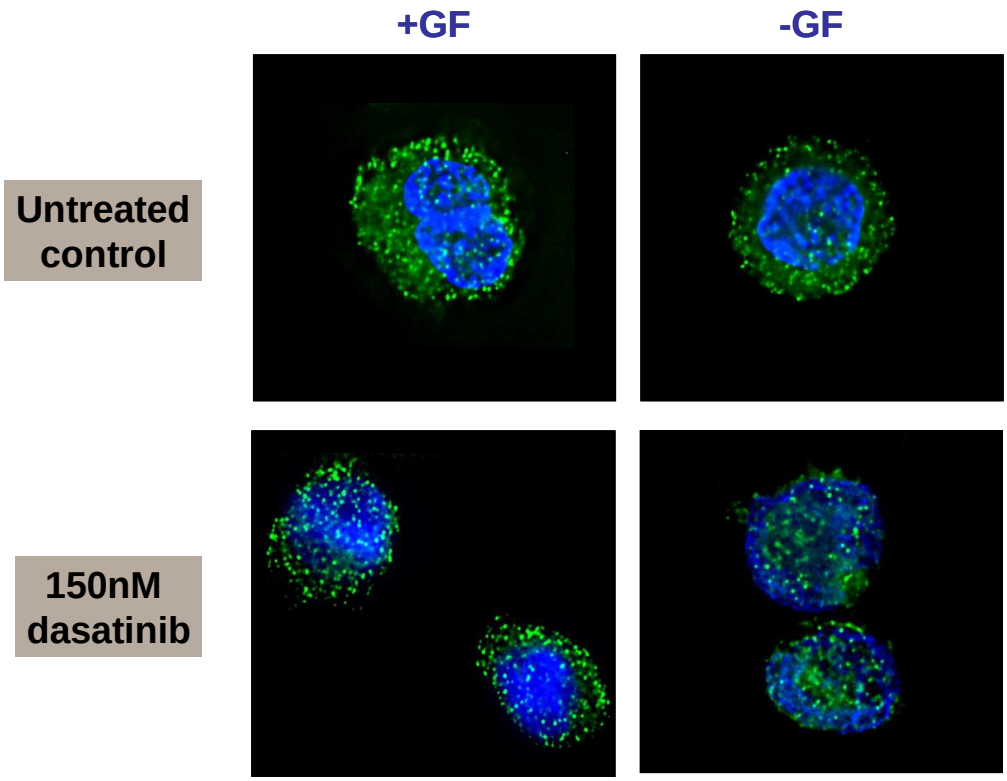

B

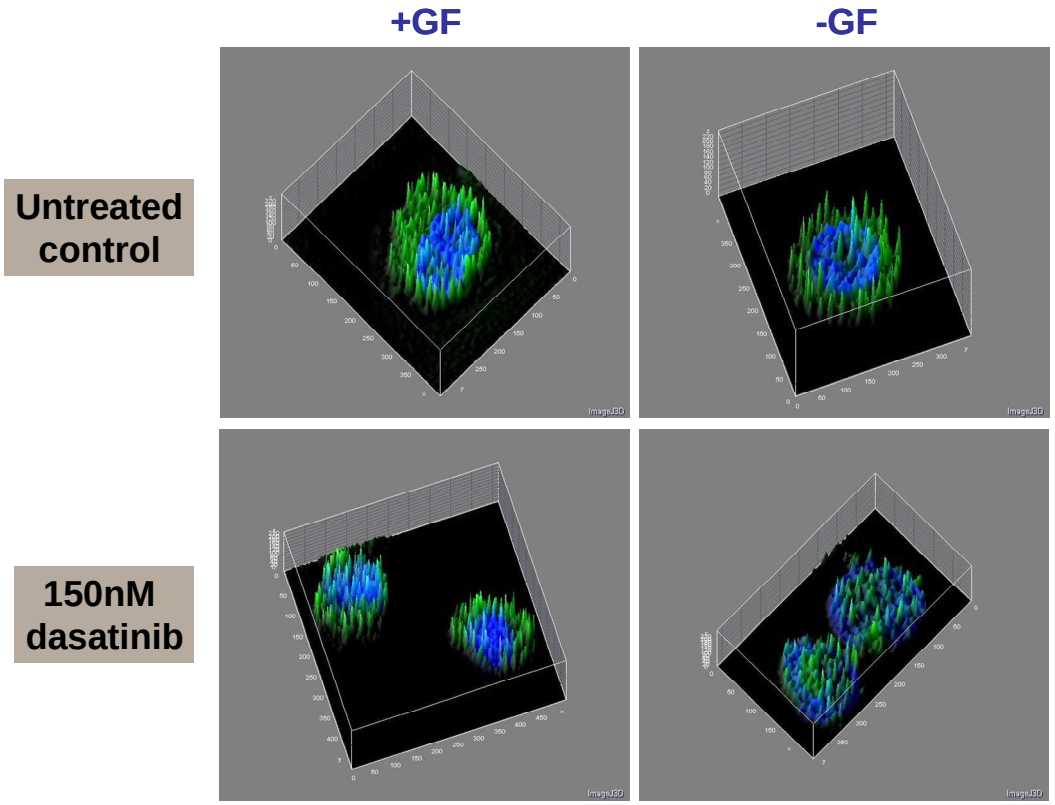

Figure 4-16 The effect of dasatinib treatment on the localisation of FoxO3a within CML cells

$CD34^+$ CML cells were cultured in SFM ± 5GF and treated ± 150nM dasatinib for 12 days. Remaining CML cells were then fixed onto multi-spot slides and stained with anti-FoxO3a antibody. Nuclei were counterstained with DAPI. Representative IF profiles (A) and surface plots using ImageJ software (B) from one patient are shown.

4.2.14 Analysis of cyclin D1 expression in dasatinib-treated CML cells

The cyclin D1 proto-oncogene is an important regulator of G_1 to S phase transition in many different cell types and its expression is often disrupted in various cancers. It has been recently reported that BCR-ABL silencing by small interfering RNAs (siRNA) resulted in significantly reduced cyclin D1 mRNA and protein expression in K562 cells (315). Furthermore, the nuclear localisation of FoxOs (as demonstrated in Figure 4-16) results in the activation of their transcriptional activity which promotes cell cycle arrest through down-regulation of cyclin D (139). Therefore, the effect of BCR-ABL activity inhibition on cyclin D1 expression was next assessed in the primary CML cells remaining after dasatinib treatment. The relative mRNA expression of cyclin D1 was measured by qRT-PCR, following 12 days treatment ± 150nM dasatinib and cultured in the absence of GFs. Figure 4-17 demonstrates that inhibition of BCR-ABL by dasatinib caused approximately a 3-fold reduction in cyclin D1 mRNA, relative to no drug control ($p=0.016$), consistent with previous studies (314). This also is in keeping with the Ki67/7AAD data presented in Figure 4-15, where the majority of cells resided within the G_0 phase of cell cycle.

These data taken together indicate that the treatment of $CD34^+$ CML cells with dasatinib leads to the nuclear localisation and subsequent activation of FoxO3a. This then contributes to the reduced transcription of the FoxO3a downstream target, cyclin D1, and maintenance of quiescence within these resistant CML cells.

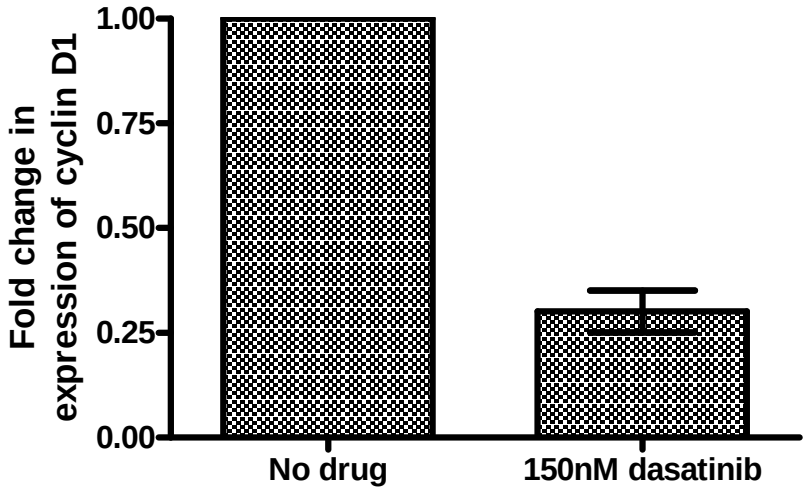

Figure 4-17 Analysis of cyclin D1 expression in dasatinib-treated CML cells

Expression of cyclin D1 mRNA transcripts as measured by qRT-PCR in $CD34^+$ CML cell samples (n=3) following treatment ± 150nM dasatinib for 12 days.

4.3 Analysis of functionality of the CML cells remaining following prolonged BCR-ABL kinase inhibtion

4.3.1 Characterisation of 12 day dasatinib-treated CML cells following additional culture with GF support

To investigate whether the dasatinib-resistant cells were still fully functional and able to proliferate when stimulated with cytokines, further analyses were carried out. First, the cells remaining following 12 days dasatinib treatment were washed with PBS to remove the drug and cultured in the presence of a potent 5GF cocktail for 7 days. A viable cell count using trypan blue dye exclusion was then performed at this time-point. Figure 4-18A demonstrates that the ± dasatinib-treated cells were found to expand 17- and 5-fold, respectively (p=0.086). The lower cell number within the dasatinib-treated arm may reflect the fact that this cell fraction contained more primitive CML cells, which were slow to proliferate as compared to the actively cycling untreated cells. The levels of p-CrkL, as a measure of BCR-ABL activity, were also determined in the cytokine-cultured cells at this time-point. Figure 4-18B shows that the dasatinib-treated cells had a level of 98% p-CrkL as compared to untreated control (100%) (p=0.95). This therefore suggests that BCR-ABL activity had been re-activated in these dasatinib-treated cells and that BCR-ABL inhibition is survivable.

Due to the fact that there was a trend towards lower viable cell counts in the dasatinib-treated CML cells as compared to the untreated cells at the day 7 time-point (Figure 4-18A), it was hypothesised that at least a proportion of the dasatinib-treated cells may have undergone an irreversible growth arrest following drug treatment. In order to address this, Ki67/7AAD staining was also carried out on the cells following the 7 days culture with 5GF. Figure 4-18C demonstrates that

the majority of both the untreated and the dasatinib-treated cells were in cycle, following drug wash out and 7 days culture with cytokines (G_0: 2.73 and 6.43%; G_1: 66.15 and 70.91% and S/G_2/M: 31 and 22.55%, for untreated and dasatinib-treated cells, respectively). These data indicate that the dasatinib treatment did not cause irreversible growth arrest in the vast majority of these cells. As this Ki67/7AAD profile is only a reflection of what is happening at a particular time-point, it is also possible that the remaining 6.43% of cells in G_0 would also go into cycle in time, particularly since the dasatinib treated cells contained more primitive cells and as suggested above would likely take longer to enter cell division upon GF stimulation. A further possibility is that these cells represent a quiescent population which, consistent with previous studies (224), remain undivided even in the presence of high GFs. In order to verify the cell cycle data, CFSE staining was also carried out. Following 12 days dasatinib treatment, the cells were washed with PBS and stained with CFSE, before being cultured for 7 days in SFM+5GF. Figure 4-18D confirms the data from the cell cycle analysis (Figure 4-18C) as the majority of both the untreated and the dasatinib-treated cells were in a state of cell division, following drug wash out and 7 days culture with cytokines (undivided population: 1.95 and 4.51% for untreated and dasatinib-treated cells, respectively). Since the proportion of undivided cells remaining following 12 days of 150nM dasatinib treatment, was an average of 3.01% (range: 2.05, 2.4 and 4.58%) (Figure 4-14), it is possible that the undivided cell fraction remaining at day 7 of culture in SFM+5GF, represents a quiescent population of CML cells which was both unaffected by prolonged treatment with dasatinib and also remained undivided after exposure to high concentrations of cytokines.

A

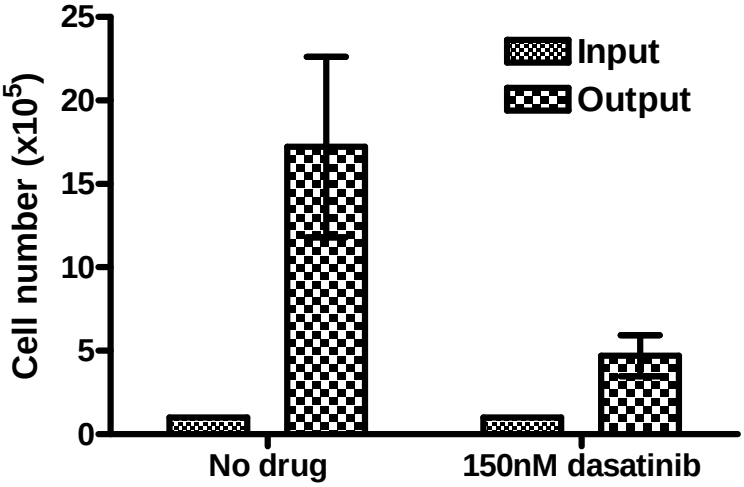
25
20
15
10
5
0
Cell number (x10^5)
Input
Output
No drug
150nM dasatinib

B

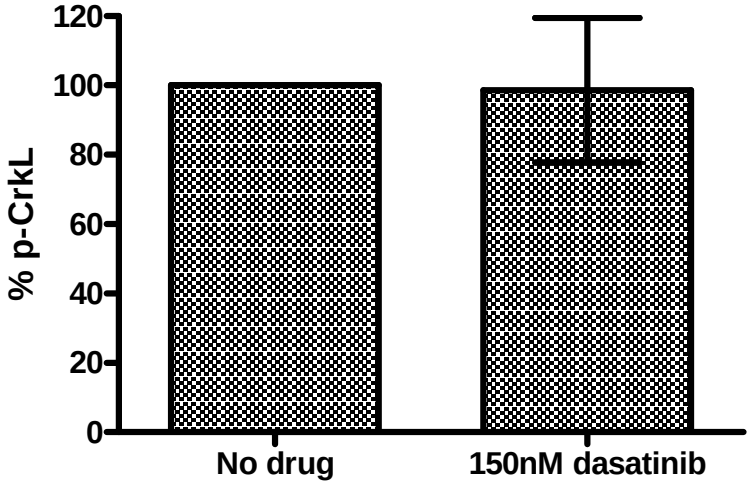
120
100
80
60
40
20
0
% p-CrkL
No drug
150nM dasatinib

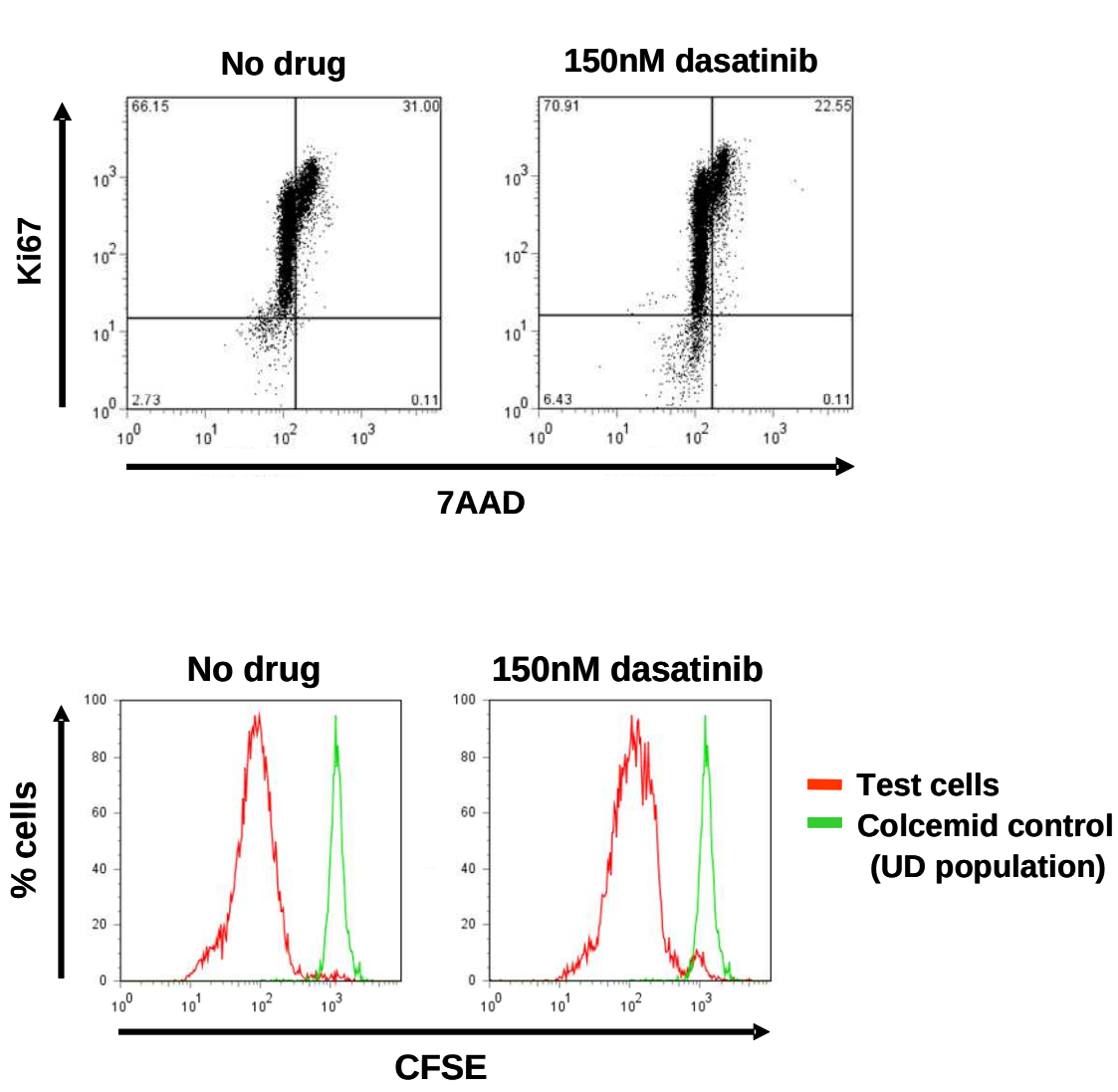

Figure 4-18 Characterisation of 12 day dasatinib-treated CML cells following additional culture with GF support

The 12 day ± 150nM dasatinib-treated cells were washed with PBS, stained with CFSE and cultured in 5GF for 7 days. At the 7-day time-point, viable cell counts were performed by trypan blue dye exclusion (A) and p-CrkL (B), Ki67/7AAD (C) and CFSE (D) were all measured by flow cytometry.

4.3.1.1 The effect of dasatinib removal and GF culture on the localisation of FoxO3a within CML cells

As stated in Section 4.2.13, the nuclear localisation of FoxO3a and its subsequent transcriptional activity, has been shown to be important for the induction of cell cycle arrest (311). Since we demonstrated that the treatment of CML cells with dasatinib induces the nuclear localisation of FoxO3a, it was next investigated whether this could be reverted following the removal of dasatinib and the culture with GFs. First, the CML cells remaining following 12 days dasatinib treatment were washed with PBS and cultured in SFM+5GF for 7 days. An aliquot of the CML cells was then fixed onto slides and stained with anti-FoxO3a antibody. Nuclei were counterstained with then DAPI and levels of FoxO3a were then visualised within these cells by IF. Figure 4-19 demonstrates a representative FoxO3a IF profile from one patient's cells. In both the untreated and dasatinib-treated CML cells, FoxO3a was found to be predominantly localised to the cytoplasm and was therefore transcriptionally inactive. This suggests that the reactivation of the PI3K/Akt pathway, by BCR-ABL and GF stimulation, following the dasatinib wash-out within the CML cells, induced the cytoplasmic localisation and inhibition of FoxO3a, which would thereby allow the cells to continue to divide.

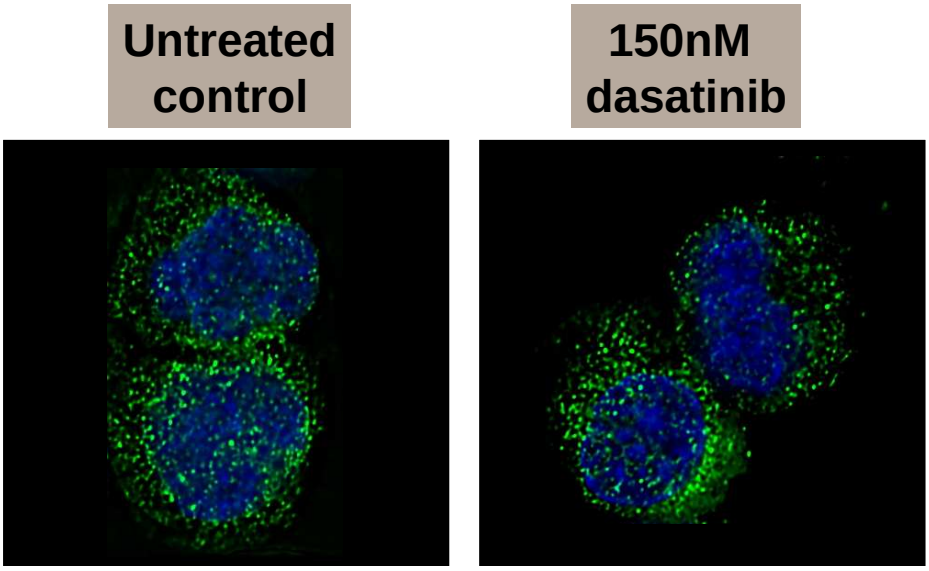

Figure 4-19 Detection of FoxO3a in dasatinib-treated CML cells following drug wash-out and additional culture with GFs

The 12 day ± 150nM dasatinib-treated cells were washed with PBS and cultured in 5GF for 7 days. Aliquots of CML cells were then fixed onto multi-spot slides and stained with anti-FoxO3a antibody. Nuclei were counterstained with DAPI.

4.3.2 Analysis of committed and primitive progenitor capacity in surviving 12 day dasatinib-treated CML cells

To determine whether the surviving CML cells had functional committed and primitive progenitor capacity, the ± dasatinib-treated cells were plated in CFC (committed progenitor) and LTC-IC (primitive progenitor) assays and compared to a baseline ($CD34^+$ CML cells which had no prior culture or treatment.) The resulting colonies were picked and analysed for Ph^+ cells by D-FISH. In each of the three patients' samples kindly tested by Mrs Elaine Allan, >98% of the cells in each of the conditions were shown to be BCR-ABL positive by D-FISH. Figure 4-20A demonstrates that the untreated arm was able to form 3 times the number of CFC as compared to the cells at baseline (100%), suggesting differentiation and expansion from stem cells, even in the absence of GFs. Dasatinib-treated cells were only able to form ~2% CFC as compared to baseline and were significantly reduced as compared to no drug control ($p=0.0125$). Next, the number of CML cells which were able to form a CFC colony, per 1000 surviving cells at day 12 was calculated. The no drug control was then normalised to 1 and the dasatinib-treated arm was calculated based on this. Figure 4-20B shows that there was a trend towards a reduction in the CFC colonies produced per 1000 cells at day 12 in the dasatinib treatment arm, as compared to untreated control. However, there was no significant difference observed between the two conditions ($p=0.25$). These data indicate that dasatinib treatment effectively targeted the more mature committed progenitor CML cell population, based on the starting cell number. However, the ability to form a CFC colony within the cells which survived the dasatinib treatment did not significantly alter, as compared to untreated control cells.

Figure 4-20C shows that compared to baseline cells, the untreated cells formed 50% less LTC-IC colonies, suggesting that half of these cells had proceeded towards terminal differentiation. Dasatinib-treated cells recovered a significantly reduced number of LTC-IC (~14%) as compared to both baseline and no drug control ($p=0.01$ and $p=0.02$, respectively). Next, the number of CML cells which were able to form a LTC-IC colony, per 1000 surviving cells at day 12 was calculated. Again, the no drug control was then normalised to 1 and the dasatinib-treated arm was calculated based on this. Figure 4-20D shows that there was a 21-fold increase in the LTC-IC colonies produced per 1000 cells at day 12 in the dasatinib treatment arm, as compared to untreated control ($p=0.025$). This mirrors the data described in Section 4.2.10, where the percentage of primitive undivided cells recovered at day 12 of dasatinib treatment was increased as compared to untreated control cells.

Overall, these data suggest that following BCR-ABL inhibition by dasatinib, within a total CML cell population, the committed CML progenitor population is targeted, whereas, the primitive quiescent CML cells with LTC-IC potential remain relatively unaffected. However, in the population which survives drug treatment, the CML cells with CFC potential remain relatively unaffected, whereas the cells with LTC-IC potential are enriched.

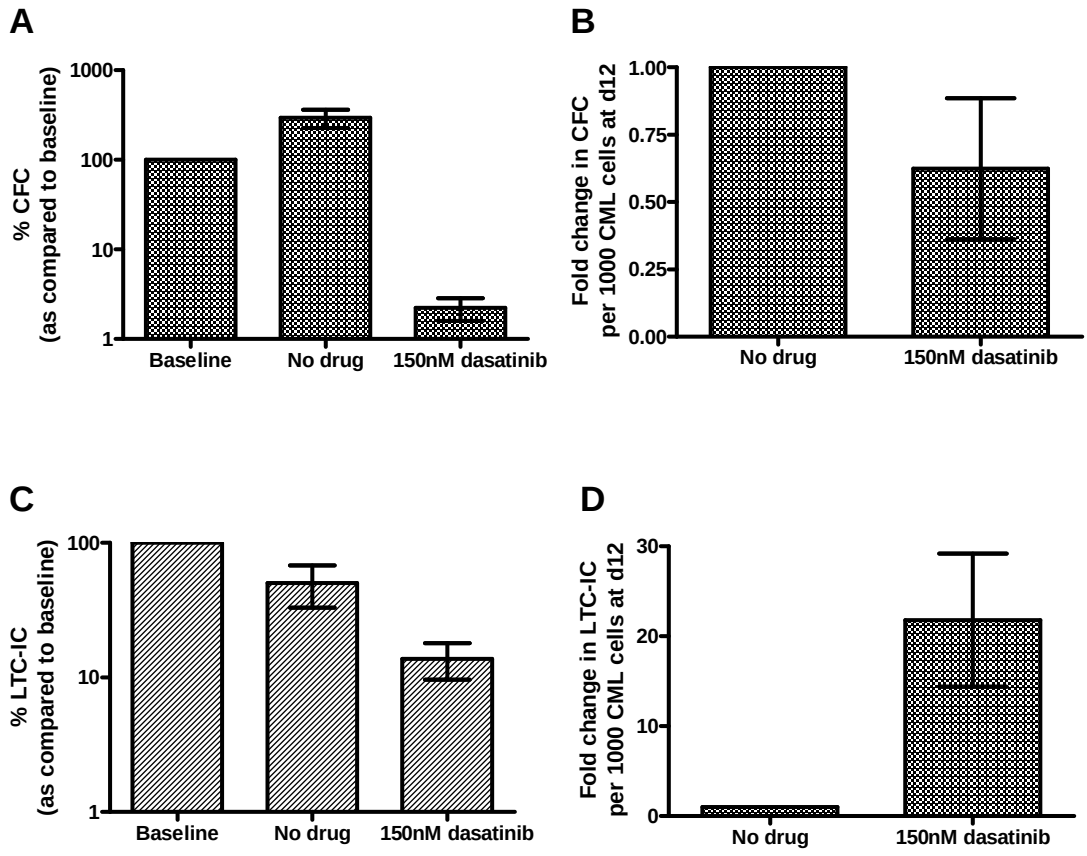

Figure 4-20 Analysis of committed and primitive progenitor capacity in surviving 12 day dasatinib-treated CML cells

Following the 150nM dasatinib treatment timecourse, the remaining CML cells (n=3) were washed with PBS to remove any drug and added to CFC (A and B) and LTC-IC (C and D) assays.

4.3.3 Analysis of murine engraftment of surviving CML cells following treatment ± 150nM dasatinib for 12 days

To further investigate the functionality of the cells that survived the 12 day 150nM dasatinib treatment timecourse, the remaining CML cells (n=3) were also transplanted into NOD/SCID mice, to determine any reconstitution potential. The surviving cells were first washed twice with PBS and sent to the animal facility at the University of Bristol, where Dr Allison Blair kindly performed all murine engraftment experiments. Engraftment was determined by the flow cytometric measurement of human CD45 in the murine BM cells. Figure 4-21 demonstrates that insufficient engraftment was achieved in both the untreated control and the dasatinib-treatment arm; therefore no definitive conclusion could be drawn from this experiment.

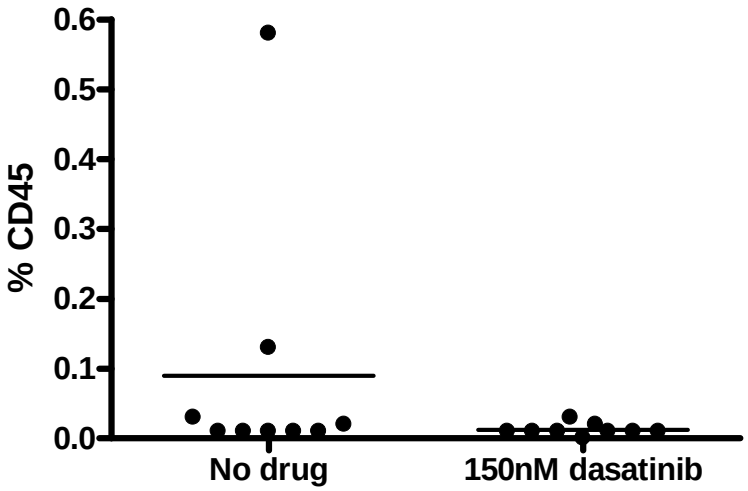

Figure 4-21 Analysis of murine engraftment of surviving CML cells following treatment ± 150nM dasatinib for 12 days

Following the treatment timecourse, the CML cells (n=3) were washed with PBS to remove any drug and transplanted into NOD/SCID mice. Three mice were transplanted per patient sample. Mice were sacrificed at 16 weeks post-transplant. Engraftment levels were determined by flow cytometric analysis of human CD45 in the murine BM cells.

4.4 Summary

The term “oncogene addiction” is used to describe the phenomenon by which some cancers acquire dependency on one or a few genes for the maintenance of the malignant phenotype and cell survival. The purpose of the work in this chapter was to determine whether CML stem cells are “addicted” to BCR-ABL kinase activity, by exposing $CD34^+$ CML cells to TKI treatment and investigating whether the inhibition of BCR-ABL kinase correlated with cell death.

In experiments designed to determine optimal treatment conditions, it was confirmed that $CD34^+$ CML cells are able to survive and proliferate in the absence of cytokine support. Furthermore, the TKI treatment of CML cells in the presence of high GFs gave the same effect as leaving the CML cells untreated in the absence of GFs. This confirms work first published by Dorsey et al. whereby IL-3 was found to protect IL-3 responsive, BCR-ABL-transformed haemopoietic progenitor cells from apoptosis caused by TKIs, including IM (303). This finding also has potential implications for the treatment of patients, in whom cytokines would be present at physiological concentrations. Studies which examined the effect of TKI exposure time and concentration also showed that each TKI exerted its effects very early in the timecourse (after 1 hour and possibly even earlier) and transient exposure was as effective as prolonged treatment, confirming the results from other investigators (310, 316). Furthermore, escalation up to clinically unachievable doses, did not give any increased cell kill over lower concentrations of the drug.

During a 12 day timecourse, dasatinib treatment in the absence of GF support resulted in a reduction in CML cell number to <2% of no drug control and <10% of the starting cell number. Investigation of possible resistance mechanisms revealed no evidence of oncogene amplification by D-FISH and no ABL-kinase domain

mutation was detected in any of the patient samples. Both D-FISH and qRT-PCR confirmed the presence of BCR-ABL within the surviving cells, ruling out the presence of normal cells as an explanation of dasatinib resistance.

Since the most primitive CML cell fraction has previously been shown to express increased levels of *BCR-ABL* transcripts and protein, there was some concern that any resistance may be caused by the fact that dasatinib was not able to effectively inhibit the increased levels of BCR-ABL activity within these primitive cell subpopulations. The experiments which measured p-CrkL levels within each CML cell division demonstrated that 150nM dasatinib treatment inhibited p-CrkL within each cell subpopulation to the same degree as the bulk population of CML $CD34^+$ cells. This level of inhibition could not be increased on dose escalation to 1000nM dasatinib and was not significantly different to the level of inhibition achieved of another downstream target, p-STAT5. Furthermore, since dasatinib treatment inhibited the phosphorylation of CrkL to the same level as that seen in non CML $CD34^+$ cells, it was concluded that the 12 day dasatinib treatment maximally inhibited BCR-ABL activity within each CML subpopulation.

Analysis of the percentage recoveries within each cell division revealed that the most primitive undivided cell fraction was higher in the dasatinib-treated cells as compared to the untreated control. A further subpopulation of CML cells, which were able to reach the earlier cell divisions, also remained. Not surprisingly, cell cycle analysis revealed that the majority of surviving CML cells following dasatinib exposure had stopped all cell division and resided within the G_0 stage of cell cycle by 12 days treatment. This was further confirmed by the observation of FoxO3a which was predominantly localised to the nucleus, with significantly reduced cyclin D1 expression in dasatinib-treated cells as compared to untreated control. This

data corroborates the findings from previous studies, whereby nuclear FoxO3a and its subsequent transcriptional activity, was important for the maintenance of both CML LICs in a CML-like disease mouse model (317) and quiescent CML stem cells *in vitro* (314). Although it is highly likely that other cell cycle regulators are involved in the anti-proliferative effect induced by dasatinib or any other TKI treatment, the FoxO axis may represent an important stem cell quiescence mechanism for future investigation.

The cells which survived the 12 day dasatinib treatment course were able to reactivate BCR-ABL activity (as measured by p-CrkL) to approximately the same level as that of untreated cells, had predominantly cytoplasmic, transcriptionally inactive FoxO3a and were also able to expand 5-fold when cultured in the presence of cytokines. Data from the CFC assay confirmed that dasatinib treatment was able to effectively target mature committed progenitor cells which were able to form colonies. However, LTC-IC data suggested that the effect of dasatinib does not target the very primitive quiescent cell population to the same extent.

Overall, these data imply that since only 10% of CML cells remain following dasatinib treatment, 90% of $CD34^+$ CML cells are “oncogene addicted” to BCR-ABL kinase activity. Due to the fact that dasatinib is a dual SRC/ABL-kinase inhibitor, it is difficult to say whether cell death is exclusively due to BCR-ABL inhibition. However, the similarity in response for IM, nilotinib and dasatinib (Section 4.1.2) suggests that sensitivity is mainly based on the potency of BCR-ABL inhibition. Since BCR-ABL kinase is fully inhibited within the surviving CML cells, it could be said that this population is BCR-ABL-kinase-independent. It was also observed that two sub-populations exist within the BCR-ABL-kinase-

independent CML cell fraction: the very primitive quiescent CML population and a further population of cells which is able to divide to the early cell divisions. It is likely that the quiescent CML cell population evades dasatinib treatment simply by virtue of their quiescent state. However, since the second BCR-ABL independent population is still able to divide even without both exogenous GF support and BCR-ABL kinase activation, which would normally allow these cells to proliferate, it is probable that these cells use other survival pathways as a mechanism of resistance against dasatinib treatment.

5. RESULTS (III) Analysis of the effects of autophagy on CML stem cell survival

Clinical IM resistance has consistently been associated with gene amplification and the detection of BCR-ABL kinase mutations. However, previous experiments performed by our own laboratory and demonstrated in the last results chapter, have shown that CML cells which survive IM or dasatinib exposure *in vitro*, do not show any evidence of amplification and do not contain any ABL-kinase domain mutations at levels that would explain their IM resistance (131). Furthermore, the previous chapter also demonstrated that BCR-ABL kinase activity was completely inhibited in the CML cells which survived prolonged dasatinib treatment. This suggests that resistance may be partly influenced by BCR-ABL independent factors or pathways, which co-operate with BCR-ABL transformation and compensate for BCR-ABL inactivation.

Autophagy is a conserved catabolic membrane-trafficking process which degrades long-lived cellular components, providing the cell with essential stores of energy. In addition to important housekeeping functions, autophagy plays an important role in cell survival under conditions of nutrient and/or oxygen deprivation (164) and hence could be predicted to play a protective role in maintaining cancer cell survival (318). Therefore, the nutrient depletion and cellular stress caused by anti-cancer agents may induce autophagy and compromise the efficacy of therapy.

To examine the role of autophagy as a BCR-ABL independent survival mechanism, experiments were designed to determine whether:

1. autophagy is induced following the TKI treatment of CML cells
2. targeting of autophagy potentiates the TKI-induced death of CML cells

5.1 Autophagy is induced following the TKI treatment of CML cells

5.1.1 Analysis of key properties of cells undergoing autophagy

In order to determine whether CML cells undergo autophagy following TKI treatment experiments were designed to study the cellular changes in CML cells induced by dasatinib treatment in more detail. $CD34^+$ CML cells, which remained viable following culture with either SFM only (Figure 5-1A-C) or SFM ± 5GF (Figure 5-1D) and treatment ± 150nM dasatinib for 12 days, were analysed by flow cytometry (Figure 5-1A+B), light microscopy (Figure 5-1C) or EM (Figure 5-1D). Flow cytometry measuring the FSC-height (FSC-H) parameter, revealed that the dasatinib-treated CML cells were significantly smaller in size as compared to untreated cells, as shown by a representative histogram from one patient's cells (Figure 5-1A) and mean FSC-H from 3 patients' cells ($p=0.02$) (Figure 5-1B). This was also demonstrated by morphology analysis using conventional light microscopy (Figure 5-1C). Figure 5-1D (upper panel) demonstrates that GF deprivation of untreated CML cells (upper right) resulted in a reduction of cytoplasm and an increase of vacuoles, as compared to untreated cells cultured in the presence of GFs (upper left). This is consistent with previous studies, whereby the cytoplasm of haemopoietic cells became progressively replaced by vesicular structures, following GF withdrawal. These investigators found that the cells had induced autophagy in order to combat the GF starvation (164). Figure 5-1D (lower panel) also shows that treatment with dasatinib caused an increase in both the size and number of these cytoplasmic vacuoles within CML cells, cultured both in the presence (lower left) and absence (lower right) of GFs. Many electron-dense

inclusions within the vacuoles were also observed within the CML cells cultured without the presence of GFs (as denoted by the black arrows).

A

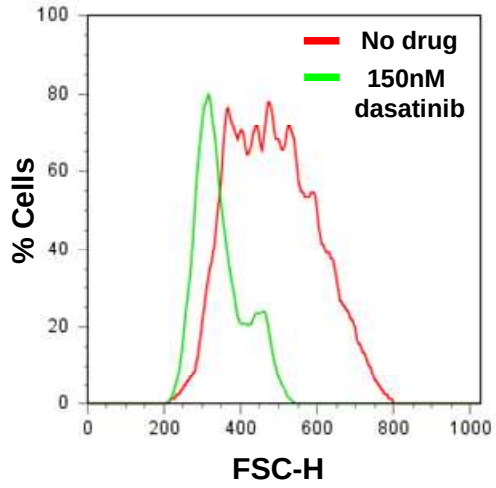

B

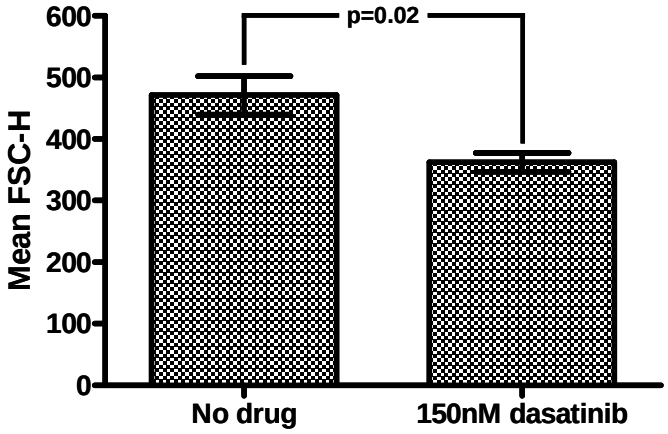

C

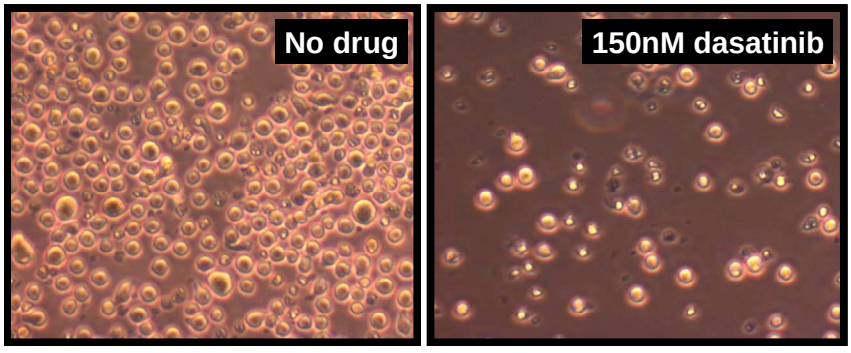

D

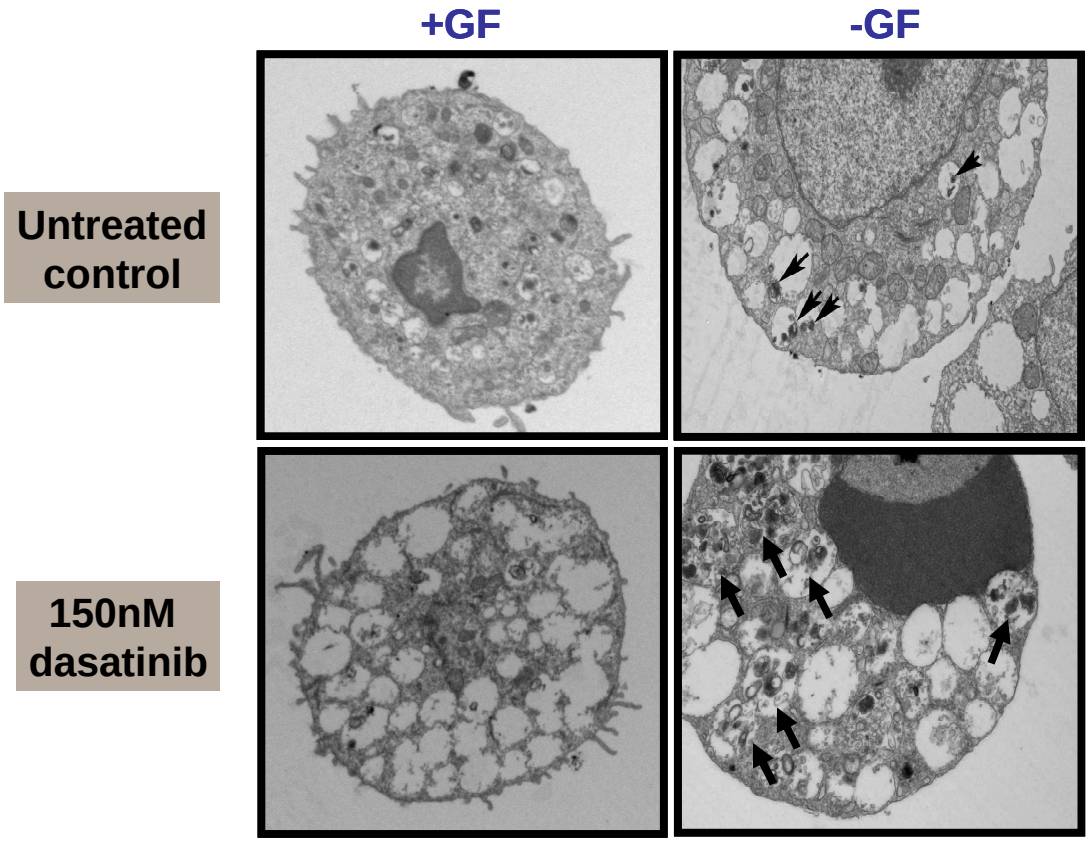

Figure 5-1 Analysis of key properties of cells undergoing autophagy

$CD34^+$ CML cells were either cultured in SFM only (A-C) or SFM ± 5GF (D) and treated ± 150nM dasatinib for 12 days. Cell size was measured using the FSC-H parameter by flow cytometry, with a representative histogram from one patient (A) and the mean from 3 patients (B) shown. Cell size was also analysed by light microscopy, with a representative morphology profile from one patient's cells demonstrated (C). The remaining CML cells were then fixed, sectioned and examined unstained by EM (D).

5.1.2 Evaluation of autophagic structure formation by EM

The autophagosome and autolysosome both contain cytoplasmic material at various stages of degradation. However, in this experiment, it was observed that many of the vesicles appeared to be empty (Figure 5-1D). Therefore, it was not possible to determine whether the electron lucent or empty vesicles were autophagic compartments or some other kind of vacuole. Since autophagy is a dynamic process, whereby an autophagosome is formed, the autophagic material is delivered to the lysosome and the material is then degraded within the lysosome, it is probable that by this time-point the majority of the autophagic material had already been degraded. Therefore in order to block this "autophagic flux", the experiment was repeated using $CD34^+$ CML cells cultured in SFM ± 5GF and treated ± 150nM dasatinib, both in the absence and presence of lysosomal protease inhibitors (pepstatin A and E-64d both at a 1:100 dilution) for 24 hours. The lysosomal protease inhibitors act by preventing the degradation of material within the autolysosome. Figures 5-2A-D confirm the previous EM data, whereby, in the absence of lysosomal protease inhibition, GF deprivation of untreated CML cells (Figure 5-2B) increased the number of cytoplasmic vacuoles as compared to untreated cells cultured with GF support (Figure 5-2A). Treatment with 150nM dasatinib increased the number of vacuoles both in the presence (Figure 5-2C) and absence (Figure 5-2D) of GFs. Addition of lysosomal protease inhibitors to the cells, had little or no effect on the untreated CML cells cultured in the presence of GFs (Figure 5-2E), however, protease inhibition increased the amount of vacuolar material (denoted by the black rings) in untreated cells cultured without GFs (Figure 5-2F) and in the dasatinib-treated cells cultured both in the presence (Figure 5-2G) and absence (Figure 5-2H) of GFs. Interestingly, the greatest accumulation of vacuolar material was observed in the dasatinib-treated cells cultured without GFs (Figure 5-2H).

Autophagosomes and autolysosomes can be defined as membrane-bound structures which contain cytoplasmic material and/or organelles. Furthermore, in conventional EM, the material within the autophagosome has the same morphology and electron density as the cytoplasm outside. Another feature of an autophagosome analysed by EM is a double limiting membrane, however this is not always the case, due to limitations in lipid preservation during sample preparation (319). Therefore, although it is difficult to determine the characteristic double membranes surrounding each vacuole within these EM images (Figures 5-2F-H), it is highly likely that these vacuoles are autophagic structures. Hence, it could be said that autophagy was likely induced following both GF deprivation and dasatinib treatment of CML cells.

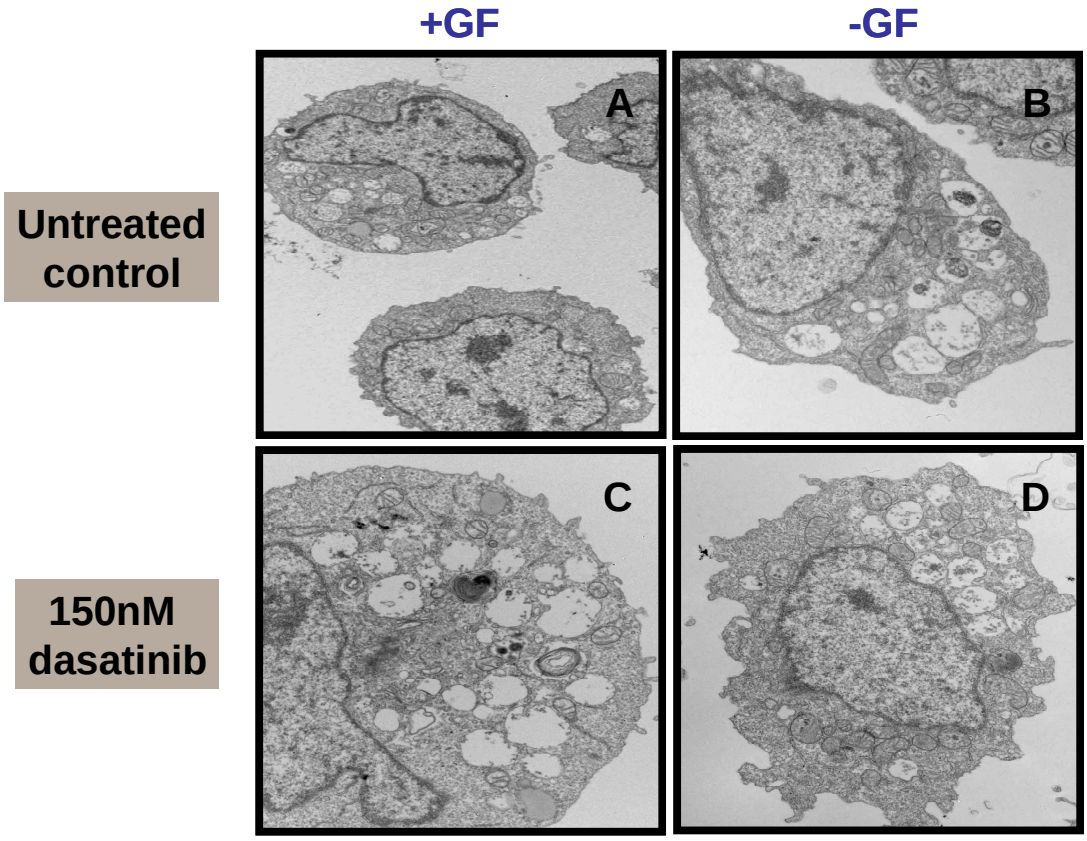

No protease inhibitors

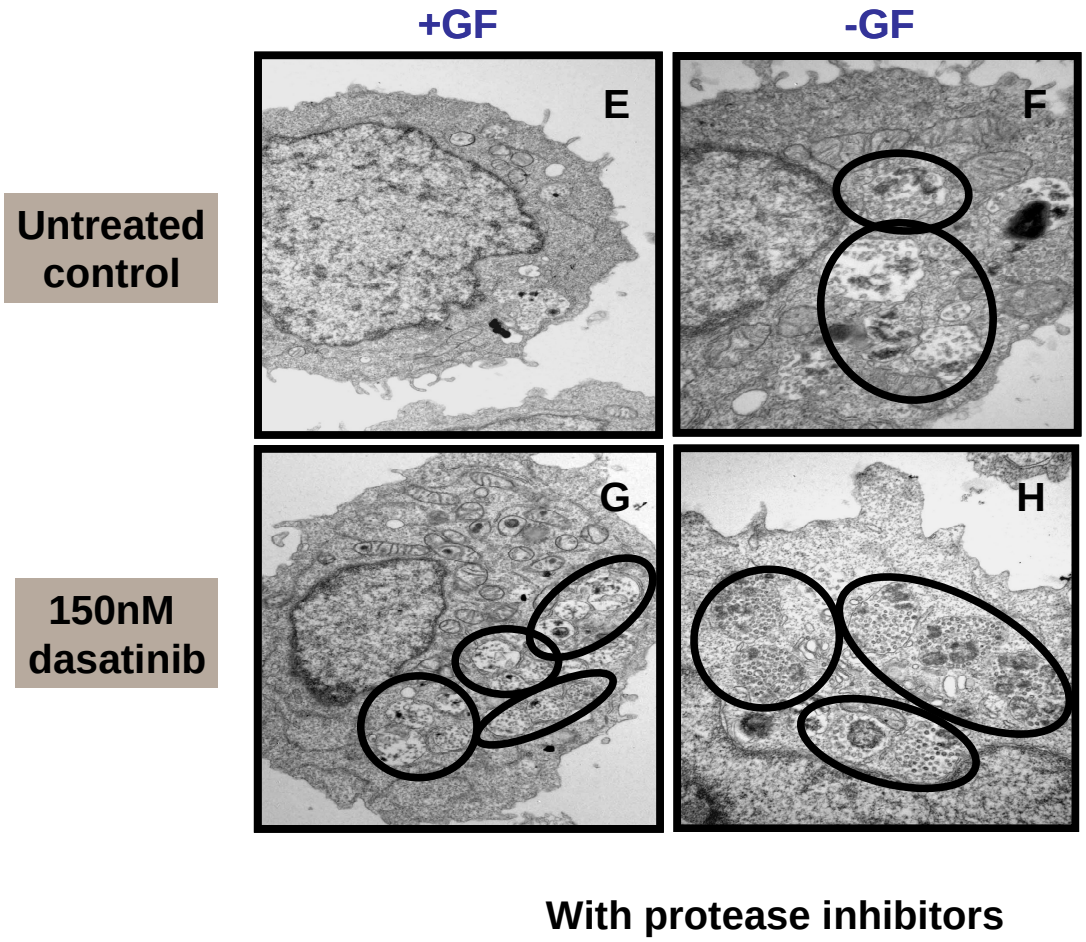

Figure 5-2 Evaluation of autophagic structure formation by EM

$CD34^+$ CML cells were cultured in SFM ± 5GF and treated ± 150nM dasatinib for 24 hours. The remaining CML cells were fixed, sectioned and examined unstained by EM (panels A-H).

5.1.3 Monitoring autophagy using LC3

The protein LC3, a mammalian homologue of Atg8, was originally identified as microtubule-associated protein 1 light chain 3. To date, LC3 is the only known mammalian protein identified that stably associates with the autophagosome membranes (166) and therefore serves as a widely used marker for autophagy. There are three human isoforms of LC3 (LC3A, LC3B, and LC3C), where LC3B is the most widely studied (320). LC3 is first cleaved at the carboxy terminus by Atg4 immediately following synthesis, to yield a cytosolic form LC3-I. During autophagy, LC3-I is conjugated with phosphatidylethanolamine (PE) to become LC3-II through lipidation by a ubiquitin-like system involving Atg7 and Atg3. Unlike the cytoplasmic LC3-I, LC3-II associates with the inner and outer membranes of the autophagosome. LC3-I can be detected on an immunoblot at a molecular mass of around 16-kDa and LC3-II at approximately 14-kDa. Following fusion with a lysosome, LC3 on the outer membrane is cleaved off by Atg4 and LC3 on the inner membrane is degraded by lysosomal enzymes resulting in low concentrations of LC3 within autolysosomes (166, 321). Therefore, the presence of endogenous LC3 as well as the conversion of LC3-I to the lower migrating form LC3-II serve as good indicators of autophagosome formation and hence, autophagy induction.

5.1.4 Formation of LC3-positive puncta in dasatinib-treated CML cells

In order to verify the EM data described in Figure 5-2, LC3 was measured in dasatinib-treated CML cells as a more specific indicator of autophagy. $CD34^+$ CML cells were cultured in SFM ± 5GF and treated ± 150nM dasatinib for 24 hours, before being fixed onto slides and stained with anti-LC3 antibody. Nuclei were counterstained with DAPI. Endogenous levels of LC3 were then visualised within these cells by fluorescence microscopy. Figures 5-3A and B demonstrate a representative LC3 IF profile from one patient's cells and the average LC3-positive puncta per cell from 3 patients, respectively. A significant increase in LC3-positive puncta was observed in the GF deprived untreated cells as compared to untreated cells cultured with GF support ($p=0.015$) (Figure 5-3A upper panel and Figure 5-3B). An even greater increase in LC3-positive puncta was observed following dasatinib treatment of cells cultured, both with and without exogenous GF support, as compared the relevant untreated control ($p=0.0004$ and $p=0.0044$ for untreated +GF versus dasatinib +GF and untreated -GF versus dasatinib -GF, respectively) (Figure 5-3A lower panel and Figure 5-3B). As with previous data, the greatest increase in autophagy induction, as measured by LC3 puncta formation, was observed in CML cells cultured without GF support and treated with dasatinib ($p=0.009$ for dasatinib treatment +GF versus -GF).

A

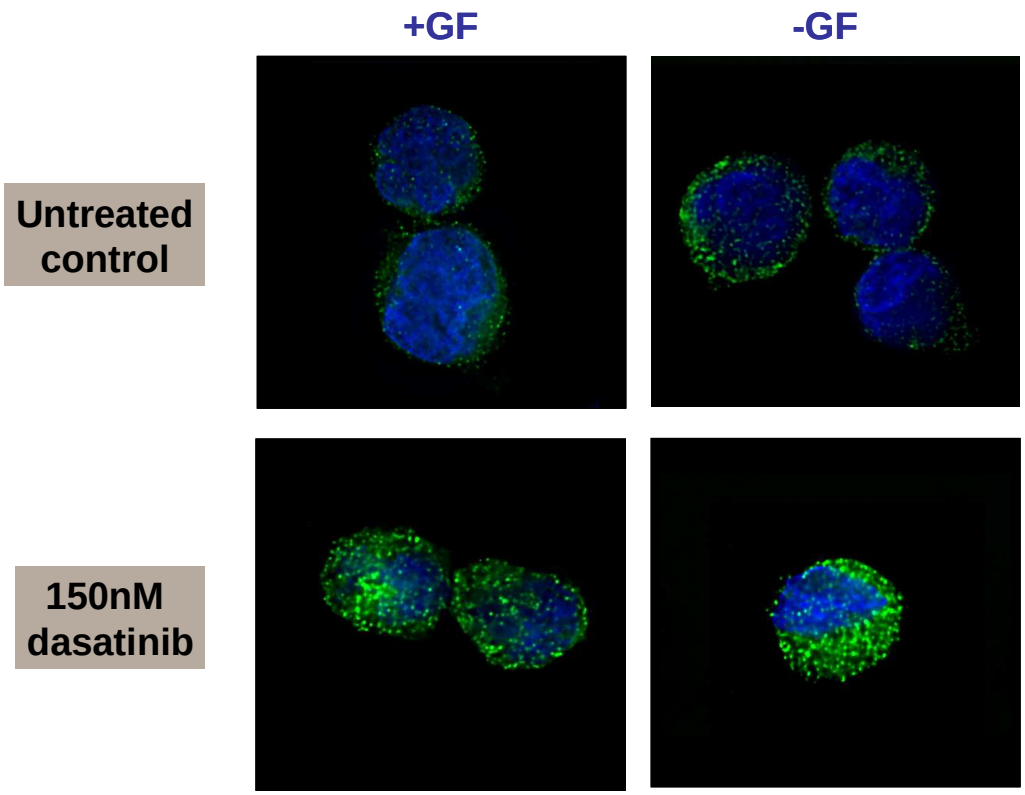

B

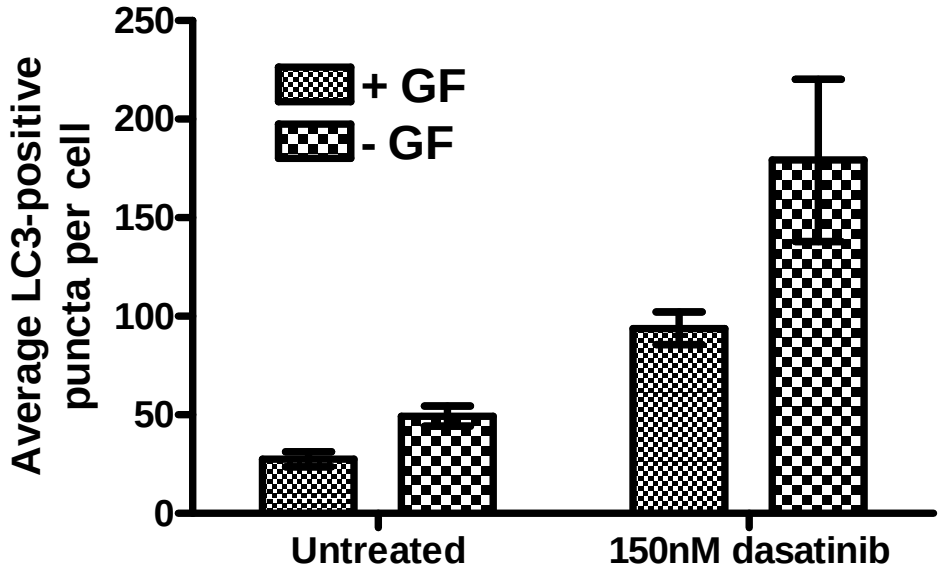

Figure 5-3 Formation of LC3-positive puncta in dasatinib-treated CML cells

$CD34^+$ CML cells were cultured in SFM ± 5GF and treated ± 150nM dasatinib for 24 hours. Remaining CML cells were then fixed onto multi-spot slides and stained with anti-LC3 antibody. Nuclei were counterstained with DAPI and LC3-positive puncta were manually counted.

A representative IF profile from one patient (A) and the average LC3-positive puncta per cell from 3 patients (B) are shown.

5.1.5 Accumulation of autophagosome-associated LC3-II in GF-starved cells

In order to completely verify the previous results, the levels of autophagosome-associated LC3-II were also measured. $CD34^+$ CML cells were left untreated and cultured in SFM ± 5GF for 24 hours, before whole cell protein lysates were made from each sample. The levels of LC3-I and LC3-II were then determined by Western blot using an anti-LC3B antibody. Beta-tubulin levels were also measured as a protein loading control. Figure 5-4 demonstrates a clear increase in the levels of autophagosome-associated LC3-II within the GF-starved CML cells as compared to cells cultured with exogenous GF support. These data, thereby, confirm the finding that autophagy is induced upon GF deprivation of CML cells.

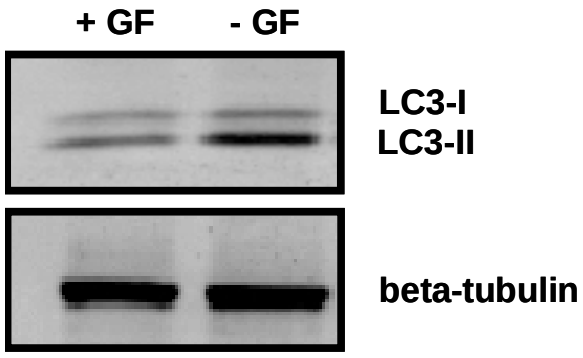

Figure 5-4 Accumulation of autophagosome-associated LC3-II in GF-starved CML cells

$CD34^+$ CML cells were cultured in SFM ± 5GF for 24 hours and whole cell protein lysates were made at this time-point. Western blot determined the levels of LC3-I and LC3-II in each sample by LC3-antibody staining. Beta-tubulin was also measured as a protein loading control.

5.1.6 Accumulation of autophagosome-associated LC3-II in dasatinib-treated CML cells

Since previous data showed that autophagy appeared to be induced upon dasatinib treatment, LC3-II levels were also measured in dasatinib-treated CML cells. $CD34^+$ CML cells were cultured in SFM only and treated with 150nM dasatinib for 24 hours, before whole cell protein lysates were made from each sample. As previously, the levels of LC3-I and LC3-II were then determined by Western blot using an anti-LC3B antibody. Levels of p-CrkL were determined as a measure of BCR-ABL activity and beta-tubulin levels were also measured as a protein loading control. Figure 5-5 demonstrates that upon dasatinib treatment of CML cells, p-CrkL and hence, BCR-ABL kinase activity is inhibited. This then results in an accumulation of autophagosome-associated LC3-II within the dasatinib-treated CML cells, as compared to untreated control. These data, thereby, confirm the finding that autophagy is induced upon dasatinib treatment of CML cells.

Overall, these data suggest that autophagy is induced following GF deprivation of CML cells. Autophagy induction is then further increased within these cells, upon BCR-ABL inhibition following dasatinib treatment.

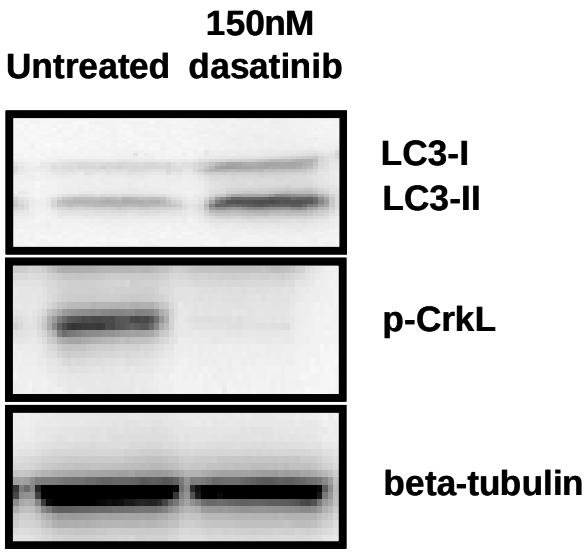

Figure 5-5 Accumulation of autophagosome-associated LC3-II in dasatinib-treated CML cells

$CD34^+$ CML cells were cultured in SFM only, treated ± 150nM dasatinib for 24 hours and whole cell protein lysates were made at this time-point. Western blot determined the levels of LC3-I and LC3-II in each sample by LC3-antibody staining. BCR-ABL activity was determined by p-CrkL-antibody staining. Beta-tubulin was also measured as a protein loading control.

5.1.7 The PI3K-Akt-mTOR signalling pathway in CML cell survival

The PI3K-Akt-mTOR axis is a cell survival pathway that is important for normal cell growth and proliferation (322). However, this pathway has also been implicated in the transformed phenotype of most cancer cells (323). Once activated by BCR-ABL, GF-signalling or cross-talk from the Ras pathway (324), it plays an important role in cell growth, protein translation and hence, survival of CML cells. It has also been demonstrated that when PI3K-Akt signalling is activated, autophagic degradation is decreased (325). The downstream effector of Akt, mTOR, has been shown to be a key negative regulator of autophagy, where it inhibits the autophagic process in the presence of abundant GFs and nutrients (326, 327). The mTOR kinase is present in two distinct protein complexes, mTORC1 and mTORC2, which have distinct mechanisms of action (328). As a central GF and nutrient sensor, mTORC1 plays a key role in the regulation of cell growth by activating protein synthesis and suppressing autophagy, through its two well characterised downstream substrates, S6K and 4EBP1. The phosphorylation levels of S6K and 4EBP1 are widely used as indicators of mTORC1 activity and decreased phosphorylation levels of these substrates are also used as markers for autophagy induction (329). It has previously been demonstrated that autophagy can be pharmacologically induced by inhibiting mTOR activity with rapamycin (163) which suppresses mTORC1-mediated S6K activation (Figure 5-6).

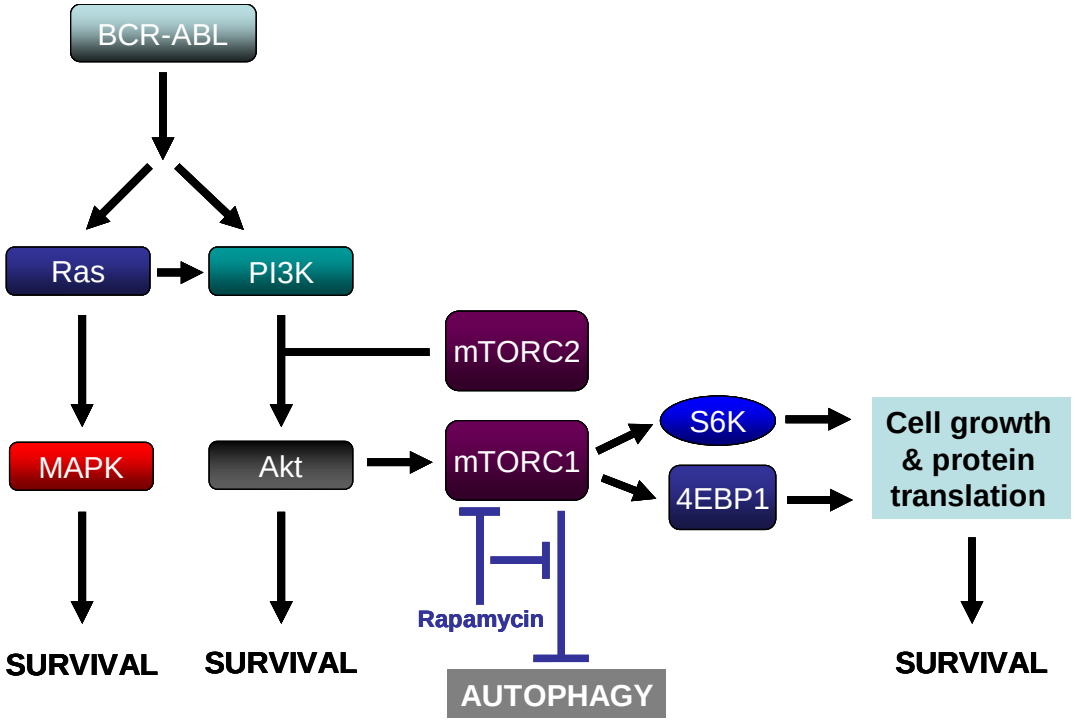

Figure 5-6 The PI3K-Akt-mTOR signaling pathway in CML cell survival

The PI3K-Akt-mTOR signaling axis is central to the transformed phenotype of CML cells. Inhibtion of the autophagy inhibitor, mTORC1, by agents such as rapamycin results in the induction of autophagy.

5.1.8 Analysis of mTOR activity in dasatinib treated K562 cells

In order to investigate the status of mTOR activity following TKI treatment of CML cells, further experiments were carried out. K562 (BCR-ABL^{+}) cells were cultured in RPMI ± serum and treated ± either 150nM dasatinib or 20nM rapamycin for 8 hours, before whole cell protein lysates were made. Western blot was then used to determined the levels of p-S6K within each sample. GAPDH was also measured as a protein loading control. Figure 5-7 shows that levels of p-S6K are reduced in serum-starved untreated K562 cells as compared to cells grown in the presence of serum-support (lane 1 versus lane 3). This is in keeping with the fact that mTOR acts as a nutrient sensor and promotes protein translation and cell growth, through phosphorylation of substrates such as S6K, in the abundance of GFs. Treatment with dasatinib caused an inhibition of p-S6K in both the absence and presence of serum (lanes 2 and 4). Treatment with the mTOR inhibitor, rapamycin, gave the same effect and also resulted in complete inhibition of p-S6K (lanes 5 and 6).

These data may suggest that autophagy induction caused by dasatinib treatment is a result of the inhibition of mTOR activity. Furthermore, this suggests that within CML cells, autophagy may also be induced by agents which act downstream of BCR-ABL, such as Ras- or PI3K-Akt-pathway inhibitors. However, to completely verify that these hypotheses are the case, further investigations would be required.

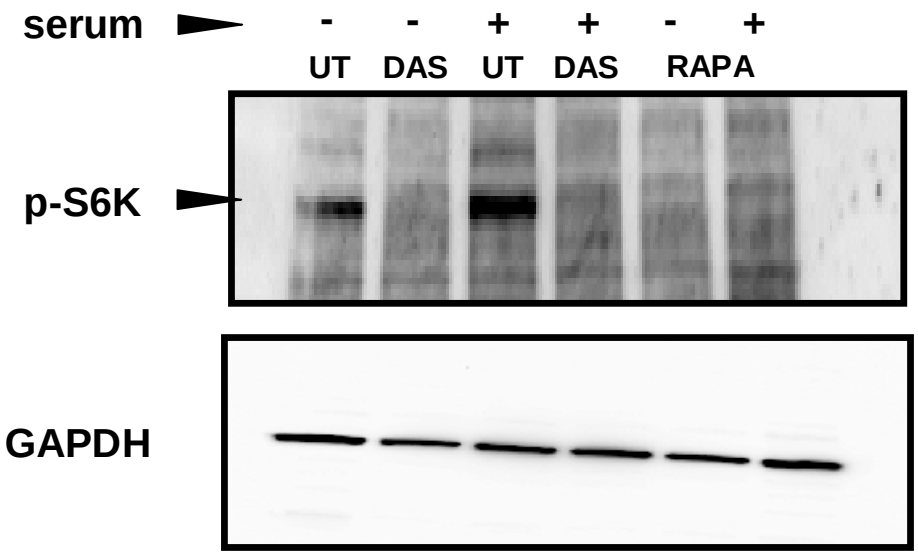

Figure 5-7 Analysis of mTOR activity in dasatinib treated K562 cells

K562 cells were cultured in RPMI ± serum and treated ± either 150nM dasatinib or 20nM rapamycin for 8 hours, before whole cell protein lysates were made. Western blot determined the levels of p-S6K. GAPDH was also measured as a protein loading control [UT: untreated; DAS: 150nM dasatinib and RAPA: rapamycin].

5.2 Targeting of autophagy potentiates the TKI-induced cell death of CML cells

5.2.1 Analysis of committed progenitor cell potential following TKI/FTI treatment in combination with autophagy inhibition of CP CML cells

A number of investigations suggest that autophagy may act as a survival signal in tumour cells (164, 330) and that the inhibition of autophagy can lead to an increase in therapy-induced cell death (171, 331). Therefore, to determine whether autophagy acts as a protective mechanism in this system, it was thought to be critical to perform further experiments designed to modulate autophagic activity within TKI-treated CML cells. In order to inhibit autophagy, the pharmacological inhibitors, CQ and BAF were used. The lysosomotropic agent, CQ, is an inhibitor of lysosomal acidification, thus raises the pH within the lysosome. BAF acts by inhibiting the activity of the H^+-ATPase responsible for the acidification of autolysosomes. Ultimately, both agents inhibit the autophagosome-lysosome fusion and thus, the final degradation of autophagic material within autolysosomes. First, the committed progenitor cell potential following TKI treatment of CML cells was tested. $CD34^+$ CP CML cells (n=3) were sorted into primitive ($CD34^+38^-$) and more mature progenitor ($CD34^+38^+$) populations, were cultured in SFM+5GF and left untreated or pretreated for 48 hours with either TKIs (IM (0.5 and 2μM); dasatinib (10 and 150nM) or nilotinib (2μM)); the farnesyl transferase inhibitor (FTI), lonafarnib (10 μM) (note: lonafarnib inhibits the Ras-pathway and was included to determine whether autophagy induction was specific to BCR-ABL inhibition) or autophagy inhibitors (CQ (10μM) or BAF (20nM)) alone or in the TKI/FTI/CQ/BAF combination. Following pre-treatment, aliquots of cells from each condition were taken for apoptosis measurement by annexin-V/viaprobe

staining determined by flow cytometry ($CD34^+38^+$ cells only) and the remaining cells were added to methycellulose for CFC analysis. The relevant drug combinations from the pre-treatment were also added to the methylcellulose. The number of CFCs obtained for each sample was then compared with a baseline - cells which had no prior culture or treatment (100%). Figure 5-8A shows that there was a trend towards an increase in apoptotic cells following combination treatment with TKI/FTI and autophagy inhibitors, as compared to both untreated control cells and TKI/FTI alone, with the greatest increase seen with 150nM dasatinib/CQ treatment (p=0.001 and 0.05 for 150nM dasatinib/CQ versus no drug and 150nM dasatinib alone, respectively). Figure 5-8B shows that within the $CD34^+38^+$ population, the untreated cells demonstrated a doubling of CFCs over the 48 hours pre-treatment, consistent with stem/progenitor cell expansion in the culture medium. Neither CQ nor BAF alone had any effect on this expansion. However, consistent with previous studies (131, 226), the TKIs (IM, dasatinib (10nM) and nilotinib) all exhibited an anti-proliferative effect, which prevented any CFC expansion over baseline. Both dasatinib, at the highest clinically achievable concentration (150nM), and lonafarnib were able to reduce the number of CFCs to 55 and 53% of baseline, respectively, suggesting some level of apoptosis was achieved by these agents alone. This effect was dramatically increased following TKI or FTI/autophagy inhibitor combination treatment, with 80-98% reduction in CFC formation versus baseline, and even more impressive as compared to the no drug control. Interestingly, lonafarnib treatment combined with autophagy inhibition gave the greatest effect, with a 98% reduction in CFC as compared to baseline. Since lonafarnib inhibits the Ras pathway, this finding indicates that BCR-ABL inhibition does not solely and directly induce autophagy within CML cells and thereby, corroborates the findings demonstrated in Figure 5-7.

Consistent with the $CD34^{+}38^{+}$ data, within the more primitive $CD34^{+}38^{-}$ cell fraction (Figure 5-8C), the untreated cells demonstrated an increase in CFC number as compared to baseline and this remained unchanged following treatment with either CQ or BAF alone. TKI treatment alone also had a protective anti-proliferative effect on CFC expansion over baseline. However, for these primitive CML cells which are consistently resistant to TKI exposure, treatment with TKI/autophagy inhibitor was extremely effective, with only 2% CFCs remaining following 150nM dasatinib/CQ exposure.

Notably, the combination treatment with TKI/BAF did not appear as effective as TKI/CQ treatment of these cells. Therefore it was decided that CQ should be used as an autophagy inhibitor for the subsequent primitive progenitor cell experiments.

Overall, these data show that autophagy inhibition greatly potentiates the effect of either TKI or FTI treatment, on the reduction of committed progenitor cell potential of relatively mature $CD34^{+}38^{+}$ and primitive $CD34^{+}38^{-}$ CML cell populations.

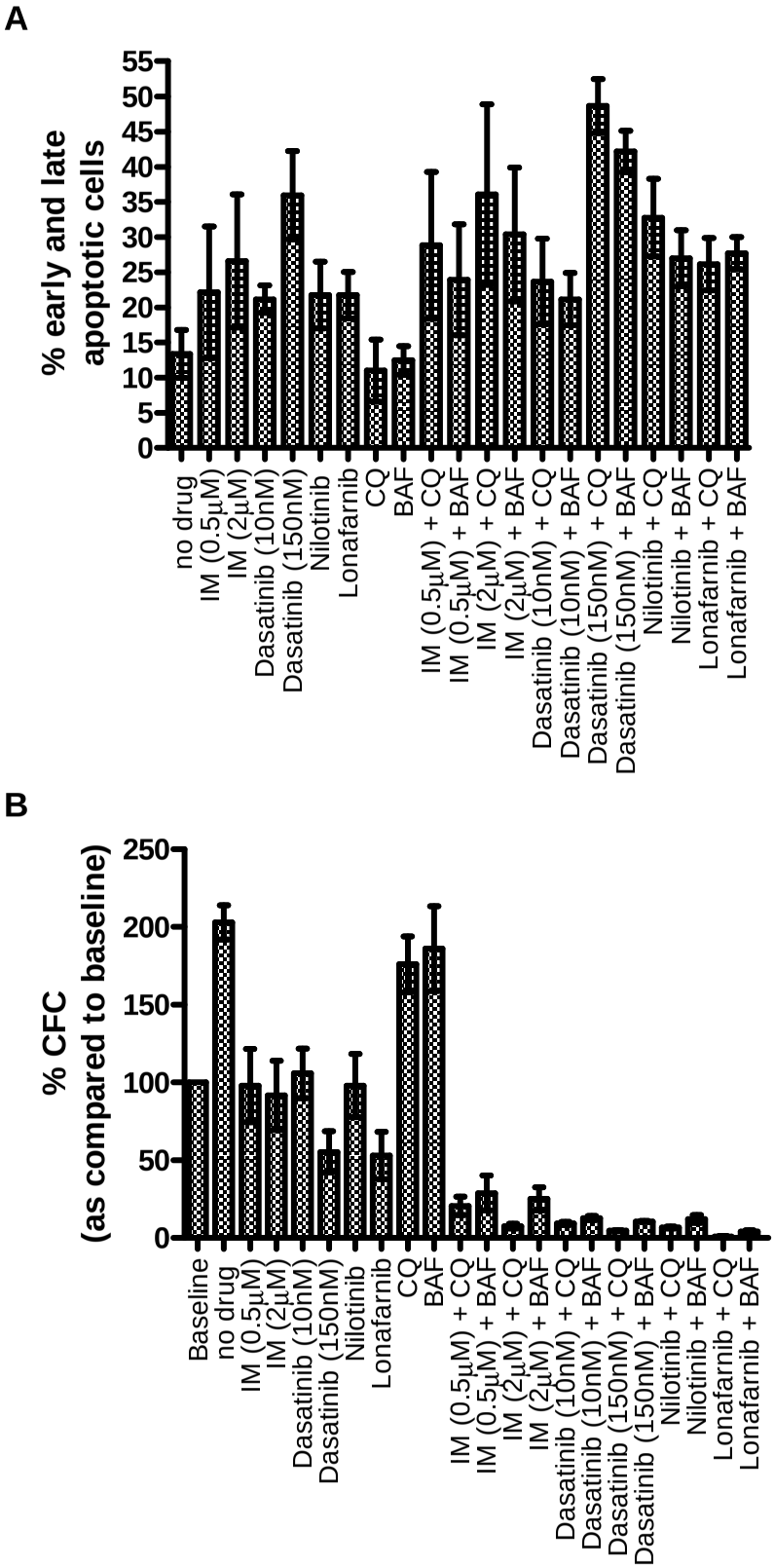
A
% early and late apoptotic cells
55
50
45
40
35
30
25
20
15
10
5
0
no drug
IM (0.5μM)
IM (2μM)
Dasatinib (10nM)
Dasatinib (150nM)
Nilotinib
Lonafarnib
CQ
BAF
IM (0.5μM) + CQ
IM (0.5μM) + BAF
IM (2μM) + CQ
IM (2μM) + BAF
Dasatinib (10nM) + CQ
Dasatinib (10nM) + BAF
Dasatinib (150nM) + CQ
Dasatinib (150nM) + BAF
Nilotinib + CQ
Nilotinib + BAF
Lonafarnib + CQ
Lonafarnib + BAF
B
% CFC (as compared to baseline)
250
200
150
100
50
0
Baseline
no drug
IM (0.5μM)
IM (2μM)
Dasatinib (10nM)
Dasatinib (150nM)
Nilotinib
Lonafarnib
CQ
BAF
IM (0.5μM) + CQ
IM (0.5μM) + BAF
IM (2μM) + CQ
IM (2μM) + BAF
Dasatinib (10nM) + CQ
Dasatinib (10nM) + BAF
Dasatinib (150nM) + CQ
Dasatinib (150nM) + BAF
Nilotinib + CQ
Nilotinib + BAF
Lonafarnib + CQ
Lonafarnib + BAF

C

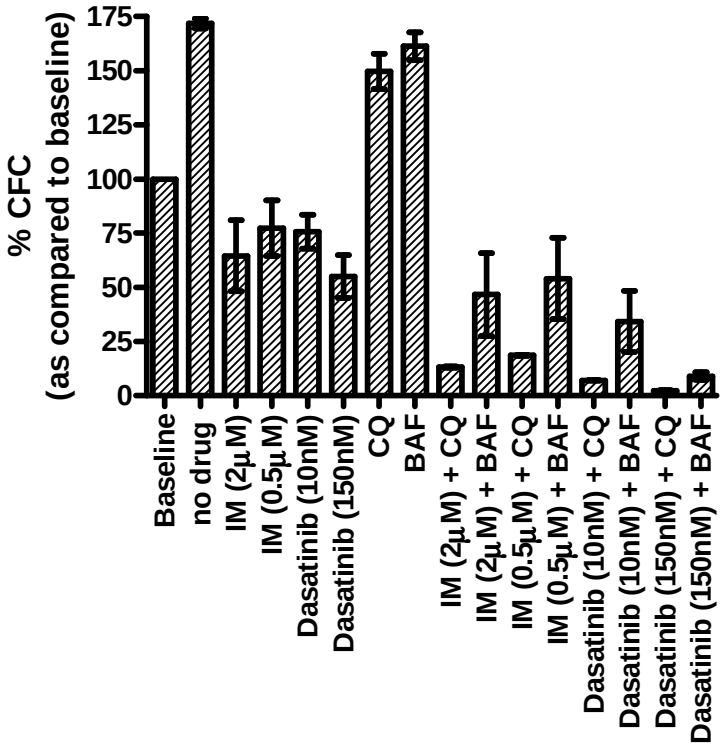

Figure 5-8 Analysis of committed progenitor cell potential following TKI/FTI treatment in combination with autophagy inhibition of CP CML cells

$CD34^+$ CP CML cells (n=3) were sorted into progenitor ($CD34^+38^+$) (A+B) and stem ($CD34^+38^-$) (C) cell populations. Cells cultured in SFM ± 5GF and left untreated or pretreated for 48 hours with IM (0.5 and 2μM), dasatinib (10 and 150nM), nilotinib (2μM) ($CD34^+38^+$ cells only) or lonafarnib (10μM) ($CD34^+38^+$ cells only), either alone or in combination with CQ (10μM) or BAF (20nM). Aliquots of cells were taken for apoptosis measurement by annexin-V/ viaprobe staining ($CD34^+38^+$ cells only) (A) and the remaining cells were then plated in methylcellulose. Colonies were counted at 14 days and compared with those derived from cells at baseline (cells with no prior culture or treatment), which were taken as 100% (B:$CD34^+38^+$ and C:$CD34^+38^-$).

5.2.2 Analysis of committed progenitor cell potential following TKI/FTI treatment in combination with autophagy inhibition of AP CML cells

Although TKI treatment has revolutionised the management of CP CML, it is less effective for the treatment of advanced phases of CML. ABL-kinase domain mutations are more common in the advanced phases of CML than in CP CML (332). Further, the acquisition of additional chromosomal abnormalities in the BCR-ABL clone, termed clonal evolution, is a criterion for the diagnosis of AP CML in the WHO guidelines for CML (333). These factors suggest that the advanced phase CML cells may develop BCR-ABL independent mechanisms of proliferation, which would thereby, render them TKI-resistant. The results in Figure 5-8 demonstrated that lonafarnib in combination with autophagy inhibition was highly effective at eliminating the CP CML cells with committed progenitor cell potential. Therefore, since lonafarnib acts on the Ras pathway rather than BCR-ABL itself, it was predicted that the lonafarnib/autophagy inhibitor combination would also be effective at targeting AP CML cells. The previous experiment, as demonstrated in Figure 5-8, was repeated using $CD34^+$ AP CML cells from one patient. Figure 5-9A shows that the greatest increase in apoptotic cells was observed with both the lonafarnib alone and lonafarnib/CQ/BAF combination (28.2, 26.6 and 28.2%, respectively, as compared to 12.1% for no drug control). As expected, Figure 5-9B shows that TKI treatment, both alone and in combination with autophagy inhibitors, was relatively ineffective at targeting AP CML cells with committed progenitor cell potential, with little or no effect as compared to both baseline and untreated control cells. However, combination treatment with lonafarnib/CQ/BAF gave the greatest effect, with a 98 and 97% reduction in CFC as compared to baseline, for lonafarnib/CQ and BAF, respectively.

Although these experiments were performed on a single patient and therefore, no definitive conclusions can be drawn as yet, these data may be an early indicator that lonafarnib treatment in combination with autophagy inhibition is an effective therapy for patients with advanced phase CML.

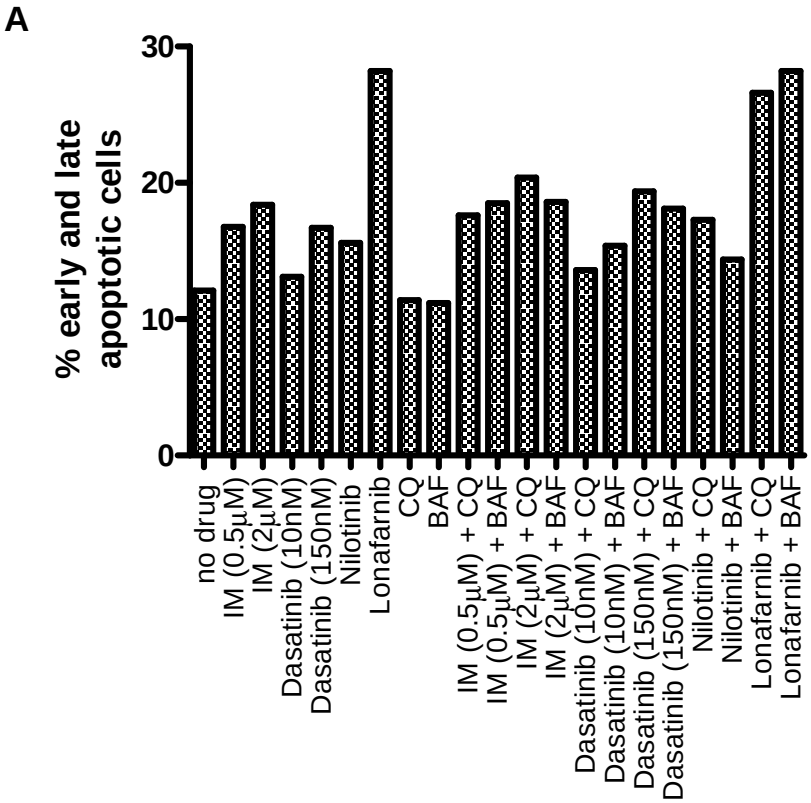

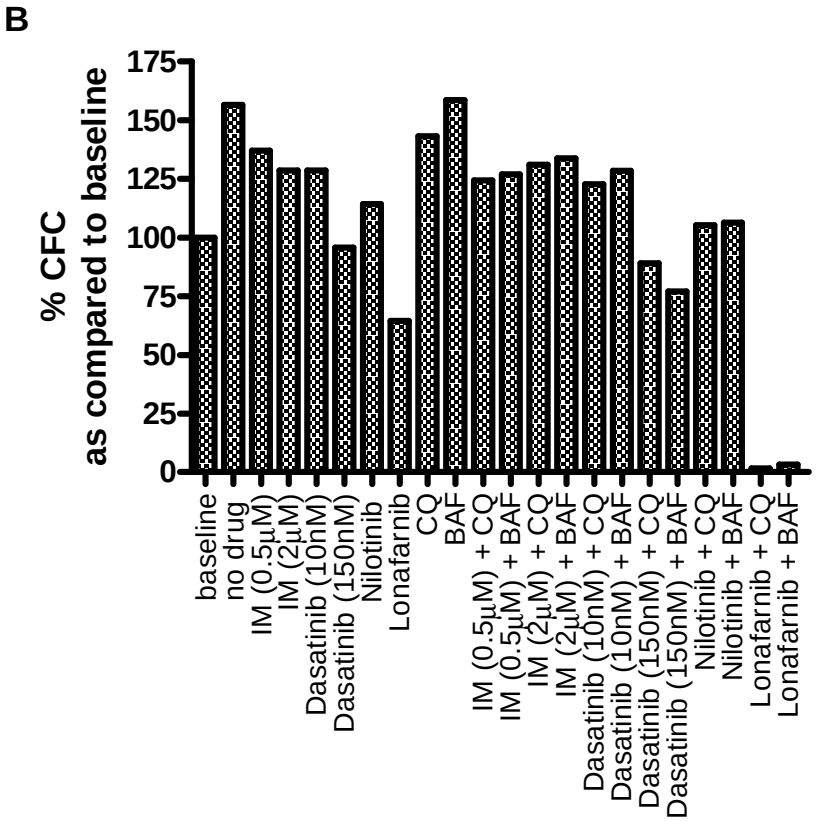

Figure 5-9 Analysis of committed progenitor cell potential following TKI/FTI treatment in combination with autophagy inhibition of AP CML cells

$CD34^+$ AP CML cells (n=1) were cultured in SFM + 5GF and left untreated or pretreated for 48 hours with IM (0.5 and 2μM), dasatinib (10 and 150nM), nilotinib (2μM) or lonafarnib (10μM), either alone or in combination with CQ (10μM) BAF (20nM). Aliquots of cells were taken for apoptosis measurement by annexin-V/viaprobe staining (A) and the remaining cells were then plated in methylcellulose. Colonies were counted at 14 days and compared with those derived from cells at baseline (cells with no prior culture or treatment), which were taken as 100% (B).

5.2.3 Analysis of primitive progenitor cell potential following TKI treatment in combination with autophagy inhibition of CML cells

Since the CFC assay measures a relatively mature, committed progenitor cell population, LTC-IC assays were also carried out to measure the effect of autophagy inhibition on the functionality of more primitive CML cells. As the presence of cytokines in the culture media may alter the requirement of autophagy for cell survival, the LTC-IC assays were carried out both in the presence and absence of a 5GF cocktail. $CD34^+$ CML cells (n=3) were left untreated or pretreated for 6 days with either TKIs (2μM IM or 150nM dasatinib); CQ alone or the TKI/CQ combination. It was noted that the presence of the drug combinations in the methylcellulose for the CFC assays (Section 5.2.1) may have exerted an anti-proliferative effect rather than the elimination of functional CML progenitor cells. Therefore, following the pre-treatment, the cells were washed twice with PBS, to remove any drug, before being added to LTC-IC assays. As it was not known how long it would take for the inhibition of autophagy by CQ to have any effect on the cells, a pre-treatment time-point of 6 days was chosen as a median of the 12 day dasatinib treatment timecourse (described in Chapter 4). If primary cellular material had been more plentiful, it would have been useful to perform a TKI/CQ treatment timecourse, in order to determine the most effective treatment times for the drug combination.

As with the CFC assay, the number of LTC-ICs obtained for each sample was then compared with a baseline. Figure 5-10A shows that in the presence of GFs, untreated and CQ-treated cells formed 67 and 47% fewer LTC-IC colonies than cells at baseline, respectively, suggesting that a large proportion of these cells had proceeded towards terminal differentiation. Consistent with the CFC data and previous studies (131), treatment with IM or dasatinib was anti-proliferative, even

in the presence of GFs, and therefore resulted in a protective effect on the number of LTC-ICs over baseline. Combination treatment with TKIs and autophagy inhibitors counteracted this protective effect and resulted in an impressive decrease in the number of LTC-ICs, with a significant reduction for treatments with IM/CQ and dasatinib/CQ combinations versus TKI alone (p= 0.04 and 0.008, respectively). Figure 5-10B shows that untreated and CQ-treated cells cultured without supplemental GFs also formed reduced numbers of colonies, as compared with baseline cells. The removal of GFs combined with TKI treatment had a dramatic effect on the number of LTC-IC colonies (6.5 and 4.1% for IM and dasatinib, respectively), suggesting that cytokines may play an important protective role for the survival of TKI-treated CML cells, consistent with the results of a previous study (235). Combination treatment with CQ resulted in an even greater decrease in LTC-IC colony numbers, as compared to TKI alone (1%; p=0.175 and 0.65%; p=0.04 for IM/CQ and dasatinib/CQ, respectively).

Overall, these data show that autophagy inhibition greatly potentiates the effect of TKI treatment, on the reduction of primitive progenitor cell potential of CML cells. Furthermore, that TKI treatment combined with autophagy inhibition of GF-starved CML cells promotes the most effective elimination of primitive CML cells.

A

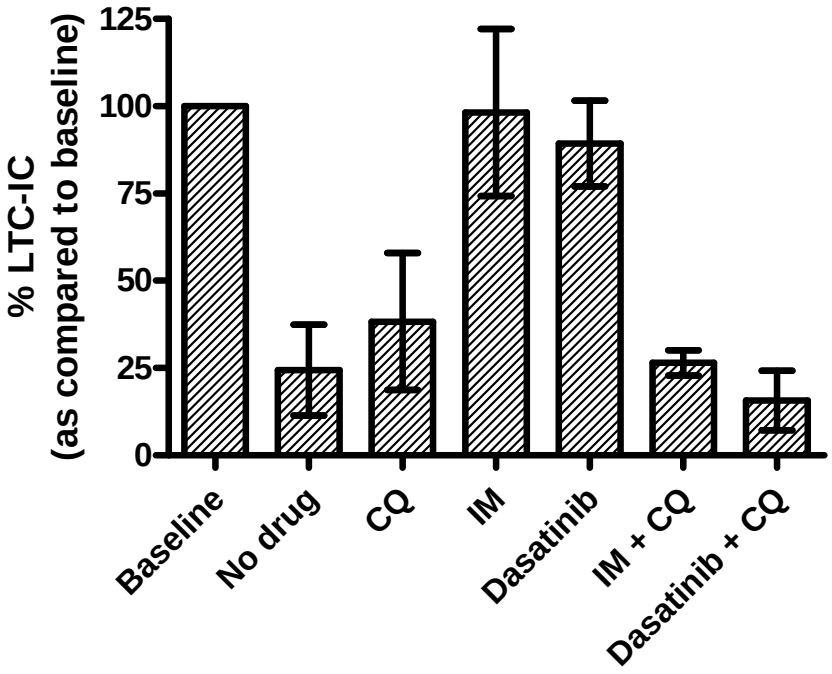
% LTC-IC
(as compared to baseline)
125
100
75
50
25
0
Baseline
No drug
CQ
IM
Dasatinib
IM + CQ
Dasatinib + CQ

B

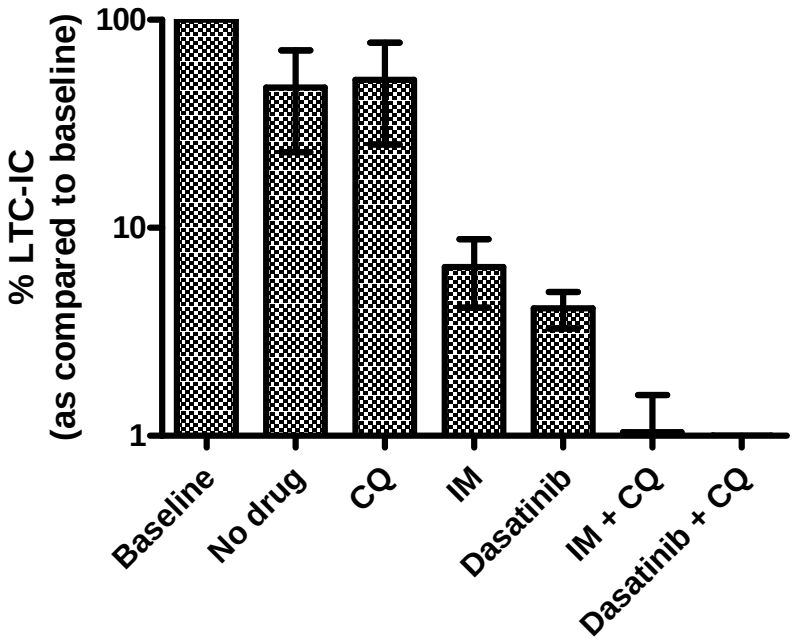

Figure 5-10 Analysis of primitive progenitor cell potential following TKI treatment in combination with autophagy inhibition of CML cells

$CD34^+$ CML cells (n=3) were cultured in SFM with (A) and without GF (B) and left untreated or pretreated for 6 days with TKIs (IM 2μM or dasatinib 150nM) or CQ (10μM) alone or the TKI/CQ combination, before being added to LTC-IC stromal feeder layers. Resulting colonies were compared with those derived from cells at baseline (cells with no prior culture or treatment), which were taken as 100%. Note: (B) is presented on a logarithmic scale due to the great differences between baseline and TKI/combination-treated arms.

5.3 Summary

The previous results chapter demonstrated that, despite culture without exogenous GF support and full inhibition of BCR-ABL kinase activity via prolonged dasatinib exposure, a small proportion CML cells survived. This indicated that resistance within these cells may be mediated by other survival signals and/or pathways. Autophagy has previously been shown to provide survival signals for cancer cells against chemotherapy. Therefore, the purpose of the work in this chapter was to investigate whether the biochemical changes within the cells which survived dasatinib treatment, were characteristic of the autophagic process and to determine whether these changes could be therapeutically exploited.

Initial experiments found that CML cells were decreased in size following treatment with dasatinib, as compared to untreated control cells. This is a typical characteristic of cells undergoing autophagy, as the lysosomal degradation of cellular components by the progressive autophagic process usually results in cell shrinkage due to self-consumption (164, 330). Further analysis by EM, revealed an increase in cytoplasmic vacuoles following GF deprivation. These vesicular structures increased in size and number following treatment with dasatinib. Further treatment with lysosomal protease inhibitors, which prevent the degradation of autophagic material, resulted in an increase in electron-dense inclusions within the vacuoles, with the greatest increase observed in dasatinib-treated CML cells cultured without GFs. These morphological and intracellular changes served as early indicators that the autophagic process was occurring.

Experiments designed to verify whether the initial intracellular changes observed were indeed due to the induction of autophagy, revealed further biochemical hallmarks of the autophagic process, following both GF-deprivation and dasatinib

treatment. These included, an increase in LC3-positive puncta and LC3-II accumulation, with the greatest increase observed, again, within the CML cells which were treated with dasatinib and cultured without GFs. Mechanistic studies also demonstrated that the induction of autophagy caused by dasatinib treatment may be due to the indirect inhibition of the PI3K/Akt/mTOR pathway.

These data suggest that autophagy may act as a survival mechanism within CML cells. Therefore, it was also investigated whether autophagy inhibition would potentiate the TKI/FTI-induced cell death of CML cells. Remarkably, the inhibition of autophagy combined with TKI/FTI treatment caused a highly significant elimination of CML cells with both committed and primitive progenitor cell potential. Interestingly, lonafarnib treatment in combination with autophagy inhibition gave an impressive reduction in CFCs from both CP-CML and AP-CML cells. This could have important implications for the treatment of CML patients with advanced phase disease and/or TKI-resistant mutations, such as T315I.

Overall, these data demonstrate that TKI/FTI treatment, results in the induction of the BCR-ABL independent survival mechanism, autophagy, in CML cells. Furthermore, the induction of autophagy could also explain the drug resistance demonstrated by the primitive CML cells treated with dasatinib (shown in Chapter 4 of this thesis). Blocking of the autophagic process then enhances the TKI/FTI-induced death of CML cells, including the inherently TKI-resistant primitive stem cell population (Figure 5-11).

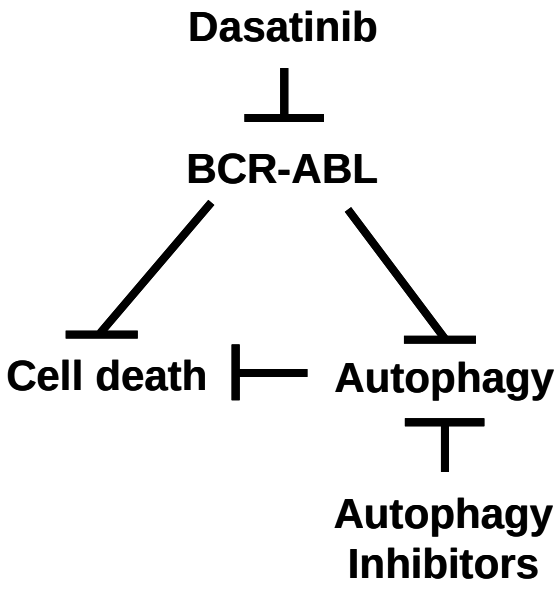

Figure 5-11 Inhibition of autophagy potentiates cell death dasatinib-treated CML cells

Following dasatinib treatment, the inhibition of BCR-ABL results in the programmed cell death of all BCR-ABL kinase-dependent CML cells. Within the surviving BCR-ABL kinase-independent CML cells, autophagy is induced as a survival mechanism. Therefore, treatment with autophagy inhibitors results in increased cell death of dasatinib-treated CML cells.

6. DISCUSSION

There is no doubt that IM treatment has revolutionised the management of CML. The remarkable activity of IM was first demonstrated in the pivotal phase III IRIS trial, whereby IM treatment significantly improved responses and survival outcomes compared with the previous standard therapy of IFNα and Ara-C (221). At the 5 year follow-up, the estimated cumulative rates of CHR, MCR, and CCR for patients treated with standard dose IM were 98, 92 and 87%, respectively. Moreover, the estimated freedom from progression and event free survival rates were an impressive 93 and 83%, respectively (222). The efficacy and safety of IM therapy was further confirmed by a recent update of the IRIS trial after a median follow up of 7 years, with an estimated overall survival rate of 86% (334). As a result, IM is widely considered as standard front-line therapy for patients with CML. However, despite these unparalleled results, an obvious outcome from the follow-up analyses is that only a small group of patients achieves a CMR. Variable levels of *BCR-ABL* mRNA can still be detected by RT-PCR in most patients receiving IM therapy (222). Furthermore, responses to IM therapy in patients with advanced stage CML are rare and usually short-term (217). The elements which contribute to this phenomenon of IM resistance have been extensively studied and are briefly summarised in Figure 6-1.

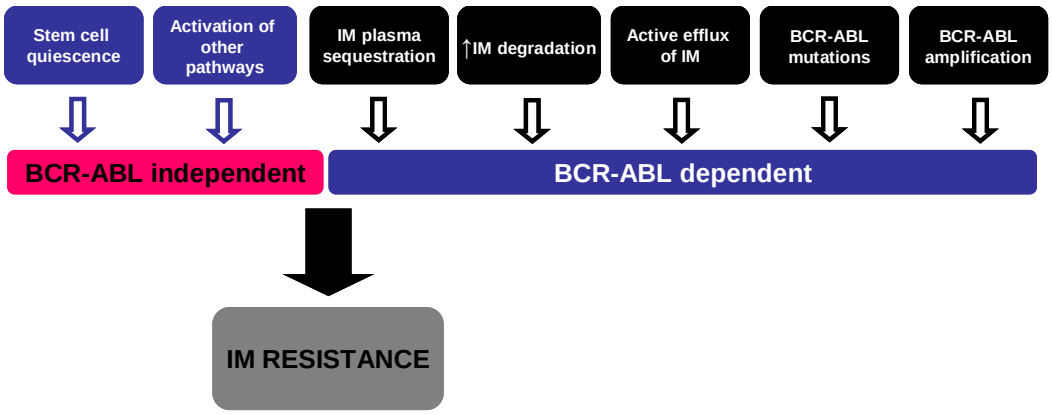

Figure 6-1 Mechanisms of IM resistance

Resistance to IM and other TKIs can be broadly subdivided into BCR-ABL-dependent and -independent mechanisms. Acquired resistance in Ph^+ leukaemias is usually BCR-ABL-dependent, with the most common form of TKI resistance attributed to the development of point mutations within the ABL-kinase domain of the *BCR-ABL* gene (238). These mutations confer structural changes whereby the ABL-kinase is unable to adopt the inactive conformation to which IM binds (206). This results in either a suboptimal response within the patient or in the worst case scenario, complete failure of therapy. The observation of IM resistance has led to the development of a second generation of TKIs such as nilotinib, a high-affinity ABL-kinase inhibitor and dasatinib, a dual SRC- and ABL-kinase inhibitor, which binds to the ABL-kinase in both its active and inactive conformations. These agents have become essential for the management of resistant and advanced-phase CML (254, 263). Nevertheless, neither of these TKIs have significant clinical activity against the “gatekeeper” T315I mutation, which confers a tyrosine-to-isoleucine substitution at position 315 and was detected in up to 15% of CML patients who failed IM therapy (335). However, the implication of BCR-ABL point mutations as the sole underlying reason for TKI resistance remains uncertain. Although, some investigators have detected mutations in $CD34^+$ cells from CML

patients both before (336) and after IM treatment (337), others have not detected any ABL-kinase mutations within the TKI-resistant CML cell population *in vitro* (131). Furthermore, it is also worth noting that the presence of BCR-ABL mutations does not always explain clinical IM resistance (245) and in $CD34^+$ cells resistance mutations have not been present at high enough levels to explain the resistance of this population.

Although less frequent than ABL-kinase domain mutations, BCR-ABL amplification has also been described as a potential BCR-ABL dependent resistance mechanism. Upregulation of BCR-ABL mRNA and protein was first reported in IM-resistant, BCR-ABL expressing cell lines, in the absence of ABL-kinase domain mutations (237). BCR-ABL amplification has also been documented in patients with advanced phase disease, who developed resistance to IM treatment (238). Further, prolonged IM exposure has also been demonstrated to enhance oncogene amplification (236). However, in a subsequent screening of IM-resistant CML patients, only 2 out of 66 had BCR-ABL gene amplification as determined by D-FISH (132). This suggests that the phenomenon of point mutations within the ABL-kinase domain is a far more common mechanism of IM resistance. That said, it has been shown that $CD34^+$ CML cells expressing increased amounts of BCR-ABL are less sensitive to IM and are prone to develop mutations faster than those that express low levels of BCR-ABL (338). Further, it has also been demonstrated that very primitive, resistant $CD34^+$ CML cells have higher transcript levels, despite having just single copy BCR-ABL (131, 298). This suggests that the levels of protein are at least partially responsible for the rate at which IM-resistant clones emerge (338) and that this increased BCR-ABL protein level still plays an important role in the propagation of disease, but possibly not as a result of amplification of the gene.

Although these mechanisms have been well-documented by many groups, resistance cannot solely be explained by oncogene mutation or amplification, as IM therapy does not eradicate all of the CML cells, even in those who respond well. For example, in patients who had achieved undetectable levels of BCR-ABL during IM treatment, molecular relapses were demonstrated in 50% of all cases when IM therapy was stopped (339). On the basis of these observations, it is predicted that this constant MRD in IM-treated patients is the result of residual LSCs. These primitive, quiescent CML cells have been shown to be resistant to IM, even at concentrations 10 fold higher than those achievable *in vivo* (224, 226). Furthermore, subsequent *in vitro* investigations have shown that this population persists in the face of treatment with the more potent TKI, nilotinib (256) and although dasatinib therapy appears to target a population of CML cells which resides deeper within the stem cell compartment, the most primitive, quiescent cells still remain (131). This rare population of quiescent CML cells, which represent approximately 0.5% of the total $CD34^+$ cells (340), may be refractory to TKI treatment simply by virtue of their dormant status. However, quiescent primitive CML stem cells may also demonstrate other mechanisms of resistance. A variety of hypotheses have been suggested as the molecular basis for this TKI refractoriness. For example, optimal TKI plasma and intracellular concentrations within the cell are necessary for therapy to succeed. Therefore, it has been suggested that drug resistance may be induced by suboptimal intracellular TKI concentration. It has been hypothesised that TKI resistance in CML stem cells is as a result of reduced drug-influx and increased drug-efflux compared with more mature cells. Primitive CML $CD34^+38^-$ stem cells apparently exhibit high level expression or activity of drug efflux proteins, such as MDR-1, and reduced expression or activity of drug influx proteins, such as the organic cation transporter-1, as compared with more mature cells (298). Therefore, such

mechanisms could possibly confer resistance against TKIs and other apoptosis-inducing drugs. However, this notion remains controversial as more recent work in the field has shown that at least the MDR-1 (249) and ABCG2 (250) transporters are unlikely players in IM resistance.

As stated previously, one important finding is that BCR-ABL is over-expressed within the quiescent CML stem cell population. Copland et al. showed that the IM-resistant CML $CD34^{+}38^{-}$ cells expressed significantly increased *BCR-ABL* transcripts and BCR-ABL protein kinase than more mature CML cells. Additionally, phosphorylation of the direct downstream target, CrkL, was increased in the most primitive CML $CD34^{+}38^{-}$ cells, as compared to the total $CD34^{+}$ fraction (131). These discoveries alone may explain why this population is so resistant to TKI treatment and suggest that BCR-ABL is still a relevant target for the treatment of CML. Following on from this, it is then necessary to ask the question: “why are the mature, proliferating CML cells targeted by TKI treatment, whereas the primitive quiescent CML cells are not?” It is suggested that oncogenic fusion TK-transformed cells are able to proliferate due to persistent survival signalling which counteracts any pro-apoptotic signals (341). The apparent dependence of a tumour cell on a single mutationally activated oncoprotein or oncoprotein-mediated signalling pathway(s) for their proliferation and/or survival has been described as “oncogene addiction” (271). Sharma et al. proposed a hypothesis to explain the oncogene addiction phenomenon. In the context of a tumour cell, the balance between pro-survival and pro-apoptotic signals derived from the activated oncoprotein favour a survival state. However, on acute inactivation of the oncoprotein, the pro-survival signals are decreased very rapidly as compared to the pro-apoptotic signals. This creates a temporal window, whereby the pro-apoptotic signalling predominates, which lasts long enough for the cell to commit

to apoptotic death (342). With regards to the fact that the primitive quiescent population is not targeted by TKI treatment, it is still currently unclear why they should be so insensitive. One could predict that they are not oncogene addicted to BCR-ABL TK activity. Studies, which have used transgenic mouse models for the inducible expression of BCR-ABL, have shown that multiple rounds of induction and reversion are possible. This thereby, indicates that the LSC population is able to persist long-term, even following BCR-ABL reversion (75, 275). Further support for this hypothesis comes from investigations which demonstrated that despite inactivation of $p190^{BCR-ABL}$ in a murine model of ALL, there was a failure to rescue the malignant phenotype, thereby suggesting that $p190^{BCR-ABL}$ is not required for the maintenance of disease in mice (343). However, this notion still remains controversial in primary CML cells, as one critical question which remains to be answered is whether BCR-ABL activity is completely inhibited by TKI within this rare primitive population of LSCs. If BCR-ABL was found to be incompletely inhibited within the stem cell population, then this would suggest that BCR-ABL is still a critical drug target for the management of CML. Therefore, efforts should be made to develop and use more potent TKIs, or manipulate drug transporters in order to increase the intracellular TKI concentrations within the CML stem cell population and effectively inhibit BCR-ABL TK activity. However, if BCR-ABL was found to be completely inhibited within the resistant pool of CML stem cells, then one could definitively say that this cell population is not oncogene addicted to BCR-ABL TK activity. This would also then suggest that these resistant primitive CML cells are perhaps reliant on other non BCR-ABL TK-related mechanisms for their proliferation and/or survival. This thesis concentrated on determining whether primitive CML stem cells are dependent on BCR-ABL TK activity for their proliferation and/or survival, with the further aim of characterising the resistant

population of CML cells and investigating any other potential cell survival mechanisms.

6.1 Is BCR-ABL relevant for the survival of cancer stem cells in CML?

Previous studies have measured BCR-ABL TK activity as an indication of TKI response of CML cells, in a number of ways: total p-Tyr by FACS (291), p-CrkL measurement by Western blot (130, 131, 290, 294), p-CrkL by flow cytometry (130, 131). Here we aimed to provide an alternative technique for the measurement of BCR-ABL TK activity, by developing a novel ELISA method designed for the high throughput of samples. Although this technique was reliable against the other methods, it proved too costly in terms of cell numbers required to give an accurate read-out for stem cell work. Therefore, for the purposes of this thesis, where the quantity of samples and the cell number within each sample was low, we decided to use flow cytometry using a method developed in house (130) and other conventional methods. Nevertheless, the ELISA would perhaps prove to be more useful in a more clinical screening setting, where the sample numbers would be higher and material less limited. Even though Western blot has proven to be an extremely reliable technique for the assessment of kinase activity, it is not feasible when working with such rare populations of CML cells. Therefore, in order to accurately assess and characterise the CML cells which are undergoing drug treatment, the only reasonable option was found to be flow cytometry. One major advantage of flow cytometry over the other methods is the ability to measure multiple parameters simultaneously, within samples containing relatively low cell numbers. This was absolutely necessary for determining BCR-ABL TK activity within specific subpopulations of CML stem cells.

Following the initial TKI timecourse studies, it was found that transient exposure to intermediate concentrations of TKI was as effective as continuous treatment with increased concentrations, which are clinically unachievable. This challenges the assumptions based on early studies with IM (205, 207, 215), where it was concluded that it was necessary for TKIs to achieve continuous BCR-ABL inhibition in order for CML cells to commit irreversibly to apoptosis. However, the results of this study are in keeping with more recent investigations (310, 316, 344), which have demonstrated that transient, potent inhibition of BCR-ABL TK activity is sufficient to commit both CML cell lines (310, 316) and primary $CD34^+$ CML cells (316, 344) irreversibly to apoptosis. This supports the "oncogenic shock" model, described previously, in which it is suggested that kinase inhibitors are effective against oncogene-addicted tumour cells because of the more rapid reduction of oncogene-mediated pro-survival versus pro-apoptotic signals following inactivation of the oncoprotein's TK activity. Here, these data suggest that once a specific threshold of kinase inhibition is exceeded within TKI-sensitive CML cells, following potent TKI exposure of up to only one hour, these cells will commit irreversibly to apoptosis. However, within the TKI-resistant CML cells, neither dose escalation of TKI to concentrations which are clinically unachievable, nor an increase in the drug exposure time from 1 to 72 hours led to an enhancement of cell death. This suggested that the cells which survived the treatment were intrinsically resistant to BCR-ABL TK inhibition. The fact that drug-sensitive CML cells commit to apoptosis following potent BCR-ABL inhibition induced by transient TKI exposure also has important implications for the treatment of CML. This has particular significance for the clinical application of more potent TKIs such as, dasatinib, whereby pulse-dosing may reduce any associated toxicities. Indeed, data from a very recent trial suggests that potent and transient kinase inhibition of BCR-ABL with dasatinib (100mg/day) achieves rapid

and durable cytogenetic responses, which are indistinguishable from those achieved with more continuous kinase inhibition, in CP CML patients with resistance, suboptimal response or intolerance to IM (345).

An interesting finding from these studies was the fact that exogenous GF support gave a protective effect over the treatment of CML cells with TKI. In fact, treatment of CML cells with TKI in the presence of a high concentration of GFs gave the same effect as removing GFs from untreated control cells. This is perhaps, logical as the pathways which are constitutively activated by BCR-ABL autophosphorylation are also activated by GF stimulation. Therefore, in this setting, the addition of exogenous GFs then negates the CML cells' requirement for BCR-ABL. Previous studies have shown that CML cells exhibit *BCR-ABL*-independent IM and nilotinib resistance, through activation of the anti-apoptotic JAK2/STAT5 pathway, as a result of adaptive autocrine and paracrine secretion of GM-CSF (235). Konig and colleagues also demonstrated that MAPK, Akt and STAT5 phosphorylation was inhibited in CML $CD34^+$ cells by nilotinib (346) and dasatinib (347) only in the absence, but not the presence of GFs. Jiang et al. showed that the deregulated growth of $CD34^+$ CML cells caused by BCR-ABL was, at least partially, dependent on the autocrine production of IL-3 and G-CSF and a stimulation of STAT5 phosphorylation. Similarly, BCR-ABL was shown to require the IL-3 receptor and subsequent downstream JAK2/STAT5-signalling for the oncogenic transformation of BCR-ABL-expressing fibroblasts (348). A very recent study by the group led by Tim Hughes also confirms these findings, where CML cells remained viable in culture with additional cytokines following short-term exposure to dasatinib. Treatment with dasatinib in combination with JAK activity inhibition then re-sensitised these cells to BCR-ABL TK inhibition, despite the presence of exogenous cytokine support. It was also observed that short-term

intense BCR-ABL TK inhibition commits $CD34^+$ CML cells to death only in the absence of GFs (344), further confirming the results of our study.

Overall, these data highlight the importance of GF signalling in the survival of CML cells treated with TKI. Further, it suggests that primitive CML progenitor cells may not be entirely dependent on BCR-ABL for proliferation and/or survival in the presence of GFs, due to the activation of cytokine-mediated signalling cascades, such as, JAK2/STAT5. This could have implications for the TKI treatment of CML patients, where cytokines would, of course, be present at physiological concentrations. Studies have demonstrated that the IL-3 receptor, CD123, is highly expressed on $CD34^+38^-$ LSCs in AML (349) and CML (350, 351) and has been shown to be an effective therapeutic target in pre-clinical AML models (352, 353). Groups have now begun to investigate the therapeutic potential of recombinant IL-3-diphtheria toxin (DT) conjugates which target CD123, both in *in vitro* and *in vivo* CML models (354) and in Ph^+ ALL (355), whereby the co-treatment with TKI and DT conjugate was more effective at eliminating Ph^+ progenitor cells than either agent alone. Furthermore, a Phase I study investigating the effects of an anti-CD123 monoclonal antibody (CSL360) in AML is currently ongoing (356). Therefore, targeting of cytokine signalling in combination with BCR-ABL TK inhibition may represent an exciting new concept for therapeutic intervention in patients with CML and Ph^+ ALL.

In this study, following a prolonged treatment timecourse of 12 days with 150nM dasatinib in the absence of exogenous cytokine support, 10% of the starting $CD34^+$ CML cells survived. Since no GFs were present in the culture media, the phenomenon of cytokine-mediated mechanisms of BCR-ABL-independent

resistance could be ruled out. Similarly, the other most common means of TKI resistance in CML cells (i.e. oncogene amplification and ABL-kinase domain mutations) were also found to be irrelevant in this TKI-resistant CML cell population. BCR-ABL TK inhibition was next measured by assessment of both p-CrkL and p-STAT5. Previous studies which have used TKI to inhibit BCR-ABL TK activity have demonstrated incomplete levels of inhibition (131). To address the question of whether a CML stem cell is oncogene addicted, BCR-ABL TK activity must be fully inhibited and the cells tracked for survival. Here, it was concluded that maximal pharmalogical inhibition of BCR-ABL TK activity was achieved in the surviving dasatinib-treated CML cells, both in the bulk population of cells and the more problematic primitive stem cell population. As with previous studies (131), those cells which survived the dasatinib treatment were primitive, residing mainly in the undivided cell fraction and the very early cell divisions. Since these BCR-ABL TK-inhibited, resistant cells were also able to grow when re-cultured in cytokines and form LTC-IC colonies, these data suggest that ~10% of primitive $CD34^+$ CML cells are not addicted to BCR-ABL TK activity for their survival. However, it would be presumptuous to say that these CML cells are not addicted to the BCR-ABL oncoprotein itself, since components in BCR-ABL, other than the kinase domain, could mediate resistance. Recent studies have identified *Alox5* as a key gene that regulates the functions of LSCs, but not normal HSCs, in mice. It was demonstrated that *Alox5* deficiency or inhibition prevented CML development initiated by BCR-ABL (357). Furthermore, *Alox5* was also found to be regulated by BCR-ABL oncoprotein, but was unaffected by TKI treatment (358). Therefore, *Alox5* represents a potential BCR-ABL dependent, but BCR-ABL TK independent, target. Previous investigations have used si- and short hairpin (sh)RNA designed to target *BCR-ABL* itself, both in Ph^+ cell lines and primary $CD34^+$ CML cells (359-361). Such a strategy should block all BCR-ABL activity and not just kinase

activity. Although in certain cases, BCR-ABL knockdown was associated with increased apoptosis, the level of down-regulation was often transient and/or incomplete. Studies performed by our own lab used shRNA against BCR-ABL, delivered by either electroporation or more stable lentiviral transduction, in combination with dasatinib treatment of CML cells. It was demonstrated that BCR-ABL oncoprotein knockdown and inhibition of kinase activity resulted in a synergistic induction of activated caspase-3, expression of annexin-V and dramatic reduction in viable K562 cells (362). However, since K562 are a BC CML cell line, they may prove to be more dependent on BCR-ABL expression for their survival. Therefore, further work is currently underway in this laboratory to use TKI to inhibit BCR-ABL TK activity, in combination with lentiviral shRNA to stably target *BCR-ABL* itself within the most primitive compartment of CML cells. If the CML cells survive both complete inhibition of BCR-ABL TK activity and complete loss of the BCR-ABL oncoprotein, then it could be definitively said that this resistant population of CML cells are truly independent of BCR-ABL for their survival.

6.2 Analysis of the effects of autophagy on CML stem cell survival

During the experiments which used dasatinib to inhibit BCR-ABL TK activity within $CD34^+$ CML cells, CFSE-staining revealed that within the CML cells which survived the prolonged treatment timecourse, two populations existed; one which remained undivided and another which was able to divide up to 3 times. This suggested that these primitive, resistant CML cells appeared to survive and proliferate by BCR-ABL-independent mechanisms. Therefore, the next experiments were then designed to investigate autophagy as a potential means of primitive CML cell survival. Autophagy has previously been shown to be an important event for the megakaryocytic differentiation of the CML cell line, K562 (363). Furthermore, since the induction of autophagy has previously been demonstrated to provide tumour cells with a protective mechanism to survive in the face of irradiation (364), alkylating agents (365) or arsenic trioxide (366), it was hypothesised that resistant CML cells could also be employing such a mechanism to survive following dasatinib treatment, especially under conditions of GF deprivation. In this study, analysis of the cellular properties of $CD34^+$ CML cells, which remained viable following the 12 days, revealed that the dasatinib-treated cells were significantly smaller in size as compared with control cells – a property of cells which are undergoing autophagy. EM also showed that both GF deprivation of untreated CML cells and dasatinib treatment of CML cells induced the formation of cytoplasmic autophagic structures. Significantly increased LC3-positive puncta and the autophagosome-asociated LC3-II were also observed in the CML cells treated with dasatinib, particularly in the cells cultured without GFs. Overall, these data suggested that autophagy is induced following GF deprivation

of CML cells and is significantly increased within these cells, upon BCR-ABL inhibition following dasatinib treatment. It was next hypothesised that autophagy was responsible for a condition by which primitive CML cells rely upon a state of metabolic inactivity, in order to survive following TKI treatment. Therefore, in order to test this hypothesis, it was assessed whether TKI-induced CML cell death could be enhanced by the chemical inhibition of autophagy by CQ or BAF. These agents act by blocking the last step of the autophagy process (i.e. the degradation of autophagosomes following fusion with lysosomes). Remarkably, it was found that the inhibition of autophagy greatly potentiates the effect of TKI treatment on the reduction of primitive CML progenitor cells, in terms of the effective eradication of functionally defined CFCs and LTC-ICs. Although CQ and BAF are relatively non-specific for the autophagy process, genetic inhibition of autophagy by RNA interference-mediated knockdown of either *ATG5* or *ATG7* yielded comparable effects in CML cell lines (172). These data thereby demonstrate that the effects of CQ and BAF depend largely on the inhibition of autophagy. However, further work is currently underway in this laboratory to investigate *ATG5* and *ATG7* knockdown within human primary CML cells, in order to completely verify that the enhancement of TKI-induced cell death caused by CQ or BAF treatment is a direct result of autophagy inhibition. Recent studies have also confirmed the importance of autophagy in CML cells, as inhibition of the autophagic process increased the effect of both the histone deacetylase inhibitor, SAHA (171), and the TKI, INNO-406 (170), for the eradication of drug-resistant CML cells.

Overall, the results of this study have provided a powerful rationale for the design and implementation of a Medical Research Council TSCRC (www.mrc.ac.uk/Fundingopportunities/Grants/TSCRC/index.htm) randomised phase II clinical called **CH**l**O**roquine **I**matinib **C**ombination to **E**liminate **S**tem cells

(***CHOICES***). The trial compares IM treatment versus HCQ in combination with IM, for patients with CML who have been on IM for 1-3 years and have achieved a MCR, with residual disease detectable by qRT-PCR (Figure 6-2).

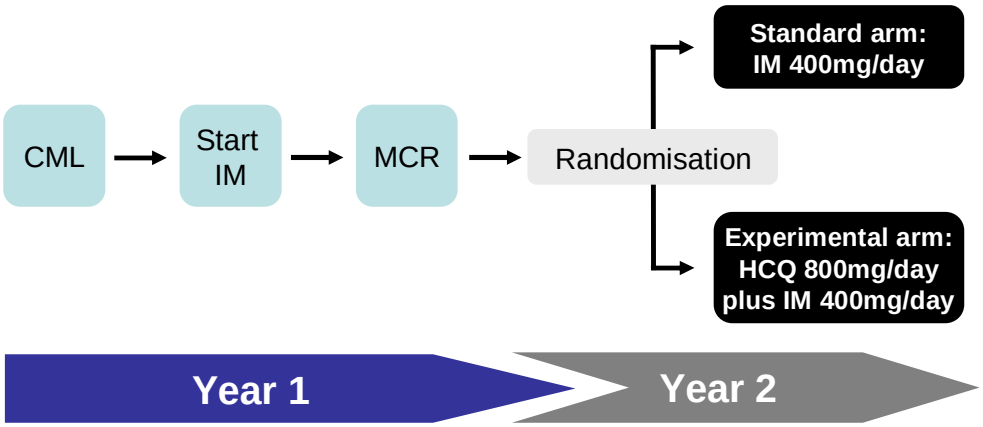

Figure 6-2 Schematic diagram of the protocol for the CHOICES trial

Although the preliminary *in vitro* data have shown the effectiveness of TKI treatment in combination with CQ for the eradication of primitive CML cells, CQ has been shown to be responsible for significant retinal toxicity in a number of patients (367). Therefore, for this trial it was replaced by HCQ, which has been used extensively in rheumatology and is well tolerated (368). Furthermore, preliminary in-house *in vitro* data indicated that HCQ was approximately equipotent to CQ when combined with TKI treatment in terms of reduction of functional CFCs from $CD34^+$ CML cells.

The primary end-points of the study are to provide preliminary evidence that HCQ given in combination with IM is more effective than IM alone in terms of *BCR-ABL* levels in CML patients who are in MCR with residual $BCR\text{-}ABL^+$ cells after at least one year of IM treatment and to determine the safety and tolerability of HCQ given

in combination with IM in these patients. The success criteria for the trial is defined as patients who have $\geq$0.5 log reductions in their 12 month PCR level of *BCR-ABL* transcripts from baseline. Secondary end-points are to determine whether the introduction of HCQ influences IM plasma levels and to confirm that whole blood HCQ levels achieved on a continuous 800mg/day dose in combination with IM are in the expected range. Correlative end-points are to confirm that HCQ at 800mg/day inhibits autophagy *in vivo* and to study the effect of HCQ given in combination with IM on residual BCR/ABL$^+$ primitive progenitors.

Recruitment for the trial started in April of this year, with 33 patients to be randomised to each treatment, making a total of 66 patients recruited in 3 UK centres.

In conclusion, the findings from this study clearly demonstrate that autophagy provides a BCR-ABL independent survival mechanism for primitive primary CML cells which have been treated with TKIs. In-house micro-array data also further backs up this notion, as the autophagy genes *ATG5* and *ATG4* were found to be upregulated in dasatinib-treated CD34$^+$ CML cells as compared to control cells. Likewise, the genes which transcribe cathepsins B and L (hydrolases which are thought to be important for the degradation of autophagic material within autolysosomes) are also increased in dasatinib-treated cells. We have also shown that the inhibition of autophagy can greatly potentiate TKI-induced CML cell death, which ultimately resulted in the initiation of a UK-wide clinical trial to investigate the benefits of the use of autophagy inhibitors in combination with TKI. Most importantly, we have demonstrated that the combination of autophagy inhibition combined with TKI is able to target the TKI-resistant CML stem cell population. Previously, it was shown that dasatinib is a much more potent inhibitor of BCR-

ABL TK activity than IM and is able to target BCR-ABL$^+$ cells deeper into the stem cell compartment (131). Here, we have shown that the combination of autophagy inhibition and BCR-ABL TK inhibition by TKI is able to target CML cells from even deeper within the stem cell compartment than dasatinib alone, as measured by the dramatic reduction in functional LTC-IC (Figure 6-3). Whether the truly quiescent CML stem cell population is targeted still remains to be seen. However, this strategy may represent a novel approach for the improvement of responses in patients with CP CML by the more effective eradication of TKI-resistant CML cells.

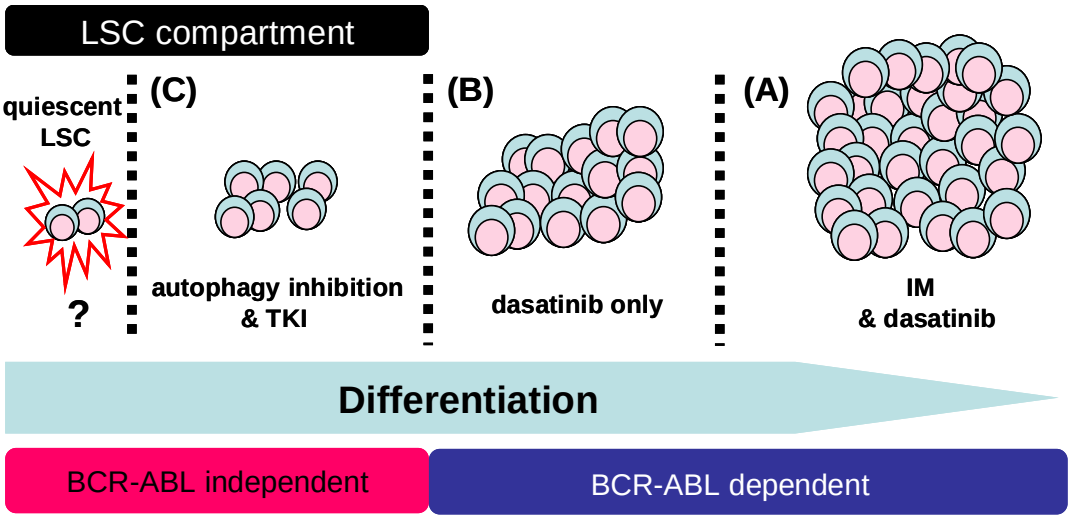

Figure 6-3 Schematic diagram to show the effects of either TKI treatment alone or in combination with autophagy inhibition on the different CML cell subpopulations

(A) More mature haemopoietic cells and the majority of progenitor cells are sensitive to both IM and dasatinib. (B) More primitive progenitor cells are resistant to IM but targeted by dasatinib. (C)The CML stem cell compartment is resistant to both IM and dasatinib, but targeted by a combination of TKI plus autophagy inhibition. It is not yet known whether the truly quiescent LSC population is affected by treatment with TKI and autophagy inhibition.

6.3 Summary and future directions

Overall, these findings suggest for the first time, that BCR-ABL targeting by TKI should no longer be the only focus of treatment for CML. Despite the success of both IM and the more potent second generation TKIs, such as dasatinib, in the treatment of CML, it is clear that quiescent stem cells still remain (131, 226). It was hypothesised that these resistant CML cells persist due to incomplete inhibition of BCR-ABL TK activity. However, here we have shown that despite maximal BCR-ABL TK inhibition, these cells are still able to survive. To attain the ultimate eradication of all CML cells, it is clear that combination therapies involving TKI and agents/therapies with activity specifically towards the cancer stem cell compartment will be required. In previous years, there were less well defined mechanisms for quiescent stem cell resistance to pro-apoptotic agents and therefore, no obvious molecular targets for therapeutic intervention. This prompted investigators to attempt to improve the effectiveness of TKI treatment by "waking up" the quiescent stem cell population, using cytokines to force them into cycle. It was demonstrated that a significant reduction of CML cells was observed following intermittent exposure to G-CSF compared to continuous treatment of IM alone, which was further enhanced when the cells were treated with a combination of IM and intermittent G-CSF (369). These impressive *in vitro* results led to a multi-centre clinical trial that further investigated the potential clinical use of cytokines in combination with IM to improve the management of CP CML. However, no significant difference was observed in patients treated with the combination as compared to continuous IM alone, indicating no further benefit compared to standard IM therapy (370). The group led by Andreas Trumpp has also used this approach in a mouse model. Here they first primed the quiescent stem cells into cycle with IFNα, which greatly sensitised these cells to the anti-proliferative agent

5-FU (371). However, since this was not a CML model, these data may have no relevance for the clearance of human primary CML cells.

In recent years, significant progress has been made in the objective for specific LSC-targeting in CML. A number of novel strategies for cancer stem cell therapy in CML are currently being investigated, with a few nearing the clinic and are briefly summarised in Table 6-1.

Strategy	Treatment	Reference
PP2A activation via SET inhibition	FTY720	(372)
Self-renewal pathway (Smoothened) inhibition	TKI and cyclopamine	(373),(374)
PML protein degradation	AraC and As_2O_3	(375)
BCR-ABL and autophagy inhibition	TKI and HCQ	(172)
BCR-ABL and histone deacetylase inhibition	TKI and LBH589	(376)

Table 6-1 Notable examples of LSC-targeted therapy in CML

In this study we have now shown that autophagy may also play a major role in the survival of LSCs following inhibition of critical oncogenic pathways. Little is known about the precise mechanism by which the autophagic process is induced by TKI in CML stem cells, therefore this remains to be elucidated by future investigations. Indeed, it is still not known why the primitive stem cell compartment is specifically able to survive through autophagy during conditions of stress. However, clues may come from the microenvironment in which they reside. The BM niche is a hypoxic tissue (377) and additionally, LSCs are more hypoxic than normal HSC in the BM, due to overcrowding from accelerated growth (378). It has also been demonstrated that $CD34^+$ human primary leukaemic cells populated the most hypoxic region of the BM (the epiphysis), when inoculated into immunodeficient mice (379). Recently, one study has suggested that a hypoxic microenvironment is important for the maintenance of CML stem cell quiescence (380). Therefore, it is likely that the quiescent CML stem cell population predominantly resides and thrives in a hypoxic BM environment. Since one of the processes which activate autophagy is prolonged hypoxia (381), it is perhaps possible that the most primitive CML cells, in particular, are already primed to use the autophagic process for survival. Therefore, understanding the hypoxic nature of LSCs and the importance for them to reside in such a microenvironment may be a further interesting avenue for future investigation.

In 1999, Holyoake et al. highlighted the importance of quiescent LSCs for the propagation of CML (224) and this population was subsequently found to persist in the face of TKI treatment (226). Significant progress has been made since then in terms of the development of agents which are able to specifically target this resistant cell population. However, little is known about why these primitive CML cells should remain quiescent? Here, we have shown that targeting autophagy is

highly effective in the eradication of primitive CML cells. Yet, it is still not clear as to whether the truly quiescent cells are targeted by this strategy and whether this population would rely on autophagy for its survival at all? One interesting finding comes from in-house microarray data in which it was observed that the essential autophagy genes, *ATG12*, *ATG2*, *ATG3* and the autolysosomal hydrolases - cathepsins L and D, were all decreased in dividing CML cells as compared to quiescent CML cells in the G_0 phase of cell cycle. Another important finding which may provide the connection between quiescence, the cell cycle arrest observed following TKI treatment and the induction of autophagy, was the observation that the dasatinib-treated cells demonstrated predominantly nuclear FoxO3a, as compared to untreated control cells. Activation of the PI3K/Akt pathway, results in FoxO inactivation which leads to enhanced cell survival and proliferation. In the absence of GF or insulin-signalling, or in the presence of stress stimuli, FoxO members reside within the nucleus, where they are active as transcription factors involved in cellular processes such as, apoptosis, cell-cycle arrest and stress resistance (382). In the normal HSC compartment, FoxOs reside within the nucleus where they are thought to play a role in cellular quiescence through their transcriptional activation of cell cycle regulators, such as p21, p27, p130 and down-regulation of cyclin D (311). FoxOs are also thought to play an important role in protecting quiescent HSCs from oxidative stress. In FoxO-deficient stem cells, there is a marked increase in reactive oxygen species which leads to an increase in the number of cycling HSCs and eventual HSC exhaustion (383). Recently, it was demonstrated that BCR-ABL inactivated the transcriptional activity of FoxOs in untreated $CD34^+$ CML cells. Furthermore, the TKI-mediated G_1 arrest seen in CML cells was found to be induced by the reactivation of FoxOs. Finally, and most importantly, primitive CML stem cells retained sustained activation of FoxOs (314) which presumably regulated their quiescence. Other studies have

also shown that FoxO3a was important for the maintenance of CML LSCs in a murine model (317). Therefore, within this study it is highly likely that the activation of FoxO3a played some part in the cell cycle arrest of the resistant dasatinib-treated CML cells.

Interestingly, as another cellular regulation mechanism, it has been demonstrated that stimulation of the energy sensor pathway, which is activated by an increased adenosine monophosphate (AMP)/ATP ratio, results in the AMP-activated protein kinase (AMPK)-mediated activation of FoxO3a (384). AMPK is a central metabolic switch which responds to low energy. It is found in all eukaryotes and governs glucose and lipid metabolism in response to changes in nutrients and intracellular energy levels. Furthermore, AMPK has been shown to be a direct downstream effector of the LKB1 tumour suppressor kinase and is involved in a mechanism representing the connection between energy metabolism and cell growth control (385). Recently, it has been reported that the conserved AMPK/FoxO3a energy sensor pathway is inducible in human tumour cells in response to metabolic stress. In colorectal and ovarian cancer cells, decreased glycolysis caused by inhibition of the p38α/HIF1α pathway, led to the nuclear accumulation of FoxO3a and the subsequent transcriptional activation of target genes whose protein products promote the autophagic process, such as, *ATG6*, *ATG7* and *ATG12* (386-388). In response to the acute energy demand that induced the autophagy process, the cells also exited the cell cycle and accumulated in the G_1 phase, which also mirrors what we observed in the dasatinib-treated CML cells tested in this study. Taken together these data indicate that there may be an important link between the cell cycle arrest induced by the nuclear accumulation of FoxO3a and the apparent reliance on autophagy for survival in TKI-resistant primitive CML stem cells.

Thus, it could be speculated that in response to acute energy depletion, caused by either GF deprivation or BCR-ABL TK inhibition, AMPK induces FoxO3a to accumulate in the nucleus of TKI-treated CML cells and triggers the transcription of target genes involved in both autophagy and cell cycle arrest. The cells would then induce autophagy and exit the cell cycle, arresting in G_0/G_1 in an attempt to retain energy for survival. The PI3K/Akt activation of mTOR has been shown to be an important negative regulator of autophagy. The known pathway by which Akt activates mTOR is via direct phosphorylation and inhibition of TSC2, which is a negative regulator of mTOR. It has also been demonstrated that Akt is a negative regulator of AMPK, which is an activator of TSC2 (389). Therefore, it seems logical that activated AMPK would have an important role in the ultimate induction of autophagy. Interestingly, it was also shown that hypoxia induced autophagy in tumour cell lines via AMPK activity (390). Thus, this could be another indicator that the very quiescent CML stem cells rely on autophagy for survival within the hypoxic conditions of the BM niche. This may also mean that the AMPK/FoxO3a axis could represent a potential approach for therapeutic intervention in CML. Of course, the link between the observation of nuclear FoxO3a, with subsequent downregulation of cyclin D1 in dasatinib-treated primitive CML cells and the high level of autophagy induction within this resistant cell population is still a little tenuous. Therefore, further work should be carried out to prove that this hypothesis is actually the case. However, this preliminary data may be an exciting early indicator of future insights in CML which are still to come.

In 1990, George Daley and colleagues used murine models to establish BCR-ABL as an oncogene to induce CML, whereby retroviral transduction of BCR-ABL cDNA into the BM of recipient mice was sufficient to induce a CML-like myeloproliferative disease (74). In the subsequent years great efforts have been

made to try to further understand the key signalling pathways and molecular drivers of malignant transformation of CML stem cells. This has yielded a wealth of preliminary data from novel agents which have demonstrated impressive results both *in vitro* and in Phase I-III clinical trials. Many efforts have been made to direct therapy towards the kinase activity of BCR-ABL. However, this thesis has shown for the first time that the most resistant primitive CML cells are likely to be independent of BCR-ABL TK activity for their survival. Furthermore, we have shown that these resistant CML stem cells rely on the BCR-ABL independent, autophagy process for survival in response to stressful conditions, such as, TKI treatment. This highlights the importance for further work directed towards the understanding of the complex biology of cancer stem cells and why they remain quiescent, both in CML and other haematological malignancies. Since the majority of CP CML cells appear to be dependent on BCR-ABL TK activity for their survival; the use of TKI to remove the burden of the CML tumour load, combined with BCR-ABL independent therapies, targeted specifically towards the quiescent LSC compartment should provide more effective future approaches for the ultimate eradication of CML.

7. REFERENCES

1. Wu AM, Till JE, Siminovitch L, McCulloch EA. A cytological study of the capacity for differentiation of normal hemopoietic colony-forming cells. J Cell Physiol1967 Apr;69(2):177-84.
2. Wu AM, Till JE, Siminovitch L, McCulloch EA. Cytological evidence for a relationship between normal hemotopoietic colony-forming cells and cells of the lymphoid system. J Exp Med1968 Mar 1;127(3):455-64.
3. Eaves C, Glimm H, Eisterer W, Audet J, Maguer-Satta V, Piret J. Characterization of human hematopoietic cells with short-lived in vivo repopulating activity. Ann N Y Acad Sci2001 Jun;938:63-70.
4. Taichman RS. Blood and bone: two tissues whose fates are intertwined to create the hematopoietic stem-cell niche. Blood2005 Apr 1;105(7):2631-9.
5. Till JE, Mc CE. A direct measurement of the radiation sensitivity of normal mouse bone marrow cells. Radiat Res1961 Feb;14:213-22.
6. Kiel MJ, He S, Ashkenazi R, Gentry SN, Teta M, Kushner JA, et al. Haematopoietic stem cells do not asymmetrically segregate chromosomes or retain BrdU. Nature2007 Sep 13;449(7159):238-42.
7. Spangrude GJ, Heimfeld S, Weissman IL. Purification and characterization of mouse hematopoietic stem cells. Science1988 Jul 1;241(4861):58-62.
8. Osawa M, Hanada K, Hamada H, Nakauchi H. Long-term lymphohematopoietic reconstitution by a single CD34-low/negative hematopoietic stem cell. Science1996 Jul 12;273(5272):242-5.
9. Krause DS, Theise ND, Collector MI, Henegariu O, Hwang S, Gardner R, et al. Multi-organ, multi-lineage engraftment by a single bone marrow-derived stem cell. Cell2001 May 4;105(3):369-77.
10. Morrison SJ, Weissman IL. The long-term repopulating subset of hematopoietic stem cells is deterministic and isolatable by phenotype. Immunity1994 Nov;1(8):661-73.
11. Morrison SJ, Wandycz AM, Hemmati HD, Wright DE, Weissman IL. Identification of a lineage of multipotent hematopoietic progenitors. Development1997 May;124(10):1929-39.
12. Kondo M, Weissman IL, Akashi K. Identification of clonogenic common lymphoid progenitors in mouse bone marrow. Cell1997 Nov 28;91(5):661-72.
13. Akashi K, Traver D, Miyamoto T, Weissman IL. A clonogenic common myeloid progenitor that gives rise to all myeloid lineages. Nature2000 Mar 9;404(6774):193-7.
14. Leary AG, Hirai Y, Kishimoto T, Clark SC, Ogawa M. Survival of hemopoietic progenitors in the G0 period of the cell cycle does not require early hemopoietic regulators. Proc Natl Acad Sci U S A1989 Jun;86(12):4535-8.
15. Leary AG, Zeng HQ, Clark SC, Ogawa M. Growth factor requirements for survival in G0 and entry into the cell cycle of primitive human hemopoietic progenitors. Proc Natl Acad Sci U S A1992 May 1;89(9):4013-7.
16. Lajtha LG. Stem cell concepts. Differentiation1979;14(1-2):23-34.
17. Schofield R. The relationship between the spleen colony-forming cell and the haemopoietic stem cell. Blood Cells1978;4(1-2):7-25.
18. Wilson A, Trumpp A. Bone-marrow haematopoietic-stem-cell niches. Nat Rev Immunol2006 Feb;6(2):93-106.
19. Dar A, Kollet O, Lapidot T. Mutual, reciprocal SDF-1/CXCR4 interactions between hematopoietic and bone marrow stromal cells regulate human stem cell

migration and development in NOD/SCID chimeric mice. Exp Hematol2006 Aug;34(8):967-75.
20. Peled A, Petit I, Kollet O, Magid M, Ponomaryov T, Byk T, et al. Dependence of human stem cell engraftment and repopulation of NOD/SCID mice on CXCR4. Science1999 Feb 5;283(5403):845-8.
21. Jin L, Tabe Y, Konoplev S, Xu Y, Leysath CE, Lu H, et al. CXCR4 up-regulation by imatinib induces chronic myelogenous leukemia (CML) cell migration to bone marrow stroma and promotes survival of quiescent CML cells. Mol Cancer Ther2008 Jan;7(1):48-58.
22. Nie Y, Han YC, Zou YR. CXCR4 is required for the quiescence of primitive hematopoietic cells. J Exp Med2008 Apr 14;205(4):777-83.
23. Scadden DT. The stem-cell niche as an entity of action. Nature2006 Jun 29;441(7097):1075-9.
24. Caux C, Favre C, Saeland S, Duvert V, Mannoni P, Durand I, et al. Sequential loss of CD34 and class II MHC antigens on purified cord blood hematopoietic progenitors cultured with IL-3: characterization of CD34-, HLA-DR+ cells. Blood1989 Sep;74(4):1287-94.
25. Krause DS, Fackler MJ, Civin CI, May WS. CD34: structure, biology, and clinical utility. Blood1996 Jan 1;87(1):1-13.
26. Hao QL, Shah AJ, Thiemann FT, Smogorzewska EM, Crooks GM. A functional comparison of CD34 + CD38- cells in cord blood and bone marrow. Blood1995 Nov 15;86(10):3745-53.
27. Kung P, Goldstein G, Reinherz EL, Schlossman SF. Monoclonal antibodies defining distinctive human T cell surface antigens. Science1979 Oct 19;206(4416):347-9.
28. Hogan CJ, Shpall EJ, Keller G. Differential long-term and multilineage engraftment potential from subfractions of human CD34+ cord blood cells transplanted into NOD/SCID mice. Proc Natl Acad Sci U S A2002 Jan 8;99(1):413-8.
29. Bhatia M, Wang JC, Kapp U, Bonnet D, Dick JE. Purification of primitive human hematopoietic cells capable of repopulating immune-deficient mice. Proc Natl Acad Sci U S A1997 May 13;94(10):5320-5.
30. Miller JS, McCullar V, Punzel M, Lemischka IR, Moore KA. Single adult human CD34(+)/Lin-/CD38(-) progenitors give rise to natural killer cells, B-lineage cells, dendritic cells, and myeloid cells. Blood1999 Jan 1;93(1):96-106.
31. Sutherland HJ, Eaves CJ, Eaves AC, Dragowska W, Lansdorp PM. Characterization and partial purification of human marrow cells capable of initiating long-term hematopoiesis in vitro. Blood1989 Oct;74(5):1563-70.
32. Yin AH, Miraglia S, Zanjani ED, Almeida-Porada G, Ogawa M, Leary AG, et al. AC133, a novel marker for human hematopoietic stem and progenitor cells. Blood1997 Dec 15;90(12):5002-12.
33. Udomsakdi C, Eaves CJ, Sutherland HJ, Lansdorp PM. Separation of functionally distinct subpopulations of primitive human hematopoietic cells using rhodamine-123. Exp Hematol1991 Jun;19(5):338-42.
34. Chaudhary PM, Roninson IB. Expression and activity of P-glycoprotein, a multidrug efflux pump, in human hematopoietic stem cells. Cell1991 Jul 12;66(1):85-94.
35. Zhou S, Schuetz JD, Bunting KD, Colapietro AM, Sampath J, Morris JJ, et al. The ABC transporter Bcrp1/ABCG2 is expressed in a wide variety of stem cells and is a molecular determinant of the side-population phenotype. Nat Med2001 Sep;7(9):1028-34.

36. Goodell MA, Brose K, Paradis G, Conner AS, Mulligan RC. Isolation and functional properties of murine hematopoietic stem cells that are replicating in vivo. J Exp Med1996 Apr 1;183(4):1797-806.
37. Shapiro HM. Flow cytometric estimation of DNA and RNA content in intact cells stained with Hoechst 33342 and pyronin Y. Cytometry1981 Nov;2(3):143-50.
38. Gordon MY, Goldman JM, Gordon-Smith EC. 4-Hydroperoxycyclophosphamide inhibits proliferation by human granulocyte-macrophage colony-forming cells (GM-CFC) but spares more primitive progenitor cells. Leuk Res1985;9(8):1017-21.
39. Sahovic EA, Colvin M, Hilton J, Ogawa M. Role for aldehyde dehydrogenase in survival of progenitors for murine blast cell colonies after treatment with 4-hydroperoxycyclophosphamide in vitro. Cancer Res1988 Mar 1;48(5):1223-6.
40. Storms RW, Trujillo AP, Springer JB, Shah L, Colvin OM, Ludeman SM, et al. Isolation of primitive human hematopoietic progenitors on the basis of aldehyde dehydrogenase activity. Proc Natl Acad Sci U S A1999 Aug 3;96(16):9118-23.
41. Passegue E, Jamieson CH, Ailles LE, Weissman IL. Normal and leukemic hematopoiesis: are leukemias a stem cell disorder or a reacquisition of stem cell characteristics? Proc Natl Acad Sci U S A2003 Sep 30;100 Suppl 1:11842-9.
42. Fialkow PJ, Gartler SM, Yoshida A. Clonal origin of chronic myelocytic leukemia in man. Proc Natl Acad Sci U S A1967 Oct;58(4):1468-71.
43. Fialkow PJ, Singer JW, Adamson JW, Vaidya K, Dow LW, Ochs J, et al. Acute nonlymphocytic leukemia: heterogeneity of stem cell origin. Blood1981 Jun;57(6):1068-73.
44. Fialkow PJ, Jacobson RJ, Papayannopoulou T. Chronic myelocytic leukemia: clonal origin in a stem cell common to the granulocyte, erythrocyte, platelet and monocyte/macrophage. Am J Med1977 Jul;63(1):125-30.
45. Park CH, Bergsagel DE, McCulloch EA. Mouse myeloma tumor stem cells: a primary cell culture assay. J Natl Cancer Inst1971 Feb;46(2):411-22.
46. Bruce WR, Van Der Gaag H. A Quantitative Assay for the Number of Murine Lymphoma Cells Capable of Proliferation in Vivo. Nature1963 Jul 6;199:79-80.
47. Bonnet D, Dick JE. Human acute myeloid leukemia is organized as a hierarchy that originates from a primitive hematopoietic cell. Nat Med1997 Jul;3(7):730-7.
48. Blair A, Hogge DE, Ailles LE, Lansdorp PM, Sutherland HJ. Lack of expression of Thy-1 (CD90) on acute myeloid leukemia cells with long-term proliferative ability in vitro and in vivo. Blood1997 May 1;89(9):3104-12.
49. Huntly BJ, Shigematsu H, Deguchi K, Lee BH, Mizuno S, Duclos N, et al. MOZ-TIF2, but not BCR-ABL, confers properties of leukemic stem cells to committed murine hematopoietic progenitors. Cancer Cell2004 Dec;6(6):587-96.
50. Cozzio A, Passegue E, Ayton PM, Karsunky H, Cleary ML, Weissman IL. Similar MLL-associated leukemias arising from self-renewing stem cells and short-lived myeloid progenitors. Genes Dev2003 Dec 15;17(24):3029-35.
51. Krivtsov AV, Twomey D, Feng Z, Stubbs MC, Wang Y, Faber J, et al. Transformation from committed progenitor to leukaemia stem cell initiated by MLL-AF9. Nature2006 Aug 17;442(7104):818-22.
52. Taussig DC, Miraki-Moud F, Anjos-Afonso F, Pearce DJ, Allen K, Ridler C, et al. Anti-CD38 antibody-mediated clearance of human repopulating cells masks the heterogeneity of leukemia-initiating cells. Blood2008 Aug 1;112(3):568-75.
53. Faderl S, Talpaz M, Estrov Z, Kantarjian HM. Chronic myelogenous leukemia: biology and therapy. Ann Intern Med1999 Aug 3;131(3):207-19.

54. Rowley JD. Letter: A new consistent chromosomal abnormality in chronic myelogenous leukaemia identified by quinacrine fluorescence and Giemsa staining. Nature1973 Jun 1;243(5405):290-3.
55. Groffen J, Stephenson JR, Heisterkamp N, de Klein A, Bartram CR, Grosveld G. Philadelphia chromosomal breakpoints are clustered within a limited region, bcr, on chromosome 22. Cell1984 Jan;36(1):93-9.
56. Ben-Neriah Y, Daley GQ, Mes-Masson AM, Witte ON, Baltimore D. The chronic myelogenous leukemia-specific P210 protein is the product of the bcr/abl hybrid gene. Science1986 Jul 11;233(4760):212-4.
57. Lugo TG, Pendergast AM, Muller AJ, Witte ON. Tyrosine kinase activity and transformation potency of bcr-abl oncogene products. Science1990 Mar 2;247(4946):1079-82.
58. Sawyers CL. Chronic myeloid leukemia. N Engl J Med1999 Apr 29;340(17):1330-40.
59. Lion T, Gaiger A, Henn T, Horth E, Haas OA, Geissler K, et al. Use of quantitative polymerase chain reaction to monitor residual disease in chronic myelogenous leukemia during treatment with interferon. Leukemia1995 Aug;9(8):1353-60.
60. Vardiman JW, Harris NL, Brunning RD. The World Health Organization (WHO) classification of the myeloid neoplasms. Blood2002 Oct 1;100(7):2292-302.
61. Laneuville P. Abl tyrosine protein kinase. Semin Immunol1995 Aug;7(4):255-66.
62. Kipreos ET, Wang JY. Cell cycle-regulated binding of c-Abl tyrosine kinase to DNA. Science1992 Apr 17;256(5055):382-5.
63. McWhirter JR, Wang JY. An actin-binding function contributes to transformation by the Bcr-Abl oncoprotein of Philadelphia chromosome-positive human leukemias. EMBO J1993 Apr;12(4):1533-46.
64. Van Etten RA, Jackson PK, Baltimore D, Sanders MC, Matsudaira PT, Janmey PA. The COOH terminus of the c-Abl tyrosine kinase contains distinct F- and G-actin binding domains with bundling activity. J Cell Biol1994 Feb;124(3):325-40.
65. Van Etten RA, Jackson P, Baltimore D. The mouse type IV c-abl gene product is a nuclear protein, and activation of transforming ability is associated with cytoplasmic localization. Cell1989 Aug 25;58(4):669-78.
66. Reuther GW, Fu H, Cripe LD, Collier RJ, Pendergast AM. Association of the protein kinases c-Bcr and Bcr-Abl with proteins of the 14-3-3 family. Science1994 Oct 7;266(5182):129-33.
67. Pendergast AM, Muller AJ, Havlik MH, Maru Y, Witte ON. BCR sequences essential for transformation by the BCR-ABL oncogene bind to the ABL SH2 regulatory domain in a non-phosphotyrosine-dependent manner. Cell1991 Jul 12;66(1):161-71.
68. McWhirter JR, Galasso DL, Wang JY. A coiled-coil oligomerization domain of Bcr is essential for the transforming function of Bcr-Abl oncoproteins. Mol Cell Biol1993 Dec;13(12):7587-95.
69. Pendergast AM, Quilliam LA, Cripe LD, Bassing CH, Dai Z, Li N, et al. BCR-ABL-induced oncogenesis is mediated by direct interaction with the SH2 domain of the GRB-2 adaptor protein. Cell1993 Oct 8;75(1):175-85.
70. Chan LC, Karhi KK, Rayter SI, Heisterkamp N, Eridani S, Powles R, et al. A novel abl protein expressed in Philadelphia chromosome positive acute lymphoblastic leukaemia. Nature1987 Feb 12-18;325(6105):635-7.

71. Kurzrock R, Shtalrid M, Talpaz M, Kloetzer WS, Gutterman JU. Expression of c-abl in Philadelphia-positive acute myelogenous leukemia. Blood1987 Nov;70(5):1584-8.
72. Melo JV, Myint H, Galton DA, Goldman JM. P190BCR-ABL chronic myeloid leukaemia: the missing link with chronic myelomonocytic leukaemia? Leukemia1994 Jan;8(1):208-11.
73. Pane F, Frigeri F, Sindona M, Luciano L, Ferrara F, Cimino R, et al. Neutrophilic-chronic myeloid leukemia: a distinct disease with a specific molecular marker (BCR/ABL with C3/A2 junction). Blood1996 Oct 1;88(7):2410-4.
74. Daley GQ, Van Etten RA, Baltimore D. Induction of chronic myelogenous leukemia in mice by the P210bcr/abl gene of the Philadelphia chromosome. Science1990 Feb 16;247(4944):824-30.
75. Koschmieder S, Gottgens B, Zhang P, Iwasaki-Arai J, Akashi K, Kutok JL, et al. Inducible chronic phase of myeloid leukemia with expansion of hematopoietic stem cells in a transgenic model of BCR-ABL leukemogenesis. Blood2005 Jan 1;105(1):324-34.
76. Teixido J, Hemler ME, Greenberger JS, Anklesaria P. Role of beta 1 and beta 2 integrins in the adhesion of human CD34hi stem cells to bone marrow stroma. J Clin Invest1992 Aug;90(2):358-67.
77. Gordon MY, Dowding CR, Riley GP, Goldman JM, Greaves MF. Altered adhesive interactions with marrow stroma of haematopoietic progenitor cells in chronic myeloid leukaemia. Nature1987 Jul 23-29;328(6128):342-4.
78. Verfaillie CM, Hurley R, Lundell BI, Zhao C, Bhatia R. Integrin-mediated regulation of hematopoiesis: do BCR/ABL-induced defects in integrin function underlie the abnormal circulation and proliferation of CML progenitors? Acta Haematol1997;97(1-2):40-52.
79. Varticovski L, Daley GQ, Jackson P, Baltimore D, Cantley LC. Activation of phosphatidylinositol 3-kinase in cells expressing abl oncogene variants. Mol Cell Biol1991 Feb;11(2):1107-13.
80. Bhatia R, Wayner EA, McGlave PB, Verfaillie CM. Interferon-alpha restores normal adhesion of chronic myelogenous leukemia hematopoietic progenitors to bone marrow stroma by correcting impaired beta 1 integrin receptor function. J Clin Invest1994 Jul;94(1):384-91.
81. Nagasawa T, Hirota S, Tachibana K, Takakura N, Nishikawa S, Kitamura Y, et al. Defects of B-cell lymphopoiesis and bone-marrow myelopoiesis in mice lacking the CXC chemokine PBSF/SDF-1. Nature1996 Aug 15;382(6592):635-8.
82. Geay JF, Buet D, Zhang Y, Foudi A, Jarrier P, Berthebaud M, et al. p210BCR-ABL inhibits SDF-1 chemotactic response via alteration of CXCR4 signaling and down-regulation of CXCR4 expression. Cancer Res2005 Apr 1;65(7):2676-83.
83. Bedi A, Zehnbauer BA, Barber JP, Sharkis SJ, Jones RJ. Inhibition of apoptosis by BCR-ABL in chronic myeloid leukemia. Blood1994 Apr 15;83(8):2038-44.
84. Skorski T, Bellacosa A, Nieborowska-Skorska M, Majewski M, Martinez R, Choi JK, et al. Transformation of hematopoietic cells by BCR/ABL requires activation of a PI-3k/Akt-dependent pathway. EMBO J1997 Oct 15;16(20):6151-61.
85. Aichberger KJ, Mayerhofer M, Krauth MT, Skvara H, Florian S, Sonneck K, et al. Identification of mcl-1 as a BCR/ABL-dependent target in chronic myeloid leukemia (CML): evidence for cooperative antileukemic effects of imatinib and mcl-1 antisense oligonucleotides. Blood2005 Apr 15;105(8):3303-11.
86. Amarante-Mendes GP, McGahon AJ, Nishioka WK, Afar DE, Witte ON, Green DR. Bcl-2-independent Bcr-Abl-mediated resistance to apoptosis:

protection is correlated with up regulation of Bcl-xL. Oncogene1998 Mar;16(11):1383-90.
87. Marley SB, Lewis JL, Scott MA, Goldman JM, Gordon MY. Evaluation of "discordant maturation' in chronic myeloid leukaemia using cultures of primitive progenitor cells and their production of clonogenic progeny (CFU-GM). Br J Haematol1996 Nov;95(2):299-305.
88. Smith DL, Burthem J, Whetton AD. Molecular pathogenesis of chronic myeloid leukaemia. Expert Rev Mol Med2003 Nov;5(27):1-27.
89. Carpino N, Wisniewski D, Strife A, Marshak D, Kobayashi R, Stillman B, et al. p62(dok): a constitutively tyrosine-phosphorylated, GAP-associated protein in chronic myelogenous leukemia progenitor cells. Cell1997 Jan 24;88(2):197-204.
90. Oda T, Heaney C, Hagopian JR, Okuda K, Griffin JD, Druker BJ. Crkl is the major tyrosine-phosphorylated protein in neutrophils from patients with chronic myelogenous leukemia. J Biol Chem1994 Sep 16;269(37):22925-8.
91. Feller SM, Knudsen B, Hanafusa H. c-Abl kinase regulates the protein binding activity of c-Crk. EMBO J1994 May 15;13(10):2341-51.
92. Druker B, Okuda K, Matulonis U, Salgia R, Roberts T, Griffin JD. Tyrosine phosphorylation of rasGAP and associated proteins in chronic myelogenous leukemia cell lines. Blood1992 May 1;79(9):2215-20.
93. Mandanas RA, Leibowitz DS, Gharehbaghi K, Tauchi T, Burgess GS, Miyazawa K, et al. Role of p21 RAS in p210 bcr-abl transformation of murine myeloid cells. Blood1993 Sep 15;82(6):1838-47.
94. Skorski T, Nieborowska-Skorska M, Szczylik C, Kanakaraj P, Perrotti D, Zon G, et al. C-RAF-1 serine/threonine kinase is required in BCR/ABL-dependent and normal hematopoiesis. Cancer Res1995 Jun 1;55(11):2275-8.
95. de Jong R, ten Hoeve J, Heisterkamp N, Groffen J. Crkl is complexed with tyrosine-phosphorylated Cbl in Ph-positive leukemia. J Biol Chem1995 Sep 15;270(37):21468-71.
96. Skorski T, Kanakaraj P, Nieborowska-Skorska M, Ratajczak MZ, Wen SC, Zon G, et al. Phosphatidylinositol-3 kinase activity is regulated by BCR/ABL and is required for the growth of Philadelphia chromosome-positive cells. Blood1995 Jul 15;86(2):726-36.
97. Carlesso N, Frank DA, Griffin JD. Tyrosyl phosphorylation and DNA binding activity of signal transducers and activators of transcription (STAT) proteins in hematopoietic cell lines transformed by Bcr/Abl. J Exp Med1996 Mar 1;183(3):811-20.
98. Hoover RR, Gerlach MJ, Koh EY, Daley GQ. Cooperative and redundant effects of STAT5 and Ras signaling in BCR/ABL transformed hematopoietic cells. Oncogene2001 Sep 13;20(41):5826-35.
99. Salgia R, Uemura N, Okuda K, Li JL, Pisick E, Sattler M, et al. CRKL links p210BCR/ABL with paxillin in chronic myelogenous leukemia cells. J Biol Chem1995 Dec 8;270(49):29145-50.
100. Gotoh A, Miyazawa K, Ohyashiki K, Tauchi T, Boswell HS, Broxmeyer HE, et al. Tyrosine phosphorylation and activation of focal adhesion kinase (p125FAK) by BCR-ABL oncoprotein. Exp Hematol1995 Oct;23(11):1153-9.
101. Salgia R, Brunkhorst B, Pisick E, Li JL, Lo SH, Chen LB, et al. Increased tyrosine phosphorylation of focal adhesion proteins in myeloid cell lines expressing p210BCR/ABL. Oncogene1995 Sep 21;11(6):1149-55.
102. Gotoh A, Miyazawa K, Ohyashiki K, Toyama K. Potential molecules implicated in downstream signaling pathways of p185BCR-ABL in Ph+ ALL involve GTPase-activating protein, phospholipase C-gamma 1, and phosphatidylinositol 3'-kinase. Leukemia1994 Jan;8(1):115-20.

103. Bassermann F, Jahn T, Miething C, Seipel P, Bai RY, Coutinho S, et al. Association of Bcr-Abl with the proto-oncogene Vav is implicated in activation of the Rac-1 pathway. J Biol Chem2002 Apr 5;277(14):12437-45.
104. Skorski T, Kanakaraj P, Ku DH, Nieborowska-Skorska M, Canaani E, Zon G, et al. Negative regulation of p120GAP GTPase promoting activity by p210bcr/abl: implication for RAS-dependent Philadelphia chromosome positive cell growth. J Exp Med1994 Jun 1;179(6):1855-65.
105. Gishizky ML, Cortez D, Pendergast AM. Mutant forms of growth factor-binding protein-2 reverse BCR-ABL-induced transformation. Proc Natl Acad Sci U S A1995 Nov 21;92(24):10889-93.
106. Pelicci G, Lanfrancone L, Salcini AE, Romano A, Mele S, Grazia Borrello M, et al. Constitutive phosphorylation of Shc proteins in human tumors. Oncogene1995 Sep 7;11(5):899-907.
107. Sawyers CL, McLaughlin J, Witte ON. Genetic requirement for Ras in the transformation of fibroblasts and hematopoietic cells by the Bcr-Abl oncogene. J Exp Med1995 Jan 1;181(1):307-13.
108. Cortez D, Kadlec L, Pendergast AM. Structural and signaling requirements for BCR-ABL-mediated transformation and inhibition of apoptosis. Mol Cell Biol1995 Oct;15(10):5531-41.
109. Goga A, McLaughlin J, Afar DE, Saffran DC, Witte ON. Alternative signals to RAS for hematopoietic transformation by the BCR-ABL oncogene. Cell1995 Sep 22;82(6):981-8.
110. Kisseleva T, Bhattacharya S, Braunstein J, Schindler CW. Signaling through the JAK/STAT pathway, recent advances and future challenges. Gene2002 Feb 20;285(1-2):1-24.
111. Chai SK, Nichols GL, Rothman P. Constitutive activation of JAKs and STATs in BCR-Abl-expressing cell lines and peripheral blood cells derived from leukemic patients. J Immunol1997 Nov 15;159(10):4720-8.
112. Ilaria RL, Jr., Van Etten RA. P210 and P190(BCR/ABL) induce the tyrosine phosphorylation and DNA binding activity of multiple specific STAT family members. J Biol Chem1996 Dec 6;271(49):31704-10.
113. de Groot RP, Raaijmakers JA, Lammers JW, Jove R, Koenderman L. STAT5 activation by BCR-Abl contributes to transformation of K562 leukemia cells. Blood1999 Aug 1;94(3):1108-12.
114. Gesbert F, Griffin JD. Bcr/Abl activates transcription of the Bcl-X gene through STAT5. Blood2000 Sep 15;96(6):2269-76.
115. Huang M, Dorsey JF, Epling-Burnette PK, Nimmanapalli R, Landowski TH, Mora LB, et al. Inhibition of Bcr-Abl kinase activity by PD180970 blocks constitutive activation of Stat5 and growth of CML cells. Oncogene2002 Dec 12;21(57):8804-16.
116. Carpenter CL, Duckworth BC, Auger KR, Cohen B, Schaffhausen BS, Cantley LC. Purification and characterization of phosphoinositide 3-kinase from rat liver. J Biol Chem1990 Nov 15;265(32):19704-11.
117. Cantley LC, Auger KR, Carpenter C, Duckworth B, Graziani A, Kapeller R, et al. Oncogenes and signal transduction. Cell1991 Jan 25;64(2):281-302.
118. Skolnik EY, Margolis B, Mohammadi M, Lowenstein E, Fischer R, Drepps A, et al. Cloning of PI3 kinase-associated p85 utilizing a novel method for expression/cloning of target proteins for receptor tyrosine kinases. Cell1991 Apr 5;65(1):83-90.
119. Kapeller R, Cantley LC. Phosphatidylinositol 3-kinase. Bioessays1994 Aug;16(8):565-76.
120. Shepherd PR, Reaves BJ, Davidson HW. Phosphoinositide 3-kinases and membrane traffic. Trends Cell Biol1996 Mar;6(3):92-7.

121. Divecha N, Irvine RF. Phospholipid signaling. Cell1995 Jan 27;80(2):269-78.
122. Vanhaesebroeck B, Leevers SJ, Ahmadi K, Timms J, Katso R, Driscoll PC, et al. Synthesis and function of 3-phosphorylated inositol lipids. Annu Rev Biochem2001;70:535-602.
123. Jain SK, Susa M, Keeler ML, Carlesso N, Druker B, Varticovski L. PI 3-kinase activation in BCR/abl-transformed hematopoietic cells does not require interaction of p85 SH2 domains with p210 BCR/abl. Blood1996 Sep 1;88(5):1542-50.
124. Sattler M, Mohi MG, Pride YB, Quinnan LR, Malouf NA, Podar K, et al. Critical role for Gab2 in transformation by BCR/ABL. Cancer Cell2002 Jun;1(5):479-92.
125. ten Hoeve J, Arlinghaus RB, Guo JQ, Heisterkamp N, Groffen J. Tyrosine phosphorylation of CRKL in Philadelphia+ leukemia. Blood1994 Sep 15;84(6):1731-6.
126. Reichman CT, Mayer BJ, Keshav S, Hanafusa H. The product of the cellular crk gene consists primarily of SH2 and SH3 regions. Cell Growth Differ1992 Jul;3(7):451-60.
127. de Jong R, ten Hoeve J, Heisterkamp N, Groffen J. Tyrosine 207 in CRKL is the BCR/ABL phosphorylation site. Oncogene1997 Feb 6;14(5):507-13.
128. Nichols GL, Raines MA, Vera JC, Lacomis L, Tempst P, Golde DW. Identification of CRKL as the constitutively phosphorylated 39-kD tyrosine phosphoprotein in chronic myelogenous leukemia cells. Blood1994 Nov 1;84(9):2912-8.
129. Sattler M, Salgia R, Okuda K, Uemura N, Durstin MA, Pisick E, et al. The proto-oncogene product p120CBL and the adaptor proteins CRKL and c-CRK link c-ABL, p190BCR/ABL and p210BCR/ABL to the phosphatidylinositol-3' kinase pathway. Oncogene1996 Feb 15;12(4):839-46.
130. Hamilton A, Elrick L, Myssina S, Copland M, Jorgensen H, Melo JV, et al. BCR-ABL activity and its response to drugs can be determined in CD34+ CML stem cells by CrkL phosphorylation status using flow cytometry. Leukemia2006 Jun;20(6):1035-9.
131. Copland M, Hamilton A, Elrick LJ, Baird JW, Allan EK, Jordanides N, et al. Dasatinib (BMS-354825) targets an earlier progenitor population than imatinib in primary CML but does not eliminate the quiescent fraction. Blood2006 Jun 1;107(11):4532-9.
132. Hochhaus A, Kreil S, Corbin AS, La Rosee P, Muller MC, Lahaye T, et al. Molecular and chromosomal mechanisms of resistance to imatinib (STI571) therapy. Leukemia2002 Nov;16(11):2190-6.
133. La Rosee P, Holm-Eriksen S, Konig H, Hartel N, Ernst T, Debatin J, et al. Phospho-CRKL monitoring for the assessment of BCR-ABL activity in imatinib-resistant chronic myeloid leukemia or Ph+ acute lymphoblastic leukemia patients treated with nilotinib. Haematologica2008 May;93(5):765-9.
134. Accili D, Arden KC. FoxOs at the crossroads of cellular metabolism, differentiation, and transformation. Cell2004 May 14;117(4):421-6.
135. Brunet A, Kanai F, Stehn J, Xu J, Sarbassova D, Frangioni JV, et al. 14-3-3 transits to the nucleus and participates in dynamic nucleocytoplasmic transport. J Cell Biol2002 Mar 4;156(5):817-28.
136. Obsilova V, Vecer J, Herman P, Pabianova A, Sulc M, Teisinger J, et al. 14-3-3 Protein interacts with nuclear localization sequence of forkhead transcription factor FoxO4. Biochemistry2005 Aug 30;44(34):11608-17.

137. Modur V, Nagarajan R, Evers BM, Milbrandt J. FOXO proteins regulate tumor necrosis factor-related apoptosis inducing ligand expression. Implications for PTEN mutation in prostate cancer. J Biol Chem2002 Dec 6;277(49):47928-37.
138. Stahl M, Dijkers PF, Kops GJ, Lens SM, Coffer PJ, Burgering BM, et al. The forkhead transcription factor FoxO regulates transcription of p27Kip1 and Bim in response to IL-2. J Immunol2002 May 15;168(10):5024-31.
139. Schmidt M, Fernandez de Mattos S, van der Horst A, Klompmaker R, Kops GJ, Lam EW, et al. Cell cycle inhibition by FoxO forkhead transcription factors involves downregulation of cyclin D. Mol Cell Biol2002 Nov;22(22):7842-52.
140. Ghaffari S, Jagani Z, Kitidis C, Lodish HF, Khosravi-Far R. Cytokines and BCR-ABL mediate suppression of TRAIL-induced apoptosis through inhibition of forkhead FOXO3a transcription factor. Proc Natl Acad Sci U S A2003 May 27;100(11):6523-8.
141. Essafi A, Fernandez de Mattos S, Hassen YA, Soeiro I, Mufti GJ, Thomas NS, et al. Direct transcriptional regulation of Bim by FoxO3a mediates STI571-induced apoptosis in Bcr-Abl-expressing cells. Oncogene2005 Mar 31;24(14):2317-29.
142. Fernandez de Mattos S, Essafi A, Soeiro I, Pietersen AM, Birkenkamp KU, Edwards CS, et al. FoxO3a and BCR-ABL regulate cyclin D2 transcription through a STAT5/BCL6-dependent mechanism. Mol Cell Biol2004 Nov;24(22):10058-71.
143. Reed JC. Bcl-2-family proteins and hematologic malignancies: history and future prospects. Blood2008 Apr 1;111(7):3322-30.
144. Zha J, Harada H, Yang E, Jockel J, Korsmeyer SJ. Serine phosphorylation of death agonist BAD in response to survival factor results in binding to 14-3-3 not BCL-X(L). Cell1996 Nov 15;87(4):619-28.
145. Neshat MS, Raitano AB, Wang HG, Reed JC, Sawyers CL. The survival function of the Bcr-Abl oncogene is mediated by Bad-dependent and -independent pathways: roles for phosphatidylinositol 3-kinase and Raf. Mol Cell Biol2000 Feb;20(4):1179-86.
146. Mayo LD, Donner DB. A phosphatidylinositol 3-kinase/Akt pathway promotes translocation of Mdm2 from the cytoplasm to the nucleus. Proc Natl Acad Sci U S A2001 Sep 25;98(20):11598-603.
147. Goetz AW, van der Kuip H, Maya R, Oren M, Aulitzky WE. Requirement for Mdm2 in the survival effects of Bcr-Abl and interleukin 3 in hematopoietic cells. Cancer Res2001 Oct 15;61(20):7635-41.
148. Pap M, Cooper GM. Role of glycogen synthase kinase-3 in the phosphatidylinositol 3-Kinase/Akt cell survival pathway. J Biol Chem1998 Aug 7;273(32):19929-32.
149. Diehl JA, Cheng M, Roussel MF, Sherr CJ. Glycogen synthase kinase-3beta regulates cyclin D1 proteolysis and subcellular localization. Genes Dev1998 Nov 15;12(22):3499-511.
150. Zhao C, Blum J, Chen A, Kwon HY, Jung SH, Cook JM, et al. Loss of beta-catenin impairs the renewal of normal and CML stem cells in vivo. Cancer Cell2007 Dec;12(6):528-41.
151. Richardson CJ, Schalm SS, Blenis J. PI3-kinase and TOR: PIKTORing cell growth. Semin Cell Dev Biol2004 Apr;15(2):147-59.
152. Bhaskar PT, Hay N. The two TORCs and Akt. Dev Cell2007 Apr;12(4):487-502.
153. Wullschleger S, Loewith R, Hall MN. TOR signaling in growth and metabolism. Cell2006 Feb 10;124(3):471-84.
154. Sarbassov DD, Guertin DA, Ali SM, Sabatini DM. Phosphorylation and regulation of Akt/PKB by the rictor-mTOR complex. Science2005 Feb 18;307(5712):1098-101.

155. Sawyers CL. Will mTOR inhibitors make it as cancer drugs? Cancer Cell2003 Nov;4(5):343-8.
156. Ly C, Arechiga AF, Melo JV, Walsh CM, Ong ST. Bcr-Abl kinase modulates the translation regulators ribosomal protein S6 and 4E-BP1 in chronic myelogenous leukemia cells via the mammalian target of rapamycin. Cancer Res2003 Sep 15;63(18):5716-22.
157. Mohi MG, Boulton C, Gu TL, Sternberg DW, Neuberg D, Griffin JD, et al. Combination of rapamycin and protein tyrosine kinase (PTK) inhibitors for the treatment of leukemias caused by oncogenic PTKs. Proc Natl Acad Sci U S A2004 Mar 2;101(9):3130-5.
158. Inoki K, Corradetti MN, Guan KL. Dysregulation of the TSC-mTOR pathway in human disease. Nat Genet2005 Jan;37(1):19-24.
159. Hay N, Sonenberg N. Upstream and downstream of mTOR. Genes Dev2004 Aug 15;18(16):1926-45.
160. Pende M, Um SH, Mieulet V, Sticker M, Goss VL, Mestan J, et al. S6K1(-/-)/S6K2(-/-) mice exhibit perinatal lethality and rapamycin-sensitive 5'-terminal oligopyrimidine mRNA translation and reveal a mitogen-activated protein kinase-dependent S6 kinase pathway. Mol Cell Biol2004 Apr;24(8):3112-24.
161. Levine B, Klionsky DJ. Development by self-digestion: molecular mechanisms and biological functions of autophagy. Dev Cell2004 Apr;6(4):463-77.
162. Kuma A, Hatano M, Matsui M, Yamamoto A, Nakaya H, Yoshimori T, et al. The role of autophagy during the early neonatal starvation period. Nature2004 Dec 23;432(7020):1032-6.
163. Rubinsztein DC, Gestwicki JE, Murphy LO, Klionsky DJ. Potential therapeutic applications of autophagy. Nat Rev Drug Discov2007 Apr;6(4):304-12.
164. Lum JJ, Bauer DE, Kong M, Harris MH, Li C, Lindsten T, et al. Growth factor regulation of autophagy and cell survival in the absence of apoptosis. Cell2005 Jan 28;120(2):237-48.
165. Xie Z, Klionsky DJ. Autophagosome formation: core machinery and adaptations. Nat Cell Biol2007 Oct;9(10):1102-9.
166. Kabeya Y, Mizushima N, Ueno T, Yamamoto A, Kirisako T, Noda T, et al. LC3, a mammalian homologue of yeast Apg8p, is localized in autophagosome membranes after processing. EMBO J2000 Nov 1;19(21):5720-8.
167. Cuervo AM. Autophagy: in sickness and in health. Trends Cell Biol2004 Feb;14(2):70-7.
168. Jin S. Autophagy, mitochondrial quality control, and oncogenesis. Autophagy2006 Apr-Jun;2(2):80-4.
169. Ertmer A, Huber V, Gilch S, Yoshimori T, Erfle V, Duyster J, et al. The anticancer drug imatinib induces cellular autophagy. Leukemia2007 May;21(5):936-42.
170. Kamitsuji Y, Kuroda J, Kimura S, Toyokuni S, Watanabe K, Ashihara E, et al. The Bcr-Abl kinase inhibitor INNO-406 induces autophagy and different modes of cell death execution in Bcr-Abl-positive leukemias. Cell Death Differ2008 Nov;15(11):1712-22.
171. Carew JS, Nawrocki ST, Kahue CN, Zhang H, Yang C, Chung L, et al. Targeting autophagy augments the anticancer activity of the histone deacetylase inhibitor SAHA to overcome Bcr-Abl-mediated drug resistance. Blood2007 Jul 1;110(1):313-22.
172. Bellodi C, Lidonnici MR, Hamilton A, Helgason GV, Soliera AR, Ronchetti M, et al. Targeting autophagy potentiates tyrosine kinase inhibitor-induced cell death in Philadelphia chromosome-positive cells, including primary CML stem cells. J Clin Invest2009 May;119(5):1109-23.

173. Aita VM, Liang XH, Murty VV, Pincus DL, Yu W, Cayanis E, et al. Cloning and genomic organization of beclin 1, a candidate tumor suppressor gene on chromosome 17q21. Genomics1999 Jul 1;59(1):59-65.
174. Liang XH, Jackson S, Seaman M, Brown K, Kempkes B, Hibshoosh H, et al. Induction of autophagy and inhibition of tumorigenesis by beclin 1. Nature1999 Dec 9;402(6762):672-6.
175. Qu X, Yu J, Bhagat G, Furuya N, Hibshoosh H, Troxel A, et al. Promotion of tumorigenesis by heterozygous disruption of the beclin 1 autophagy gene. J Clin Invest2003 Dec;112(12):1809-20.
176. Yue Z, Jin S, Yang C, Levine AJ, Heintz N. Beclin 1, an autophagy gene essential for early embryonic development, is a haploinsufficient tumor suppressor. Proc Natl Acad Sci U S A2003 Dec 9;100(25):15077-82.
177. Steelman LS, Pohnert SC, Shelton JG, Franklin RA, Bertrand FE, McCubrey JA. JAK/STAT, Raf/MEK/ERK, PI3K/Akt and BCR-ABL in cell cycle progression and leukemogenesis. Leukemia2004 Feb;18(2):189-218.
178. Burgess AW, Metcalf D. Characterization of a serum factor stimulating the differentiation of myelomonocytic leukemic cells. Int J Cancer1980 Nov 15;26(5):647-54.
179. Roberts AW. G-CSF: a key regulator of neutrophil production, but that's not all! Growth Factors2005 Mar;23(1):33-41.
180. Ozer H, Armitage JO, Bennett CL, Crawford J, Demetri GD, Pizzo PA, et al. 2000 update of recommendations for the use of hematopoietic colony-stimulating factors: evidence-based, clinical practice guidelines. American Society of Clinical Oncology Growth Factors Expert Panel. J Clin Oncol2000 Oct 15;18(20):3558-85.
181. Duhrsen U, Villeval JL, Boyd J, Kannourakis G, Morstyn G, Metcalf D. Effects of recombinant human granulocyte colony-stimulating factor on hematopoietic progenitor cells in cancer patients. Blood1988 Dec;72(6):2074-81.
182. Pan L, Delmonte J, Jr., Jalonen CK, Ferrara JL. Pretreatment of donor mice with granulocyte colony-stimulating factor polarizes donor T lymphocytes toward type-2 cytokine production and reduces severity of experimental graft-versus-host disease. Blood1995 Dec 15;86(12):4422-9.
183. Sattler M, Salgia R. Activation of hematopoietic growth factor signal transduction pathways by the human oncogene BCR/ABL. Cytokine Growth Factor Rev1997 Mar;8(1):63-79.
184. Chang JM, Metcalf D, Lang RA, Gonda TJ, Johnson GR. Nonneoplastic hematopoietic myeloproliferative syndrome induced by dysregulated multi-CSF (IL-3) expression. Blood1989 May 1;73(6):1487-97.
185. Wong PM, Chung SW, Dunbar CE, Bodine DM, Ruscetti S, Nienhuis AW. Retrovirus-mediated transfer and expression of the interleukin-3 gene in mouse hematopoietic cells result in a myeloproliferative disorder. Mol Cell Biol1989 Feb;9(2):798-808.
186. Just U, Katsuno M, Stocking C, Spooncer E, Dexter M. Targeted in vivo infection with a retroviral vector carrying the interleukin-3 (multi-CSF) gene leads to immortalization and leukemic transformation of primitive hematopoietic progenitor cells. Growth Factors1993;9(1):41-55.
187. Hariharan IK, Adams JM, Cory S. bcr-abl oncogene renders myeloid cell line factor independent: potential autocrine mechanism in chronic myeloid leukemia. Oncogene Res1988;3(4):387-99.
188. Sirard C, Laneuville P, Dick JE. Expression of bcr-abl abrogates factor-dependent growth of human hematopoietic M07E cells by an autocrine mechanism. Blood1994 Mar 15;83(6):1575-85.
189. Li S, Gillessen S, Tomasson MH, Dranoff G, Gilliland DG, Van Etten RA. Interleukin 3 and granulocyte-macrophage colony-stimulating factor are not

required for induction of chronic myeloid leukemia-like myeloproliferative disease in mice by BCR/ABL. Blood2001 Mar 1;97(5):1442-50.
190. Jiang X, Lopez A, Holyoake T, Eaves A, Eaves C. Autocrine production and action of IL-3 and granulocyte colony-stimulating factor in chronic myeloid leukemia. Proc Natl Acad Sci U S A1999 Oct 26;96(22):12804-9.
191. Strife A, Lambek C, Wisniewski D, Wachter M, Gulati SC, Clarkson BD. Discordant maturation as the primary biological defect in chronic myelogenous leukemia. Cancer Res1988 Feb 15;48(4):1035-41.
192. Geary CG. The story of chronic myeloid leukaemia. Br J Haematol2000 Jul;110(1):2-11.
193. Galton DA. Myleran in chronic myeloid leukaemia; results of treatment. Lancet1953 Jan 31;264(6753):208-13.
194. Kantarjian HM, Deisseroth A, Kurzrock R, Estrov Z, Talpaz M. Chronic myelogenous leukemia: a concise update. Blood1993 Aug 1;82(3):691-703.
195. Goldman JM, Apperley JF, Jones L, Marcus R, Goolden AW, Batchelor R, et al. Bone marrow transplantation for patients with chronic myeloid leukemia. N Engl J Med1986 Jan 23;314(4):202-7.
196. Silver RT, Woolf SH, Hehlmann R, Appelbaum FR, Anderson J, Bennett C, et al. An evidence-based analysis of the effect of busulfan, hydroxyurea, interferon, and allogeneic bone marrow transplantation in treating the chronic phase of chronic myeloid leukemia: developed for the American Society of Hematology. Blood1999 Sep 1;94(5):1517-36.
197. Gratwohl A, Hermans J, Goldman JM, Arcese W, Carreras E, Devergie A, et al. Risk assessment for patients with chronic myeloid leukaemia before allogeneic blood or marrow transplantation. Chronic Leukemia Working Party of the European Group for Blood and Marrow Transplantation. Lancet1998 Oct 3;352(9134):1087-92.
198. Interferon alfa versus chemotherapy for chronic myeloid leukemia: a meta-analysis of seven randomized trials: Chronic Myeloid Leukemia Trialists' Collaborative Group. J Natl Cancer Inst1997 Nov 5;89(21):1616-20.
199. Talpaz M, Kantarjian HM, McCredie K, Trujillo JM, Keating MJ, Gutterman JU. Hematologic remission and cytogenetic improvement induced by recombinant human interferon alpha A in chronic myelogenous leukemia. N Engl J Med1986 Apr 24;314(17):1065-9.
200. Guilhot F, Chastang C, Michallet M, Guerci A, Harousseau JL, Maloisel F, et al. Interferon alfa-2b combined with cytarabine versus interferon alone in chronic myelogenous leukemia. French Chronic Myeloid Leukemia Study Group. N Engl J Med1997 Jul 24;337(4):223-9.
201. Anafi M, Gazit A, Zehavi A, Ben-Neriah Y, Levitzki A. Tyrphostin-induced inhibition of p210bcr-abl tyrosine kinase activity induces K562 to differentiate. Blood1993 Dec 15;82(12):3524-9.
202. Okabe M, Uehara Y, Miyagishima T, Itaya T, Tanaka M, Kuni-Eda Y, et al. Effect of herbimycin A, an antagonist of tyrosine kinase, on bcr/abl oncoprotein-associated cell proliferations: abrogative effect on the transformation of murine hematopoietic cells by transfection of a retroviral vector expressing oncoprotein P210bcr/abl and preferential inhibition on Ph1-positive leukemia cell growth. Blood1992 Sep 1;80(5):1330-8.
203. Honma Y, Matsuo Y, Hayashi Y, Omura S. Treatment of Philadelphia-chromosome-positive human leukemia in SCID mouse model with herbimycin A, bcr-abl tyrosine kinase activity inhibitor. Int J Cancer1995 Mar 3;60(5):685-8.
204. Shiotsu Y, Neckers LM, Wortman I, An WG, Schulte TW, Soga S, et al. Novel oxime derivatives of radicicol induce erythroid differentiation associated with preferential G(1) phase accumulation against chronic myelogenous leukemia cells

through destabilization of Bcr-Abl with Hsp90 complex. Blood2000 Sep 15;96(6):2284-91.
205. Druker BJ, Tamura S, Buchdunger E, Ohno S, Segal GM, Fanning S, et al. Effects of a selective inhibitor of the Abl tyrosine kinase on the growth of Bcr-Abl positive cells. Nat Med1996 May;2(5):561-6.
206. Schindler T, Bornmann W, Pellicena P, Miller WT, Clarkson B, Kuriyan J. Structural mechanism for STI-571 inhibition of abelson tyrosine kinase. Science2000 Sep 15;289(5486):1938-42.
207. Buchdunger E, Zimmermann J, Mett H, Meyer T, Muller M, Druker BJ, et al. Inhibition of the Abl protein-tyrosine kinase in vitro and in vivo by a 2-phenylaminopyrimidine derivative. Cancer Res1996 Jan 1;56(1):100-4.
208. Carroll M, Ohno-Jones S, Tamura S, Buchdunger E, Zimmermann J, Lydon NB, et al. CGP 57148, a tyrosine kinase inhibitor, inhibits the growth of cells expressing BCR-ABL, TEL-ABL, and TEL-PDGFR fusion proteins. Blood1997 Dec 15;90(12):4947-52.
209. Beran M, Cao X, Estrov Z, Jeha S, Jin G, O'Brien S, et al. Selective inhibition of cell proliferation and BCR-ABL phosphorylation in acute lymphoblastic leukemia cells expressing Mr 190,000 BCR-ABL protein by a tyrosine kinase inhibitor (CGP-57148). Clin Cancer Res1998 Jul;4(7):1661-72.
210. Buchdunger E, Matter A, Druker BJ. Bcr-Abl inhibition as a modality of CML therapeutics. Biochim Biophys Acta2001 Aug 31;1551(1):M11-8.
211. Deininger MW, Goldman JM, Lydon N, Melo JV. The tyrosine kinase inhibitor CGP57148B selectively inhibits the growth of BCR-ABL-positive cells. Blood1997 Nov 1;90(9):3691-8.
212. Gambacorti-Passerini C, le Coutre P, Mologni L, Fanelli M, Bertazzoli C, Marchesi E, et al. Inhibition of the ABL kinase activity blocks the proliferation of BCR/ABL+ leukemic cells and induces apoptosis. Blood Cells Mol Dis1997 Dec;23(3):380-94.
213. Kasper B, Fruehauf S, Schiedlmeier B, Buchdunger E, Ho AD, Zeller WJ. Favorable therapeutic index of a p210(BCR-ABL)-specific tyrosine kinase inhibitor; activity on lineage-committed and primitive chronic myelogenous leukemia progenitors. Cancer Chemother Pharmacol1999;44(5):433-8.
214. Marley SB, Deininger MW, Davidson RJ, Goldman JM, Gordon MY. The tyrosine kinase inhibitor STI571, like interferon-alpha, preferentially reduces the capacity for amplification of granulocyte-macrophage progenitors from patients with chronic myeloid leukemia. Exp Hematol2000 May;28(5):551-7.
215. le Coutre P, Mologni L, Cleris L, Marchesi E, Buchdunger E, Giardini R, et al. In vivo eradication of human BCR/ABL-positive leukemia cells with an ABL kinase inhibitor. J Natl Cancer Inst1999 Jan 20;91(2):163-8.
216. Druker BJ, Talpaz M, Resta DJ, Peng B, Buchdunger E, Ford JM, et al. Efficacy and safety of a specific inhibitor of the BCR-ABL tyrosine kinase in chronic myeloid leukemia. N Engl J Med2001 Apr 5;344(14):1031-7.
217. Druker BJ, Sawyers CL, Kantarjian H, Resta DJ, Reese SF, Ford JM, et al. Activity of a specific inhibitor of the BCR-ABL tyrosine kinase in the blast crisis of chronic myeloid leukemia and acute lymphoblastic leukemia with the Philadelphia chromosome. N Engl J Med2001 Apr 5;344(14):1038-42.
218. Kantarjian H, Sawyers C, Hochhaus A, Guilhot F, Schiffer C, Gambacorti-Passerini C, et al. Hematologic and cytogenetic responses to imatinib mesylate in chronic myelogenous leukemia. N Engl J Med2002 Feb 28;346(9):645-52.
219. Sawyers CL, Hochhaus A, Feldman E, Goldman JM, Miller CB, Ottmann OG, et al. Imatinib induces hematologic and cytogenetic responses in patients with chronic myelogenous leukemia in myeloid blast crisis: results of a phase II study. Blood2002 May 15;99(10):3530-9.

220. Talpaz M, Silver RT, Druker BJ, Goldman JM, Gambacorti-Passerini C, Guilhot F, et al. Imatinib induces durable hematologic and cytogenetic responses in patients with accelerated phase chronic myeloid leukemia: results of a phase 2 study. Blood2002 Mar 15;99(6):1928-37.
221. O'Brien SG, Guilhot F, Larson RA, Gathmann I, Baccarani M, Cervantes F, et al. Imatinib compared with interferon and low-dose cytarabine for newly diagnosed chronic-phase chronic myeloid leukemia. N Engl J Med2003 Mar 13;348(11):994-1004.
222. Druker BJ, Guilhot F, O'Brien SG, Gathmann I, Kantarjian H, Gattermann N, et al. Five-year follow-up of patients receiving imatinib for chronic myeloid leukemia. N Engl J Med2006 Dec 7;355(23):2408-17.
223. Hughes TP, Kaeda J, Branford S, Rudzki Z, Hochhaus A, Hensley ML, et al. Frequency of major molecular responses to imatinib or interferon alfa plus cytarabine in newly diagnosed chronic myeloid leukemia. N Engl J Med2003 Oct 9;349(15):1423-32.
224. Holyoake T, Jiang X, Eaves C, Eaves A. Isolation of a highly quiescent subpopulation of primitive leukemic cells in chronic myeloid leukemia. Blood1999 Sep 15;94(6):2056-64.
225. Holyoake TL, Jiang X, Jorgensen HG, Graham S, Alcorn MJ, Laird C, et al. Primitive quiescent leukemic cells from patients with chronic myeloid leukemia spontaneously initiate factor-independent growth in vitro in association with up-regulation of expression of interleukin-3. Blood2001 Feb 1;97(3):720-8.
226. Graham SM, Jorgensen HG, Allan E, Pearson C, Alcorn MJ, Richmond L, et al. Primitive, quiescent, Philadelphia-positive stem cells from patients with chronic myeloid leukemia are insensitive to STI571 in vitro. Blood2002 Jan 1;99(1):319-25.
227. Holtz MS, Slovak ML, Zhang F, Sawyers CL, Forman SJ, Bhatia R. Imatinib mesylate (STI571) inhibits growth of primitive malignant progenitors in chronic myelogenous leukemia through reversal of abnormally increased proliferation. Blood2002 May 15;99(10):3792-800.
228. Bhatia R, Holtz M, Niu N, Gray R, Snyder DS, Sawyers CL, et al. Persistence of malignant hematopoietic progenitors in chronic myelogenous leukemia patients in complete cytogenetic remission following imatinib mesylate treatment. Blood2003 Jun 15;101(12):4701-7.
229. Jorgensen HG, Allan EK, Mountford JC, Richmond L, Harrison S, Elliott MA, et al. Enhanced CML stem cell elimination in vitro by bryostatin priming with imatinib mesylate. Exp Hematol2005 Oct;33(10):1140-6.
230. Michor F, Hughes TP, Iwasa Y, Branford S, Shah NP, Sawyers CL, et al. Dynamics of chronic myeloid leukaemia. Nature2005 Jun 30;435(7046):1267-70.
231. Baccarani M, Saglio G, Goldman J, Hochhaus A, Simonsson B, Appelbaum F, et al. Evolving concepts in the management of chronic myeloid leukemia: recommendations from an expert panel on behalf of the European LeukemiaNet. Blood2006 Sep 15;108(6):1809-20.
232. Donato NJ, Wu JY, Stapley J, Lin H, Arlinghaus R, Aggarwal BB, et al. Imatinib mesylate resistance through BCR-ABL independence in chronic myelogenous leukemia. Cancer Res2004 Jan 15;64(2):672-7.
233. Donato NJ, Wu JY, Stapley J, Gallick G, Lin H, Arlinghaus R, et al. BCR-ABL independence and LYN kinase overexpression in chronic myelogenous leukemia cells selected for resistance to STI571. Blood2003 Jan 15;101(2):690-8.
234. Wu J, Meng F, Lu H, Kong L, Bornmann W, Peng Z, et al. Lyn regulates BCR-ABL and Gab2 tyrosine phosphorylation and c-Cbl protein stability in imatinib-resistant chronic myelogenous leukemia cells. Blood2008 Apr 1;111(7):3821-9.

235. Wang Y, Cai D, Brendel C, Barett C, Erben P, Manley PW, et al. Adaptive secretion of granulocyte-macrophage colony-stimulating factor (GM-CSF) mediates imatinib and nilotinib resistance in BCR/ABL+ progenitors via JAK-2/STAT-5 pathway activation. Blood2007 Mar 1;109(5):2147-55.
236. le Coutre P, Tassi E, Varella-Garcia M, Barni R, Mologni L, Cabrita G, et al. Induction of resistance to the Abelson inhibitor STI571 in human leukemic cells through gene amplification. Blood2000 Mar 1;95(5):1758-66.
237. Mahon FX, Deininger MW, Schultheis B, Chabrol J, Reiffers J, Goldman JM, et al. Selection and characterization of BCR-ABL positive cell lines with differential sensitivity to the tyrosine kinase inhibitor STI571: diverse mechanisms of resistance. Blood2000 Aug 1;96(3):1070-9.
238. Gorre ME, Mohammed M, Ellwood K, Hsu N, Paquette R, Rao PN, et al. Clinical resistance to STI-571 cancer therapy caused by BCR-ABL gene mutation or amplification. Science2001 Aug 3;293(5531):876-80.
239. Branford S, Rudzki Z, Walsh S, Grigg A, Arthur C, Taylor K, et al. High frequency of point mutations clustered within the adenosine triphosphate-binding region of BCR/ABL in patients with chronic myeloid leukemia or Ph-positive acute lymphoblastic leukemia who develop imatinib (STI571) resistance. Blood2002 May 1;99(9):3472-5.
240. Shah NP, Nicoll JM, Nagar B, Gorre ME, Paquette RL, Kuriyan J, et al. Multiple BCR-ABL kinase domain mutations confer polyclonal resistance to the tyrosine kinase inhibitor imatinib (STI571) in chronic phase and blast crisis chronic myeloid leukemia. Cancer Cell2002 Aug;2(2):117-25.
241. Nagar B, Bornmann WG, Pellicena P, Schindler T, Veach DR, Miller WT, et al. Crystal structures of the kinase domain of c-Abl in complex with the small molecule inhibitors PD173955 and imatinib (STI-571). Cancer Res2002 Aug 1;62(15):4236-43.
242. O'Hare T, Eide CA, Deininger MW. Bcr-Abl kinase domain mutations, drug resistance, and the road to a cure for chronic myeloid leukemia. Blood2007 Oct 1;110(7):2242-9.
243. Azam M, Latek RR, Daley GQ. Mechanisms of autoinhibition and STI-571/imatinib resistance revealed by mutagenesis of BCR-ABL. Cell2003 Mar 21;112(6):831-43.
244. Hughes T, Deininger M, Hochhaus A, Branford S, Radich J, Kaeda J, et al. Monitoring CML patients responding to treatment with tyrosine kinase inhibitors: review and recommendations for harmonizing current methodology for detecting BCR-ABL transcripts and kinase domain mutations and for expressing results. Blood2006 Jul 1;108(1):28-37.
245. Khorashad JS, Anand M, Marin D, Saunders S, Al-Jabary T, Iqbal A, et al. The presence of a BCR-ABL mutant allele in CML does not always explain clinical resistance to imatinib. Leukemia2006 Apr;20(4):658-63.
246. Dai H, Marbach P, Lemaire M, Hayes M, Elmquist WF. Distribution of STI-571 to the brain is limited by P-glycoprotein-mediated efflux. J Pharmacol Exp Ther2003 Mar;304(3):1085-92.
247. Mahon FX, Belloc F, Lagarde V, Chollet C, Moreau-Gaudry F, Reiffers J, et al. MDR1 gene overexpression confers resistance to imatinib mesylate in leukemia cell line models. Blood2003 Mar 15;101(6):2368-73.
248. Ferrao PT, Frost MJ, Siah SP, Ashman LK. Overexpression of P-glycoprotein in K562 cells does not confer resistance to the growth inhibitory effects of imatinib (STI571) in vitro. Blood2003 Dec 15;102(13):4499-503.
249. Hatziieremia S, Jordanides NE, Holyoake TL, Mountford JC, Jorgensen HG. Inhibition of MDR1 does not sensitize primitive chronic myeloid leukemia CD34+ cells to imatinib. Exp Hematol2009 Jun;37(6):692-700.

250. Jordanides NE, Jorgensen HG, Holyoake TL, Mountford JC. Functional ABCG2 is overexpressed on primary CML CD34+ cells and is inhibited by imatinib mesylate. Blood2006 Aug 15;108(4):1370-3.
251. Weisberg E, Manley PW, Breitenstein W, Bruggen J, Cowan-Jacob SW, Ray A, et al. Characterization of AMN107, a selective inhibitor of native and mutant Bcr-Abl. Cancer Cell2005 Feb;7(2):129-41.
252. O'Hare T, Walters DK, Stoffregen EP, Jia T, Manley PW, Mestan J, et al. In vitro activity of Bcr-Abl inhibitors AMN107 and BMS-354825 against clinically relevant imatinib-resistant Abl kinase domain mutants. Cancer Res2005 Jun 1;65(11):4500-5.
253. Golemovic M, Verstovsek S, Giles F, Cortes J, Manshouri T, Manley PW, et al. AMN107, a novel aminopyrimidine inhibitor of Bcr-Abl, has in vitro activity against imatinib-resistant chronic myeloid leukemia. Clin Cancer Res2005 Jul 1;11(13):4941-7.
254. Kantarjian H, Giles F, Wunderle L, Bhalla K, O'Brien S, Wassmann B, et al. Nilotinib in imatinib-resistant CML and Philadelphia chromosome-positive ALL. N Engl J Med2006 Jun 15;354(24):2542-51.
255. Kantarjian HM, Giles F, Gattermann N, Bhalla K, Alimena G, Palandri F, et al. Nilotinib (formerly AMN107), a highly selective BCR-ABL tyrosine kinase inhibitor, is effective in patients with Philadelphia chromosome-positive chronic myelogenous leukemia in chronic phase following imatinib resistance and intolerance. Blood2007 Nov 15;110(10):3540-6.
256. Jorgensen HG, Allan EK, Jordanides NE, Mountford JC, Holyoake TL. Nilotinib exerts equipotent antiproliferative effects to imatinib and does not induce apoptosis in CD34+ CML cells. Blood2007 May 1;109(9):4016-9.
257. Abram CL, Courtneidge SA. Src family tyrosine kinases and growth factor signaling. Exp Cell Res2000 Jan 10;254(1):1-13.
258. Stanglmaier M, Warmuth M, Kleinlein I, Reis S, Hallek M. The interaction of the Bcr-Abl tyrosine kinase with the Src kinase Hck is mediated by multiple binding domains. Leukemia2003 Feb;17(2):283-9.
259. Danhauser-Riedl S, Warmuth M, Druker BJ, Emmerich B, Hallek M. Activation of Src kinases p53/56lyn and p59hck by p210bcr/abl in myeloid cells. Cancer Res1996 Aug 1;56(15):3589-96.
260. Golas JM, Arndt K, Etienne C, Lucas J, Nardin D, Gibbons J, et al. SKI-606, a 4-anilino-3-quinolinecarbonitrile dual inhibitor of Src and Abl kinases, is a potent antiproliferative agent against chronic myelogenous leukemia cells in culture and causes regression of K562 xenografts in nude mice. Cancer Res2003 Jan 15;63(2):375-81.
261. Cortes J, Kantarjian HM, Baccarani M, Brummendorf TH, Liu D, Ossenkoppele G, et al. A Phase 1/2 Study of SKI-606, a Dual Inhibitor of Src and Abl Kinases, in Adult Patients with Philadelphia Chromosome Positive (Ph+) Chronic Myelogenous Leukemia (CML) or Acute Lymphocytic Leukemia (ALL) Relapsed, Refractory or Intolerant of Imatinib. Blood (ASH Annual Meeting Abstracts)2006;108: Abstract 168.
262. Konig H, Holyoake TL, Bhatia R. Effective and selective inhibition of chronic myeloid leukemia primitive hematopoietic progenitors by the dual Src/Abl kinase inhibitor SKI-606. Blood2008 Feb 15;111(4):2329-38.
263. Talpaz M, Shah NP, Kantarjian H, Donato N, Nicoll J, Paquette R, et al. Dasatinib in imatinib-resistant Philadelphia chromosome-positive leukemias. N Engl J Med2006 Jun 15;354(24):2531-41.
264. Lombardo LJ, Lee FY, Chen P, Norris D, Barrish JC, Behnia K, et al. Discovery of N-(2-chloro-6-methyl- phenyl)-2-(6-(4-(2-hydroxyethyl)- piperazin-1-yl)-2-methylpyrimidin-4- ylamino)thiazole-5-carboxamide (BMS-354825), a dual

Src/Abl kinase inhibitor with potent antitumor activity in preclinical assays. J Med Chem2004 Dec 30;47(27):6658-61.
265. Tokarski JS, Newitt JA, Chang CY, Cheng JD, Wittekind M, Kiefer SE, et al. The structure of Dasatinib (BMS-354825) bound to activated ABL kinase domain elucidates its inhibitory activity against imatinib-resistant ABL mutants. Cancer Res2006 Jun 1;66(11):5790-7.
266. Hochhaus A, Baccarani M, Deininger M, Apperley JF, Lipton JH, Goldberg SL, et al. Dasatinib induces durable cytogenetic responses in patients with chronic myelogenous leukemia in chronic phase with resistance or intolerance to imatinib. Leukemia2008 Jun;22(6):1200-6.
267. Guilhot F, Apperley J, Kim DW, Bullorsky EO, Baccarani M, Roboz GJ, et al. Dasatinib induces significant hematologic and cytogenetic responses in patients with imatinib-resistant or -intolerant chronic myeloid leukemia in accelerated phase. Blood2007 May 15;109(10):4143-50.
268. Cortes J, Rousselot P, Kim DW, Ritchie E, Hamerschlak N, Coutre S, et al. Dasatinib induces complete hematologic and cytogenetic responses in patients with imatinib-resistant or -intolerant chronic myeloid leukemia in blast crisis. Blood2007 Apr 15;109(8):3207-13.
269. Weinstein IB, Begemann M, Zhou P, Han EK, Sgambato A, Doki Y, et al. Disorders in cell circuitry associated with multistage carcinogenesis: exploitable targets for cancer prevention and therapy. Clin Cancer Res1997 Dec;3(12 Pt 2):2696-702.
270. Weinstein IB. Disorders in cell circuitry during multistage carcinogenesis: the role of homeostasis. Carcinogenesis2000 May;21(5):857-64.
271. Weinstein IB. Cancer. Addiction to oncogenes--the Achilles heal of cancer. Science2002 Jul 5;297(5578):63-4.
272. Jackson EL, Willis N, Mercer K, Bronson RT, Crowley D, Montoya R, et al. Analysis of lung tumor initiation and progression using conditional expression of oncogenic K-ras. Genes Dev2001 Dec 15;15(24):3243-8.
273. Chin L, Tam A, Pomerantz J, Wong M, Holash J, Bardeesy N, et al. Essential role for oncogenic Ras in tumour maintenance. Nature1999 Jul 29;400(6743):468-72.
274. Felsher DW, Bishop JM. Reversible tumorigenesis by MYC in hematopoietic lineages. Mol Cell1999 Aug;4(2):199-207.
275. Huettner CS, Zhang P, Van Etten RA, Tenen DG. Reversibility of acute B-cell leukaemia induced by BCR-ABL1. Nat Genet2000 Jan;24(1):57-60.
276. Colomer R, Lupu R, Bacus SS, Gelmann EP. erbB-2 antisense oligonucleotides inhibit the proliferation of breast carcinoma cells with erbB-2 oncogene amplification. Br J Cancer1994 Nov;70(5):819-25.
277. Zhou P, Jiang W, Zhang YJ, Kahn SM, Schieren I, Santella RM, et al. Antisense to cyclin D1 inhibits growth and reverses the transformed phenotype of human esophageal cancer cells. Oncogene1995 Aug 3;11(3):571-80.
278. Aoki K, Yoshida T, Matsumoto N, Ide H, Sugimura T, Terada M. Suppression of Ki-ras p21 levels leading to growth inhibition of pancreatic cancer cell lines with Ki-ras mutation but not those without Ki-ras mutation. Mol Carcinog1997 Oct;20(2):251-8.
279. Verma UN, Surabhi RM, Schmaltieg A, Becerra C, Gaynor RB. Small interfering RNAs directed against beta-catenin inhibit the in vitro and in vivo growth of colon cancer cells. Clin Cancer Res2003 Apr;9(4):1291-300.
280. Lyons AB, Parish CR. Determination of lymphocyte division by flow cytometry. J Immunol Methods1994 May 2;171(1):131-7.

281. Li X, Dancausse H, Grijalva I, Oliveira M, Levi AD. Labeling Schwann cells with CFSE-an in vitro and in vivo study. J Neurosci Methods2003 May 30;125(1-2):83-91.
282. Coulombel L, Eaves AC, Eaves CJ. Enzymatic treatment of long-term human marrow cultures reveals the preferential location of primitive hemopoietic progenitors in the adherent layer. Blood1983 Aug;62(2):291-7.
283. Sutherland HJ, Eaves CJ, Lansdorp PM, Thacker JD, Hogge DE. Differential regulation of primitive human hematopoietic cells in long-term cultures maintained on genetically engineered murine stromal cells. Blood1991 Aug 1;78(3):666-72.
284. Hogge DE, Lansdorp PM, Reid D, Gerhard B, Eaves CJ. Enhanced detection, maintenance, and differentiation of primitive human hematopoietic cells in cultures containing murine fibroblasts engineered to produce human steel factor, interleukin-3, and granulocyte colony-stimulating factor. Blood1996 Nov 15;88(10):3765-73.
285. Gerdes J, Lemke H, Baisch H, Wacker HH, Schwab U, Stein H. Cell cycle analysis of a cell proliferation-associated human nuclear antigen defined by the monoclonal antibody Ki-67. J Immunol1984 Oct;133(4):1710-5.
286. Jordan CT, Yamasaki G, Minamoto D. High-resolution cell cycle analysis of defined phenotypic subsets within primitive human hematopoietic cell populations. Exp Hematol1996 Sep;24(11):1347-55.
287. Smith PK, Krohn RI, Hermanson GT, Mallia AK, Gartner FH, Provenzano MD, et al. Measurement of protein using bicinchoninic acid. Anal Biochem1985 Oct;150(1):76-85.
288. Gabert J, Beillard E, van der Velden VH, Bi W, Grimwade D, Pallisgaard N, et al. Standardization and quality control studies of 'real-time' quantitative reverse transcriptase polymerase chain reaction of fusion gene transcripts for residual disease detection in leukemia - a Europe Against Cancer program. Leukemia2003 Dec;17(12):2318-57.
289. Hayette S, Michallet M, Baille ML, Magaud JP, Nicolini FE. Assessment and follow-up of the proportion of T315I mutant BCR-ABL transcripts can guide appropriate therapeutic decision making in CML patients. Leuk Res2005 Sep;29(9):1073-7.
290. White D, Saunders V, Lyons AB, Branford S, Grigg A, To LB, et al. In vitro sensitivity to imatinib-induced inhibition of ABL kinase activity is predictive of molecular response in patients with de novo CML. Blood2005 Oct 1;106(7):2520-6.
291. Schultheis B, Szydlo R, Mahon FX, Apperley JF, Melo JV. Analysis of total phosphotyrosine levels in CD34+ cells from CML patients to predict the response to imatinib mesylate treatment. Blood2005 Jun 15;105(12):4893-4.
292. Shah NP, Tran C, Lee FY, Chen P, Norris D, Sawyers CL. Overriding imatinib resistance with a novel ABL kinase inhibitor. Science2004 Jul 16;305(5682):399-401.
293. Corbin AS, La Rosee P, Stoffregen EP, Druker BJ, Deininger MW. Several Bcr-Abl kinase domain mutants associated with imatinib mesylate resistance remain sensitive to imatinib. Blood2003 Jun 1;101(11):4611-4.
294. Singer CF, Hudelist G, Lamm W, Mueller R, Handl C, Kubista E, et al. Active (p)CrkL is overexpressed in human malignancies: potential role as a surrogate parameter for therapeutic tyrosine kinase inhibition. Oncol Rep2006 Feb;15(2):353-9.
295. Patel H, Marley SB, Gordon MY. Conventional Western blotting techniques will not reliably quantify p210BCR-ABL1 levels in CML mononuclear cells. Blood2007 Feb 1;109(3):1335; author reply 6.

296. Patel H, Marley SB, Gordon MY. Detection in primary chronic myeloid leukaemia cells of p210BCR-ABL1 in complexes with adaptor proteins CBL, CRKL, and GRB2. Genes Chromosomes Cancer2006 Dec;45(12):1121-9.
297. Maxwell SA, Kurzrock R, Parsons SJ, Talpaz M, Gallick GE, Kloetzer WS, et al. Analysis of P210bcr-abl tyrosine protein kinase activity in various subtypes of Philadelphia chromosome-positive cells from chronic myelogenous leukemia patients. Cancer Res1987 Mar 15;47(6):1731-9.
298. Jiang X, Zhao Y, Smith C, Gasparetto M, Turhan A, Eaves A, et al. Chronic myeloid leukemia stem cells possess multiple unique features of resistance to BCR-ABL targeted therapies. Leukemia2007 May;21(5):926-35.
299. Roumiantsev S, Shah NP, Gorre ME, Nicoll J, Brasher BB, Sawyers CL, et al. Clinical resistance to the kinase inhibitor STI-571 in chronic myeloid leukemia by mutation of Tyr-253 in the Abl kinase domain P-loop. Proc Natl Acad Sci U S A2002 Aug 6;99(16):10700-5.
300. Jamieson CH, Ailles LE, Dylla SJ, Muijtjens M, Jones C, Zehnder JL, et al. Granulocyte-macrophage progenitors as candidate leukemic stem cells in blast-crisis CML. N Engl J Med2004 Aug 12;351(7):657-67.
301. Wu J, Meng F, Kong LY, Peng Z, Ying Y, Bornmann WG, et al. Association between imatinib-resistant BCR-ABL mutation-negative leukemia and persistent activation of LYN kinase. J Natl Cancer Inst2008 Jul 2;100(13):926-39.
302. O'Hare T, Eide CA, Deininger MW. Persistent LYN signaling in imatinib-resistant, BCR-ABL-independent chronic myelogenous leukemia. J Natl Cancer Inst2008 Jul 2;100(13):908-9.
303. Dorsey JF, Cunnick JM, Lanehart R, Huang M, Kraker AJ, Bhalla KN, et al. Interleukin-3 protects Bcr-Abl-transformed hematopoietic progenitor cells from apoptosis induced by Bcr-Abl tyrosine kinase inhibitors. Leukemia2002 Sep;16(9):1589-95.
304. Barber DL, Mason JM, Fukazawa T, Reedquist KA, Druker BJ, Band H, et al. Erythropoietin and interleukin-3 activate tyrosine phosphorylation of CBL and association with CRK adaptor proteins. Blood1997 May 1;89(9):3166-74.
305. Oda A, Miyakawa Y, Druker BJ, Ishida A, Ozaki K, Ohashi H, et al. Crkl is constitutively tyrosine phosphorylated in platelets from chronic myelogenous leukemia patients and inducibly phosphorylated in normal platelets stimulated by thrombopoietin. Blood1996 Dec 1;88(11):4304-13.
306. Reedquist KA, Fukazawa T, Panchamoorthy G, Langdon WY, Shoelson SE, Druker BJ, et al. Stimulation through the T cell receptor induces Cbl association with Crk proteins and the guanine nucleotide exchange protein C3G. J Biol Chem1996 Apr 5;271(14):8435-42.
307. Sattler M, Salgia R, Shrikhande G, Verma S, Pisick E, Prasad KV, et al. Steel factor induces tyrosine phosphorylation of CRKL and binding of CRKL to a complex containing c-kit, phosphatidylinositol 3-kinase, and p120(CBL). J Biol Chem1997 Apr 11;272(15):10248-53.
308. Sattler M, Salgia R, Shrikhande G, Verma S, Uemura N, Law SF, et al. Differential signaling after beta1 integrin ligation is mediated through binding of CRKL to p120(CBL) and p110(HEF1). J Biol Chem1997 May 30;272(22):14320-6.
309. Smit L, van der Horst G, Borst J. Sos, Vav, and C3G participate in B cell receptor-induced signaling pathways and differentially associate with Shc-Grb2, Crk, and Crk-L adaptors. J Biol Chem1996 Apr 12;271(15):8564-9.
310. Shah NP, Kasap C, Weier C, Balbas M, Nicoll JM, Bleickardt E, et al. Transient potent BCR-ABL inhibition is sufficient to commit chronic myeloid leukemia cells irreversibly to apoptosis. Cancer Cell2008 Dec 9;14(6):485-93.
311. Burgering BM. A brief introduction to FOXOlogy. Oncogene2008 Apr 7;27(16):2258-62.

312. Brunet A, Bonni A, Zigmond MJ, Lin MZ, Juo P, Hu LS, et al. Akt promotes cell survival by phosphorylating and inhibiting a Forkhead transcription factor. Cell1999 Mar 19;96(6):857-68.
313. Komatsu N, Watanabe T, Uchida M, Mori M, Kirito K, Kikuchi S, et al. A member of Forkhead transcription factor FKHRL1 is a downstream effector of STI571-induced cell cycle arrest in BCR-ABL-expressing cells. J Biol Chem2003 Feb 21;278(8):6411-9.
314. Pellicano F, Cilloni D, Helgason GV, Messa F, Panuzzo C, Arruga F, et al. FOXO transcription factor activity is partially retained in quiescent CML stem cells and induced by tyrosine kinase inhibitors in CML progenitor cells. Blood2009 Dec 1.
315. Rangatia J, Bonnet D. Transient or long-term silencing of BCR-ABL alone induces cell cycle and proliferation arrest, apoptosis and differentiation. Leukemia2006 Jan;20(1):68-76.
316. Snead JL, O'Hare T, Adrian LT, Eide CA, Lange T, Druker BJ, et al. Acute dasatinib exposure commits Bcr-Abl-dependent cells to apoptosis. Blood2009 Oct 15;114(16):3459-63.
317. Naka K, Hoshii T, Muraguchi T, Tadokoro Y, Ooshio T, Kondo Y, et al. TGF-beta-FOXO signalling maintains leukaemia-initiating cells in chronic myeloid leukaemia. Nature2010 Feb 4;463(7281):676-80.
318. Lum JJ, DeBerardinis RJ, Thompson CB. Autophagy in metazoans: cell survival in the land of plenty. Nat Rev Mol Cell Biol2005 Jun;6(6):439-48.
319. Eskelinen EL. To be or not to be? Examples of incorrect identification of autophagic compartments in conventional transmission electron microscopy of mammalian cells. Autophagy2008 Feb 16;4(2):257-60.
320. He H, Dang Y, Dai F, Guo Z, Wu J, She X, et al. Post-translational modifications of three members of the human MAP1LC3 family and detection of a novel type of modification for MAP1LC3B. J Biol Chem2003 Aug 1;278(31):29278-87.
321. Tanida I, Ueno T, Kominami E. Human light chain 3/MAP1LC3B is cleaved at its carboxyl-terminal Met121 to expose Gly120 for lipidation and targeting to autophagosomal membranes. J Biol Chem2004 Nov 12;279(46):47704-10.
322. Cantley LC. The phosphoinositide 3-kinase pathway. Science2002 May 31;296(5573):1655-7.
323. Engelman JA, Luo J, Cantley LC. The evolution of phosphatidylinositol 3-kinases as regulators of growth and metabolism. Nat Rev Genet2006 Aug;7(8):606-19.
324. Kaur H, Park CS, Lewis JM, Haugh JM. Quantitative model of Ras-phosphoinositide 3-kinase signalling cross-talk based on co-operative molecular assembly. Biochem J2006 Jan 1;393(Pt 1):235-43.
325. Arico S, Petiot A, Bauvy C, Dubbelhuis PF, Meijer AJ, Codogno P, et al. The tumor suppressor PTEN positively regulates macroautophagy by inhibiting the phosphatidylinositol 3-kinase/protein kinase B pathway. J Biol Chem2001 Sep 21;276(38):35243-6.
326. Klionsky DJ, Emr SD. Autophagy as a regulated pathway of cellular degradation. Science2000 Dec 1;290(5497):1717-21.
327. Meijer AJ, Codogno P. Regulation and role of autophagy in mammalian cells. Int J Biochem Cell Biol2004 Dec;36(12):2445-62.
328. Guertin DA, Sabatini DM. Defining the role of mTOR in cancer. Cancer Cell2007 Jul;12(1):9-22.
329. Klionsky DJ, Abeliovich H, Agostinis P, Agrawal DK, Aliev G, Askew DS, et al. Guidelines for the use and interpretation of assays for monitoring autophagy in higher eukaryotes. Autophagy2008 Feb 16;4(2):151-75.

330. Degenhardt K, Mathew R, Beaudoin B, Bray K, Anderson D, Chen G, et al. Autophagy promotes tumor cell survival and restricts necrosis, inflammation, and tumorigenesis. Cancer Cell2006 Jul;10(1):51-64.
331. Amaravadi RK, Yu D, Lum JJ, Bui T, Christophorou MA, Evan GI, et al. Autophagy inhibition enhances therapy-induced apoptosis in a Myc-induced model of lymphoma. J Clin Invest2007 Feb;117(2):326-36.
332. Soverini S, Colarossi S, Gnani A, Rosti G, Castagnetti F, Poerio A, et al. Contribution of ABL kinase domain mutations to imatinib resistance in different subsets of Philadelphia-positive patients: by the GIMEMA Working Party on Chronic Myeloid Leukemia. Clin Cancer Res2006 Dec 15;12(24):7374-9.
333. Cortes JE, Talpaz M, O'Brien S, Faderl S, Garcia-Manero G, Ferrajoli A, et al. Staging of chronic myeloid leukemia in the imatinib era: an evaluation of the World Health Organization proposal. Cancer2006 Mar 15;106(6):1306-15.
334. O'Brien SG, Guilhot F, Goldman JM, Hochhaus A, Hughes TP, Radich JP, et al. International Randomized Study of Interferon Versus STI571 (IRIS) 7-Year Follow-up: Sustained Survival, Low Rate of Transformation and Increased Rate of Major Molecular Response (MMR) in Patients (pts) with Newly Diagnosed Chronic Myeloid Leukemia in Chronic Phase (CML-CP) Treated with Imatinib (IM) Blood (ASH abstracts)2008;Abstract: 186.
335. Cortes J, Jabbour E, Kantarjian H, Yin CC, Shan J, O'Brien S, et al. Dynamics of BCR-ABL kinase domain mutations in chronic myeloid leukemia after sequential treatment with multiple tyrosine kinase inhibitors. Blood2007 Dec 1;110(12):4005-11.
336. Jiang X, Saw KM, Eaves A, Eaves C. Instability of BCR-ABL gene in primary and cultured chronic myeloid leukemia stem cells. J Natl Cancer Inst2007 May 2;99(9):680-93.
337. Chu S, Xu H, Shah NP, Snyder DS, Forman SJ, Sawyers CL, et al. Detection of BCR-ABL kinase mutations in CD34+ cells from chronic myelogenous leukemia patients in complete cytogenetic remission on imatinib mesylate treatment. Blood2005 Mar 1;105(5):2093-8.
338. Barnes DJ, Palaiologou D, Panousopoulou E, Schultheis B, Yong AS, Wong A, et al. Bcr-Abl expression levels determine the rate of development of resistance to imatinib mesylate in chronic myeloid leukemia. Cancer Res2005 Oct 1;65(19):8912-9.
339. Rousselot P, Huguet F, Rea D, Legros L, Cayuela JM, Maarek O, et al. Imatinib mesylate discontinuation in patients with chronic myelogenous leukemia in complete molecular remission for more than 2 years. Blood2007 Jan 1;109(1):58-60.
340. Jorgensen HG, Allan EK, Graham SM, Godden JL, Richmond L, Elliott MA, et al. Lonafarnib reduces the resistance of primitive quiescent CML cells to imatinib mesylate in vitro. Leukemia2005 Jul;19(7):1184-91.
341. Turner SD, Alexander DR. Fusion tyrosine kinase mediated signalling pathways in the transformation of haematopoietic cells. Leukemia2006 Apr;20(4):572-82.
342. Sharma SV, Fischbach MA, Haber DA, Settleman J. "Oncogenic shock": explaining oncogene addiction through differential signal attenuation. Clin Cancer Res2006 Jul 15;12(14 Pt 2):4392s-5s.
343. Perez-Caro M, Gutierrez-Cianca N, Gonzalez-Herrero I, Lopez-Hernandez I, Flores T, Orfao A, et al. Sustained leukaemic phenotype after inactivation of BCR-ABLp190 in mice. Oncogene2007 Mar 15;26(12):1702-13.
344. Hiwase DK, White DL, Powell JA, Saunders VA, Zrim SA, Frede AK, et al. Blocking cytokine signaling along with intense Bcr-Abl kinase inhibition induces apoptosis in primary CML progenitors. Leukemia2010 Feb 4.

345. Shah NP, Kim DW, Kantarjian H, Rousselot P, Llacer PE, Enrico A, et al. Potent, transient inhibition of BCR-ABL with dasatinib 100 mg daily achieves rapid and durable cytogenetic responses and high transformation-free survival rates in chronic phase chronic myeloid leukemia patients with resistance, suboptimal response or intolerance to imatinib. Haematologica2010 Feb;95(2):232-40.
346. Konig H, Holtz M, Modi H, Manley P, Holyoake TL, Forman SJ, et al. Enhanced BCR-ABL kinase inhibition does not result in increased inhibition of downstream signaling pathways or increased growth suppression in CML progenitors. Leukemia2008 Apr;22(4):748-55.
347. Konig H, Copland M, Chu S, Jove R, Holyoake TL, Bhatia R. Effects of dasatinib on SRC kinase activity and downstream intracellular signaling in primitive chronic myelogenous leukemia hematopoietic cells. Cancer Res2008 Dec 1;68(23):9624-33.
348. Tao WJ, Lin H, Sun T, Samanta AK, Arlinghaus R. BCR-ABL oncogenic transformation of NIH 3T3 fibroblasts requires the IL-3 receptor. Oncogene2008 May 15;27(22):3194-200.
349. Jordan CT, Upchurch D, Szilvassy SJ, Guzman ML, Howard DS, Pettigrew AL, et al. The interleukin-3 receptor alpha chain is a unique marker for human acute myelogenous leukemia stem cells. Leukemia2000 Oct;14(10):1777-84.
350. Neering SJ, Bushnell T, Sozer S, Ashton J, Rossi RM, Wang PY, et al. Leukemia stem cells in a genetically defined murine model of blast-crisis CML. Blood2007 Oct 1;110(7):2578-85.
351. Florian S, Sonneck K, Hauswirth AW, Krauth MT, Schernthaner GH, Sperr WR, et al. Detection of molecular targets on the surface of CD34+/CD38-- stem cells in various myeloid malignancies. Leuk Lymphoma2006 Feb;47(2):207-22.
352. Jin L, Lee EM, Ramshaw HS, Busfield SJ, Peoppl AG, Wilkinson L, et al. Monoclonal antibody-mediated targeting of CD123, IL-3 receptor alpha chain, eliminates human acute myeloid leukemic stem cells. Cell Stem Cell2009 Jul 2;5(1):31-42.
353. Feuring-Buske M, Hiddemann W, Buske C. [Pathogenesis and biology of leukemias]. Internist (Berl)2002 Oct;43(10):1179-89.
354. Frolova O, Wang RY, Korchin B, Watt JC, Cortes J, Frankel AE, et al. Targeting IL3 Receptor in Chronic Myeloid Leukemia. Blood (ASH abstracts)2009;Abstract: 2172.
355. Kim HP, Frankel AE, Hogge DE. A diphtheria toxin interleukin-3 fusion protein synergizes with tyrosine kinase inhibitors in killing leukemic progenitors from BCR/ABL positive acute leukemia. Leuk Res2010 Feb 4.
356. Roberts AW, He S, Bradstock KF, Hertzberg MS, Durrant STS, Ritchie D, et al. A Phase 1 and Correlative Biological Study of CSL360 (anti-CD123 mAb) in AML Blood (ASH abstracts)2008;Abstract: 2956.
357. Chen Y, Hu Y, Zhang H, Peng C, Li S. Loss of the Alox5 gene impairs leukemia stem cells and prevents chronic myeloid leukemia. Nat Genet2009 Jul;41(7):783-92.
358. Hu Y, Swerdlow S, Duffy TM, Weinmann R, Lee FY, Li S. Targeting multiple kinase pathways in leukemic progenitors and stem cells is essential for improved treatment of Ph+ leukemia in mice. Proc Natl Acad Sci U S A2006 Nov 7;103(45):16870-5.
359. Scherr M, Battmer K, Winkler T, Heidenreich O, Ganser A, Eder M. Specific inhibition of bcr-abl gene expression by small interfering RNA. Blood2003 Feb 15;101(4):1566-9.
360. Li MJ, McMahon R, Snyder DS, Yee JK, Rossi JJ. Specific killing of Ph+ chronic myeloid leukemia cells by a lentiviral vector-delivered anti-bcr/abl small hairpin RNA. Oligonucleotides2003;13(5):401-9.

361. Wohlbold L, van der Kuip H, Miething C, Vornlocher HP, Knabbe C, Duyster J, et al. Inhibition of bcr-abl gene expression by small interfering RNA sensitizes for imatinib mesylate (STI571). Blood2003 Sep 15;102(6):2236-9.
362. Myssina S, Helgason GV, Serrels A, Jorgensen HG, Bhatia R, Modi H, et al. Combined BCR-ABL inhibition with lentiviral-delivered shRNA and dasatinib augments induction of apoptosis in Philadelphia-positive cells. Exp Hematol2009 Feb;37(2):206-14.
363. Colosetti P, Puissant A, Robert G, Luciano F, Jacquel A, Gounon P, et al. Autophagy is an important event for megakaryocytic differentiation of the chronic myelogenous leukemia K562 cell line. Autophagy2009 Nov;5(8):1092-8.
364. Ito H, Daido S, Kanzawa T, Kondo S, Kondo Y. Radiation-induced autophagy is associated with LC3 and its inhibition sensitizes malignant glioma cells. Int J Oncol2005 May;26(5):1401-10.
365. Kanzawa T, Germano IM, Komata T, Ito H, Kondo Y, Kondo S. Role of autophagy in temozolomide-induced cytotoxicity for malignant glioma cells. Cell Death Differ2004 Apr;11(4):448-57.
366. Kanzawa T, Kondo Y, Ito H, Kondo S, Germano I. Induction of autophagic cell death in malignant glioma cells by arsenic trioxide. Cancer Res2003 May 1;63(9):2103-8.
367. Finbloom DS, Silver K, Newsome DA, Gunkel R. Comparison of hydroxychloroquine and chloroquine use and the development of retinal toxicity. J Rheumatol1985 Aug;12(4):692-4.
368. Munster T, Gibbs JP, Shen D, Baethge BA, Botstein GR, Caldwell J, et al. Hydroxychloroquine concentration-response relationships in patients with rheumatoid arthritis. Arthritis Rheum2002 Jun;46(6):1460-9.
369. Jorgensen HG, Copland M, Allan EK, Jiang X, Eaves A, Eaves C, et al. Intermittent exposure of primitive quiescent chronic myeloid leukemia cells to granulocyte-colony stimulating factor in vitro promotes their elimination by imatinib mesylate. Clin Cancer Res2006 Jan 15;12(2):626-33.
370. Heaney NB, Holyoake TL. Therapeutic targets in chronic myeloid leukaemia. Hematol Oncol2007 Jun;25(2):66-75.
371. Essers MA, Offner S, Blanco-Bose WE, Waibler Z, Kalinke U, Duchosal MA, et al. IFNalpha activates dormant haematopoietic stem cells in vivo. Nature2009 Apr 16;458(7240):904-8.
372. Neviani P, Santhanam R, Oaks JJ, Eiring AM, Notari M, Blaser BW, et al. FTY720, a new alternative for treating blast crisis chronic myelogenous leukemia and Philadelphia chromosome-positive acute lymphocytic leukemia. J Clin Invest2007 Sep;117(9):2408-21.
373. Zhao C, Chen A, Jamieson CH, Fereshteh M, Abrahamsson A, Blum J, et al. Hedgehog signalling is essential for maintenance of cancer stem cells in myeloid leukaemia. Nature2009 Apr 9;458(7239):776-9.
374. Dierks C, Beigi R, Guo GR, Zirlik K, Stegert MR, Manley P, et al. Expansion of Bcr-Abl-positive leukemic stem cells is dependent on Hedgehog pathway activation. Cancer Cell2008 Sep 9;14(3):238-49.
375. Ito K, Bernardi R, Morotti A, Matsuoka S, Saglio G, Ikeda Y, et al. PML targeting eradicates quiescent leukaemia-initiating cells. Nature2008 Jun 19;453(7198):1072-8.
376. Bhatia R, Snyder DS, Lin A, Arceo J, Seymour L, Deininger M, et al. A Phase I Study of the HDAC Inhibitor LBH589 in Combination with Imatinib for Patients with CML in Cytogenetic Remission with Residual Disease Detectable by Q-PCR Blood (ASH abstracts)2009;Abstract: 2194.

377. Parmar K, Mauch P, Vergilio JA, Sackstein R, Down JD. Distribution of hematopoietic stem cells in the bone marrow according to regional hypoxia. Proc Natl Acad Sci U S A2007 Mar 27;104(13):5431-6.
378. Jensen PO, Mortensen BT, Hodgkiss RJ, Iversen PO, Christensen IJ, Helledie N, et al. Increased cellular hypoxia and reduced proliferation of both normal and leukaemic cells during progression of acute myeloid leukaemia in rats. Cell Prolif2000 Dec;33(6):381-95.
379. Ninomiya M, Abe A, Katsumi A, Xu J, Ito M, Arai F, et al. Homing, proliferation and survival sites of human leukemia cells in vivo in immunodeficient mice. Leukemia2007 Jan;21(1):136-42.
380. Takeuchi M, Kimura S, Kuroda J, Ashihara E, Kawatani M, Osada H, et al. Glyoxalase-I is a novel target against Bcr-Abl(+) leukemic cells acquiring stem-like characteristics in a hypoxic environment. Cell Death Differ2010 Feb 5.
381. Scherz-Shouval R, Shvets E, Fass E, Shorer H, Gil L, Elazar Z. Reactive oxygen species are essential for autophagy and specifically regulate the activity of Atg4. EMBO J2007 Apr 4;26(7):1749-60.
382. Greer EL, Brunet A. FOXO transcription factors at the interface between longevity and tumor suppression. Oncogene2005 Nov 14;24(50):7410-25.
383. Tothova Z, Kollipara R, Huntly BJ, Lee BH, Castrillon DH, Cullen DE, et al. FoxOs are critical mediators of hematopoietic stem cell resistance to physiologic oxidative stress. Cell2007 Jan 26;128(2):325-39.
384. Greer EL, Oskoui PR, Banko MR, Maniar JM, Gygi MP, Gygi SP, et al. The energy sensor AMP-activated protein kinase directly regulates the mammalian FOXO3 transcription factor. J Biol Chem2007 Oct 12;282(41):30107-19.
385. Shackelford DB, Shaw RJ. The LKB1-AMPK pathway: metabolism and growth control in tumour suppression. Nat Rev Cancer2009 Aug;9(8):563-75.
386. Chiacchiera F, Matrone A, Ferrari E, Ingravallo G, Lo Sasso G, Murzilli S, et al. p38alpha blockade inhibits colorectal cancer growth in vivo by inducing a switch from HIF1alpha- to FoxO-dependent transcription. Cell Death Differ2009 Sep;16(9):1203-14.
387. Chiacchiera F, Simone C. Inhibition of p38alpha unveils an AMPK-FoxO3A axis linking autophagy to cancer-specific metabolism. Autophagy2009 Oct;5(7):1030-3.
388. Matrone A, Grossi V, Chiacchiera F, Fina E, Cappellari M, Caringella AM, et al. p38alpha is required for ovarian cancer cell metabolism and survival. Int J Gynecol Cancer Feb;20(2):203-11.
389. Hahn-Windgassen A, Nogueira V, Chen CC, Skeen JE, Sonenberg N, Hay N. Akt activates the mammalian target of rapamycin by regulating cellular ATP level and AMPK activity. J Biol Chem2005 Sep 16;280(37):32081-9.
390. Papandreou I, Lim AL, Laderoute K, Denko NC. Hypoxia signals autophagy in tumor cells via AMPK activity, independent of HIF-1, BNIP3, and BNIP3L. Cell Death Differ2008 Oct;15(10):1572-81.